The Pennsylvania State University

The Graduate School

Department of Civil and Environmental Engineering

EVALUATION OF PASSIVE SYSTEMS FOR THE

TREATMENT OF MINE DRAINAGE

A Thesis in

Environmental Engineering

By

Heath C. Roscoe

Submitted in Partial Fulfillment
of the Requirements
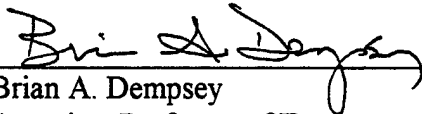for the Degree of

Master of Science

May 1999

I grant The Pennsylvania State University the nonexclusive right to use this work for the University's own purpose and to make single copies of the work available to the public on a not-for-profit basis if copies are not otherwise available.
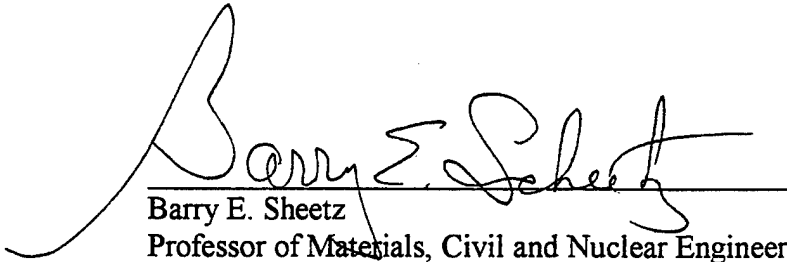
Heath C. Roscoe

We approve the thesis of Heath C. Roscoe.

Date of Signature

Brian A. Dempsey 26 March 99
Brian A. Dempsey
Associate Professor of Environmental Engineering
Thesis Advisor
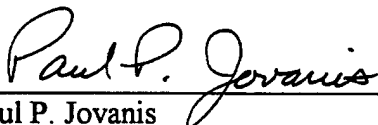
Barry E. Sheetz 26 March 99
Barry E. Sheetz
Professor of Materials, Civil and Nuclear Engineering

Robert S Hedin 26 March 1999
Robert S. Hedin
President, Hedin Environmental, Inc.
Special Signatory

Paul P. Jovanis 26 March 1999
Paul P. Jovanis
Professor of Civil Engineering
Head of the Department of Civil and Environmental
            Engineering

ABSTRACT

Acid Mine Drainage (AMD) is a serious environmental problem and the focus of a great deal of research. Passive treatment systems associated with wetlands and Anoxic Limestone Drains (ALDs) provide a low-cost, low-maintenance treatment in contrast to continuous chemical metering. The ALD adds alkalinity to the water allowing for a more rapid formation of iron precipitates. The abiotic oxidation ponds associated with these systems are expected to precipitate about 10-20 g/m^2-day of iron. The focus of this research is to evaluate two different ALD passive treatment systems in order to find ways to improve the efficiency of the abiotic oxidation of ferrous, thereby reducing the amount of land area required to treat the discharge. The two systems evaluated differed in that one system is a channel system, while the other is a series of ponds. The channel system has a large excess of alkalinity while the pond system has net mineral acidity. The study of the systems was conducted over a one-year period starting in January 1998 and ended in January 1999. The evaluation of each system included monitoring the chemistry and using MINTEQA2, a chemical equilibrium computer program to assist in the analysis. Of all the major cations in solution, ferrous is the only one that is removed in the system. The mechanisms for ferrous removal are the heterogeneous or homogeneous oxidation to ferric then subsequent precipitation, and also some adsorption onto the ferric oxide precipitate. The rate constants for homogeneous and heterogeneous oxidation of ferrous were determined from field data to be 6.8 $x10^{+14}$ L/M^3-sec and 2.2 $x10^{-8}$ L/mg-sec respectively for the channel; the pond system was not determined. These constants are

similar to values being reported in lab experiments. Sulfate decreased slightly in both systems and the removal mechanism was determined to be adsorption onto the ferric oxides produced. The oxygen gas transfer constant was also monitored and determined to be 1.96 cm/hr across the abiotic oxidation ponds. The constant for the channel system changed depending on the flow and ranged from 21.4 cm/hr for high flows to 3.9 cm/hr for low flows. The iron removal rate for the pond system was 21.0 g/day-m^2 which is typical of other values reported in literature. However, the channel system reported higher rates of removal, up to 56.5 g/day-m^2 which corresponded to high flows, and an average value of 41.6 g/day-m^2 through the study period. The sludge that formed in the pond system was identified as goethite with some lepidocrocite. These results matched predictions of models used to predict the AMD precipitate under the same chemistry. A significant amount of quartz (10% of sludge weight) was found in the bottom of the sediment layer, and is believed to come from the dissolution of the limestone in the drain and the impurities left behind being washed out, as well as being washed in from the surrounding area through rain events.

TABLE OF CONTENTS

LIST OF FIGURES

LIST OF TABLES

ACKNOWLEDGMENTS

GLOSSARY OF TERMS

A	Specific surface area (m^2/g); figure 2-4
A^{-z}	Anion with Z charge in solution
AA	Atomic Absorption
γ	Activity of ion; equation (3.6)
ALD	Anoxic Limestone Drain
AMD	Acid Mine Drainage
B1	Bend # 1 at the C & K Coal treatment site
B2	Bend #2 at the C & K Coal treatment site
B3	Bend #3 at the C & K Coal treatment site
CK	C & K Coal passive treatment system site
DO	Dissolved Oxygen
ΔH_{rxn}	Enthalpy of reaction; equation (3.3)
EP1	Effluent of Pond #1 at Howe Bridge
EP2	Effluent of Pond #2 at Howe Bridge
F	Faraday's constant (96,485 C/mol); figure 2-4
FAS	ferrous ammonium sulfate solution
FE	Final Effluent
HB	Howe Bridge passive treatment site
μ	Ionic Strength of solution; equation (3.4)
IP1	Influent to Pond #1 at Howe Bridge
IP2	Influent to Pond #2 at Howe Bridge

K^{int} Intrinsic equilibrium constant; equation (2.14) and (2.17)

K^{app} Apparent equilibrium constant; equation (2.14 and 2.17)

M^{2+} Divalent metal cation

MRL   Material Resources Laboratory

ψ Potential at surface (volts); figure 2-4

QA   Quality Assurance

QC   Quality Control

R   Gas Constant 1.99×10^{-3} kcal/mol; equation (3.4)

σ Surface charge density (C/m^2)

S   Solid concentration (g/L); figure 2-4

$\equiv$ Indicates surface of species

TIC   Total Inorganic Carbon

TOC   Total Organic Carbon

XRD   X-ray Diffraction

Z   Charge of particular species

Chapter 1

INTRODUCTION

1.1 General

Coal and metal mining disturb large amounts of geological material and expose them to air and water. With this exposure, sulfide minerals commonly associated with coal mining are oxidized and hydrolyzed resulting in Acid Mine Drainage (AMD). AMD emerging from pre-existing coal spoils is a common occurrence in the coalfields of Pennsylvania. This water typically contains elevated levels of acidity, iron, aluminum, and manganese. As this water flows into other streams and rivers, it becomes less toxic through dilution, but can still be harmful to the aquatic life.

AMD commonly leads to formation of metal precipitates that are part of a major water-pollution problem in regions with a history of coal and metal mining. Letterman and Mitsch (1978), for example reported particulate deposition rates of up to 3 g/m^2-day in a stream receiving acid coalmine drainage. Such voluminous blankets of sediment have bad impacts on native fish populations and benthic communities. It also can shorten the effective lifetime of reservoirs, catchment basins and wetlands constructed for treatment of AMD (Fennessy and Mitsch, 1989; Eger et al., 1993; Hedin and Nairn, 1993).

An estimated 5000 miles of Pennsylvania streams are currently degraded to some extent by acid water discharges from old, abandoned surface and deep mines (Alcorn, 1996). Since no company or individual is held responsible for reclaiming these abandoned mines, no treatment of the AMD occurs and continual contamination of the

surface and groundwater results. The responsibility then falls on the federal, state and local governments. Clean-up costs for Pennsylvania alone are estimated at $15 billion for abandoned mines (Herlihy et al, 1990).

An inexpensive approach to treating AMD is through wetlands and Anoxic Limestone Drains (ALDs). The major cost for this approach is land for the abiotic oxidation ponds, which are expected to precipitate about 10-20 g/m^2-day of iron (Watzlaf and Hyman, 1995). The ALD raises the pH of the water to circumneutral levels (pH 6-7) and introduces bicarbonate alkalinity. The water then exits the drain with the new pH, which promotes metal precipitation into the ponds while bicarbonate alkalinity neutralizes acidity produced by hydrolysis (Hedin and Nairn, 1993). This system will be the focus of this study.

1.2 Desired Goals

The purpose of this research is to monitor the ALD passive treatment systems on their ability to treat mine drainage. A 12-month study period was used to evaluate factors that are responsible for the performance of these systems. The evaluation looked at flow data, temperature effects, metal concentrations, sulfate concentrations, alkalinity and types of precipitates formed in the two systems.

In doing so, the following hypotheses will be tested:

1. Rate constants for the oxidation of ferrous can be determined in a field environment by careful measurements of the parameters of the system.

2. Removal mechanisms associated with ferrous and sulfate for these systems can be identified using MINTEQA2 and analytical procedures in the lab.

3. The inability to accurately predict ferrous removal with alkalinity decrease is a result of ferrous adsorption and sulfate adsorption by replacement of OH^- onto the surface of the ferric oxide precipitate.

4. Very little if any, microbiological activity for the oxidation of ferrous occurs in the passive treatment systems where the pH value is above 5.

5. AMD precipitation models can be used to accurately predict the formation of solids in an ALD passive treatment system.

6. Flow has a major impact on the iron rate of removal and oxidation of ferrous in the ALD passive treatment systems.

7. The heterogeneous oxidation process is a significant part of the total oxidation rate in the ALD passive treatment systems with pH values around 6.

8. The rate of oxygenation of water is enhanced in a channel system rather than a pond system.

1.3 Site Background

The two ALD passive treatment systems evaluated in this study are located in Jefferson County in Pennsylvania. Both systems are located approximately 4 miles north of the town of Corsica along state route 949. The sites are approximately 2 miles apart from each other and treat separate mine discharges.

The study of the sites started on the 31st of January 1998 with the first sampling trip. Eleven successive trips occurred after this approximately 30 days apart from each other, with the final sampling trip occurring on the 24th of January 1999.

The first site, called Howe Bridge (HB) is net acidic. This means that the amount of alkalinity generated in the ALD is not enough to account for the mineral acidity produced by the oxidation and hydrolysis of ferrous iron to ferric hydroxide. HB's flow comes from a contaminated aquifer. HB has two different AMD influents each treated by an ALD that discharge into pond #1. The outlet for influent #2 is submerged in pond #1. The water then moves through two more oxidation-settling ponds then discharges into a local stream. A layout of the system and the dimensional data can be seen in figure 1-1 and table 1-1 on the next page.

The next site is called C&K Coal (CK) and is net alkaline. This means that the amount of alkalinity produced in the ALD is larger than the acidity produced by ferrous iron going to ferric hydroxide. The AMD influent flows through an ALD then is discharged into a channel system which in turn flows through three successive settling ponds then into a wetland. Information about this system can be seen in figure 1-2 and table 1-2.
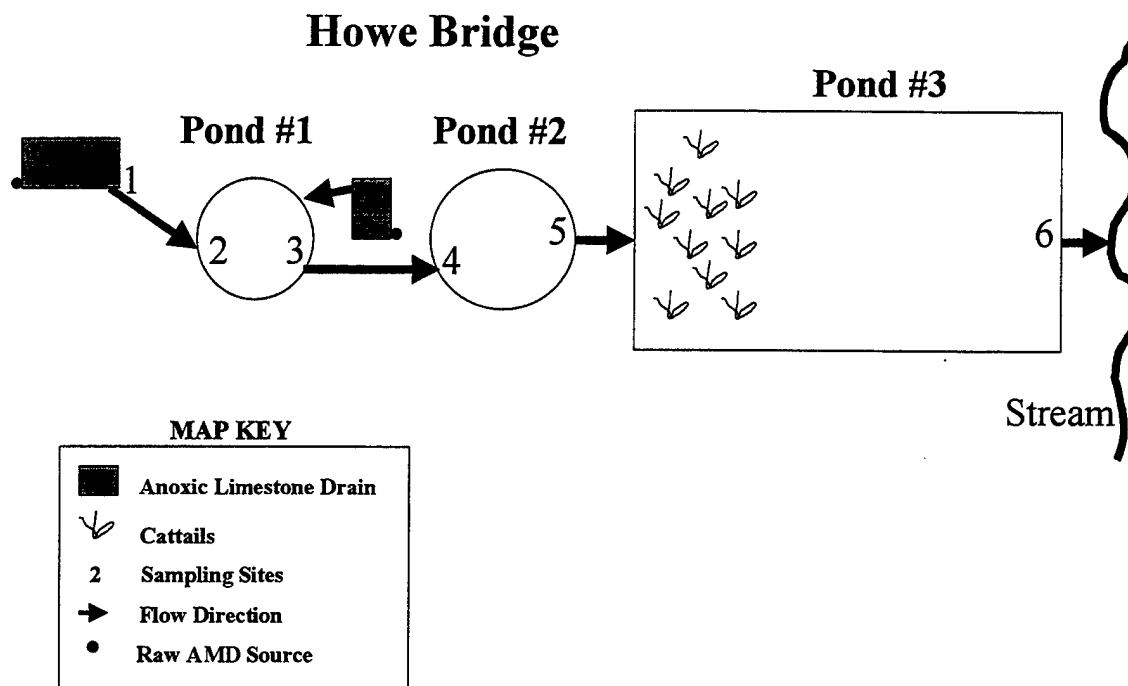
Howe Bridge

Figure 1-1: Howe Bridge site layout.

Table 1-1: Dimensional data for Howe Bridge.*

LOCATION	Surface Area (ft^2)	Volume (ft^3)	Dimensions LxWxD (ft)
Race #1**	76	19	38x2x0.25
Pond #1	1218	1218	42x29x1
Race #2**	159	79.5	53x3x.0.5
Pond #2	5000	15000	50x100x3
Race #3**	300	75	30x10x0.25
Pond #3	31540	94620	380x83x3

*   Note: These measurements were taken on 29 March 1998 with a 100 foot tape
        measurer.

** Note: Race is the part of land that water flows over prior to entering the pond.
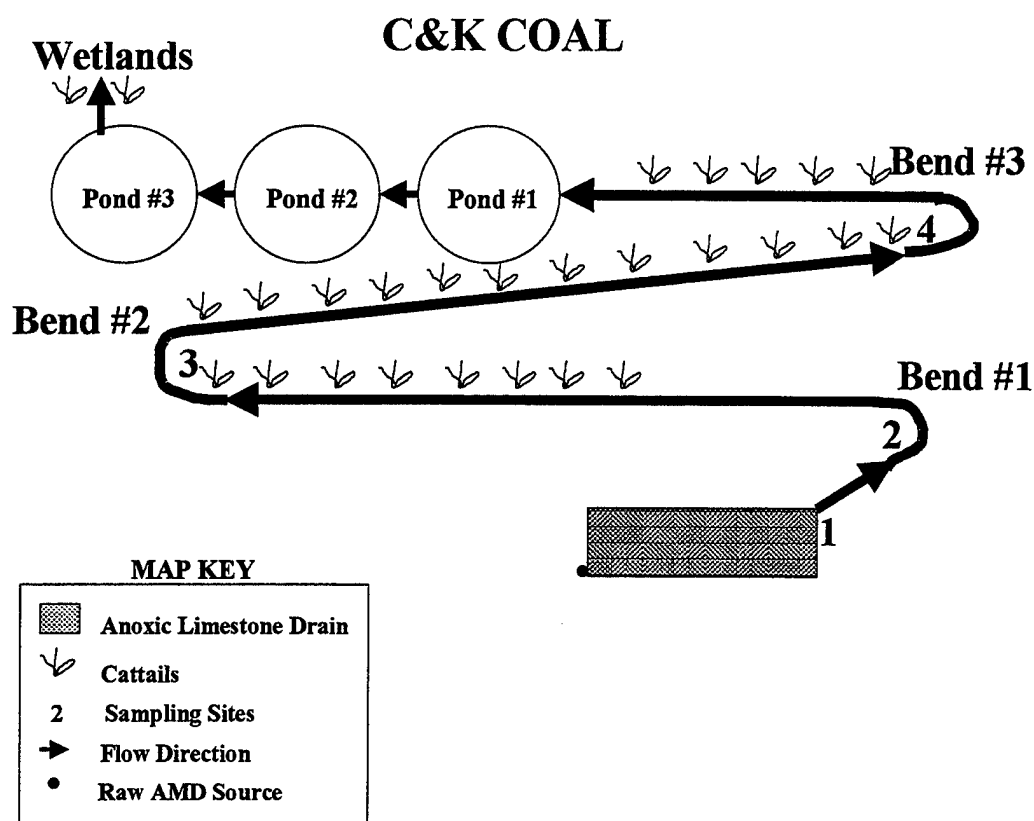
C&K COAL

Figure 1-2: Site layout of the CK Coal system.

Table 1-2: Dimensional data for the CK system.

LOCATION	Surface Area (ft^2)	Volume (ft^3)	Dimensions LxWxD (ft)
Bend #1	300	150	30x10x0.5
Bend #2	5250	5250	375x14x1
Bend #3	6650	3325	475x14x0.5
Pond #1	8870	**	**
Pond #2	6500	**	**
Pond #3	12910	**	**

* Note: These measurements were taken on 29 March 1998 with a 100 foot tape measurer.

** Note: Depth of the water for the ponds is unknown.

Figure 1-3: Howe Bridge Pond #1. Photo taken on 26 September 1998.

Figure 1-4: Iron film on-top of the water at Howe Bridge Pond #1. Photo was taken on 24 October 1998.

Figure 1-5: Bend #1 at C & K Coal. Photo taken on 24 October 1998.
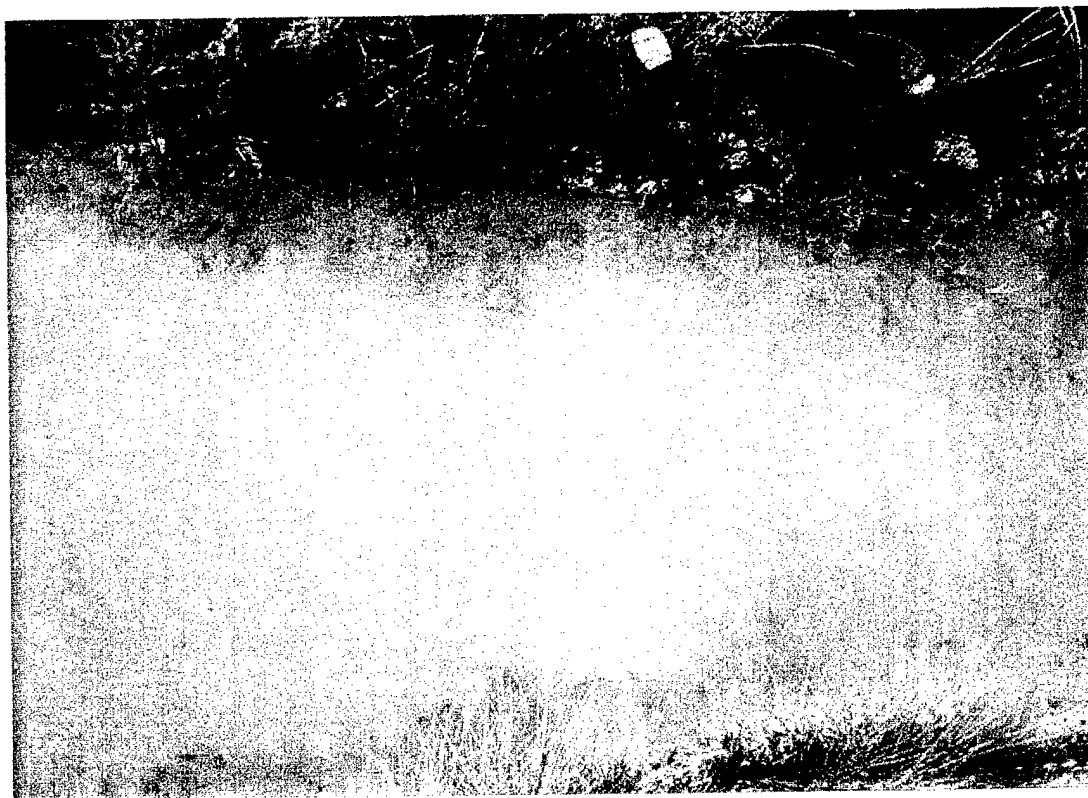
Figure 1-6: Precipitate forming at C & K Coal between the influent and Bend #1. Photo taken on 24 October 1998.

Chapter 2

LITERATURE REVIEW

2.1 Description of Acid Mine Drainage Problem

In the Appalachian region, numerous streams have been altered by AMD. It is estimated that 80% of the pollution in the streams comes from abandoned mines. Abandoned underground mine workings are the largest source of mine drainage, responsible for an estimated 70% of the pollution problem. If aerated water comes into contact with pyrite-rich coal and strata, then the pyrite oxidizes forming AMD. Water exiting the spoil bank or mine becomes an acid mine drainage discharge (Appalachian Regional Commission, 1969).

Pollution of water resources by AMD causes considerable expense and loss of revenue. Severe impacts on the stream ecology, such as "dead" streams or fish kills, affect both the environment and revenue lost for recreational use. Precipitation of the metals in AMD causes increased sedimentation and corrosion of metal structures in the waterways (Appalachian Regional Commission, 1969).

The most common contaminants in AMD in Pennsylvania coalfields are Fe, Mn, Al, and SO_4 ions. In addition, the mine drainage may contain Cu, Zn, Cd, Pb, and As at levels near or beyond threshold limit concentrations. These metals may interact to increase the toxicity of the water (Alcorn, 1996).

2.2 Formation of Acid Mine Drainage

The oxidation and hydrolysis of pyrite and related iron disulfide minerals that are present in coal and related strata is the cause of AMD. An understanding of the mechanisms of AMD production is helpful in explaining the methodology or prevention and remediation. Pyrite oxidizes in the presence of water and oxygen to form highly acidic, sulfate rich drainage. In the Appalachian coalfields, the following four chemical equations are accepted to explain the processes (Skousen, 1995).

$$FeS_2(s) + 7/2\ O_2 + H_2O \rightarrow Fe^{2+} + 2\ SO_4^{2-} + 2\ H^+ \qquad (2.1)$$

$$Fe^{2+} + \tfrac{1}{4}\ O_2 + H^+ \rightarrow Fe^{3+} + \tfrac{1}{2}\ H_2O \qquad (2.2)$$

$$Fe^{3+} + 3\ H_2O \rightarrow Fe(OH)_3\ (s) + 3\ H^+ \qquad (2.3)$$

$$FeS_2(s) + 14\ Fe^{3+} + 8\ H_2O \rightarrow 15\ Fe^{2+} + 2\ SO_4^{2-} + 16\ H^+ \qquad (2.4)$$
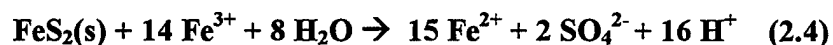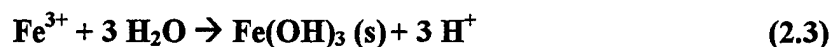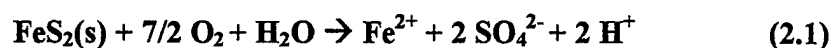
If any of the processes represented by the equations were slowed or stopped, the generation of AMD would also slow or cease. Removal of air and /or water from the system, two of the three principal reactants, would stop pyrite from oxidizing (Skousen, 1995).

The first equation is the oxidation of pyrite, in which the pyrite is converted into ferrous iron, sulfate and acidity. In oxygen depleted environments, limited amounts of other species of sulfur may be produced, such as SO_3^{2-}, $S_2O_3^{2-}$ and S_2^{2-}. When they come into contact with oxygen, the species are quickly oxidized to SO_4^{2-} (Williams, et al 1982).

The slowest, or rate determining step, is equation (2.2), the oxidation of ferrous iron to ferric iron. At pH > 4.5, the reaction proceeds quickly, allowing the production of sufficient acidity to produce AMD. In this pH region, the reaction can be depicted by the equation (Singer and Stumm, 1970)

$$-d[Fe^{2+}]/dt = k[Fe^{2+}][O_2][OH^-]^2 \qquad (2.5)$$

where $k = 8.0 \times 10^{13}$ liter^{2}mole^{-2}atm^{-1} at 25^{0}C. The half time for this reaction is very small in this pH range. At a pH of 7.0, half of the iron is oxidized in 4 minutes (Singer and Stumm, 1970).

In an abiotic environment below a pH of 4.5, the rate of oxidation of ferrous iron slows down significantly. At pH < 3.5, the oxidation rate of ferrous iron is independent of pH, the following relationship applies

$$-d[Fe^{2+}]/dt = k'[Fe^{2+}][O_2] \qquad (2.6)$$

where $k' = 1.0 \times 10^{-7}$ atm^{-1}min^{-1} at 25°C. The half time of the reaction under these conditions is approximately 1000 days (Singer and Stumm, 1970). However, a family of autotrophic bacteria, *Thiobacillus ferrooxidans*, has been identified which can catalyze the oxidation of ferrous iron at low pH values.

T. ferrooxidans is the best characterized of the acidophilic thiobacilli (i.e., those that will grow only at low pH) was first isolated from coal AMD by Colmer and Hinkle

(1947). This thiobacillus is an obligate acidophile that has a pH range of 1.0 to 3.5, and an optimum near 2.0. It is capable of obtaining energy from the oxidation of a number of metal sulfides as well as reduced-sulfur compounds such as thiosulfate, and sulfide and elemental sulfur. It also can get energy via the oxidation of ferrous to ferric iron. *T. ferrooxidans* is a mesophile with a temperature optimum near 35°C and with 40°C the maximum for growth. Some isolates have been shown to be capable of iron oxidation and growth at temperatures as low as 2°C (Leduc et al., 1993). Because it is an autotroph, it obtains all of its carbon by fixation of CO_2, and only low concentrations of inorganic nitrogen and phosphorous compounds, as well as trace amounts of magnesium are required (Gould et al., 1990).

Equation (2.3) shows the hydrolysis of ferric iron to ferric hydroxide. The equilibrium concentration of ferric iron is pH dependent. According to the equilibrium theory, at pH 2, hundreds of mg/L of ferric iron can be dissolved in water, at pH 3, less than 5 mg/L and at pH 4 less than 0.1 mg/L. In general, at pH values greater than 4, once ferrous iron is oxidized to ferric iron, it will precipitate as ferric hydroxide fairly rapidly. Thus at pH > 4, the removal of ferrous iron from mine water is usually limited by the rate of iron oxidation, equation (2.2) (Watzlaff and Hyman, 1995).

Equation (2.4) shows a secondary pathway for pyrite oxidation, which requires an excess of ferric iron. This reaction creates much more acidity than the first three equations combined per molecule of pyrite oxidized, and is much more significant under extremely acidic conditions. Due to the rapid hydrolysis associated with this reaction,

ferric iron typically does not exist in substantial amounts in non-aerated mine drainage
(Alcorn, 1996).

2.3 Methods for Treating Acid Mine Drainage

The selection of a treatment system to control AMD is often site specific. An
active mine site has many more options than an abandoned site, and can often
accommodate more effective and expensive control measures. Abandoned or closed sites
typically require after the fact treatment with limited resources available (Alcorn, 1996).
Treatment methods for AMD come under two general categories, conventional and
passive.

2.3.1 Conventional Treatment Systems

Conventional, or chemical treatment systems eliminate acidity, remove heavy
metals by precipitation, and capture any other harmful substances which may be present
in mine drainage. Chemical treatment technology is well established, but requires
continuous operation, maintenance and high cost (Skousen et al., 1990). Four chemicals
are typically used in treating AMD: calcium carbonate (limestone), calcium hydroxide
(hydrated lime), sodium carbonate (soda ash), and sodium hydroxide (caustic soda).
Ammonia is also being used, but not as much as the four mentioned before (Skousen and
Ziemkiewicz 1995). Conventional treatment is typically only favored for short term
treatment or treatment of waters which are so polluted that passive treatment is not
possible.

2.3.2 Passive Treatment Systems

Development of passive treatment systems began with research projects which demonstrated the natural Sphagnum (peat moss) wetlands remediated AMD without receiving damage (Brodie, 1993). These findings prompted more projects investigating if constructed wetlands could treat coalmine drainage. Other treatment methods arose and some of these include: Aerobic wetlands (treatment with bacteria), Anaerobic wetlands (compost wetlands), and Anoxic Limestone Drains with oxidation/settling ponds.

Aerobic wetland systems are applicable when the mine drainage water contains enough alkalinity to precipitate all of the ferrous iron to ferric hydroxide. In these systems, oxidation and precipitation occur naturally through the system without any addition of chemicals (Faulkner et al., 1995).

The compost wetland can treat AMD by means of anaerobic bacteria activity and limestone dissolution. The activity of certain bacteria such as *Desulfovibrio spp.* and *Desulfotomachulum spp.* reduces the sulfate to sulfide followed by the precipitation of metal sulfides and production of bicarbonate alkalinity (Gazea et al., 1996).

The third type of system is the anoxic limestone drain. ALDs are used to treat net acidic mine drainage. ALDs are typically followed by a series of constructed wetlands or settling ponds. The ALD passive treatment system is the subject of this study and will be discussed in greater detail in the following sections.

2.4 Anoxic Limestone Drains (ALDs)

ALDs are buried beds of limestone. Acid water is diverted through these drains and, through reaction with the limestone, pH and alkalinity of the water are increased. Limestone is a cheap and effective way to generate alkalinity, but must be done under the right conditions or its effectiveness is limited. By keeping the limestone and mine water anoxic, limestone dissolution can occur without armoring reactions that make the limestone useless in a surface environment. ALDs then must be followed by an aerobic system in which metal oxidation and precipitation reactions can occur (Hedin and Nairn, 1992).

2.4.1 Factors Important for ALD Treatment for AMD

The following factors are important in using ALDs for treatment of AMD:

1. Flow rate (max and min)

2. Dissolved oxygen content

3. Alkalinity

4. Ferric and ferrous iron concentrations

5. Aluminum concentrations

Flow rates of about 100 gpm have generally been the upper limit for passive treatment systems because of size and area limitations. However, some flows have been treated up to 800 gpm in the Tennessee Valley Authority. Most passive systems perform best on flows of less than 100 gpm (Skousen and Ziemkiewicz, 1995).

Dissolved Oxygen (DO) content relates to the oxidation/reduction status of the water. At oxygen concentrations of 2 mg/L or less and with low ferric iron concentration, ALDs are effective because limestone armoring is thought to be negligible. If the DO were higher and more ferric iron present, limestone armoring increases dramatically and decreases the effective life of the system (Skousen and Ziemkiewicz, 1995).

Alkalinity in water is important because it neutralizes mineral acidity (primarily from Fe and Al ions), raises pH and helps in removal of manganese. The alkalinity generated in an ALD is mostly in the form of bicarbonate (HCO_3^-). Upon oxidation after exiting the drain, the precipitation reactions occur more readily in alkaline water. ALDs have been observed to generate up to 300 mg/L of alkalinity in water when functioning properly (Hedin and Nairn, 1992).

Ferrous iron occurs in waters under reduced or low oxygen conditions. When oxygen in introduced into reduced water, ferrous iron oxidizes to ferric iron. As DO concentrations increase, less iron will be in the ferrous state (Fe^{2+}) and more will be in the ferric state (Fe^{3+}). Measuring the quantity of ferrous and ferric iron is critical to determine the potential of using an ALD. For an ALD to work, most of the iron should be in the ferrous or reduced state. Ferrous iron will not precipitate at the pH levels attained in an ALD. If ferric iron is present in the acid water and with the generation of alkalinity, ferric hydroxide will precipitate in the drain (Skousen and Ziemkiewicz, 1995).

Aluminum is found in all AMD at varying concentrations. Aluminum precipitates in water at or above pH 5.0 through hydrolysis (the splitting of water H^+ and OH^-) and does not require oxidation. So the use of an ALD will cause aluminum to precipitate in the drain. If high concentrations of aluminum are found in the water (>25 mg/L), the potential exist for aluminum to clog the drain (Skousen and Ziemkiewicz, 1995).

2.4.2 Alkalinity Generation

The carbonate system is the most important buffering system in natural waters, as well as one of the most complex. The chemical species that make up the carbonate system include gaseous carbon dioxide (CO_2), dissolved or aqueous carbon dioxide ($CO_{2\ (aq)}$), carbonic acid (H_2CO_3), bicarbonate (HCO_3^-), carbonate (CO_3^{-2}), and carbonate containing solids such as calcium carbonate ($CaCO_3$) (Nairn et al., 1992).

When acid waters contact limestone, the limestone dissolves and produces dissolved calcium and dissolved carbon dioxide (2.7). Dissolved CO_2 is a weak acid and continues to react with limestone, producing dissolved calcium and bicarbonate ion (2.8). The conventional notation for dissolved CO_2 is "H_2CO_3*", and includes both $CO_{2(aq)}$ and carbonic acid (Stumm and Morgan, 1981). This relationship is shown in reaction (2.9).

$$CaCO_3 + 2\ H^+ \rightarrow Ca^{+2} + H_2CO_3* \tag{2.7}$$

$$CaCO_3 + H_2CO_3* \rightarrow Ca^{+2} + 2\ HCO_3^- \tag{2.8}$$

$$CO_{2(aq)} + H_2O \leftrightarrow H_2CO_3 \tag{2.9}$$
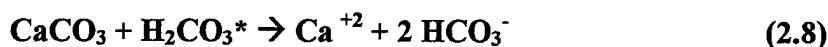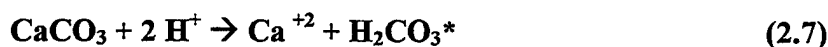
The bicarbonate alkalinity produced in reaction (2.8) is available for acid neutralization reactions. When the reactions of ferrous to ferric (2.2), then ferric to ferric hydroxide (2.3) occur after the water discharges from the drain, the alkalinity introduced in the ALD buffer the proton acidity produced and maintains circumneutral pH levels (Nairn et al., 1992).

Since ALDs are assumed to be closed systems, the partial pressure of carbon dioxide (pCO$_2$) becomes quite important in the potential rate of limestone dissolution and thus, alkalinity generation. The equilibrium constant for reaction (2.9) is near $10^{-2.8}$ and the great majority of dissolved CO$_2$ is present as CO$_{2(aq)}$. Therefore, reactions (2.7) and (2.8) can be viewed as:

$$CaCO_3 + 2\ H^+ \rightarrow Ca^{+2} + H_2O + CO_2 \qquad (2.10)$$

$$CaCO_3 + H_2O + CO_2 \rightarrow Ca^{+2} + 2\ HCO_3^- \qquad (2.11)$$
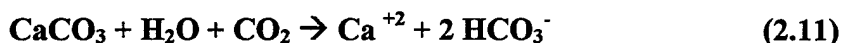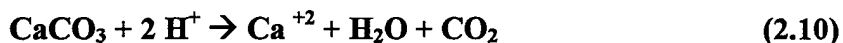
As limestone dissolves, CO$_2$ is produced and, in a closed system, pCO$_2$ increases (2.10). The CO$_2$ produced continues to react with the limestone producing bicarbonate alkalinity (2.11). As pCO$_2$ increases, the alkalinity able to be dissolve in water will increase (Nairn et al., 1992).

By excluding oxygen, ALDs provide an environment for continued limestone dissolution without some of the armoring problems encountered when oxygen is present. Also, their buried and closed nature allows the generation of much greater alkalinity

concentrations than possible in an open system, due to the presence of elevated pCO_2

(Naim et al., 1992).

2.5 Mineralogy of Deposits Formed by AMD

There are thirteen iron oxides, oxyhydroxides and hydroxides known to date. The

most important ones related to AMD are listed in Table 2-1. All iron oxides and

hydroxides consist of Fe, O and/or OH. They differ in composition, in the valence of Fe

and , above all crystal structure (Schwertmann and Cornell, 1991).

Most sediments from AMD are bright, yellow-to-red coloration. It has been noted

that the sediments have a tendency for the pigmentation to vary under the influence of

such factors as particle size, aggregation, chemical composition, admixtures, etc. There

is a misconception that that color sediments can not be measured with any degree of

confidence (Bigham, 1994). However, colors of such materials can be measured

precisely in the laboratory using diffuse reflectance spectrophotometers (Torrent and

Barron, 1993). These technical advances, coupled with a better understanding of the

spectral characteristics and genesis of minerals from AMD should enable useful

interpretations concerning not only mineralogy, but also local geochemical conditions to

be derived from color measurements (Schwertmann and Cornell, 1991; Bigham, 1994).

The iron oxides and their corresponding colors can be seen in figures 2-1 and 2-2.

The Munsell System was developed in the early 1900's by the artist A. H.

Munsell. Today it finds world-wide use as a basis for color specification, including

AMD precipitates. The colors are arranged and defined in terms of the three accepted

dimensions of color: hue, value and chroma. Hue refers to the relation of a color to red

(R), yellow (Y), green (G), blue (B) and purple (P). These letters are preceded by a

number from 1 to 10 to indicate gradations of hue. For example, goethite ranges from 7.5

YR to 10.0 YR (Schwertmann and Cornell, 1991). This color system will be used in this

chapter to identify solids.

X-ray powder diffraction is used for identification and purity control of ferric

oxides. It can also provide information concerning crystal size and disorder, structural

parameters (unit cell edge lengths), and surface area (Schwertmann and Cornell, 1991).

Well-crystallized minerals formed as a result of AMD can commonly be identified

readily by X-ray diffraction (XRD). Problems arise when a poorly crystallized phase(s)

is present as a minor constituent (<25 wt%) in a sample that also contains well-

crystallized components. This problem can be overcome by a combination of XRD

and selective-dissolution analysis (Bigham, 1994; Schulze, 1981). Schwertmann et al.

(1982) reported that 15 wt% was about the lower limit of detection using this method for

poorly crystallized ferrihydrite occurring in natural spring deposits and soil samples.

Table 2-1: Properties of minerals in AMD from Bigham 1994.

Mineral Name	Goethite	Lepidocrocite	Ferrihydrite	Schwertmannite	Jarosite
Ideal Formula	FeOOH	FeOOH	$Fe_5OH_8-4H_2O$	$Fe_8O_8(OH)_6SO_4$	$KFe_3(OH)_6(SO4)_2$
Crystal System	Orthorhom	Orthorhomic	Trigonal	Tetragonal	Hexagonal
Cell size (Å)	a = 4.608	a = 3.88	a = 5.08	a = 10.66	a = 7.92
	b = 9.956	b = 12.54	c = 9.4	c = 6.04	c = 17.16
	c = 3.022	c = 3.07			
Color	Yellow Br	Orange	Reddish Br	Yellow	Straw Yellow
Crystal shape	Short rods	Laths	Spherical	Pin cushion	Pseudocubic
Crystallinity	Moderate	Moderate	Poor	Poor	Good
XRD Spacing	2.69 (Å)	2.47, 1.94 (Å)	1.97, 1.73, 1.47 (Å)	2.28, 1.66, 1.51 (Å)	3.08 (Å)

Goethite   Lepidocrocite   Akaganéite

Hematite   Magnetite   Maghemite

Fe(III) hydroxy-
Ferrihydrite   Feroxyhyte   Sulfate
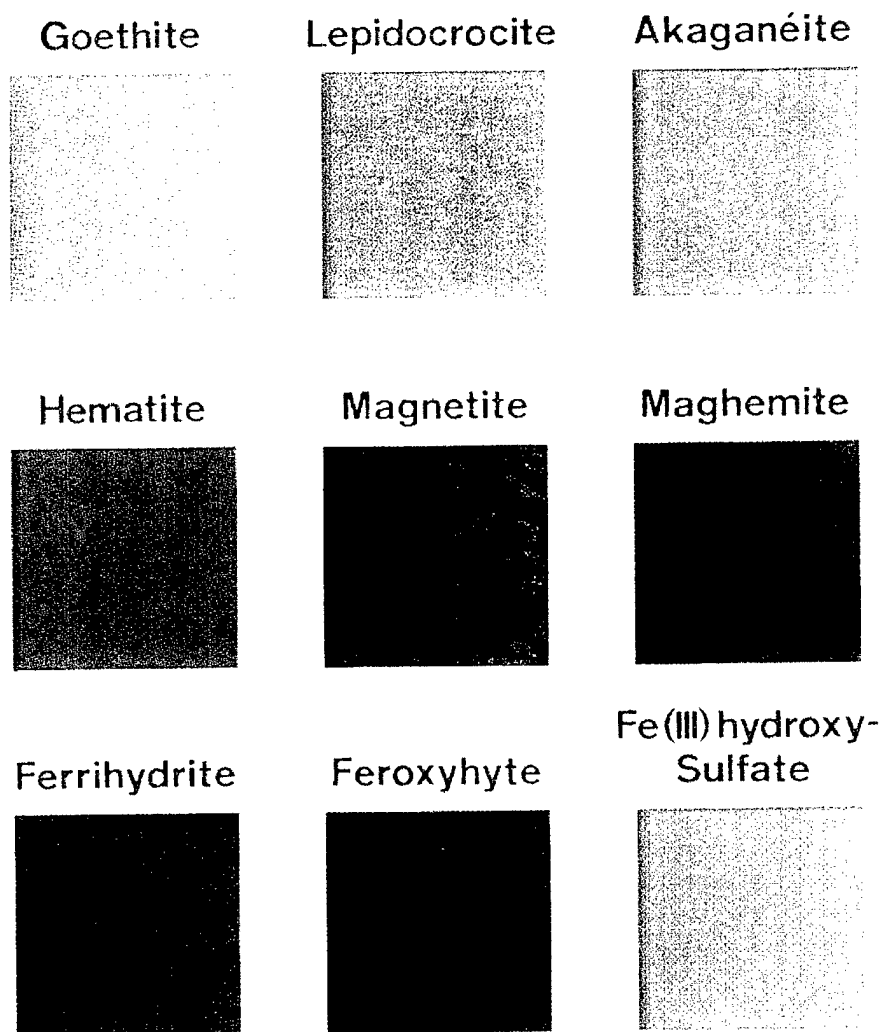
Figure 2-1: Colors of common iron oxides from Schwertmann and Cornell, 1991.

Goethite

Mn-Goethite

1-2 μm

~ 0.2 μm

Cr-Goethite

~ 0.5 μm

~ 0.1 μm

Hematite

~ 0.4 μm

~ 0.1 μm
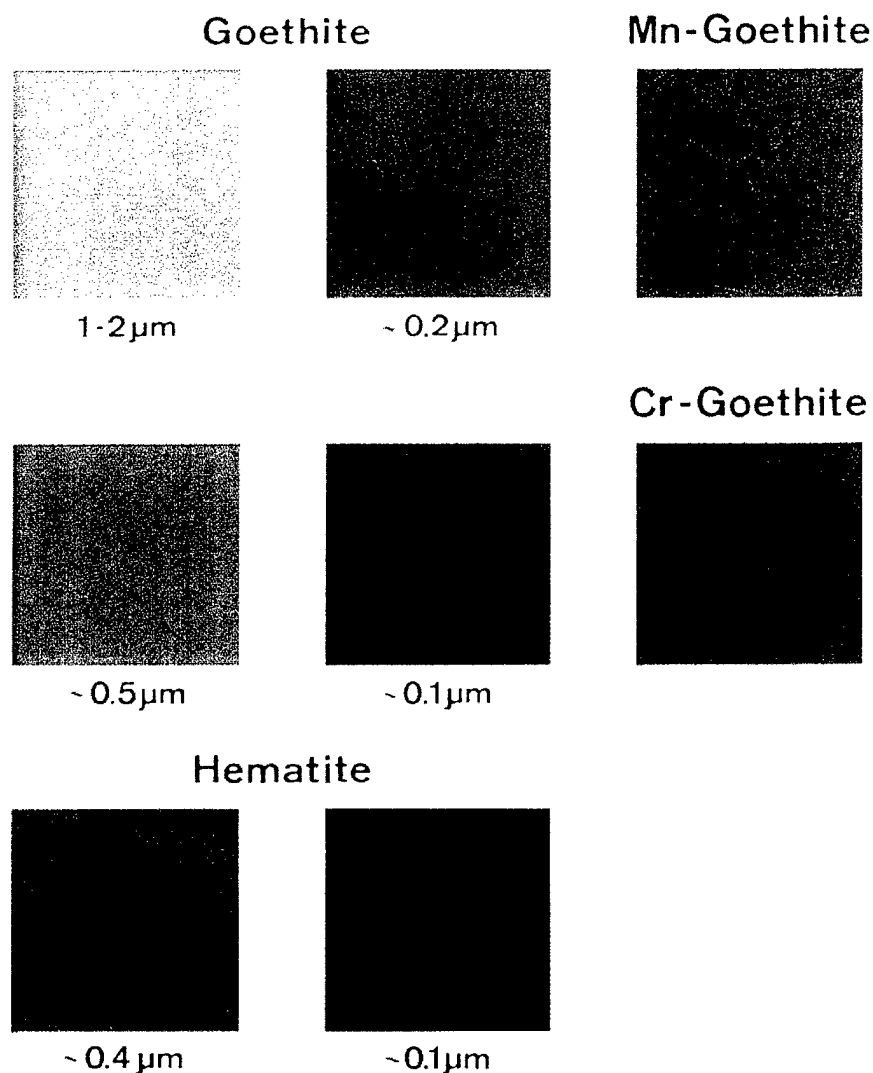
Figure 2-2: Colors of goethite, lepidocrocite and hematite with large and small crystals. The right hand column shows a goethite with 6 mole % Mn for Fe substitution and with 10 mole % Cr for Fe substitution. The crystal sizes given are approximations taken from micrographs and refer to the size of the largest dimension of the crystals. This information comes from Schwertmann and Cornell, 1991.

2.5.1 Goethite (FeOOH)

Goethite is one of the most widely used iron oxides in the world today. Goethite is considered the most stable form of ferric oxide, and it occurs in almost every type of surface environment (Schwertmann and Fitzpatrick, 1992). In AMD precipitates, goethite is rarely the dominant phase, and commonly is observed as a minor constituent. Precipitated goethites are usually yellowish brown in color with Munsell hues ranging between 7.5 YR and 10 YR. Well crystallized/synthetic goethites typically display a fibrous or lath-like morphology while AMD precipitates usually form short, rod-like particles (Brady et al., 1986; Bigham, 1994). Goethite may be synthesized from either ferric or ferrous systems. The synthesis from ferrous involves the oxidation of ferrous to ferric. The initial precipitate may be a so-called green rust (Schwertmann and Cornell, 1991).

2.5.2 Lepidocrocite (FeOOH)

Lepidocrocite is generally less widespread than its polymorph, goethite, but it does occur frequently as orange accumulations in certain environments. These are characterized by the presence of ferrous from which lepidocrocite forms by oxidation. The presence of this mineral, therefore, indicates a deficiency of oxygen (Schwertmann and Cornell,1991). In carbonate rich solutions, formation of lepidocrocite is prevented and goethite forms from the ferrous. Lepidocrocite is commonly recognizable in the field by bright orange colors having Munsell hues in the 5 YR to 7.5 YR range. Lepidocrocite is found throughout the surface environment particularly in soils, however its

observations as a product of AMD is limited (Bigham, 1994). Milnes et al. (1992) reported finding poorly crystallized lepidocrocite in sludge taken from a uranium mine in Australia.

2.5.3 Ferrihydrite ($Fe_5OH_8 \cdot 4H_2O$)

Ferrihydrite is very popular and often misused synonym for "amorphous" ferric hydroxide. The occurrence of ferrihydrite appears to be limited to those situations where ferrous is oxidized rapidly and/or where crystallization inhibitors are present. Such inhibitors include organics, phosphate and silicate species, all of which are widespread in the natural environment, and have a high affinity for the ferric oxide surface. Ferrihydrite occurring in soils has a rusty, reddish-brown color with Munsell hues in the 5 YR to 7.5 YR range (Bigham 1994). Natural and synthetic samples both usually consist of highly aggregated spherical particles with diameters in the order of 2 to 6 nm. Ferrihydrite is poorly crystallized. Even though it is poorly crystallized, Carlson and Schwertmann (1981) report that it can be detected with XRD.

2.5.4 Schwertmannite ($Fe_8O_8(OH)_6SO_4$)

Schwertmannite is a new mineral that only recently has been approved by the Commission on New Minerals and Mineral Names. Schwertmannite seems to be the most common mineral associated with acid sulfate waters. Favorable conditions for its formation are pH values less than 4. The ferrous in these systems must be oxidized by the assistance of microorganisms called *Thiobacillus ferroxydans*. It requires the

presence of high sulfate concentrations greater than 1000 mg/L. Its color is bright

yellow, and probably accounts for the term "yellow boy" that is commonly used by

miners. Schwertmannite is very poorly crystallized (Bigham, 1994).

2.5.5 Jarosite ($KFe_3(OH)_6(SO4)_2$)

Jarosite is a common mineral in acid, high-sulfate waters. It appearance is usually

straw colored with Munsell hues in the 2.5 YR range. Jarosite is often credited as an

important phase in fresh precipitates from acidic surface waters carrying AMD. Jarosite

is usually well crystallized and easily identified from its characteristic XRD pattern.

2.5.6 Role of Bacteria in AMD precipitates

The biggest player in AMD for microorganisms is the *Thiobacillus ferrooxidans*.

There is clear evidence that the bacteria can indirectly catalyze subsequent decomposition

reactions by oxidizing ferrous whenever the pH of the water drops below 4.5. Rapid

oxidation under acidic conditions is related to the fact that the activity of ferric becomes

significant at low pH values, so that ferric replaces oxygen as the primary oxidant

(Bigham, 1994).

T. ferrooxidans have been thought to accelerate the formation of precipitates

associated with AMD by catalyzing the oxidation of iron (Colmer and Hinkle, 1947).

Iron-encrusted bacterial remains have been isolated from AMD sediments (Milnes et al.,

1992). However, it is unlikely that the type of mineral produced is controlled by the

physiology of the organism. The oxidation of iron is biologically induced, and the rate of

oxidation is under metabolic control, but the mineralization process itself is extracellular (Lowesnstam and Weiner, 1989). In other words, the geochemical parameters such as pH, $[SO_4^{2-}]$, and $[HCO_3^-]$ determine the mineralogical fate of iron once it is oxidized either by microorganisms or abiotic mechanisms (Bigham, 1994).

2.5.7 Proton Activity

AMD is usually assumed to be acidic. However, the pH of the mine drainage may range from less than 2 to as high as 8.5 depending on the stage of reactions and geological setting (Mills, 1985). Bigham et al, (1992) studied a variety of AMD sites with pH values in the range of 2.7 to 7.8. They found that goethite occurred over the full range of pH values, but it was the primary component in only two places, both of which had a pH > 6. Slightly acidic pH conditions favored the formation of ferrihydrite. The most acidic pH ranges showed that jarosite formed mostly. Brown (1971) noted that the solution pH should not raise above 3 if jarosite is to be the most stable phase. Schwertmannite was the most common mineral identified by Bigham et al., (1992). It was present in more that 60% of the specimens analyzed from a pH of under 3 to pH > 6. It was most abundant in pH values of 3 to 4.

2.5.8 Dissolve Sulfate

Sulfate is the most common anion in AMD, and it is reasonable to expect the activity of sulfate to plan a major role in mineral speciation. Jarosite is easily synthesized from acid solutions containing excess sulfate and suitable concentrations of metal cations

by using both abiotic and biotic approaches (Brown, 1970). It is not clear what level of sulfate is needed for the formation of jarosite in field conditions, however jarosite was only detected in AMD streams when the sulfate concentration exceeded 3000 mg/L (Bigham et al., 1992).

Currently no thermodynamic data exist for schwertmannite, but field and laboratory experiments show the sulfate concentrations in the range of 1000 to 3000 mg/L are optimal for its formation with the proper pH condition (Bigham, 1994). Several laboratory studies have also shown sulfate to enhance the formation of goethite over other iron oxyhydroxides even though sulfate is not a structural component of this mineral (Dousma et al., 1979). Bigham et al. (1992) found that under field conditions ferrihydrite seems to be insensitive to sulfate concentrations, however once ferrihydrite is formed, it seems to transform rapidly to goethite in the presence of sulfate.

2.5.9 Dissolve Carbonate

Most alkaline mine drainage if found is mining districts with abundant limestone or dolomite in the rock column, and the water is usually charged with dissolved carbonate. Ferrihydrate and goethite appear to be the normal oxidation products of alkaline mine drainage. Field and laboratory examples show that goethite formation is enhanced over lepidocrocite when ferrous solutions are oxidized in the presence of bicarbonate (Schwertmann and Fitzpatrick, 1977).

2.5.10 Model for Mineral Formation in AMD

Bigham et al., (1992) created a model that can be seen in figure 2-3. This model is based on the field observations and physical data collected. It has a strong kinetic bias with little considerations of solubility controls and other important thermodynamic data (Bigham, 1994).

The proposed model show ferrous and sulfate being released to the solution through bacterially catalyzed decomposition of iron sulfides. The model is incomplete with respect to lepidocrocite. The conditions favoring its precipitation are unclear (Bigham, 1994).
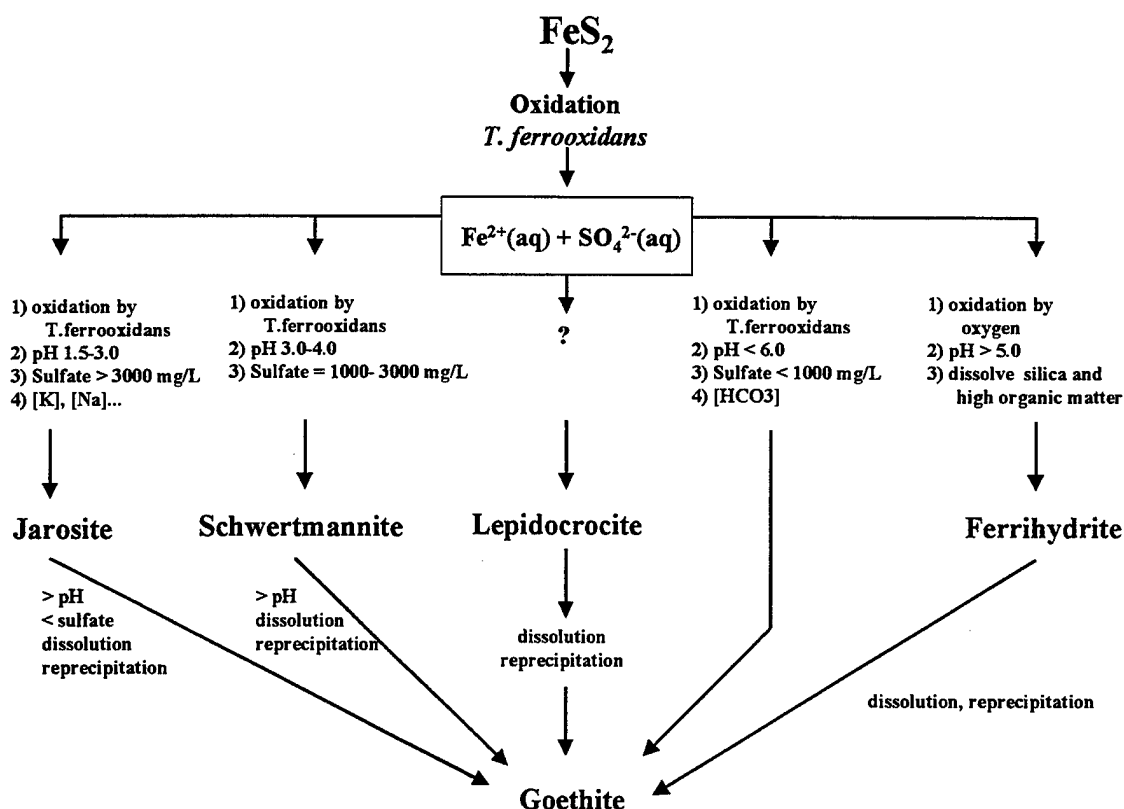
Figure 2-3: Biochemical model for the precipitation of various minerals occurring in mine drainage (Modified from Bigham et al., 1992).

2.6 Ion Adsorption onto Ferric Oxide

Iron hydrous oxide can sorb a host of chemical species. It is one of the dominant sorbents in nature because of its tendency to be finely dispersed and to coat other particles. Experimental data on sorption has been described by various empirical means, including partition coefficients, isotherm equations, and conditional equilibrium sorption constants. Sorption of inorganic ions onto iron hydrous oxides is also strongly dependent on solution pH, ionic strength, and presence of competing ions (Dzombak, and Morel, 1990).

It is important to note that there are many models that try to explain the ion adsorption onto a surface. For the purpose of this research, the diffuse layer model (or two-layer model) proposed by Stumm and co-workers will be used. In this model, the oxide/water interface is considered to comprise of two layers of charge: a surface layer and a diffuse layer of counterions in solution. All specifically sorbed ions are assigned to one surface layer, and all nonspecifically sorbed counterions are assigned to the diffuse layer (Dzombak, and Morel, 1990). This concept of the oxide/water interface incorporated in the diffuse layer model is seen in figure 2-4.

$$\sigma = \frac{F}{AS} [(\equiv XOH_2^+) + (\equiv XOM^+) - (\equiv XO^-) - (\equiv XA^-)]$$

$$\sigma + \sigma_d = 0$$
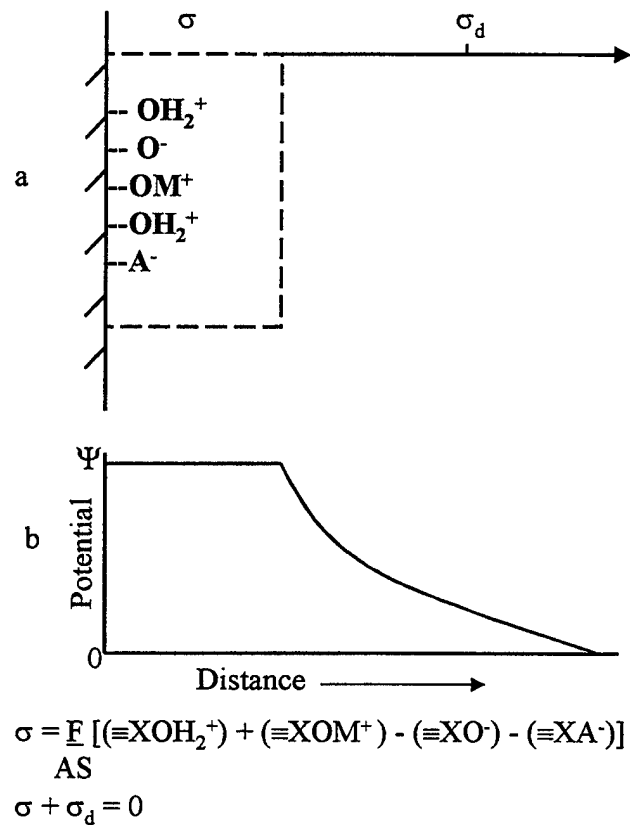
Figure 2-4: (a) Schematic representation of ion binding on an oxide surface. This conceptualization is used in the diffuse layer surface complexation model. (b) Potential decay in the diffuse layer. A is specific surface area (m^2/g); S is solid concentration (g/L); F is Faraday constant (96,485 C/mol) (Dzombak and Morel, 1990).

2.6.1 Cation Adsorption

Surface complexation of cations by hydrous oxides involves the formation of bonds with surface oxygen atoms and the release of protons from the surface. For example,

$$\equiv XOH^0 + M^{2+} \rightarrow \equiv XOM^+ + H^+ \qquad K_M^{app} \qquad (2.12)$$

or, equivalently,

$$\equiv XOH^0 + M^{2+} + H_2O \rightarrow \equiv XMOH_2^+ + H^+ \quad K_M^{app} \qquad (2.13)$$
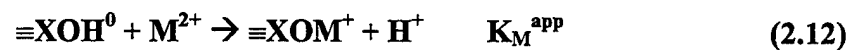
where M^{2+} represents the divalent cation (Dzombak and Morel, 1990).

A strong pH dependence is observed because the reactive surface sites are hydroxyl groups that can coordinate and dissociate protons. As pH is increased, cation sorption on hydrous oxides also increases.

Cations sorb onto oxide surfaces in response to both chemical and coulombic forces. Long range electrostatic effects due to the surface charge on the oxides can be taken into account explicitly by inclusion of a coulombic term in the mass law expression for sorption reactions:

$$K_M^{int} = K_M^{app} \exp(\Delta ZF\Psi/RT) \qquad (2.14)$$

Where K_M^{int} and K_M^{app} are apparent and intrinsic equilibrium constants for sorption of a hypothetical cation M^{2+}. Where ΔZ is the net change in the charge number of the surface species and Ψ is the surface potential. The role of the coulombic effect on cation sorption has been questioned because of the very small effect on ionic strength on cation sorptions that is observed experimentally (Dzombak and Morel, 1990).

For the purpose of this study, cations that are most commonly found in AMD were looked at. These include Ca^{2+}, Mg^{2+} and Fe^{2+}. Experimental data and assumptions

from Dzombak and Morel (1990) were used for these cations as they sorb onto ferric

oxide can be found in chapter 4, section 4.1.4.

2.6.2 Anion Adsorption

Anion sorption of anions on hydrous oxides occurs via a ligand exchange reaction

in which hydroxyl surface groups are replaced by the sorbing ions (Dzombak and Morel,

1990). Anion sorption can be described with the reaction such as

$$\equiv XOH^0 + A^{3-} + H^+ \rightarrow \equiv XA^{2-} + H_2O \qquad K_{1A}^{app} \qquad (2.15)$$

and/or

$$\equiv XOH^0 + A^{3-} + 2H^+ \rightarrow \equiv XHA^- + H_2O \qquad K_{2A}^{app} \qquad (2.16)$$
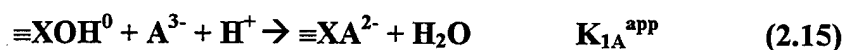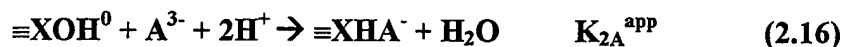
where A^{3-} is a hypothetical trivalent anion. Once again we see that pH will have an

impact to the sorption of the anion to the surface. Changes in pH in the degree of

protonation of anions sorbed on surfaces seem to parallel their degree of protonation in

solution with current experimental data (Dzombak and Morel, 1990).

The electrostatic field near charged oxide surfaces affects the sorption of anions in

the same way it influences proton exchange. The effect of nonspecific electrostatic

interactions on anion sorption is taken explicitly into account by separation of a

coulombic term from the apparent sorption constant; that is

$$K_A{}^{int} = K_A{}^{app} \exp (\Delta ZF\Psi/RT) \qquad\qquad (2.17)$$

Where $K_A{}^{int}$ and $K_A{}^{app}$ are apparent and intrinsic equilibrium constants for sorption of a hypothetical anion A^{z-} (Dzombak and Morel, 1990).

For the purpose of this study, the anion sulfate was investigated. Information concerning the sorption of this anion onto the surface of ferric oxide is shown in greater detail in chapter 4, section 4.4.3.

2.6.3 MINTEQ A2 Computer Program

MINTEQA2 is a geochemical equilibrium speciation model capable of computing equilibria among the dissolved, adsorbed, solid, and gas phases in an environmental setting. MINTEQA2 includes an extensive database of reliable thermodynamic data that is also accessible to PRODEFA2, an interactive program designed to be executed prior to MINTEQA2 for the purpose of creating the required input file (Allison, 1991).

This model was used to predict the speciation and adsorption of cations and anions for the local chemistry of the HB and CK systems. This data is further explained in chapter 4.

Chapter 3

METHODS

3.1 Sample Handling and Data Collection

The first thing done when arriving to either the HB or CK passive treatment systems was equipment calibration (pH and Dissolve Oxygen meters) and the measurement of the air temperature. Sample collection always started at the end of the system (final effluent) and progressed up to the beginning (influent). Water samples were collected during every trip at the indicated sites shown by the numerals on figures 1-1 and 1-2. There were 6 sampling sites for HB and 4 sampling sites for CK. At each sampling site a 200 mL acidified sample was taken for future analysis for metals. A 60 mL Total Inorganic Carbon (TIC) sample was also collected at this time for future analysis, but no acid was added. These two types of samples were immediately put on ice. The pH, Dissolved Oxygen (DO) and water temperature were then taken using the proper equipment. Field titrations for alkalinity and total iron were also performed but not at all the indicated sites. A list of the dates and sampling sites tested for the field titrations can be found in Appendix A. The last thing completed when leaving the passive treatment system was a flow measurement. For CK it was measured at the influent. HB required two flow measurements, and will be explained further in section 3.1.8.

3.1.1   Metal Samples

Samples for metal analysis were collected in a 200 mL wide mouth plastic bottle. These bottles were new and had not been used prior. Prior to collecting the water sample, 0.5 mL of 0.89 Normal H_2SO_4 acid was placed in the bottle with a clean plastic calibrated

dropper. This amount of acid was tested and calculated to sufficiently lower the pH of the water entering the bottle to below a pH of 2. Keeping the pH below 2 significantly slowed the oxidation process of ferrous and kept the other metal ions in solution free from forming any precipitate. The bottle was marked with a marker and placed in a cooler with ice. Once the sample was transported to the lab, it was placed in the refrigerator that was kept around 4° C. The sample was stored here until needed for future analysis. The storage time was usually no longer that 96 hours.

3.1.2   Total Inorganic Carbon Samples

Samples for TIC analysis were collected using a 60 cc plastic syringe. When taking the sample, the tip of the syringe was placed under the water. Water was drawn in. This water was swirled around in the syringe and discharged so that no air was left in the syringe. The tip was again placed under the water and the sample was drawn slowly ensuring that no air entered the syringe. This was done to prevent the loss of CO_2, which would cause the calculated alkalinity to be lower than the true value. The cap to the syringe was applied and the sample was marked with a marker. It was immediately placed in the cooler of ice. Once the sample was transported back to the lab it was placed in the refrigerator that was kept around 4° C. The sample was stored here until needed for future analysis. The storage time was no longer than 48 hours.

3.1.3   Sulfate Samples

Sulfate samples were collected the same manner as the TIC, using the same 60 cc syringe and procedures.

3.1.4 Core Samples

Core samples were collected using 1 ¼ inch PVC pipe and black 1 ¼ inch rubber

stoppers. Waidders were used to enter the water where the sample was taken. The PVC pipe

was cut to the proper length prior to the sampling trip. Once in the water, the PVC pipe was

inserted into the sediment until its end reached the clay bottom. Enough pressure was applied

to fully push the pipe into the clay bottom to plug that end. At this time the top of the pipe

would be submerged under the surface of the water, but not yet into the sediments. A rubber

stopper was inserted into the top of the pipe ensuring that no air was trapped in the pipe. The

pipe was removed from the sediments ensuring that no sediment material lost from the

bottom. The bottom of the pipe was inspected to see that it was indeed plugged with the clay

and a stopper was then inserted. The pipe was placed upright in a bucket and transported to

the cold room that was kept around 10°C. The core samples remained in the pipe no longer

than 96 hours before being removed for analysis.

The core samples were removed from the pipe in the lab. Clean plastic sheets were

laid out on the table. The top of the pipe was unplugged and drained of all its water. The

bottom was unplugged and the pipe was placed horizontal on the plastic sheet. The core

sample was then forced through the pipe with a metal push rod ejector that was the same size

as the inside diameter of the pipe. Once the core sample was on the sheet, a clean knife was

used to cut the sample in three places (Top, Middle and Bottom). After each cut the knife

was cleaned. Samples taken from the core were from the inner part of the core that did not

touch the pipe or the sheet. This sample was placed in a clean uncontaminated plastic 60 mL

wide mouth bottle. The bottle was capped and immediately place on ice. Samples were then

transported to the Material Resource Laboratory (MRL) building for analysis on the X-ray diffraction machine.

3.1.5 pH

The pH was measured using the VWR Scientific 2000 hand held pH meter equipped with a VWR Scientific combination pH-Temperature probe (no 34105-032). The meter was calibrated using Fisher Scientific standards pH 4 and 7 buffers. After each calibration the meter would indicate the current slope reading for the machine. The slope reading was always above 98 and below 101, indicating that it was working properly. Calibration of the meter occurred prior to measuring the pH at each passive treatment system. The probe was then placed directly in the water for measurement of the pH. The probe was placed in an acidic solution moving from sampling site to sampling site. This was to ensure that precipitation of the sample water did not occur around the frit, which could cause it to clog.

3.1.6 Dissolved Oxygen

The DO was measured using the YSI model 54a DO meter and model 5750 DO probe. The instrument was calibrated by placing the probe in a small bottle that was half filled with deionized water. After measuring the temperature, the meter was set to read the oxygen saturation level in the 100% relative humidity atmosphere. The calibration of the DO meter occurred prior to using it for measurements on each of the two systems. The probe performance at low DO was verified periodically by measuring the DO in a sulfite solution. The probe membrane was checked and changed regularly using the YSI replacement membranes.

3.1.7 Temperature

The water temperature was measured using the VWR Scientific 2000 hand held pH meter equipped with a VWR Scientific combination pH-Temperature probe (no 34105-032). The temperature probe was periodically check against a thermometer in the lab. The probe was placed directly in the water for measurement of the temperature.

3.1.8 Flow

Flow was measured using a 5 gallon plastic bucket. The bucket was marked on the inside with a water-proof marker in one liter increments. The bucket was placed under the influent flow and timed with a stopwatch. This was repeated 3 times and an average was taken for liters per second. At Howe Bridge, the flow had to be measured twice. Once at the front end of the system, and once at the place where the water enters pond #2. The reason for this is the second influent pipe to Howe Bridge is submerged in pond #1 (figure 1-1). The influent flow was then subtracted from the flow at pond #2 to get the second submerged influent flow.

3.1.9 TIC with bisulfide

This was done once to check for microbial activity that may be occurring in the samples prior to analysis. Acid washed volumetric 100 mL flasks were used for the sample collection. The flasks were placed under the water at the sampling sites and left there for approximately 3 hours. The samples were then injected with Na_2SO_3 (bisulfide) while still under the water and immediately capped and placed in a cooler of ice. The bisulfide reacted with the oxygen in the sample by the following reaction:

$$Na_2SO_3 + 1/2\ O_2 \rightarrow Na_2SO_4 \qquad\qquad (3.1)$$

The proper sulfide requirement was calculated using the stoichiometric relationship and the measured DO at the site, with approximately 10-20% extra. When the samples were returned back to the lab and analyzed, they were also checked for DO content, and in all cases, the DO level was below 0.2 mg/L.

3.2 Analytical Techniques

3.2.1 Field Alkalinity Titration

The titration was performed using the HACH digital titrator, model 16900-01. A 100 mL sample was taken using a graduated cylinder. The cylinder was flushed three times with the sample water prior to collecting the sample for titrating. A 1.6 Normal H_2SO_4 titration cartridge was placed on the titrator and zeroed. The 100 mL sample was transferred to a flushed 250 mL Erlenmeyer flask. One bromocresol green–methyl red indicator packet was added to the flask and swirled to mix. The titrator delivery tube was placed below the surface of the sample and the dispensing knob was turned until the color changed to light pink, indicating the pH end point of 4.5. The alkalinity calculation in mg/L was the number of digits used in the titration. This method was checked against a standard solution of sodium carbonate made up in the lab and came within 1% of the value of the standard solution.

3.2.2 Field Iron Titration

The titration was performed using the HACH digital titrator, model 16900-01. A 20 mL sample was taken using a graduated cylinder. The cylinder was flushed three times with the sample prior to collecting the sample for titrating. A 0.0716 Molar TitraVer standard solution titration cartridge was placed on the titrator and zeroed. The 20 mL sample was diluted to 50 mL with deionized water. It was transferred to the flushed 150 mL erlenmeyer flask. One citrate buffer packet was added and swirled to mix. This was used to buffer the solution. Then one sodium periodate packet was added, swirled to mix. Sodium periodate oxidizes the ferrous to ferric. Lastly, one sulfosalicylic acid packet was added, swirled to mix. When sulfosalicylic acid is present, the ferric iron forms a red complex. The titrator delivery tube was placed below the surface of the sample and the dispensing knob was turned until the color changed from red to pale yellow. The total iron calculation in mg/L was the number of digits used multiplied by 0.25.

3.2.3 UV-Vis Spectrophotometry

The Shimadzu digital double-beam spectrophotometer UV-210A was used along with the 1,10 phenanathroline colormetric technique to determine the amount of ferrous iron in a sample. The method used is described in Standard Methods (1989), section 3500 Fe-D.

Standardization was done by titrating a solution of ferrous against a solution of prepared standard grade $K_2Cr_2O_7$ to a red-brown ferroin end point. This technique is commonly used to determine ferrous in chemical oxygen demand experiments, as described in Standard Methods (1989) sections 5220-B and 5220-C.

A concentrated stock standard of ferrous was prepared by dissolving 24.5 g of ferrous ammonium sulfate in deionized water, adding 5 mL of concentrated H_2SO_4 and diluting to 250 mL. A primary standard solution of $K_2Cr_2O_7$ was prepared by drying a small amount at 120^0C for about 12 hrs, cooling in a desiccator. Then dissolving 3 g of it in a 250 mL volumetric flask with deionized water. The standard titration was carried out at one tenth scale of the procedure recommended by Standard Methods (1998). One mL of $K_2Cr_2O_7$ standard was pipetted into a small acid washed beaker, 9 mL of DI water and 5 mL of concentrated H_2SO_4 were then added to the beaker. The beaker was then cooled in a water bath. One drop of ferroin indicator was added to the beaker and the contents of the beaker were then titrated with the ferrous ammonium sulfate solution (Ames, 1998). The titration reaction is as follows:

$$Cr_2O_7^{2-} + 6Fe^{2+} + 14H^+ \rightarrow 2\ Cr^{3+} + 6\ Fe^{3+} + 7H_2O \qquad (3.2)$$
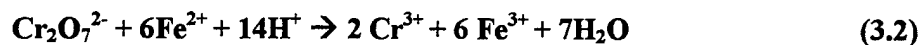
Knowing the stoichiometry, the true concentration of ferrous in the ferrous ammonium sulfate solution can be calculated. The standardization titration was done three times and an average was used for the true concentration. Dilutions of this concentration were made and then used for the standards for the 1,10 phenanthroline determination of ferrous (Ames, 1998).

The samples and standards were made using 100 mL volumetric flask. The appropriate amount of standard was added using the solution in the above paragraph. Four standards were made ranging from zero to below 4mg/L ferrous. The samples were made by pipetting 1 mL of sample from the acidified stored samples into the flasks. Then 10 mL of

ammonium acetate-acetic acid buffer was pipetted into the flasks, followed by 10 mL of 1,10 phenanthroline solution. The flask was then filled to the 100 mL mark with DI water and mixed thoroughly (Ames, 1998).

A standard curve was developed by preparing a series of samples as described above from four standards of the diluted FAS solution. The absorbance was measured by the spectrophotmeter at a wavelength of 510 um within 15 minutes of the samples being prepared. During the measurements, a standard was measured every 5 readings to ensure the standard curve did not shift during the experiment.

3.2.4 Total Inorganic Carbon Analyzer

The TIC was measured on the Dormann Carbon Analyzer. Inorganic carbon (Carbonate) is converted to $H_2CO_3^*$, which is stripped out of the solution as CO_2 by the nitrogen carrier gas in the reaction vessel. It is then detected by the non-dispersive IR detector (NDIR).

The instrument was standardized against dried sodium carbonate (Na_2CO_3). A 100 ppm (as C) solution of Na_2CO_3 was prepared the day of the experiment. A series of different volumes of the standard were injected into the machine, and a calibration curve was developed plotting the amount of carbon injected against the instrument reading (Ames, 1998).

The TIC samples were removed from the refrigerator. The sample for the machine was drawn out of the 60 cc syringe with a gas tight 1 mL syringe and injected into the machine. The appropriate reading for each of the samples was recorded and plotted against

the standard curve. During the experiment, a standard was injected every 5 readings to confirm that the standard curve did not shift during the experiment.

3.2.5 Atomic Absorption Spectrometry

Metal concentrations were measured using atomic absorption spectrometry (AA) using the Perkin Elmer model 3030-B spectrometer. The instrument settings suggested by the pre-programmed analytical methods were used for all analyses. The metals analyzed for this study were calcium, magnesium, manganese and iron. The setting outlined by the machines manual can be seen in table 3-1.

Table 3-1: Standard atomic absorption conditions for calcium, magnesium, manganese and iron.

Metal	Wavelength (nm)	Slit (nm)	Relative noise	Sensitivity (mg/L)	Sensitivity Check (mg/L)	Linear Range (mg/L)*
Calcium	422.7	0.7	1.0	0.092	4.0	5.0
Magnesium	285.2	0.7	1.0	0.0078	0.30	0.5
Manganese	279.5	0.2	1.0	0.052	2.5	2.0
Iron	248.3	0.2	1.0	0.10	5.0	5.0

Note: The Linear range is from zero to the value reported in the column.

The machine was set to take five readings with a 5 second read time and a 0.5 second delay between readings. The standard solutions were used and plotted against their respective readings from the machine to make the calibration curve. Standards were prepared by pipetting from a 1000 ppm standard AA solution from Fisher Chemicals for each metal. Standards for each metal were made in accordance with the linear range for that metal reported in the above table. The appropriate volume was added to the volumetric flask with a micropipeter. Samples were prepared from the stored acidified samples in the refrigerator.

One mL from each sample was pipetted from the sample and into a 100 mL volumetric flask. One mL of HNO₃ was added to the standards and samples to keep the pH below 2. The flasks were then filled to the water mark with DI water. Samples were aspirated directly from the volumetric flasks. The instrument zero and standard curve were checked every five samples with the blank and a standard.

After a few analyses, it was noted that the total iron being reported from the AA analysis was less than the ferrous being reported through the UV-Vis spectrophotometry. This did not make sense. An investigation showed that the iron analysis for the AA was being affected negatively by the calcium sulfate and magnesium sulfate in the AMD chemistry. To correct this problem, a standard addition was performed. The appropriate amount of calcium sulfate and magnesium sulfate was added to each of the standards for their respective system (HB and CK) and analyzed. It was assumed that the calcium sulfate and magnesium sulfate concentrations were constant throughout the passive treatment system. This is not entirely correct, and as a result the total iron reported for the system will have error to it depending on the difference between the concentration of the metal sulfate salts in the samples solution to the standard solution.

3.2.6   Total Organic Carbon Analyzer

Total Organic Carbon (TOC) was checked only once to confirm what was already suspected, that the water at both sites contained low amounts of TOC in the abiotic areas. TOC concentrations were determined by the Total Organic Carbon Analyzer, Model TOC-5000A from Shimadzu. Its operation is based on the combustion/non-dispersive infrared gas analysis method widely employed for TOC measurement. Kirk Novak, Ph.D. candidate was

responsible for setting up, calibration and the operation of the machine. Samples were prepared from the acidified samples taken for the metals analysis.

3.2.7   X-ray Diffraction

Core samples were analyzed using the Scintag X2 Advanced Diffraction System with a Peltier detector. Radiation used was $CuK\alpha$. Generator settings were set at 45 KV – 40 mA. The machine utilizes a theta – theta goniometer. Software for this machine was the Scintag DMSNT (Data Management System Software for Microsoft Windows NT, version 1.34). The XRD data printouts had no background corrections made to it. Peaks were found using the peak finding program using the digital filter setting. The operator for the machine was Tanya Baker.

Core samples were brought to the MRL building in 60 mL plastic bottles and on ice. The samples were exposed to the atmosphere for approximately 30-120 minutes prior to being placed on the machine. Samples were taken from the bottles and placed on the sampling tray for the machine with a metal scoop. The machine was set to do a slow scan with a range of 17.00-44.00 ($^\circ 2\theta$), with a step size of 0.020 Deg/min. It is noted that the samples when taken out of the core were an olive green color. While placing the core sample on the machine tray and during the analysis, the sample turned from the olive green color to a bright orange red color.

3.2.8   Ion Chromatograph

Sulfate concentrations were measured using the Dionex DX 500 high performance liquid chromatography system. The IONPAC AS11 Analytical column (P/N 044076) was

used in conjunction with the machine. The eluent used was 10 mM NaOH, and was made by Brian Jackobson, the machine operator. Prior to running the machine for sulfate, a test was done with other major anions that may be in the AMD chemistry. Samples with 5 mg/L of HCO_3^-, PO_4^{3-}, Cl^- and SO_4^{2-} were tested on the machine to find what time each of the anions peaked for IONPAC column. It was determined that the sulfate peak occurred around 2.05 minutes.

Standards were made with a primary standard of Na_2SO_4. A 1.479 g of Na_2SO_4 was weighed and put in a 1000 mL volumetric flask and topped off with DI water. This made a 1000 ppm solution of sulfate. The standards used for the calibration curve for the machine were taken from this standard. The standards made were 5, 10, 15 and 20 mg/L of sulfate. When operating the machine, one set the standards were placed in the auto-sampler to be read first. Next, came the field samples, and the last 4 samples, again were the standards. This was done to confirm the calibrations curve.

The field samples were taken from the TIC samples in the refrigerator. One mL of each sample was pipetted into a 100 mL volumetric flask and topped off with DI water. These were placed in the auto-sampler between the standards.

3.2.9 Bulk Analysis, Core sample

The core sample for the bulk analysis was prepared the same as the core samples for the XRD (section 3.1.4). The sample was taken to the MRL building where Scott Atkinson performed a microwave digestion in 7 mL of HCl, 2 mL HF and 1mL HNO_3. The cations were then analyzed using Direct Current Plasma (DCP) spectrometer. The Anions were analyzed using the ion chromatograph. A core sample was weighed and placed in a 105°C

oven with a vacuum. It was then weighed again then placed in an 1000°C oven were Loss on

Ignition (LOI) was performed. The results of this analysis can be found in Appendix L.

3.2.10 Bulk Analysis, Water sample

The bulk analysis water samples were filtered. They were filtered using the Antlia,

pneumatic hand pump system from Schleicher and Schnell. The metal analysis sample was

acidified after filtering using 0.89 N H_2SO_4 acid to ensure the pH was below 2. The sample

was put in a clean 200 mL wide mouth bottle, marked and put on ice. Once back in the lab it

was stored in the refrigerator, until it was moved to the MRL building for analysis by Scott

Atkinson.

The anion sample was also filtered using the same device mentioned above. It was

placed in a 200 mL wide mouth plastic bottle, but no acid was added. It followed the same

path of the metal sample to Scott Atkinson. For cation analysis the DCP was used. The

anions entailed using the ion chromatograph. The results of this analysis can be found in

Appendix L.

3.3 Quality Assurance and Control

3.3.1 Atomic Absorption

As previous mentioned, during the operation of the AA machine, a standard solution

was tested every four to five sample readings. This standard solution was usually the one

that was most closely the same value as the AMD samples. This was done in order to ensure

that the calibration curve had not shifted during the experiment. One of the checks for the 6

July 1998 experiment can be seen in figures 3-1 and 3-2.

Standard (mg/L)	Absorbance Reading
0	0.000
1	0.061
2	0.116
3	0.163

$y = 18.321x - 0.0573$

$R^2 = 0.9967$
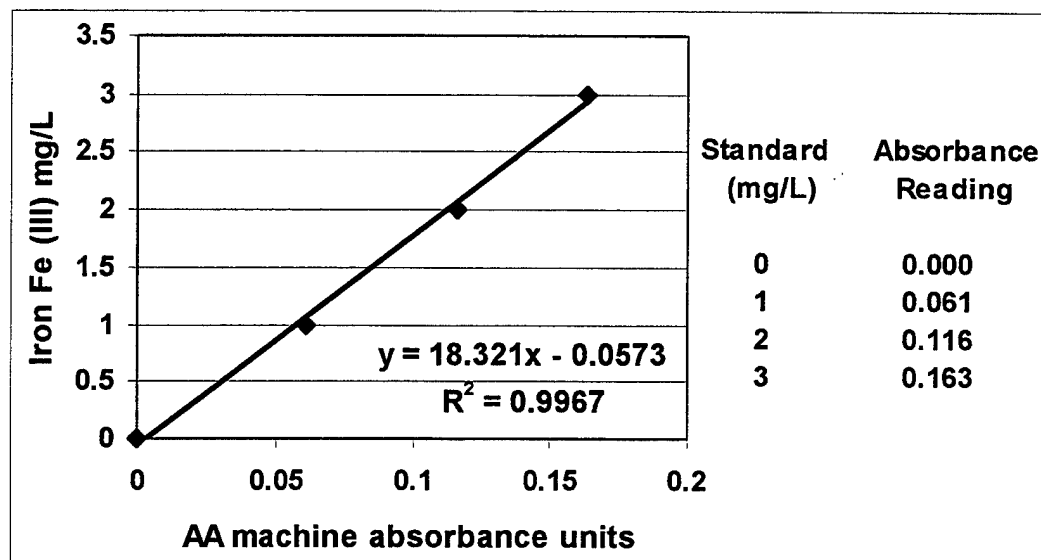
Figure 3-1: Total iron calibration curve for the HB 6 July 1998 experiment.

2 mg/L standard
formula corrected
value (2.068)

Sample	Reading	Formula Correction
QC #1	0.114	2.031
QC #2	0.116	2.068
QC #3	0.116	2.068
QC #4	0.115	2.049
Std Dev.	0.0009	0.0175
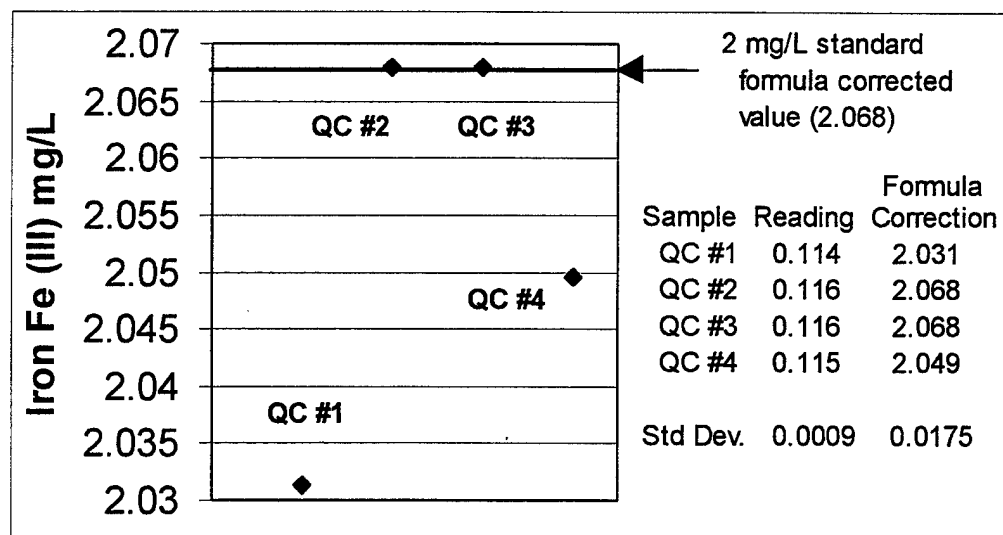
Figure 3-2: Quality Control of the AA for the HB 6 July 1998. The standard checked was the 2 mg/L standard.

Note: The 2 mg/L standard had an adsorbance reading of 0.116. When this value is entered into the linear regression formula, it gives a corrected value of 2.068 mg/L.

The calibration curve had an R^2 value of 0.9967 indicating a good fit for the initial standard readings. It must be noted that a R^2 value of 0.9999 is sought for to reduce the error in the analysis. The linear regression was performed by the Microsoft Excel spreadsheet. The 2 mg/L sample had an AA absorbance reading of 0.116 units. Two of the four Quality Control (QC) checks matched this reading with the other two being slightly lower. The standard deviation for the absorbance units was 0.0009 units. It can be implied from this data that the standard curve can be used for the evaluation of the data. The other experiments in which this QC was conducted on the AA machine can be found in Appendix C.

3.3.2   UV-Vis Spectrophotometry

QC checks were also performed on the UV-Vis Spectrophotometry experiment. This entailed reading a given standard, (standard which was closest in value to the AMD sample readings) every 4-5 readings during the experiment. This was done to ensure that the calibration curve created by the machine readings in the beginning had not shifted during the experiment. An example of one of these checks performed on 17 August 1998 can be seen in figures 3-3 and 3-4.

Standard (mg/L)	Absorbance Units
0	0.096
0.923	0.293
1.859	0.512
3.718	0.899

$y = 4.6108x - 0.4482$
$R^2 = 0.9995$
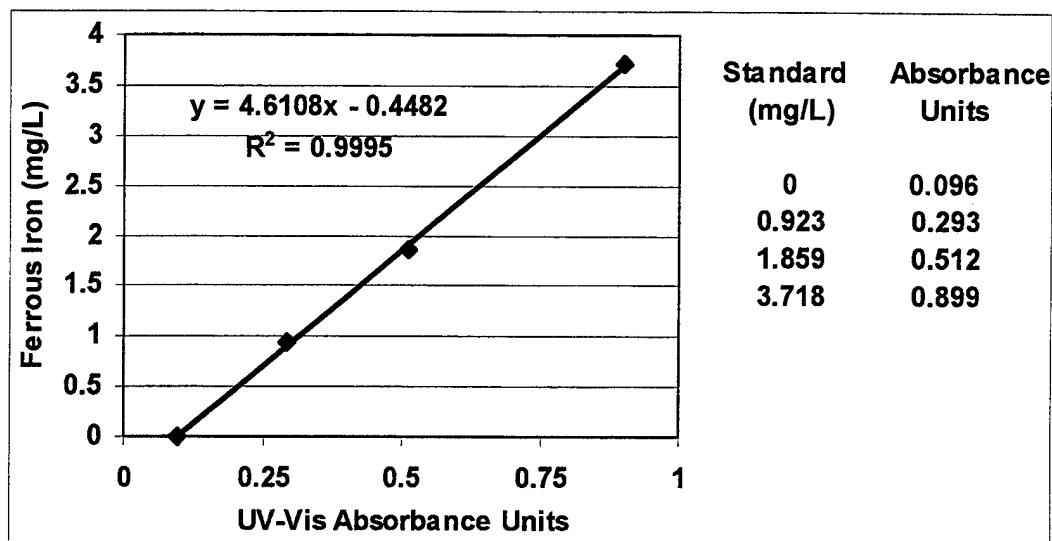
Figure 3-3: Ferrous concentration calibration curve on the UV-Vis for 17 August 1998 experiment.

Sample	Abs Units	Corrected
QC #1	0.513	191.71
QC #2	0.511	190.79
QC #3	0.510	190.33
OC #4	0.514	192.17
QC #5	0.512	191.25
QC #6	0.515	192.63
Std Dev	0.002	0.863

standard 1.859 mg/L value corrected (191.2)
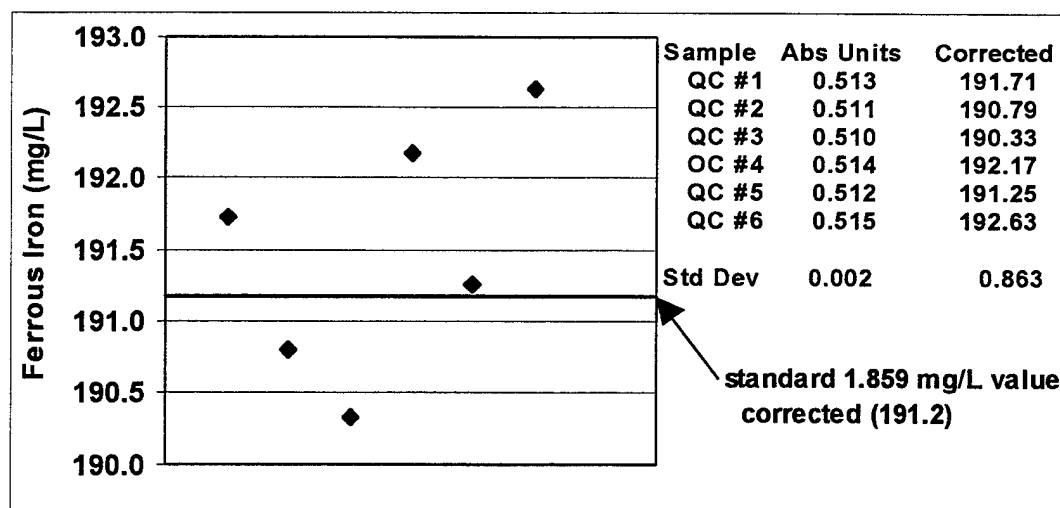
Figure 3-4: QC check for the 1.859 mg/L standard for ferrous concentration for the UV-Vis on 17 August 1998.

The R^2 value in figure 3-3 indicates a good fit for the line. The standard used for this test was the 1.859 mg/L ferrous standard. The machine reported an absorbance value of

0.512 which when corrected with the linear regression formula came to 191.25 mg/L. Of the six QC samples, 4 readings were above the expected line, while two were below. There is no indication from this check that the machine has shifted. The standard deviation is also small. Thus, this calibration curve was used to calculate the ferrous concentration for this day. The rest of the UV-Vis QC checks for other days can be found in Appendix D.

3.3.3 Total Inorganic Carbon

The QC checks for the TIC machine were done similar to the AA and UV-Vis experiments. A standard was injected into the machine once every 5 readings. Once again, this was to check the calibration curve created at the beginning of operating the machine had not shifted. An example of this can be seen in figures 3-5 and 3-6.
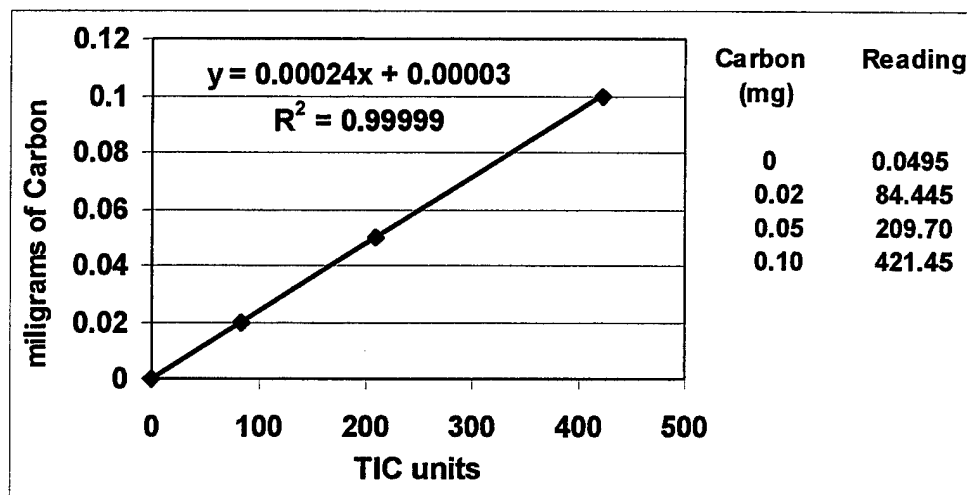
Figure 3-5: Calibration curve for TIC samples on 25 Oct. 1998.

Sample	Reading	Correction
QC#1	209.8	0.0503
QC#2	209.0	0.0501
QC#3	210.2	0.0504
QC#4	209.5	0.0502
QC#5	210.4	0.0504
Std Dev.	0.558	0.0001

Standard value (0.0502)
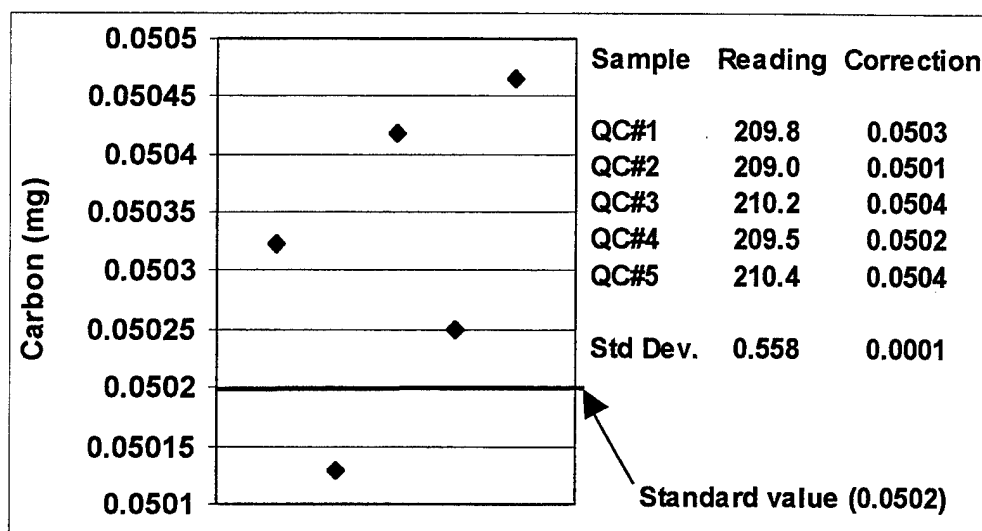
Figure 3-6: QC check for TIC calibration curve samples for the 25 October experiment.

The R^2 value (0.99) was very good for this calibration curve. The standard used for the check was the 0.05 mg of C. When corrected with the linear regression formula it obtained a value of 0.0502 mg of C. Three of the five reading fell above this expected value, while two fell below. The standard deviation is quite small for these corrected values. This calibration curve was used. In appendix E, the rest of the QC checks for TIC can be located.

3.3.4 Field Iron

The field iron titration done in the field was compared with the total iron done on the AA machine in the laboratory and ferrous concentrations on the UV-Vis machine. The AA values for total iron have some error already in the value. This was explained in section 3.2.5. Titrations were done to ensure that the values obtained on the AA and UV-Vis were close. The total iron at the influent should be very close to actual ferrous concentration at that location. The reason for this is when building an ALD, ferric concentrations must be

kept small to ensure that the ferric does not precipitate out in the drain and cause armoring of the limestone. Also at pH values above 4 ferric concentrations are less than 0.1 mg/L (Watzlaff and Hyman, 1995). Below in figure 3-7 shows the field iron titration values against what the UV-Vis and AA machine in the laboratory reported.

The field titration value was subtracted by the lab value. In a perfect world, the values should be the same and result in a value of zero. The mean value for this data was 3.93 mg/L. This value is expected since the assumptions used for the lab values did not take into account the ferric concentrations when using the UV-Vis at the influent readings, which would cause the value to be above zero. Also it is hard to say what impact the error for the AA machine using a constant standard addition for each system would be for this value.

3.3.5 Field Alkalinity

Field alkalinity was performed similarly to the field iron. Field alkalinity values in mg/L were compared to the values obtained by the TIC machine. The lab value was subtracted from the field value. A value of zero would result in a perfect match, however, this was not the case. Figure 3-8 shows this comparison.

The mean value is around 12 mg/L higher than the expected value of zero. This was not expected. In order to verify the experimental procedures, redundancy was the focus for the next sampling trip. On the 5 August sampling trip, 5 readings each for the HB system at Influent to Pond#2 (IP2), Effluent to Pond #2 (EP2), and 5 readings each for CK system at Bend #1 (B1), and Bend #2 (B2) were done for the field alkalinity. Five TIC samples were also taken at each of the same sites and brought back to the lab for analysis. The mean values and standard deviations for these samples can be seen in table 3-2.
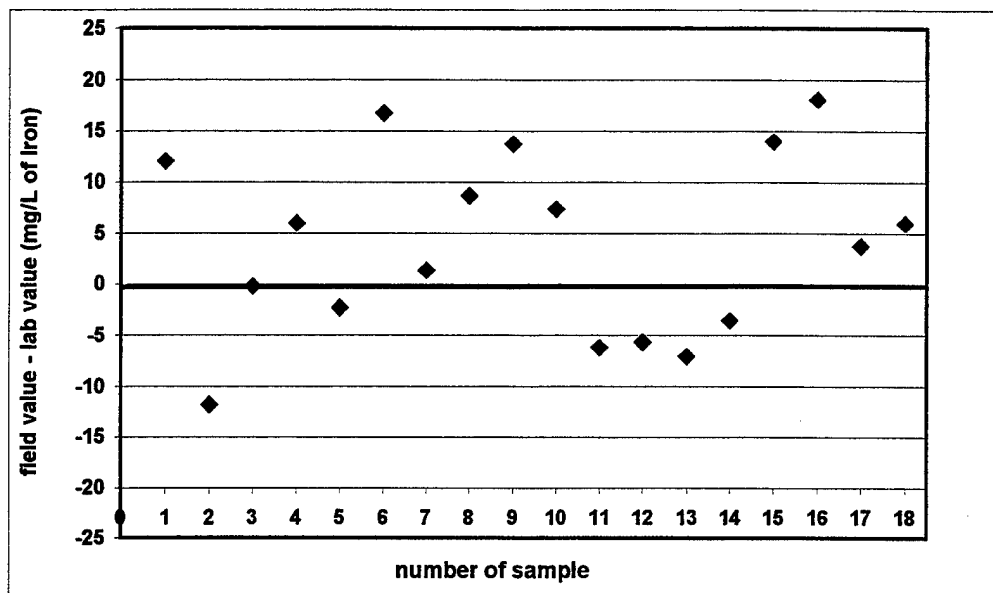
Sample Number	fld value (mg/L)	lab value (mg/L)	fld - lab (mg/L)	Location
1	278	266	12	HB 1 Mar at Pipe
2	92.5	104.3	-11.8	CK 1 Mar at Pipe
3	9.2	9.4	-0.2	CK 1 Mar at FE
4	100	94	6	CK 29 Mar at Pipe
5	0	2.3	-2.3	CK 29 Mar at FE
6	274	257.25	16.75	HB 29 Mar At Pipe
7	2	0.65	1.35	CK 13 May at FE
8	110	101.3	8.7	CK 6 Jun at pipe
9	270	256.3	13.7	HB 3 July at Pipe
10	260	252.6	7.4	HB 3 July at IP1
11	95	101.23	-6.23	CK 3 July at pipe
12	30	35.7	-5.7	CK 3 July at B3
13	251	258.1	-7.1	HB 5 Aug at pipe
14	249	252.6	-3.6	HB 5 Aug IP1
15	265	251	14	HB 26 Aug at Pipe
16	265	246.9	18.1	HB 26 Sep at pipe
17	92	88.2	3.8	CK 26 Aug at pipe
18	250	244	6	HB 24 Oct @ pipe
	Std Dev.	8.927113		
	Mean:	3.937222		

Figure 3-7: QA of total iron field titration and lab results.

Sample Number	fld value (mg/L)	lab value (mg/L)	fld - lab (mg/L)	Location
1	155	145	10	HB 6 Jun at Pipe
2	270	255	15	CK 6 Jun at Pipe
3	270	267	3	CK 3 July at pipe
4	270	276	-6	CK 3 July at B1
5	180	140	40	CK 3 July at B3
6	150	144	6	HB 3 July at Pipe
7	140	133	7	HB 3 July at IP1
8	80	47	33	HB 3 July at EP2
9	300	309	-9	CK 6 Aug at pipe
10	284	292	-8	CK 5 Aug at B1
11	182	183	-1	CK 5 Aug at B2
12	152	140	12	CK 5 Aug at B3
13	155	148	7	HB 5 Aug at pipe
14	149	148	1	HB 5 Aug IP1
15	140	100	40	HB 5 Aug EP1
16	137	107	30	HB 5 Aug IP2
17	42	33	9	HB 5 Aug EP2
18	299	288	11	CK 26 Aug B1
19	160	142	18	CK 26 Aug B2
20	139	137	2	CK 26 Aug B3
21	290	283	7	CK 26 Sep B1
22	180	165	15	CK 26 Sep B2
23	170	175	-5	CK 26 Sep B3
24	155	157	-2	HB 26 Aug at Pipe
25	136	111	25	HB 26 Aug EP1
26	132	111	21	HB 26 Aug IP2
27	74	63	21	HB 26 Aug EP2
28	148	121	27	HB 26 Sep at Pipe
29	144	126	18	HB 26 Sep IP1
30	126	121	5	HB 26 Sep EP1
31	128	109	19	HB 26 Sep IP2
32	58	48	10	HB 26 Sep EP2
33	140	138	2	HB 24 Oct @pipe
34	135	105	30	HB 24 Oct EP1
35	118	97	21	HB 24 Oct IP2
36	40	23	17	HB 24 Oct EP2
37	300	311	-11	CK 24 Oct @ Pipe
38	250	221	29	CK 24 Oct B1
39	180	160	20	CK 24 Oct B2
40	170	171	-1	CK 24 Oct B3
		Std Dev:	13.3	
		Mean:	12.2	

Figure 3-8: QA of alkalinity for field titrations and lab results.

The standard deviation for all of the experiments is low, indicating a good degree of precision when conducting the experiment. When looking at these four sites and calculating the field values minus the lab values you get a mean value of 7.5 mg/L above the expected zero line. The possible reasons for why the field value is larger than the lab value is explained in further detail in chapter 4.

Table 3-2: Redundancy check for alkalinity values (mg/L) for the 5 August trip.

	Field IP2	Field EP2	Field B1	Field B2	TIC IP2	TIC EP2	TIC B1	TIC B2
Read # 1	136	41	286	184	107.1	32.0	290.4	182.3
Read #2	138	42	288	180	108.3	32.7	291.7	183.3
Read #3	135	42	280	181	106.7	35.9	291.9	178.4
Read #4	137	43	281	181	107.9	33.8	293.4	186.8
Read #5	138	42	283	185	104.9	32.9	294.2	184.5
Std Dev:	1.3	0.7	3.4	2.2	1.3	1.5	1.5	3.1
Mean:	136.8	42.0	283.6	182.2	106.98	33.46	292.32	183.06

3.4 Manipulation of Data

3.4.1 Corrections for Temperature

The equilibrium constants K for $H_2CO_3^*$, $FeHCO_3^+$, $MgHCO_3^+$, $MnHCO_3^+$, $CaHCO_3^+$ and water needed to be corrected for temperature. The Van't Hoff equation (3.3) was used to make the correction.

$$\ln K_{(T2)} = \ln K_{(T1)} - \frac{\Delta H_{rxn}}{R} \left(\frac{1}{T_2} - \frac{1}{T_1} \right) \qquad (3.3)$$

Where $\ln K_{(T2)}$ is the Equilibrium constant at temperature T_2

$\ln K_{(T1)}$ is the Equilibrium constant at temperature T_1

R is the gas constant 1.99×10^{-3} kcal/mol

ΔH_{rxn} is the enthalpy of reaction

The values for the equilibrium constant K for the mentioned above species for 25^0C are listed in table 3-3.

Table 3-3: Log K equilibrium constants at 25^0C for bicarbonate species.

Species	Log K (MHL/M*HL)
$FeHCO_3^+$	1.10
$MgHCO_3^+$	1.07
$MnHCO_3^+$	1.00
$CaHCO_3^+$	1.27
$H_2CO_3^*$	-6.35
HCO_3^-	-10.33

3.4.2 Corrections for ionic strength

The ionic strength was calculated using equation 3.4:

$$\mu = \frac{1}{2} \sum (C_i Z_i^2) \tag{3.4}$$

Where C_i is the concentration of ionic species i

             Z_i is the charge of species i.

The values for C_i were determined from the analysis of the water chemistry at the two passive treatment systems. Once the ionic strength was determined, the activity of the specific species could be found using the Güntelberg approximation (3.5) of the Debye-Hückel theory.

$$-\log \gamma_i = \frac{0.5 Z_i^2 \mu^{\frac{1}{2}}}{1 + \mu^{\frac{1}{2}}} \qquad (3.5)$$

The corrected value for the equilibrium constant K was then calculated using equation (3.6).

$$\text{Log K'} = \text{Log (K/}\gamma) \qquad (3.6)$$

The use of these equations can be seen in the next section, corrections for carbonate speciation and calculation of alkalinity.

3.4.3 Corrections for Carbonate Speciation

The computer program MINTEQA2 was run given the water chemistry concentrations and environmental conditions found at each of the passive treatment sites. The program calculated that approximately 10% of the HCO_3^- was being bound in the $MHCO_3^+$ species. The metal bicarbonate species are listed in table 3-3 with their respective K values. This caused a different approach in calculating the alkalinity for the systems. The old method of calculating alkalinity was using the Hederson Hasselback equation (3.7).

$$pH = pKa + \log ([HCO_3^-]/[H_2CO_3]) \qquad (3.7)$$

The TIC was measured for each sample in order to determine the alkalinity of the solution. The TIC reading was assumed to be the total concentration (C_T) for the inorganic carbon in the solution. The new method used to calculate alkalinity is equation (3.8).

$$Alk = (\alpha_1 + 2\alpha_2 + \alpha_3 + \alpha_4 + \alpha_5)C_T + K_w/[H^+] - 10^{-pH}/\gamma_{H^+} \qquad (3.8)$$

Where

C_T is the total inorganic carbon concentration in mol/L

K_w is the temperature and ionic strength corrected equilibrium constant for water

γ_{H^+} is the activity of $[H^+]$

$\alpha_1 = 1/[HCO_3^-]([H^+]/K_{a1} + 1 + K_{a2}/[H^+] + K_3[Fe^{2+}] + K_4[Mg^{2+}] + K_5[Mn^{2+}] + K_6[Ca^{2+}]$

$2\alpha_2 = 1/[CO_3^{-2}]([H^+]^2/K_{a1}K_{a2} + [H+]/K_{a2} + 1 + K_3[Fe^{2+}][H^+] + K_4[Mg^{2+}][H^+] +$

$\qquad K_5[Mn^{2+}][H^+] + K_6[Ca^{2+}][H^+])$

$\alpha_3 = 1/[FeHCO_3^+]([H^+]/K_{a1}K_3[Fe^{2+}] + 1/K_3[Fe^{2+}] + K_{a2}/K_3[H^+][Fe^{2+}] +$

$\qquad K_4[Mg^{2+}]/K_3[Fe^{2+}] + K_5[Mn^{2+}]/K_3[Fe^{2+}] + K_6[Ca^{2+}]/K_3[Fe^{2+}])$

α_4, α_5, and α_6 are similar to α_3, just replace the values for $FeHCO_3^+$

$\qquad$ with the other $MHCO_3^+$ in question

Where

K_{a1} is the temperature and ionic strength corrected equilibrium constant for H_2CO_3

K_{a2} is the temperature and ionic strength corrected equilibrium constant for HCO_3^-

K_3 is the temperature and ionic strength corrected equilibrium constant for $FeHCO_3^+$

K_4 is the temperature and ionic strength corrected equilibrium constant for $MgHCO_3^+$

K_5 is the temperature and ionic strength corrected equilibrium constant for $MnHCO_3^+$

K_6 is the temperature and ionic strength corrected equilibrium constant for $CaHCO_3^+$

In equation (3.8), the α values represent the percentage of TIC (C_T) made up by each species in solution. This equation offers a more exact way to calculate alkalinity knowing

where the bicarbonate species is bound. This method of calculating the alkalinity did narrow

the gap between the values being reported in the field titrations and those done

experimentally in the lab. The mean value of 12.2 mg/L difference reported in section 3.3.6

is the result of using this equation. Prior to using this equation, and using the Hederson

Hasselbach method a mean value of around 20 mg/L was the difference. However, there is

still a discrepancy and this will be discussed in chapter four.

Chapter 4

RESULTS AND DISCUSSION

4.1 Metals Concentrations

4.1.1 MINTEQA2 Predictions

In Appendices F and G are MINTEQA2 results for the initial conditions for HB pond #2 and CK at pipe run for a pH of 6. The major cation and anion concentrations from the field samples collected at the sites and analyzed on the lab equipment were used to create the input file to run the computer program. The following tables are a summary of the results for the computer model. It must be noted that in this case, adsorption of the cations onto the surface of ferric oxide was not looked at. Cation adsorption will be discussed later in this chapter.

Table 4-1: CK initial conditions at the pipe (Influent). The pH for these results is 6.0. No precipitation was allowed. MINTEQA2 reads distributions of species up to 1%, if smaller, it does not report.

Major Cation or Anion	Initial Conditions (mg/L)	Percent Distribution of Dissolved Species (No precipitation)
Fe^{2+}	100	78.2 % bound as Fe^{2+}
		21.8 % bound as $FeSO_4$
Fe^{3+}	2*	98.8 % bound as $FeOH_2^+$
Ca^{2+}	300	72.9 % bound as Ca^{2+}
		26.6 % bound as $CaSO_4$
Mg^{2+}	200	75.2 % bound as Mg^{2+}
		24.1 % bound as $MgSO_4$
Mn^{2+}	40	75.7 % bound as Mn^{2+}
		23.4 % bound as $MnSO_4$
SO_4^{-2}	1300	67.6 % bound as SO_4^{-2}
		14.2 % bound as $MgSO_4$
		14.3 % bound as $CaSO_4$
		2.8 % bound as $FeSO_4$
		1.2 % bound as $MnSO_4$
CO_3^{-2}	180	60.3 % bound as H_2CO_3
		37.7 % bound as HCO_3^-
		1.2 % bound as $MgHCO_3^+$

*Note: Initially there is very little ferric that comes out of the drain at CK. This number was picked to simulate the oxidation of ferrous to ferric in order to see what out put the computer program would give.

Table 4-2: Saturation indices and chemical formulas for supersaturated species for the CK initial conditions at the pipe. The pH for these results is 6.0.

Name	Sat. Index	Chemical Formula
Ferrihydrite	2.235	$Fe_5OH_8\text{-}4H_2O$
$Fe_3(OH)_8$	2.839	$Fe_3(OH)_8$
Goethite	6.141	$FeOOH$
Hematite	17.228	Fe_2O_3
Jarosite	2.916	$KFe_3(SO_4)_2(OH)_6$
Maghemite	7.865	Fe_2O_3
Magnetite	17.639	$FeO\text{-}Fe_2O_3$
Mag-Ferrite	4.716	$MgFe_2O_4$
Lepidocrocite	5.754	$FeOOH$

Table 4-3: HB Pond #2 conditions. The pH for these results is 6.0.
No precipitation was allowed. MINTEQA2 reads distributions of species up to
1%, if smaller, it does not report.

Major Cation or Anion	Initial Conditions (mg/L)	Percent Distribution of Dissolved Species (No precipitation)
Fe^{2+}	158	75.4 % bound as Fe^{2+}
		24.6 % bound as $FeSO_4$
Fe^{3+}	25*	98.7 % bound as $FeOH_2^+$
Ca^{2+}	225	70.7 % bound as Ca^{2+}
		29.3 % bound as $CaSO_4$
Mg^{2+}	140	73.3 % bound as Mg^{2+}
		26.6 % bound as $MgSO_4$
Mn^{2+}	40	73.8 % bound as Mn^{2+}
		26.2 % bound as $MnSO_4$
SO_4^{-2}	1200	70.6 % bound as SO_4^{-2}
		11.4 % bound as $MgSO_4$
		11.7 % bound as $CaSO_4$
		5.0 % bound as $FeSO_4$
		1.4 % bound as $MnSO_4$
CO_3^{-2}	25	61.6 % bound as H_2CO_3
		36.8 % bound as HCO_3^-

* Note: This number was chosen to represent the amount of ferrous going to ferric for the detention time of the pond.

Table 4-4: Saturation indices and chemical formulas for HB Pond #2 conditions for supersaturated species. The pH for these results is 6.0.

Name	Sat. Index	Chemical Formula
Ferrihydrite	3.662	$Fe_5OH_8 \cdot 4H_2O$
$Fe_3(OH)_8$	5.890	$Fe_3(OH)_8$
Goethite	7.685	$FeOOH$
Hematite	20.330	Fe_2O_3
Jarosite	7.701	$KFe_3(SO_4)_2(OH)_6$
Maghemite	10.721	Fe_2O_3
Magnetite	21.092	$FeO \cdot Fe_2O_3$
Mag-Ferrite	7.967	$MgFe_2O_4$
Lepidocrocite	7.182	$FeOOH$

Tables 4-2 and 4-4 for both sites indicates that ferric iron would be the major metal removed in the system. There is a possibility for the removal of magnesium with mag-ferrite and ferrous iron with magnetite. The formation of these precipitates is unlikely because of the more stable phase for ferric oxide precipitation under these conditions would be ferrihydrite, lepidocrocite, goethite and hematite.

The thermodynamic phase relations in the Fe_2O_3-H_2O system is complicated by a large number of metastable phases with similar solubility. Hematite and goethite solubilities and stabilities are so close that grain size and surface Gibbs free energy have an important influence on the phase stability. With regard for to coarse-grained minerals, goethite appears to be stable relative to hematite (Langmuir, 1969). Both goethite and hematite have slow growth kinetics at surficial temperatures, so the initial solid products from the hydrolysis of ferric are poorly crystalline, metastable phases such as ferrihydrite (Chukhrov et al., 1973) or microcrystalline goethite (Alpers et al., 1994).

Ferrihydrite has been shown to be the precursor to hematite, to which transforms by solid-state dehydration reaction (Schwertmann, 1985). When this transformation takes place in the presence of water, there is a competing tendency for ferrihydrite to dissolve back into solution and for the ferric iron to precipitate as fine-grained goethite. Schwertmann and Murad (1983) showed that ferrihydrite aged in solutions with a wide spectrum of pH values and showed a wide variation in terms of proportions of hematite and goethite. Hematite formed around pH values of 8. Goethite formed below 6 and above 11 (Alpers, et al., 1994).

Dissolved ions also play an important role in determining goethite and hematite formation. The presence of calcium and magnesium in solution has been found to favor the precipitation of hematite rather than goethite under certain conditions (Alpers, et al., 1994). The presence of copper can catalyze the oxidation of ferrous to ferric (Thornber, 1985), leading to the precipitation of ferrihydrite, then onto hematite.

During the formation of these stable phases, ferric iron is being removed from the system. At the same time, ferrous iron is being oxidized to ferric reducing its overall concentration in the system. As more ferric is produced, it reacts rapidly with water forming these stable phases and precipitating out of the system. The cycle will continue until all of the ferrous is gone, or the pH drops low enough to significantly slow the oxidation reaction of ferrous to ferric, and keeping more dissolved ferric iron in solution. If the pH drops low enough, biotic oxidation can take over.

4.1.2 Field Observations

The major cations in the HB and CK system are ferrous, magnesium, calcium and manganese. These four cations will be the focus for metal concentrations for the two systems. The following tables and figures are from the 24 October 1998 sampling trip. The concentrations of the metals were obtained from analysis on the AA spectrometer and UV-Vis spectrometer. These metal concentrations for the other sampling trips can be found in Appendix B. Over the one-year period of sampling, the concentration of each metal did not change significantly and remained relatively the same value.

Table 4-5: CK system, analysis of metals for 24 October 1998 trip with a flow of 12 gpm.

Metal	At Pipe (mg/L)	Bend #1 (mg/L)	Bend #2 (mg/L)	Bend #3 (mg/L)
Fe2+	82.7	60.9	0.4	<0.02
Ca2+	337.5	321.5	321.5	*ND
Mg2+	173.5	176.6	175.0	*ND
Mn2+	48.22	44.9	44.3	*ND

*ND: Not Done
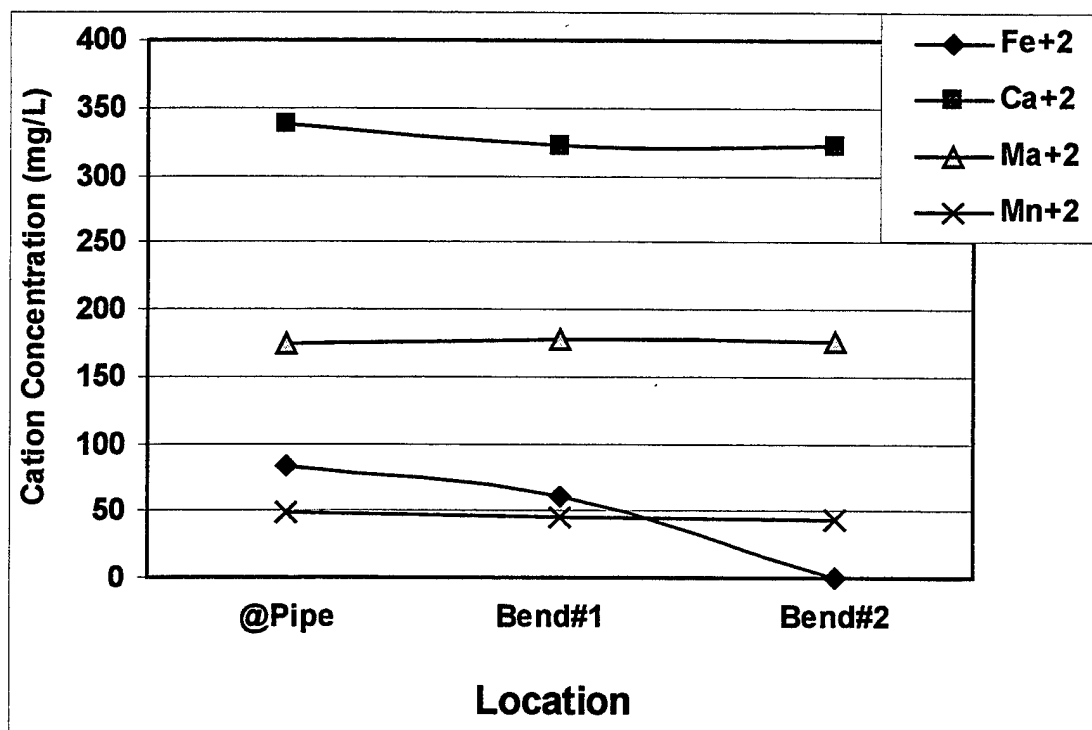
Figure 4-1: Major metal concentrations through the CK system for the 24 October 1998 sampling trip.

Table 4-6: HB system, analysis of metals for 24 October 1998 trip with a flow of 36 gpm.

Metal	At Pipe (mg/L)	EP1 (mg/L)	IP2 (mg/L)	EP2 (mg/L)	FE (mg/L)
Fe2+	243.5	211.8	210.4	158.4	48.6
Ca2+	225	208.9	ND	208.9	192.8
Mg2+	110.5	111.9	ND	108.9	110.4
Mn2+	37.9	35.3	ND	35.9	35.3

*ND: Not Done
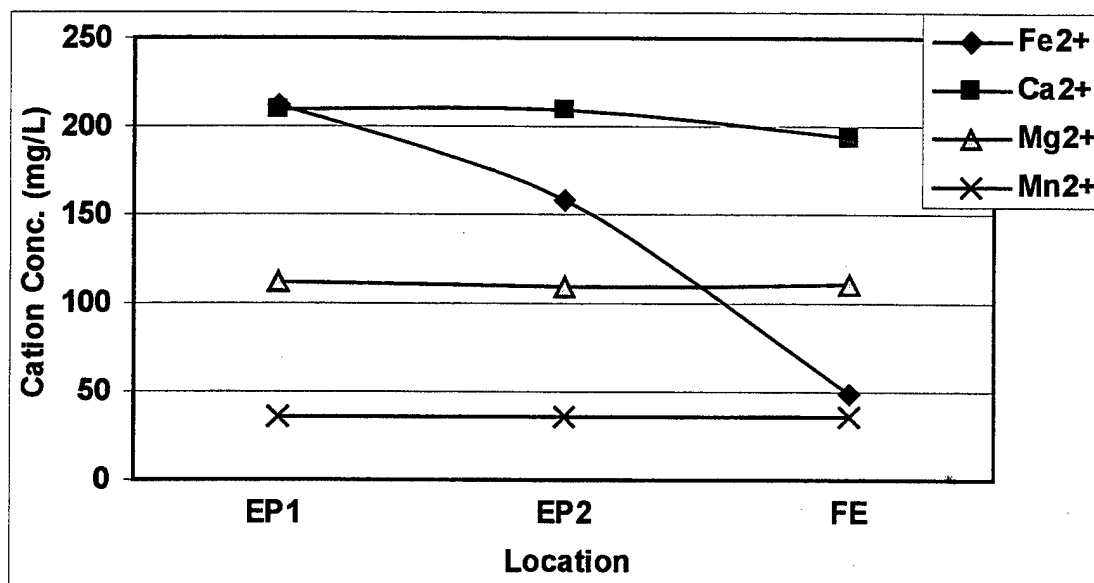
Figure 4-2: Metals concentration through HB system for the 24 October 1998 sampling trip.

It can be inferred from the above tables and figures that of the four major cations in the system, ferrous is the only metal that decreases with any degree of significance. The other metal cations seem to maintain their initial concentration, with some slight decreases. These small decreases will be discussed later in the cation adsorption section.

These observations are similar to Hedin et al., (1994) for the HB system in 1994. The ferrous loss in the system is primarily the result of oxidation to ferric, then precipitation. These observations also fall into line with what MINTEQA2 predicted for these systems. There is also some indication that ferrous and possibly the other metals in solution may be adsorbed onto the precipitating ferric oxide. This will be discussed in a following section.

4.1.3   Ferrous Oxidation and Precipitation

As previous mentioned in chapter 2, Singer and Stumm (1970) reported the following equation for the oxidation of ferrous to ferric above a pH of 4.5.

$$-d[Fe^{2+}]/dt = k_1[Fe^{2+}][O_2][OH^-]^2 \qquad (4.1)$$

where $k_1 = 8.0 \times 10^{13}$ liter^{2}mole^{-2}atm^{-1} at 25°C and is known as the homogeneous rate constant. Sung and Morgan (1980) stated that small amounts of ferric has a catalytic effect on the ferrous oxidation rate. This new rate equation has been called the heterogeneous rate equation and can be seen below.

$$-d[Fe^{2+}]/dt = (k_1 + k_2[Fe^{3+}][H^+])[Fe^{2+}][H^+]^{-2}P_{O2} \qquad (4-2)$$

The term heterogeneous refers to the interaction of liquid and solid phases when ferrous is oxidized on the surface of ferric solids. The catalytic effect of ferric is

significant in terms of improving the oxidation rate in passive treatment systems because ferric solids can be resuspended in the water by means of stirring or turbulence (Ames, 1998).

Ames (1998) reported that the heterogeneous process will dominate below pH values of 5, while the homogeneous process will dominate at pH values greater than 8. The pH ranges between 5 and 8 will be influenced by both processes, and the ferric concentration becomes an important factor.

Equations (4.1) and (4.2) can be rewritten in terms of $[H^+]$. The homogeneous equation will be:

$$-d[Fe^{2+}]/dt = k'_1[Fe^{2+}]DO/[H^-]^2 \qquad (4.3)$$

Where k_1' is the homogeneous rate constant in terms of [H+]. The heterogeneous equation can be written as equation (4.4).

$$-d[Fe^{2+}]/dt = (k_2DO[Fe^{3+}][Fe^{2+}]/[H^+] \qquad (4.4)$$

By combining equations (4.3) and (4.4), Ames (1998) was able to find a linear

relationship between k_1' and k_2. Equation (4.5) shows this relationship.

$$\frac{-d[Fe^{2+}]/dt\ [H^+]^2}{[Fe^{2+}]\ DO} = k_2[H^+][Fe^{3+}] + k_1' \qquad (4.5)$$

By plotting the field data obtained into equation (4.5), k_2 will be the slope and

k_1' the intercept of the line. The field data used for this analysis was from the CK system.

The HB system could not be used due to the second influent flow coming into Pond #1

and not having enough sample points to complete the analysis prior to pond #3. An

example of this procedure for the CK system can be seen in figure 4-3. The data for the

other trips can be found in Appendix K.

Location	Flow Time (Hours)	Ferrous (mg/L)	DO (mg/L)	Ferric (mg/L)	pH	d(fe)/dt mg/L-hr	d[Fe+2]/dt*[H]^2 [DO]*[Fe+2] M/sec
At Pipe	0	89.8	0	12.3	6.15	0	
Bend #2	2.5	64.5	8.5	19.1	6.16	10.12	6.72E-14
Bend #3	4.66	37.7	8.5	23.9	6.24	12.41	1.01E-13

Location	Converson to [OH] units 1/M^3 sec	AVE [H] mol	AVE[Fe+2] mg/L	AVE[Fe+3] mg/L	[H]*[Fe+3] M mg/L
At Pipe					
Bend #2	6.72E+14	7.00E-07	77.2	15.7	1.10E-05
Bend #3	1.01E+15	6.31E-07	51.1	21.5	1.36E-05
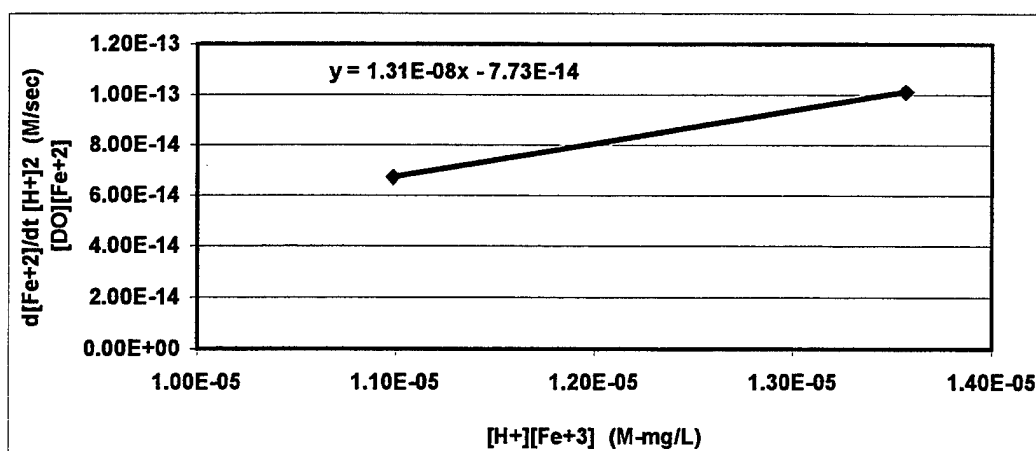
Figure 4-3: Linearized data for determination of k'$_1$ and k$_2$ for the 13 May sampling trip.

The k'$_1$ and k$_2$ rate constants obtained with the above procedure are shown in table 4-7 for the rest of the sampling trips.

Table 4-7: Oxidation rate constants for heterogeneous and homogeneous reactions for the CK system.

Date of Trip to CK Coal	Ave. Water Temp ^{0}C	k'$_1$ WRT [H$^+$] M/sec	k$_1$ WRT [OH$^-$] 1/M^3-sec	k$_2$ WRT [H$^+$] L/mg-sec
1 March 98	11.7	2.0E-15	2.0E+13	3.4E-09
29 March 98	16.9	1.1E-14	1.1E+14	4.6E-09
13 May 98	16.7	7.7E-14	7.7E+14	1.3E-08
6 June 98	17.6	1.8E-13	1.8E+15	6.8E-08
3 July 98	19.2	-4.4E-14	-4.4E+14	3.2E-09

These rate constants for the field were then compared to the rate constants of past researchers. This data can be seen in table 4-8, which came from Ames (1998).

Table 4-8 Comparison of rate constants with past research.

Researcher(s)	Temperature °C	k_1 (1/M³-sec)	k_2 (L/mg-sec)
Ames (1998)	19.3-23.5	9.3E+14	3.1E-08
Stumm and Lee (1961)	20.5	1.1E+15	
Morgan and Dirkner (1966)	25	2.7E+14	
Schenk and Weber (1968)	25	2.8E+14	
Theis (1972)	25	1.9E+15	
Kester et al., (1975)	(?)	1.3E+13	
Tamura et al., (1976)	25	2.0E+14	2.6E-08
Sung and Morgan (1980)	25	3.3E+13	2.6E-08
This study Average	**11.7-19.2**	**6.8E+14**	**2.2E-08**

Sources of error for this analysis primarily come from the calculation of ferric iron, which was discussed in a previous section. If this were a great source of error, it would have a dramatic effect on the equation since the heterogeneous rate is 1st order with respect to the ferric concentration. Other sources of error may include interference from anions. Stumm and Lee (1961) reported a decline in the oxidation rate in the presence of sulfate. The activity of sulfate is very high in the CK system, with a concentration around 1300 mg/L. These authors also noted a catalytic effect from copper. The concentration of copper is unknown for this system. Tamura (1976) reported that ferrous in the presence of silica may be oxidized more rapidly. It is difficult to control the concentrations of these catalytic or inhibitory ions in the field, but they

should be considered when designing and modeling a passive treatment system (Ames, 1998).

In table 4-7, the 3-July trip reported negative value for the homogeneous rate constant. This also was reported by Ames (1998). His explanation for this behavior was that if k_2 is very dominant, then little confidence can be placed on k'_1. What this means is that if the system is mostly heterogeneous, then the homogeneous rate constant will not be valid. The trip on 3 July was different than most trips. On this particular day, a stratification of the water was observed. The upper 3-4 inches of water was very turbid from B1 to B2. The lower 6 inches were clear and cool. The ferric concentration data reported for B1 on this day was very high, 45.2 mg/L ferric. This would indicate a strong shift to heterogeneous rate equation with this high activity of ferric.

Ames (1998) also came up with a formula to calculate the fraction of the overall rate due to the heterogeneous and homogeneous processes:

$$\text{Heterogeneous Fraction} = \frac{k_2\ [Fe(III)][H^+]}{k_1 + k_2\ [Fe(III)][H+]} \tag{4.6}$$

This formula was used to calculate the fraction of the oxidation processes for the CK system from the data used during the determination of the oxidation constants. Table 4-9 list the results of this analysis.

Table 4-9: Percent distribution of oxidation processes between heterogeneous and homogeneous rate constants for the CK system.

Date of Trip to CK	% k_1	% k_2
1 March 98	<1%	99%
29 March 98	<1%	99%
13 May 98	<1%	99%
6 June 98	<1%	99%
3 July 98	<1%	99%

The following figures show the concentration of ferrous versus time in each of the passive treatment systems. These figures also show the effect of temperature, and flow on the oxidation rate of ferrous.
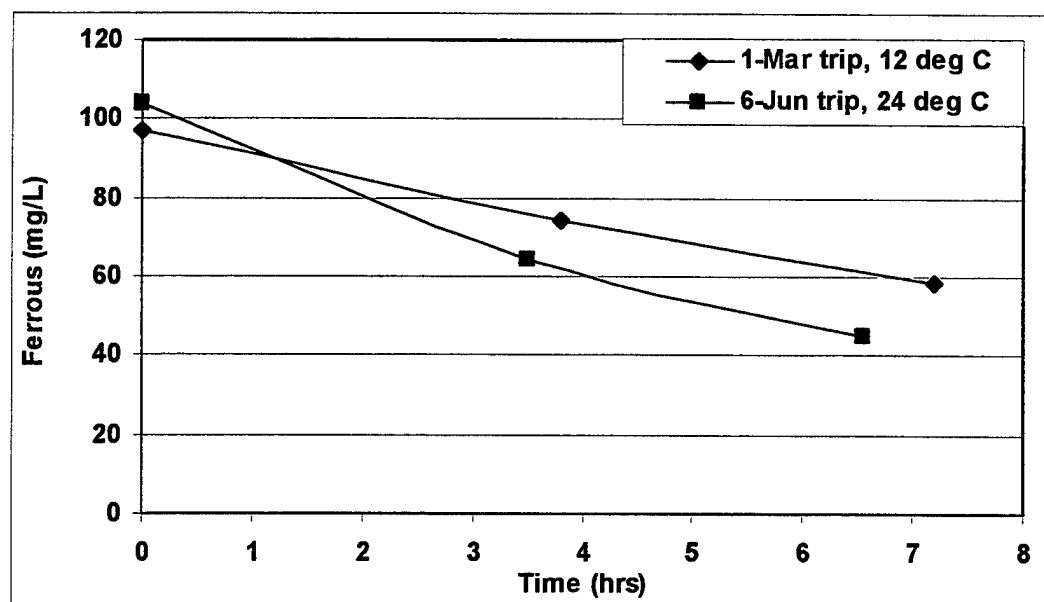
Figure 4-4: Effects of temperature on ferrous oxidation in the CK system. The standard deviation between the two flows is 8.4 gal/min.
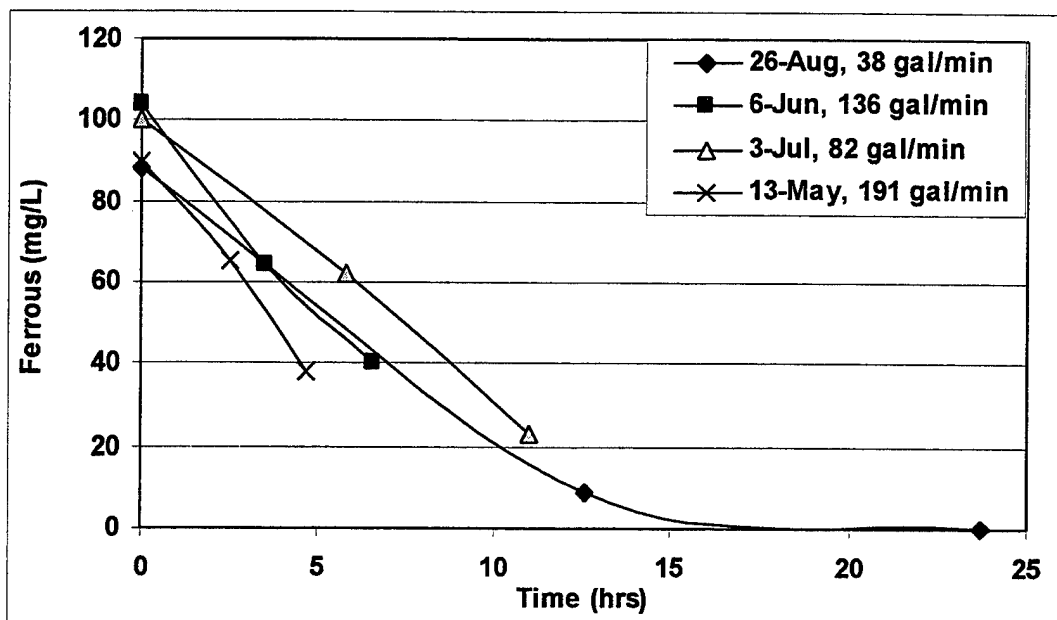
Figure 4-5: Effects of flow variation in the CK system for ferrous removal. The graph shows the time it took to get from the influent to bend #3. Temperature for the water between all four trips had a standard deviation of 1.7 degrees Celsius.
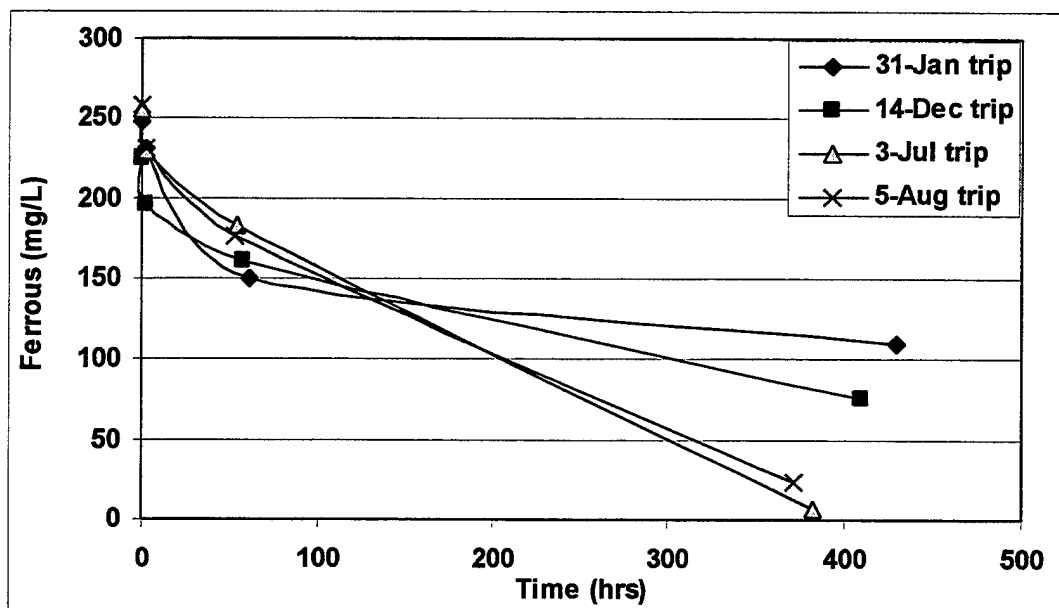
Figure 4-6: Comparison of ferrous concentration through the HB system at different periods of the year.
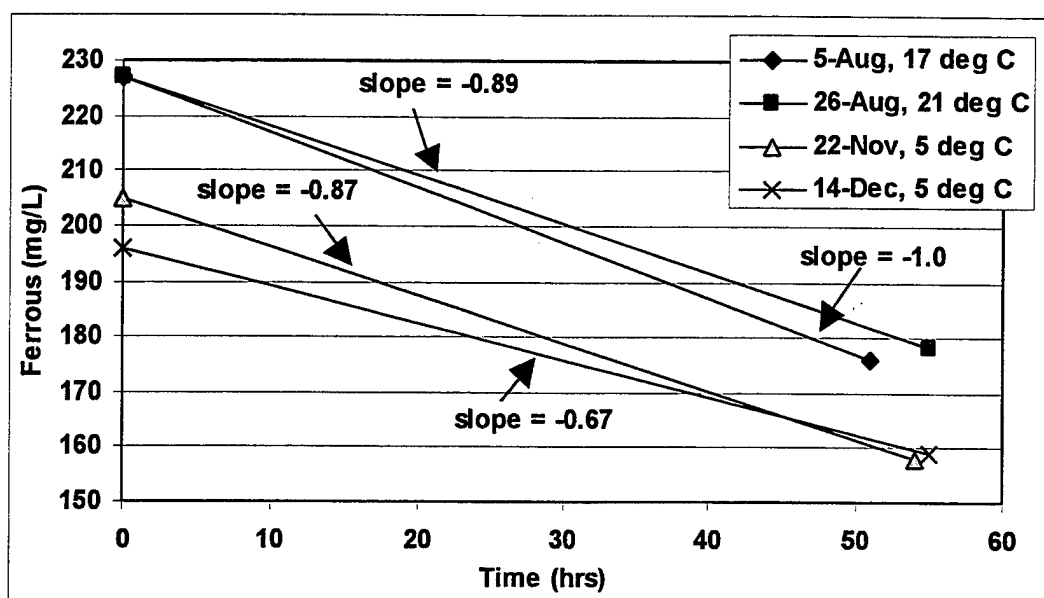
Figure 4-7: Ferrous concentration from influent of Pond #2 to the effluent of Pond #2. The two highest water temperatures dates were compared to the two lowest. Flows for the 4 dates have a standard deviation of 1.5 gal/min.

The effect of temperature in the field system can be seen in figures 4-4, 4-6 and 4-7. The effect of temperature on the rate was no surprise. For the CK system, the two dates shown in figure 4-4 are the closest in respect for equal flows and chemistry. The 1 March trip had a flow of 124 gal/min while the 6 June flow was 136 gal/min. The water was much colder on the March trip than on the June trip, which would suggest a increase in the ferrous oxidation rate for the June trip. This indeed was the case.

The effect of temperature for the HB system was also observed (figure 4-7). HB flow throughout the year changed very little. The two hottest flows and coldest flows were compared for ferrous removal. The results show a increase in ferrous oxidation for

the hottest water temperatures and decrease for the coldest. The rate is indicated by the slope on the figure.

The effect of increase flow/mixing is also shown in figure 4-5. The result of this analysis come as no surprise also. With increase mixing/flow, comes an increase in DO into the system and possible resuspension of ferric oxides which becomes a catalyst for the heterogeneous oxidation of ferrous. Four flows were picked with similar temperatures. The standard deviation of the temperature was 1.7 °C between the four flows. The two highest flows had the greatest slopes indicating a higher rate of oxidation.

Figure 4-6 shows 4 separate trips to the HB system over the year. What is important to note about this system is that the 3rd pond is biotic. The pH drops to below 3 in this pond and in the summer months the biological activity is responsible for the oxidization rate of the ferrous. During the winter, the temperature is to cold to support the biological activity, and the rate of ferrous removal slows significantly. This is evident is this figure.

4.1.4   Cation adsorption

Figures 4-1 and 4-2 show the metal cation's concentrations through each of the two passive treatment systems. As previously mention, ferrous is the main ion that decreases in each of the systems. There is an indication that some of the ferrous could be adsorbing onto the surface of the ferric oxide. The alkalinity decrease in the system is less than expected than the amount of ferrous that is being oxidized. This data will be shown in the alkalinity portion of this chapter. Dzombak and Morel (1990) looked at ion

adsorption in great detail, however, it seems that there has not been much work done on ferrous adsorption as it relates to ferric oxide. Information concerning the other cations in the system primarily come from their book, but ferrous information was assumed. These assumptions will be discussed later.

MINTEQA2 was used to predict the amount of adsorption of the major cations in these two systems onto ferric oxide using the constant capacitance model. Two separate runs for HB pond #2 were completed varying the pH. One case was run with the concentration of ferric oxide at 71.5 mg/L. This value is a result of the decrease in ferrous in pond #2 being converted to ferric oxide. The other case was for a ferric oxide concentration of 1 g/L. This value was picked because of the possible resuspension of solids and the sediment/water interface.

For the ferric oxide, one adsorption surface was picked with two sites, one weak and one strong. The site concentrations came from Dzombak and Morel (1990) and are as follows:

$$\text{Low affinity site } [\equiv Fe^W OH^o] = 0.2 \text{ mol/mol of Fe}$$

$$\text{High affinity site } [\equiv Fe^S OH^o] = 0.005 \text{ mol/mol of Fe}$$

The density of the ferric oxide used was 3.5 g/cm^3. The reactions and equilibrium constants picked for the input file to MINTEQA2 for the HB cations came from Dzombak and Morel (1990) and can be seen below in table 4-10.

Table 4-10: Reactions and equilibrium constants used for the input file for MINTEQA2.

Reaction	Equilibrium constants
H^+	
$\equiv FeOH^\circ + H^+ = \equiv FeOH_2^+$	$LogK_1^{int} = 7.27$
$\equiv FeOH^\circ = \equiv FeO^- + H^+$	$LogK_2^{int} = -8.91$
Ca^{2+}	
$\equiv Fe^S OH^\circ + Ca^{+2} = \equiv FeOHCa^{+2}$	$LogK_1^{int} = 4.97$
$\equiv Fe^W OH^\circ + Ca^{+2} = \equiv FeOCa^+ + H^+$	$LogK_2^{int} = -5.85$
Mg^{2+}	
$\equiv Fe^S OH^\circ + Mg^{+2} = \equiv FeOHMg^{+2}$	$LogK_1^{int} = 4.80*$
$\equiv Fe^W OH^\circ + Mg^{+2} = \equiv FeOMg^+ + H^+$	$LogK_2^{int} = -4.60$
Fe^{2+}	
$\equiv Fe^S OH^\circ + Fe^{+2} = \equiv FeOHFe^{+2}$	$LogK_1^{int} = -0.43**$
$\equiv Fe^W OH^\circ + Fe^{+2} = \equiv FeOFe^+ + H^+$	$LogK_2^{int} = -3.25**$
SO_4^{-2}	
$\equiv FeOH^\circ + SO_4^{-2} + H^+ = \equiv FeSO_4^- + H_2O$	$LogK_1^{int} = 7.78$
$\equiv FeOH^\circ + SO_4^{-2} = \equiv FeOHSO_4^{-2}$	$LogK_2^{int} = 0.79$

* This value was not available and was interpolated from the values given by calcium and strontium in Dzombak and Morel (1990).

** These values were not available in current literature and were interpolated using the values for Co and Mn, which surround ferrous in the periodic table from Dzombak and Morel (1990).

The results of the computer model run can be seen in figure 4-8. MINTEQA2 predicts that calcium will not adsorb onto the 71.5 mg/L case, and will only adsorb up to 0.1% for the 1 g/L case at high pH values. Magnesium will adsorb up to 0.1% for the 71.5 mg/L case, and up to 2.1% for the higher concentration of ferric oxide at the higher pH values. The cation that adsorbs the most is the ferrous. At a pH value of 6, it is shown to adsorb up to 0.1% for the 71.5 mg/L case and up to 2.5% for the 1 g/L case. Sulfate will be discussed in a later section.
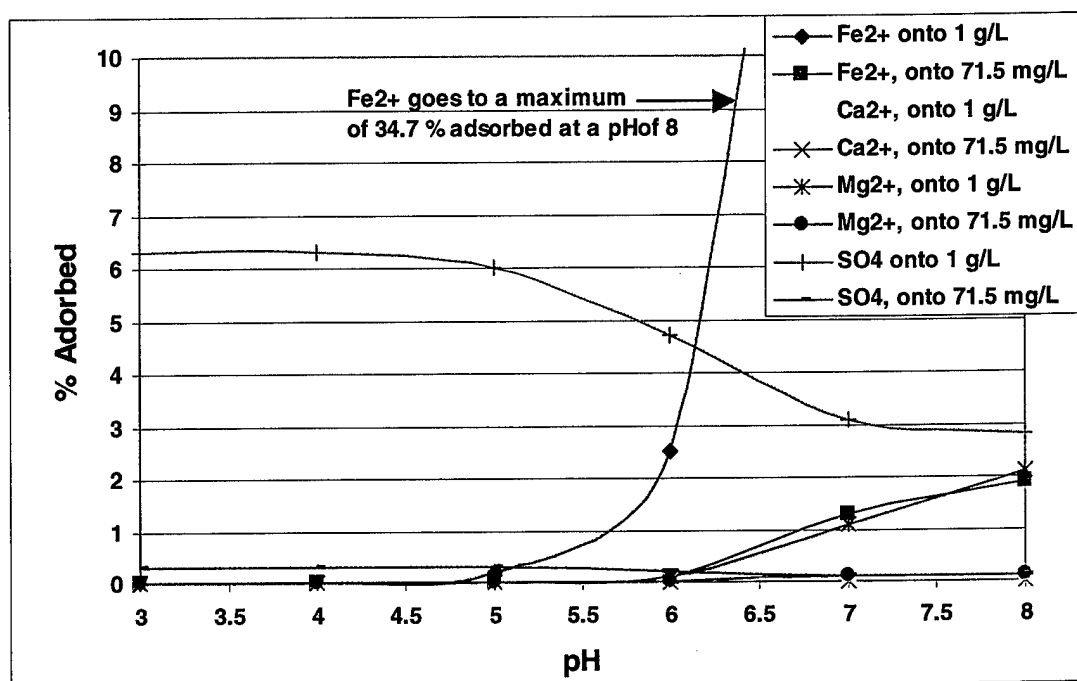
Figure 4-8: Results of MINTEQA2 for major ions at HB pond #2.

The trend for this plot is as pH increases, there is increasing adsorbance. When the concentration of ferric oxide is increased, there is increased adsorbance. These trends fall into line with what Dzombak and Morel (1990) also predict for cation adsorption onto ferric oxide. Ferrous is the cation that seems to respond most quickly as the pH increases and increasing ferric oxide concentration. It most be noted that the equilibrium value for this reaction was interpolated since there is no reportable value found in literature. More research is needed to accurately predict this reaction.

Since the concentration of ferric oxide is not known for the site, it is difficult to say exactly what percent of each cation should adsorb. However, the concentration of

ferric oxide should be between the values indicated. Assuming this, it is safe to say that there should not be any decrease in calcium and minor losses for magnesium concentrations in the system. This is what is observed from the field data. It must also be noted that very little calcium and magnesium was found in the sediments during the core bulk analysis (Appendix L), indicating they are not being removed from the system.

Another observance is that more ferrous is decreasing in the system than what is predicted by the alkalinity decrease. Ferrous adsorption on to ferric oxide could be one of the mechanism causing the two not to match.. There is approximately a 15% difference from the actual ferrous lost across pond #2 than what the alkalinity predicts (table 4-11). At a pH value of 6, the maximum percent absorbed ferrous for the 1 g/L case is 2.5% of ferrous in solution, equating to approximately a 5 mg/L adsorbed. It is possible that the equilibrium constant for the ferrous adsorbance may be incorrect, and could cause this number to increase or decrease depending on the correct value. It must also be noted that the change in alkalinity could be effected by the adsorbed sulfate and absorbed ferrous by taking up sites instead of the OH^- ion, which would cause an error in the ferrous prediction. This will be addressed later.

Ferrous also seems to be present in the sludge. When analyzing the sludge with XRD for the bulk analysis, the color was a olive green. In the time span of 30 minutes, the olive green changed to a orange red color, indicating ferrous oxidation. Due to time and equipment constraints, this was not investigated further. It must also be noted that there has not been any documented research on this in the literature.

4.2 Alkalinity

Alkalinity decreases in the system due to the flowing reactions:

REDOX: **½ reaction:** $Fe^{2+} \rightarrow Fe^{3+} + e^-$ (4.7)

½ reaction: $\frac{1}{4} O_2 + e\text{-} + H^+ \rightarrow \frac{1}{2} H_2O$ (4.8)

Addition: $Fe^{2+} + H^+ + \frac{1}{4} O_2 \rightarrow Fe^{3+} + \frac{1}{2} H_2O$ (4.9)

Note: One proton of acidity generated on left hand side of equation.

Hydrolysis: $Fe^{3+} + 3H_2O \rightarrow Fe(OH)_3 + 3H^+$ (4.10)

Note: Three protons of acidity generated on right hand side of equation.

The net acidity for these reactions is 2 protons of acidity generated. Take the 3 protons of acidity generated in equation (4.10) minus the 1 proton of acidity taken away in reaction (4.9). One 1 mole of ferrous going to ferric hydroxide corresponds to 2 moles of H^+ being generated. The alkalinity required to neutralized the acidity generated is:

Alkalinity required: $2 H^+ + 2HCO_3^- \rightarrow 2 H_2CO_3$ (4.11)

For every mole of H^+ generated, one mole of HCO_3^- must be used. For every mole of ferrous being oxidized and going to ferric hydroxide, 2 moles of bicarbonate must be used.

4.2.1   Ferrous removal and alkalinity usage

The alkalinity calculations from the beginning of the study have not matched the ferrous decrease. Possible reasons for these discrepancies are:

1) Adsorption of ferrous onto ferric oxide.

2) Adsorption of sulfate onto ferric oxide.

3) Precipitation of an iron sulfate hydroxyl.

The first reason was addressed partly in section 4.1.4. Ferrous adsorption onto ferric oxide is possible. MINTEQA2 predicted up to 2.5% of the ferrous in solution could be adsorbed onto the surface of the ferric oxide precipitate. This value may change depending on the actual equilibrium constant for ferrous adsorption, which is unknown at this time. Also mention previously was the initial color of the sludge being a olive green color and once exposed to air quickly oxidized to a orange red color. Ferrous is being removed from the system as ferrous and not as previously believe as going to ferric and precipitating out.

Table 4-11: Ferrous lost versus alkalinity predicted for HB IP2.

Date of Trip	HB IP2 Fe^{2+} (mg/L)	HB EP2 Fe^{2+} (mg/L)	Fe^{2+} Lost (mg/L)	Lab ALK Predicted Fe^{2+} Loss (mg/L)	Field ALK Predicted Fe^{2+} Loss (mg/L)	% Difference actual vs lab	% Difference actual vs Field
6-Jun-98	226.5	174.6	51.9	45.5	ND	12.3	
3-Jul-98	230.6	182.2	48.4	40.1	ND	17.1	
5-Aug-98	227.6	176.4	51.2	41.4	53.1	19.1	-3.7
26-Aug-98	223.4	178.2	45.2	32.4	32.4	28.3	28.3
26-Sep-98	219.2	177.2	42	34.3	39.1	18.3	6.9
24-Oct-98	210.4	158.4	52	40.5	43.5	22.1	16.3
22-Nov-98	204.9	158.1	46.8	ND	41.3		11.8

Table 4-12: Ferrous lost versus alkalinity predicted for CK system.

Date of Trip	CK @ Pipe Fe^{2+} (mg/L)	CK Bend #3 Fe^{2+} (mg/L)	Fe^{2+} Lost (mg/L)	Lab ALK Predicted Fe^{2+} Loss (mg/L)	Field ALK Predicted Fe^{2+} Loss (mg/L)	% Difference actual vs lab	% Difference actual vs Field
6-Jun-98	104.5	45.2	59.3	63.1	ND	-6.4	
3-Jul-98	99.9	22.7	77.2	70.5	50.2	8.7	
5-Aug-98	90.5	7.35	83.15	94.3	82.6	-13.4	0.7

In table 4-11, the HB amount of actual ferrous lost across pond #2 is greater than the amount predicted by both field and lab alkalinity values for all cases except one. Only three measurements were taken at CK because of the dynamics of the system. The flow for CK decreased rapidly from June to Dec due to the drought in the area.

If ferrous is leaving the system as ferrous and not oxidizing to ferric, this would explain why delta ferrous is larger than what is predicted by the alkalinity. However, the numbers above indicate a large amount of ferrous that needs to be adsorbed in order for this to explain this phenomenon. MINTEQA2 only predicted a max of 2.5% under optimum conditions, not the approximate value of 15% being reported above.

Another explanation could be the adsorption of sulfate onto the surface of the ferric oxide. Figure 4-8 predicts sulfate being adsorbed. Sulfate may be competing for adsorption sites that are being assumed to be taken up by the OH^- ion in equation (4.10). If this were to happen, the alkalinity prediction for ferrous above would be in error. This will be discussed further in this chapter in section 4.4.3.

The precipitation of an iron hydroxyl sulfate could also explain the difference. If the ferric were precipitating out of the system in a form other than what is describe in equation (4.10), this may also cause the alkalinity prediction of ferrous to be in error.

Instead of generating 3 protons of acidity with equation (4.10), depending on the species make up, there may be only 2 protons of acidity generated. The sulfate will replace one or maybe two of the OH⁻ ions, causing the alkalinity prediction of ferrous to be in error.

4.2.2   Lab results vs. field results

While the above section may explain the discrepancy between the ferrous loss and alkalinity predicted, there is still a large discrepancy between lab alkalinity and field values. This discrepancy was reported in chapter 3 figure 3-8. The field values were an average of 12.2 mg/L as $CaCO_3$ higher than what the lab reported for the same location. Possible explanation for this may be:

1) Loss of CO_2 during storage due to microbial activity.

2) Loss of CO_2 during sampling, handling and storage.

3) Formation of Siderite.

Microbial activity does have its place in AMD, however it was assumed that the first part of the HB system and CK systems were abiotic. To validate this assumption an experiment was set up to inject sulfite into the TIC samples prior to removing them from the water. This would remove all the O_2 that was in the water that is required for microbiological activity. An outline of the experimental procedures can be found in chapter three. The results can be seen in figures 4-9 and 4-10.
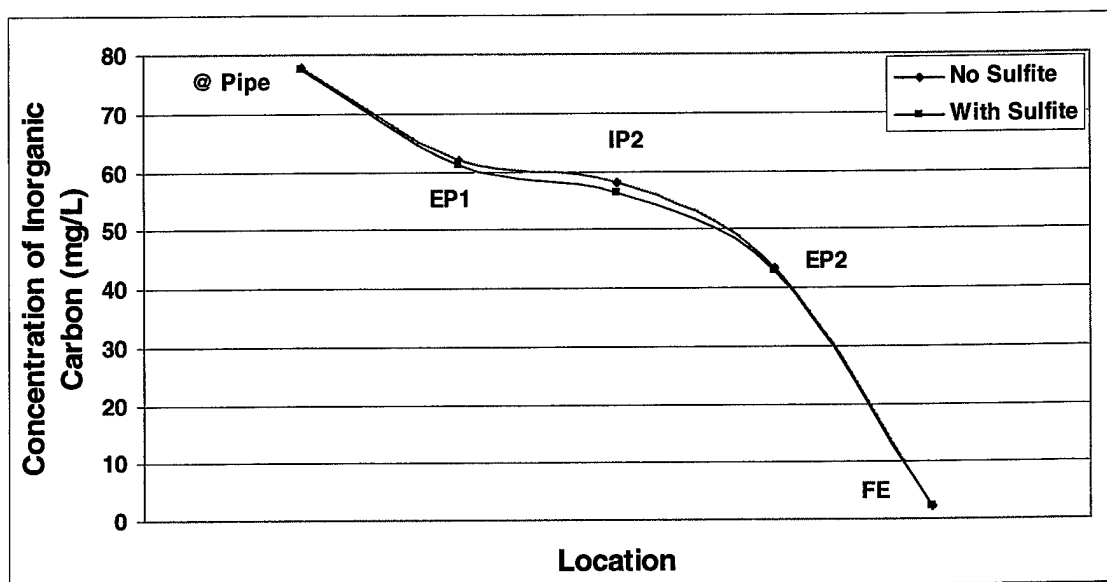
Figure 4-9: Comparison of TIC samples with and without sulfite addition for the HB trip 26 Aug 98.
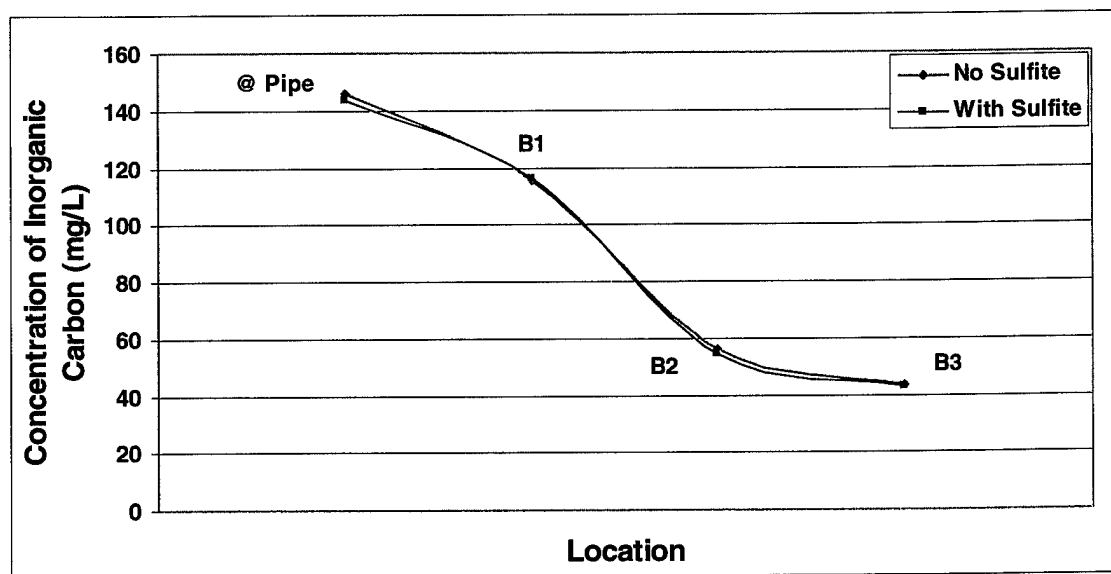
Figure 4-10: Comparison of TIC samples with and without sulfite addition for the CK trip on 26 Aug 98.

The two figures above show that there is a small change between taking samples with or without sulfite. The sulfite reduced the DO levels in the sample close to zero minimizing any effect of microbiological activity. It appears that microbiological activity was close to zero already since the two lines are practically on top of each other for the two plots above. The assumption made that the systems are abiotic is valid. There should be no loss of CO_2 due to microbiological activity in the sample.

The next possible explanation for the discrepancy was the loss of CO_2 during storage, handling and sampling. Great care was taken when collecting the TIC samples. It was important to collect the sample ensuring no air came into the sample syringe or bottle. A possible explanation was CO_2 loss through the plastic collection device. An experiment was set up to collect the samples with the plastic syringes and glass bottles. The results can be seen in figures 4-11 and 4-12.
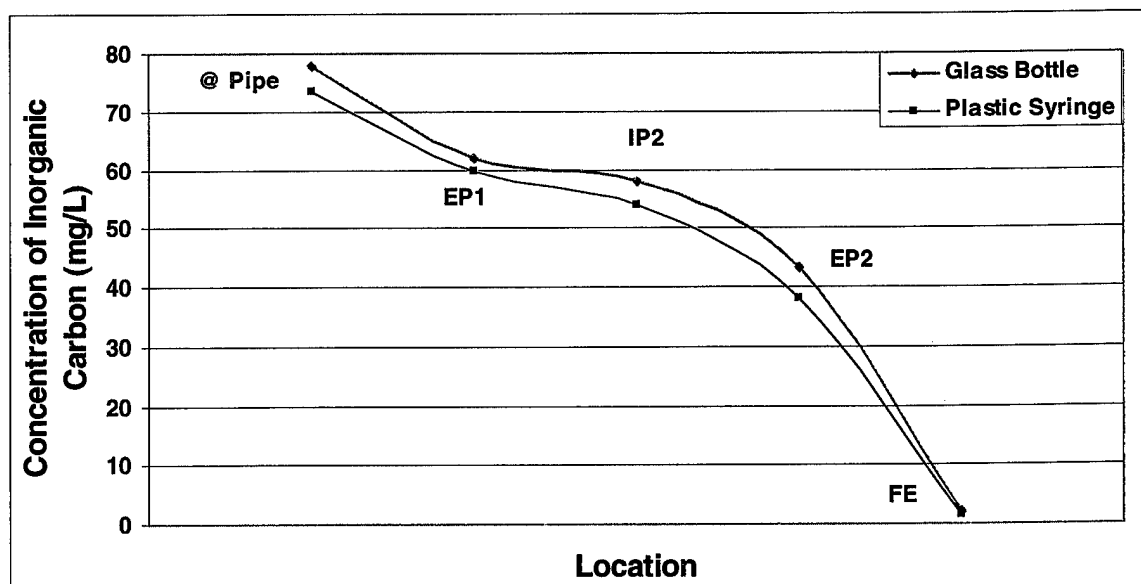
Figure 4-11: Comparison of TIC samples with glass versus plastic syringe for the HB trip on 26 August 1998.
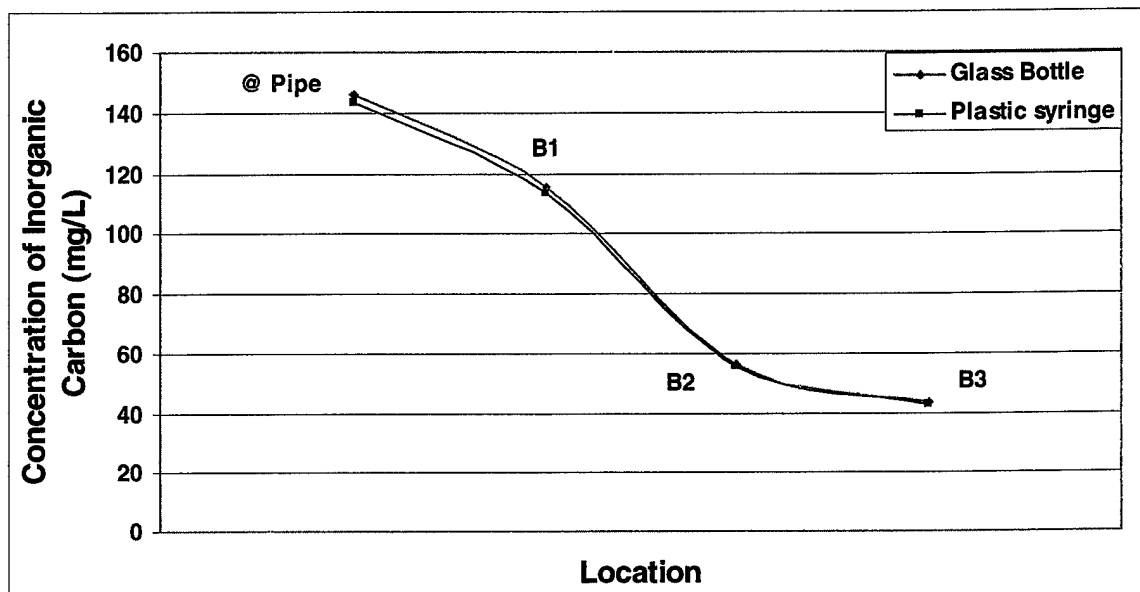
Figure 4-12: Comparison of TIC samples with glass versus plastic syringe for the CK trip on 26 Aug 98.

In figure 4-11, it appears that there may have been some loss of CO_2 in the syringe than in the bottle. When taking this difference and changing it to alkalinity as $CaCO_3$, it would account for an approximate 5-6 mg/L of the 12.2 mg/L difference. Plastic syringes were not used after this experiment for subsequent sampling trips. The difference between field and lab after the 26th of August trip was lowered to around 11 mg/L instead of the 12.2 mg/L. In figure 4-12 for the CK samples, there was almost no indication that there was any CO_2 being lost in the syringe samples versus the glass bottles.

Another possibility for the discrepancy could be the formation of siderite. Siderite is near saturation and in some cases supersaturated depending on where you are for each system. If colloidal siderite is forming, a lot of the alkalinity is tied up as

$FeCO_3$, leaving less as HCO_3^-, and therefore the pH would be lower. The TIC in the siderite should be liberated during the TIC analysis, but may not be during the field alkalinity titration. The sludge that was collected at pond #2 at HB was analyzed for siderite by XRD. No phase for siderite was found in the sludge. This hypothesis was not investigated further, and may be the focus of future research.

4.3 Iron Removal Rate

The area adjusted iron removal rate (IRR) was calculated taking the change in ferrous multiplying the flow and dividing by the surface area (S.A.). The formula can be seen below in equation (4.12).

$$\mathbf{IRR = \frac{dFe^{2+} \times FLOW}{S.A.}} \qquad (4.12)$$

Tables 4-13 and 4-14 show the IRR for the two systems throughout the year with different flows and temperatures.

Table 4-13: Iron Removal Rates for pond #2 at HB. Water temperature comes from the effluent of the pond.

Date of Trip	Water Temp °C	FLOW (gal/min)	HB Pond #2 IRR (g/day-m2)
1 March	7.1	32.0	21.7
29 March	11.3	32.1	24.6
13 May 98	12.9	32.0	31.0
6 June 98	11.1	33.0	20.1
3 July 98	13.9	36.0	20.5
5 August 98	16.5	37.0	22.3
26 August 98	21.2	33.8	17.9
26 September 98	11.3	36.0	17.8
25 October 98	7.3	36.0	21.9
22 November 98	4.8	34.6	19.0
Average:	**11.7**	**34.3**	**21.7**
Standard Deviation:	**4.8**	**1.9**	**3.9**

Table 4-14: Iron Removal Rates for the CK system from pipe to B2. Water temperature is taken from B2.

Date of Trip	Water Temp °C	FLOW (gal/min)	CK system from Pipe to B3 IRR (g/day-m2)
1 March 98	12.8	124	30.7
29 March	20.4	159	56.5
18 May 98	21.1	191	51.1
6 June 98	21.1	136	57.2
3 July 98	16.9	82	33.0
5 August 98	24.0	50	31.5
Average:	**19.4**	**123**	**41.6**
Standard Deviation:	**3.9**	**51.2**	**12.6**

HB had a relatively constant flow during the study period. The standard deviation was 1.9 gal/min unlike the 51.2 gal/min that occurred for the CK system. HB had an average of 21.7 g/day-m^2 for its IRR. This is very close to other removal rates reported in the literature (Hedin, et al., 1994). CK however, shows a very large IRR of 41.6

g/day-m^2 with a standard deviation of 12.6 g/day-m2. This is due to the large variation in the flow during the study period. The equation used to calculate the IRR is heavily dependent on the flow. If all other factors remain the same, and flow increases, the IRR will increase. However, the chemistry of the water changes with changing flow. The delta ferrous value with the larger flows decreases. The reason for this is the time it takes the ferrous to travel from the pipe to B2 is much faster than the time it takes to oxidize the ferrous completely to ferric.

Comparing the two sites for IRR can not be done objectively. The conditions are not the same. HB has a much larger driving force due to the large concentration of ferrous, where CK does not. However, even though HB has the greater driving force (greater concentration of ferrous), the CK system is the one that removes more ferrous per unit of area under its conditions.

To increase the IRR, flow is not necessarily the factor you want to increase. Treating large flows require large amounts of land. However, it offers some incites to making the delta ferrous value larger since the two seem to be related. Flow has also been shown to cause the rate of ferrous oxidation to increase due to increased DO levels and possible resuspension of solids allowing for heterogeneous oxidation processed to influence. Finding ways to increase the DO levels in the water and ferric concentrations should increase the rate of oxidation of ferrous, thereby increasing the delta ferrous value in equation (4.12). This will increase the IRR.

Surface area must also be considered for these calculations. It was assumed that for both systems that the S.A. remained the same. This is valid for HB where the flow

changed very little. The CK system is in the shape of a trapezoid. As flow increases so must the S.A. with increasing depth. Since the sides of the CK channel were very steep, the increase in the S.A. was assumed to be minimal.

4.3.1 DO and Flow

Ferrous oxidation to ferric is dependent of oxygen. The rate at which the oxygen transfers into the water is very import. Hustwit et al., (1992) proposed that oxygen transfer is the rate-limiting step in the oxidation process of ferrous to ferric. The rate of oxygen transfer is governed by equation (4.13).

$$d[O_2]/dt = K_L a([O_2]_{sat} - [O_2]_t) \qquad (4.13)$$

Where $[O_2]_{sat}$ and $[O_2]_t$ are the saturation and time dependant oxygen concentrations. The rate constant $K_{L(O2)}$, equals the rate at which oxygen is used to convert Fe(II) to Fe(III) according to equation (2.2) plus the increment in DO across the pond or down the length of channel. This is seen in equation (4.14).

$$K_{L(O2)} = \frac{\left(\dfrac{d[O_2]}{dt} - \dfrac{\frac{1}{4}[Fe(II)]}{dt} \right) V}{A \, ([O_2]_{sat} - [O_2]_t)} \qquad (4.14)$$

Where V is the volume of the pond or system and A is the air-water surface area. The constant will have dimensions of length per time. Thus the surface of the pond can be related to the oxygen transfer rate, and ultimately the oxidation of ferrous (Ames 1998).

The design of passive treatment systems should have sufficient surface area so the oxygen transfer is not the rate-determining step in the oxidation of ferrous. Oxygen transfer rates can be increased by adding turbulence to the water like weirs, waterfalls or rip rap filled channels (Ames, 1998).

The equation (4.14) was then subsequently used to calculate the $K_{L(O2)}$. These values are reported in tables 4-15 and 4-16.

Table 4-15: $K_{L(O2)}$ for pond #2 at HB.

Date of Trip	Water Temp °C	FLOW (gal/min)	HB Pond #2 $K_{L(O2)}$ (cm/hr)	Race #2 HB $K_{L(O2)}$ (cm/hr)
1 March	7.1	32.0	1.04	14.8
29 March	11.3	32.1	1.52	18.6
13 May 98	12.9	32.0	1.62	41.0
6 June 98	11.1	33.0	2.75	5.1
3 July 98	13.9	36.0	1.71	3.5
5 August 98	16.5	37.0	1.83	15.8
26 August 98	21.2	33.8	2.11	13.2
26 September 98	11.3	36.0	1.29	9.9
25 October 98	7.3	36.0	3.30	11.9
22 November 98	4.8	34.6	2.43	18.4
Average:	**11.7**	**34.3**	**1.96**	**15.2**
Standard Dev:	**4.8**	**1.9**	**0.69**	**10.4**

Table 4-16: $K_{L(O2)}$ for CK system from Pipe to B2.

Date of Trip	Water Temp °C	FLOW (gal/min)	CK system from Pipe to B2 $K_{L(O2)}$ (cm/hr)
1 March 98	12.8	124	10.2
29 March 98	20.4	159	14.5
13 May 98	21.1	191	21.4
6 June 98	21.1	136	13.8
3 July 98	16.9	82	5.2
5 August 98	24.0	50	3.9
Average:	**19.4**	**123.6**	**11.5**
Standard Deviation:	**3.9**	**51.2**	**6.5**

For the HB system, the flow is relatively steady as well as the $K_{L(O2)}$ for pond #2. However, the race (small channel prior to pond #2) has a much larger rate. The average for HB pond #2 is 1.96 cm/hr, but the average for the race with the same flow is 15.2 cm/hr. The channel for the same flow has a greater oxygenation rate than the pond. This is also the case for the CK system. The CK system also shows that the flow effects the rate of oxygen transfer into the system. At high flows, $K_{L(O2)}$ is at it highest and it decreases as flow decreases. As mentioned before, it has been shown in figure 4-5 that an increased flow increases the rate of oxidation of ferrous.

Ames (1998) showed similar increases in his experiments. In all of his cases, as the rate of mixing was increased in his batch reactors, the $K_{L(O2)}$ also increased. Ames (1998) also reported a thin iron precipitate film that formed on the surface of the water. The film was made up of plate like sections that resisted flow with the motion of his reactors. He also reported in some cases an appearance of an oil slick on top of his reactors. Although not proven, he hypothesized that the film may have created a barrier slowing the rate of oxidation to the water.

These same two types of films produced in the lab under abiotic conditions are also seen in the field (figure 1-4). Temperature dependence does not seem to matter. These films are present during the winter months as well as the summer. They are mainly seen on the ponds and attached to the vegetation (cattails). No correlation was drawn between the film and gas transport rates for the field. This is an area for possible future study.

4.4 Sulfate Removal

4.4.1 MINTEQA2 Predictions

Both of the passive treatment systems have very high concentrations of sulfate (HB approx. 1200 mg/L and CK approx. 1300 mg/L). When the initial conditions were put into MINTEQA2, it predicted many dissolve species of the metal cations with the dissolved sulfate (tables 4-1 and 4-3). However, with such a high activity of sulfate in the solution, MINTEQA2 did not predict any sulfate species as supersaturated. There is an indication that some sulfate may be leaving the system through analysis of wet samples from the field on the IC machine. Hedin et al., (1994) also reported a decrease of sulfate in the HB system. During the analysis of the sludge, it showed sulfate as approximately 0.1 % of the make up. If sulfate is leaving the system, then what is the mechanism it is using to do so? There are two possible explanation that will be discussed, one is that the sulfate is being adsorbed onto the ferric oxide, and two is the sulfate is being precipitated out of the system.

4.4.2 Field Observations

Three sampling trips were conducted for collection of samples for sulfate analysis. In all three cases the IC indicated a decrease in sulfate through both systems. Below in figure 4-13 is the results for the second trip at HB on 22 November 1998.
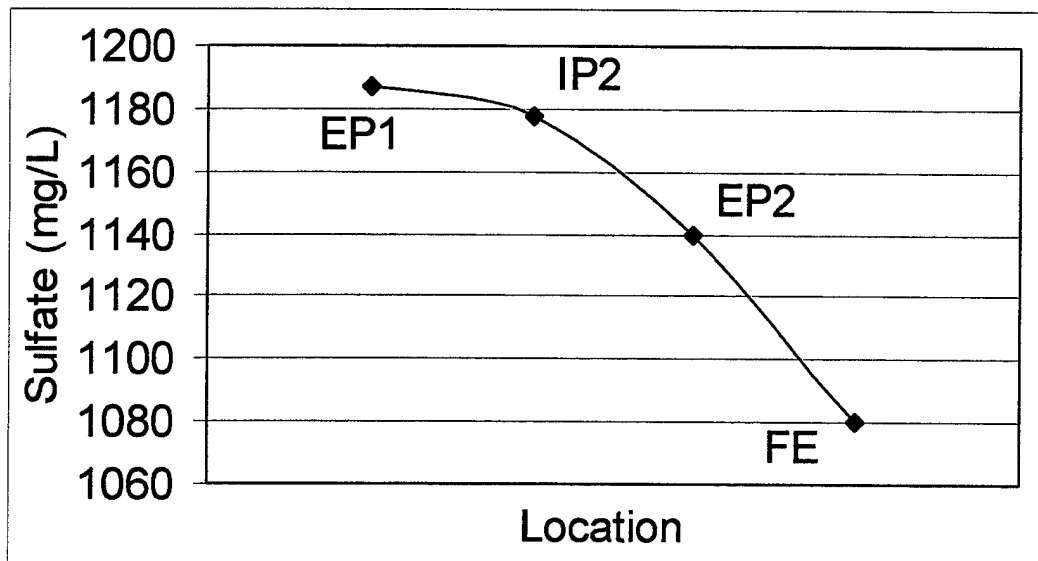
Figure 4-13: Sulfate concentration through HB on 22 November 1998.

The first two trips indicated large decreases in sulfate in the HB and CK systems. The first trip on 26 September 1998 indicated a 300 mg/L sulfate decrease through the CK system and a 90 mg/L decrease at HB in pond #2. The second trip on 22 November 1998 shown above indicated a 38 mg/L decrease in pond #2. These number seemed very high and a additional trip was taken on 14 December 1998 for redundancy to collect 5 samples from the influent and 5 samples from the effluent of pond #2 at HB. The results can be seen in table 4-17.

Table 4-17: Results of sulfate analysis for the IC machine for HB pond #2,
14 December trip.

Sample number	HB IP2 (mg/L)	HB EP2 (mg/L)
#1	919.5	912.4
#2	934.7	939.5
#3	941.5	957.6
#4	901.0	894.4
#5	852.1	805.5
Average:	**909.7**	**901.8**
Standard Deviation:	**35.8**	**59.1**

From the table above there is an decrease shown again for pond #2 of 7.8 mg/L when taking the average of the five samples. However, the standard deviation is quite large. Large enough that the data is not valid using statistical procedures. However, there is still some indication that sulfate is being removed from the system and it needed to be investigated further.

4.4.3 Anion Adsorption

One of the possible mechanisms that could cause sulfate to be removed from the system is anion adsorption onto the ferric oxide surface. MINTEQA2 reported that sulfate will adsorb onto the ferric oxide surface (figure 4-8). The percent adsorbed varies with pH, at low pH values the percent adsorbed is larger than for high. This trend is also predicted by Dzombak and Morel (1990). The maximum percent adsorbed predicted by MINTEQA2 for sulfate at a pH value of 6 was 4.7 % for the 1 g/L ferric oxide case. Thus, it is quite possible that the sulfate in the sediments may be the result of adsorption.

4.4.4 Schwertmannite Precipitation

Another possible explanation for the loss of sulfate is the precipitation by an iron hydroxyl sulfate. The most common of these in AMD is schwertmannite. MINTEQA2 did not recognize this species since it was just recently approved as a mineral. However, it is possible to add schwertmannite to the data base. Currently there is no thermodynamic data on schwertmannite, but Schwertmann et al., (1996) were able to come up with a K_{sp} value and the chemical reaction. This information was added to MINTEQA2's database. The output of the run is located in Appendix J. The output shows that schwertmannite is supersaturated at a pH value of 6 and may precipitate. The output also suggest that ferric is the limiting factor for the precipitation. For schwertmannite it takes 8 moles of ferric to remove 1 mole of sulfate.

Bigham et al. (1994) showed that schwertmannite can form at high pH values above 6. During the XRD analysis of the solids (appendix P), there was no indication that schwertmannite was present. The conditions to form schwertmannite are present in the HB system, but its formation is unlikely because goethite formation is better suited for the given conditions.

4.5 Identification of Solids

One of the goals for this study was to identify the sludge that is made in these systems. To do this, the XRD procedure outlined in chapter 3 was used with the help of its operator and Dr. Barry Sheetz for analysis of the data. Samples from HB pond #2 were analyzed for two sampling trips on 4 and 27 January 1999. The core sample was

opened and 3 samples from the core were taken and labeled "Top" "Middle" and

"bottom". The spacing between the samples was approximately 6 inches. The bottom

sample was taken approximately three inches above the clay liner that sealed the end of

the core tube. The "Top" "Middle" and "bottom" samples where then taken to the MRL

building and analyzed on the XRD machine.

4.5.1 MINTEQA2 and Bigham Model Predictions

As previously mentioned, MINTEQA2 produced a printout of all the

supersaturated solids that may form in these passive treatment systems. This information

can be found in Table 4-2 and 4-4 or in Appendix G and E. The Bigham model found in

figure 2-3 for the HB pond #2 conditions predicts the formation of lepidocrocite then

subsequent dissolution and reprecipitation as goethite. The species identified by

MINTEQA2 and the Bigham model were checked against the XRD data for the sludge at

HB pond #2. The raw data for these checks can be found in Appendix P.

4.5.2 Positive Identification

Of all the checks done, three species were found to be part of the sludge at pond

#2. Table 4-18 list those species checked and the outcome.

Table 4-18: Results of XRD analysis for the HB core samples at pond #2.

Mineral	Chemical Formula	Color	Results
Ferrihydrite	$Fe_5OH_8\text{-}4H_2O$	Yellow-brown	A
Schwertmannite	$Fe_8O_8(OH)_6SO_4$	Yellow-brown	A
Goethite	$FeOOH$	Dark brown	D
Hematite	Fe_2O_3	Red-brown	A
Jarosite	$KFe_3(SO_4)_2(OH)_6$	Yellow-brown	A
Maghemite	Fe_2O_3		A
Magnetite	$FeO\text{-}Fe_2O_3$	Black	A
Mag-Ferrite	$MgFe_2O_4$	Red-brown	A
Lepidocrocite	$FeOOH$	Red-brown	T
Fibroferrite	$Fe(SO_4)(OH)\text{-}5\ H_2O$	Yellow-green	A
Amarantite	$Fe(SO_4)(OH)\text{-}3\ H_2O$	Brownish-red	A
Siderite	$FeCO_3$	Yellow-brown	A
Quartz	SiO_2	White	D*

D = Dominate Signal, T = Trace Signal, A = Absent Signal.
* Note Quartz was dominant for the "Bottom" sample.

The following figures 4-14, 4-15 and 4-16 show a positive match for goethite,

quartz and lepidocrocite. In the figures, the bottom graph shows the computer generation

of the peaks of the raw data in the top graph. The top graph shows the raw data and the

particular mineral being analyzed by the vertical lines on the x-axis as that particular

mineral's signature. A match is found when the mineral's signature lines line up with the

raw data peaks.
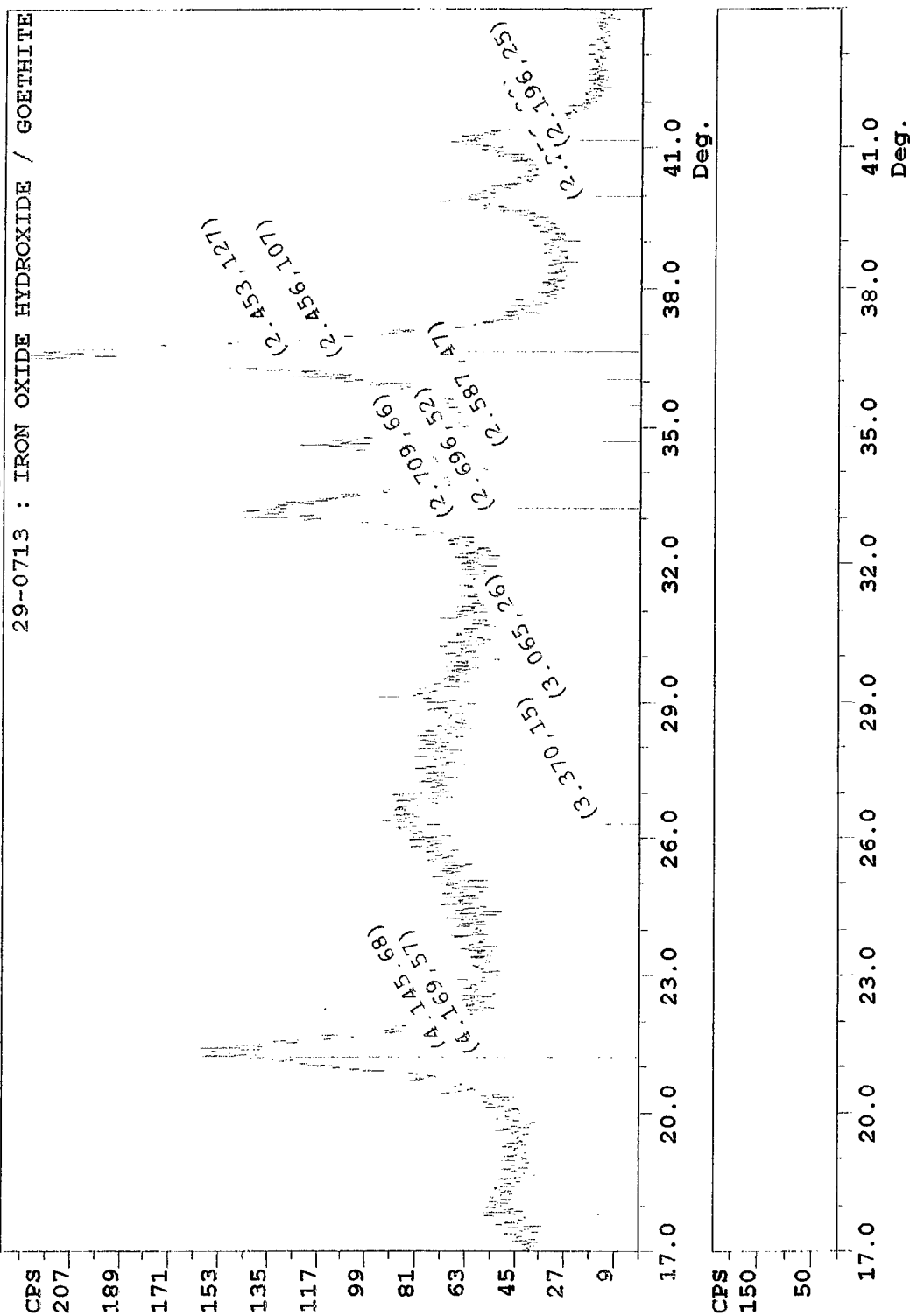
Figure 4-14: Positive identification of goethite.
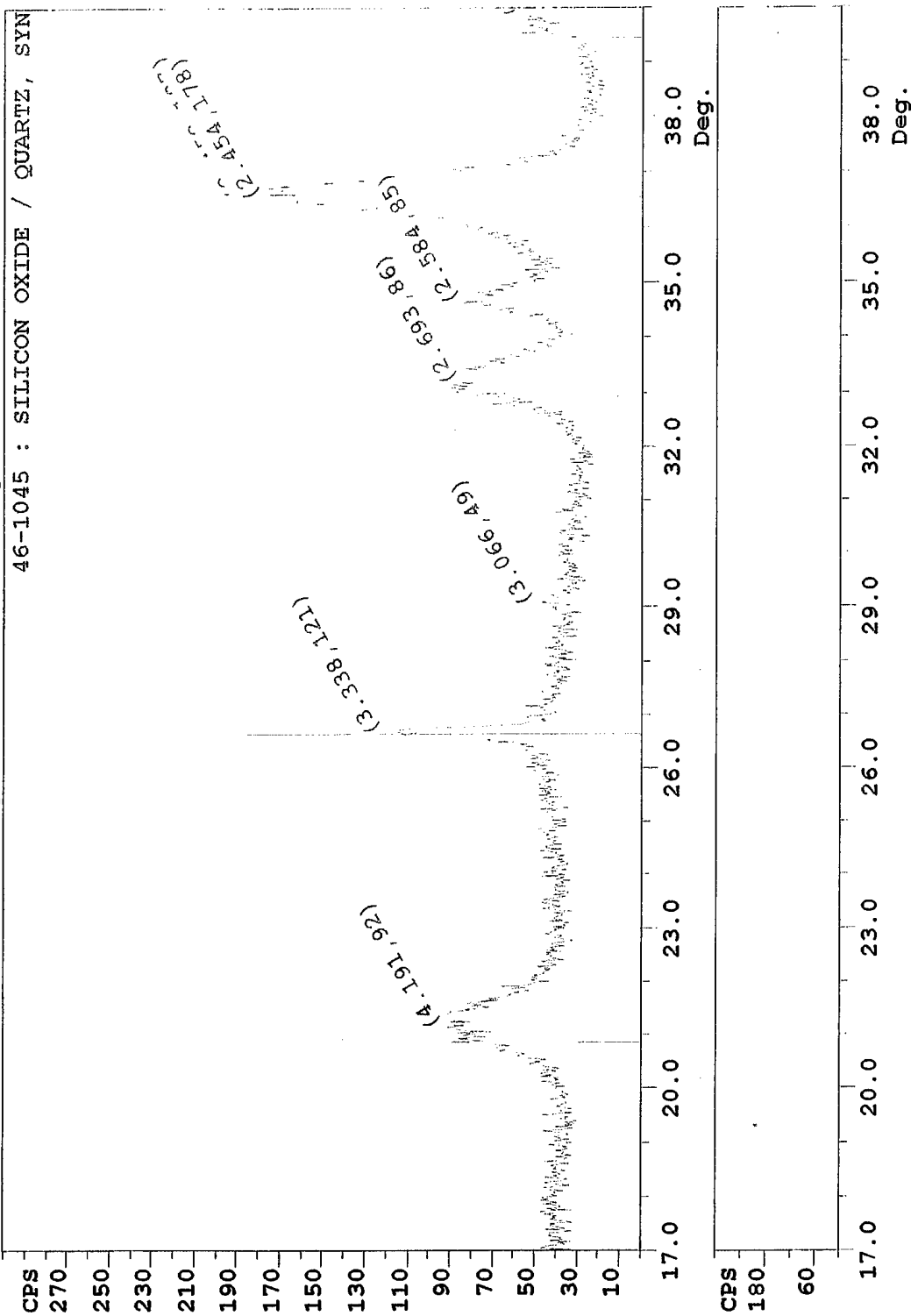
Figure 4-15: Positive identification of quartz.
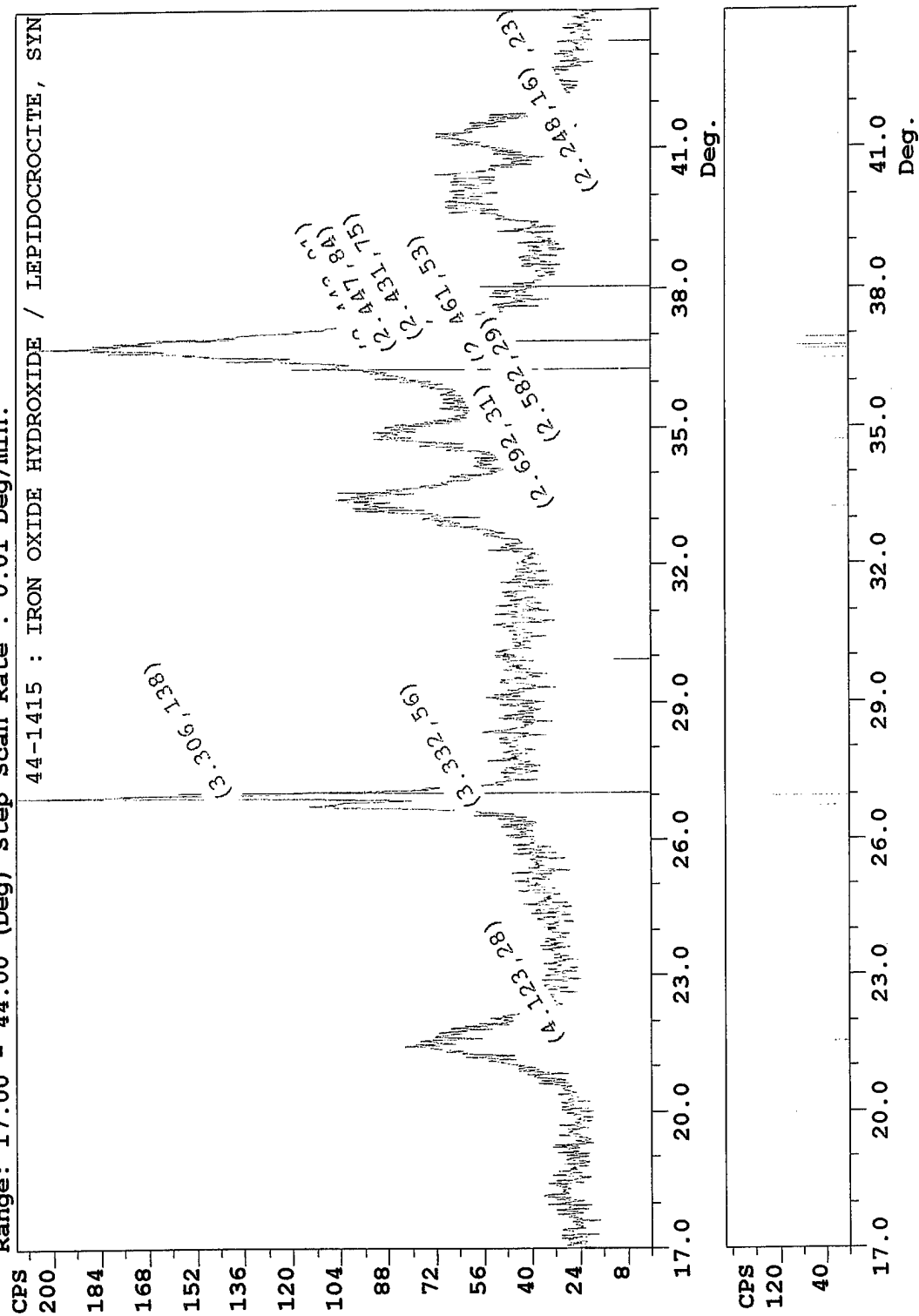
Figure 4-16: Positive identification of minor phases of lepidocrocite.

4.5.3 Content of Sludge.

For the "Top" sample of the core, iron made up 13.7% of the total weight. The total moisture content was 81.7%. Loss on Ignition (LOI) accounted for 2.9 %, which was probably organic material from leaves and sticks that fell into the pond. Metals such as magnesium, manganese, calcium, aluminum, and sodium combined comprised less than 0.1 % of the total weight, while quartz was 0.35% of the weight. As the depth increased so did the concentrations of the metals and the quartz. Sulfate accounted for approximately 0.1 % from top to bottom in the core sample.

For the "Bottom" sample of the core, iron made up 15.4 % of the total weight, a slight increase. The water content was 67%, a decrease indicating the sludge is becoming more dense with depth. The LOI accounted for approximately 3.4 %. The aluminum concentration increased dramatically to 1.55 % of the total weight. Potassium went from practically zero to 0.26 %. There were also slight increases from calcium, magnesium and manganese, but this increased still only combined for less than 0.2 % of the total weight. The big surprise was the dramatic increase in quartz, which was 10.5 % of the total weight in the "Bottom" sample. Table 4-19 shows the results of the bulk analysis of the sludge.

Table 4-19: Bulk analysis on the core sample taken from HB pond #2 on 24 Jan 1998.

Wt. %	HB IP2 Top layer	HB IP2 Middle layer	HB IP2 Bottom layer
Al_2O_3	0.053	0.158	1.550
B_2O_3	0.004	0.005	0.008
BaO	<0.002	<0.002	0.007
CaO	0.034	0.036	0.054
CoO	<0.002	<0.002	<0.002
Cr_2O_3	<0.002	<0.002	<0.002
Fe_2O_3	13.7	16.4	15.4
K_2O	0.005	0.021	0.260
MgO	0.020	0.024	0.079
MnO	0.034	0.049	0.051
MoO_3	<0.002	0.003	0.004
Na_2O	0.004	0.008	0.060
NiO	<0.002	<0.002	<0.002
SiO_2	0.35	1.27	10.5
SrO	<0.002	<0.002	<0.002
TiO_2	<0.002	0.007	0.118
V_2O_5	<0.002	<0.002	<0.002
ZnO	0.01	0.016	0.015
F	<0.001	<0.001	<0.001
Cl	0.008	0.006	<0.001
Nitrate	<0.001	<0.001	<0.001
Phosphate	<0.002	<0.002	<0.002
SO_3	0.127	0.084	0.108
Moisture	81.7	76.6	66.9
$LOI\text{-}1000^0C$	84.6	80.0	70.4

As mentioned previously, the large increase in quartz was not expected. Possible reasons for its large increase:

1) Quartz and aluminum are migrating up from the clay liner.

2) Quartz is entering the system through weathering processes and is more dense than the iron precipitate causing it to be in greater quantities deeper in the sediments.

3) Quartz is entering the system through the dissolution of the limestone in the drain and the impurities left behind in the drain (quartz) is being washed out.

In-order for the first reason to occur, a low pH is needed to dissolve the clay and silica at the sediment/clay liner interface. The pH of the sediment was determined to be 5.6. This pH is to high for the dissolution of the clay and then reprecipitation as quartz, and this hypothesis was ruled out.

The second reason seemed quite plausible and Dr. Hedin (1996) also reported finding quartz in similar sludge samples of AMD. He hypothesized that the quartz entered the system through weathering processes that washed the quartz into the pond. Analysis done by Scott Atkinson and Maria Klimkiewicz from MRL shows that the quartz is detrital (sharp edged), indicating it comes from a breaking off or weathering processes. If it were to come from precipitation in the system it would have a coli-flowered shape (Sheetz 1999). Since it is detrital, the source must be found to produce this significant amount of quartz in the bottom layer of the sediment. It is quite possible for the rain to wash this quartz into the ponds, then having a greater density than the goethite, causing it to collect in the bottom sediment layer. It does seem likely that the large amount of quartz found in the bottom sediment layer came when the pond was

constructed leaving the surrounding area absent of vegetation allowing rain to wash in the quartz.

The third hypothesis is that the quartz came from the anoxic limestone drain. The purity of the limestone used in the drain was approximately 90%. Depending on the purity will cause the amount of quartz that makes up part of the impurities to increase or decrease. As the limestone dissolves and gives up alkalinity to the AMD water, the impurities are left behind. As more dissolution occurs the impurities will be washed out of the drain since nothing is holding them in place. As these particles wash out of the drain, they will settle out depending on the size and work their way through the sediment layer to the bottom, since they will have a greater density than the goethite precipitate. Figure 4-17 shows the increase of quartz has you go deeper into the sediment layer.

This second and third hypothesis seem the most likely of the three to explain the occurrence of this large amount of quartz in the sediment. These hypothesis has not been proven due to time constraints. It would be relatively easy to prove by taking sediment samples from the front of the system to the end. If the quartz is in greater abundance and larger particle sizes in the beginning than the end of the system, then this will prove the third theory. If the quartz did not leave the treatment system and collected in the sediment, it seems quite plausible that calculations could be made to determine the life of the limestone drain, if the amount of quartz was known initially when the drain was implaced.
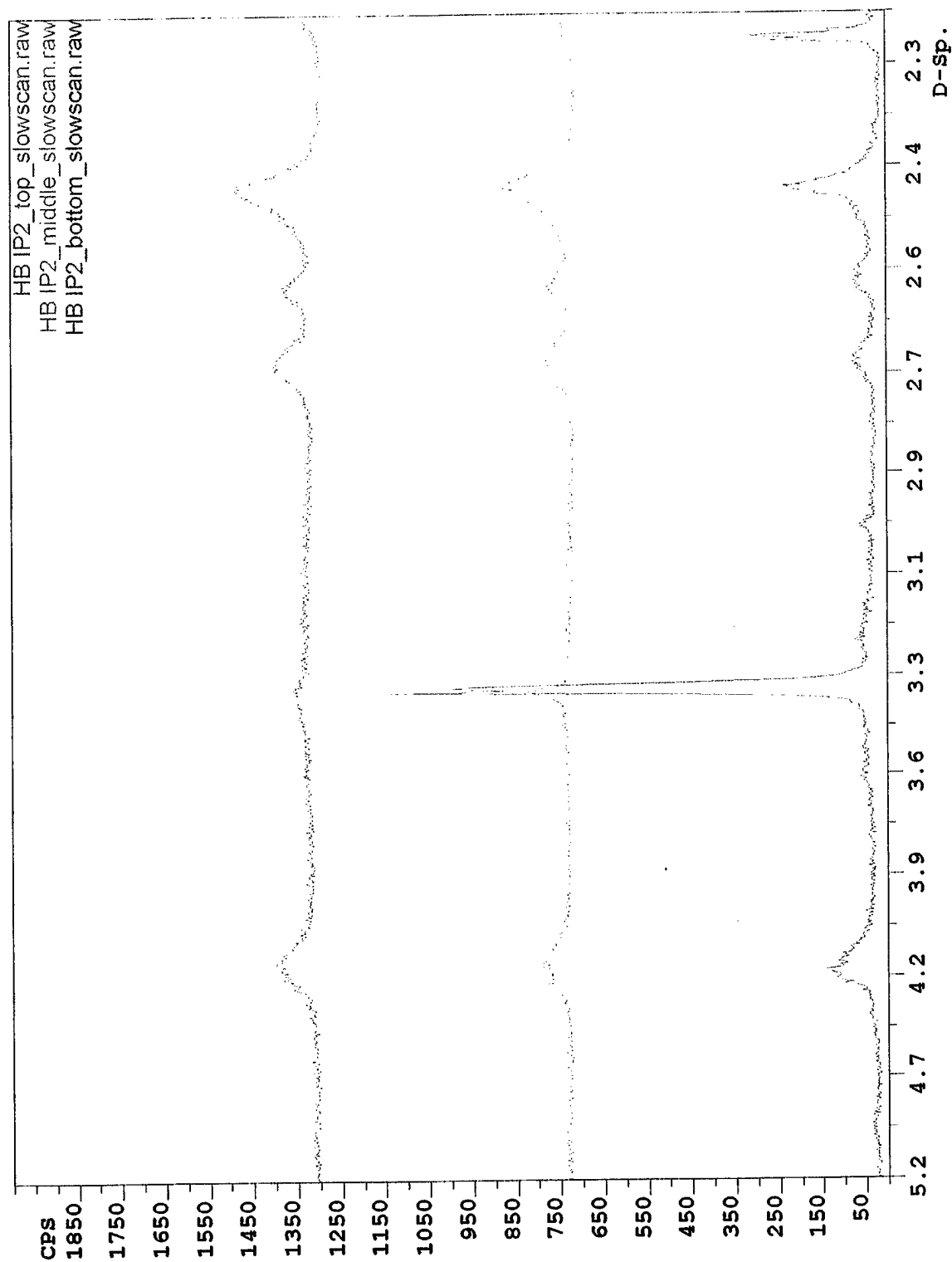
Figure 4-17: Quartz peaks increase with increasing depth in the sediment layer.

Chapter 5

CONCLUSIONS

5.1 Conclusions

The following conclusions can be drawn from this research:

1.   Treating mine drainage with abiotic ponds removed large quantities of iron when there is net alkalinity in the system. There is no indication that other metals such as magnesium, manganese or calcium will be removed through precipitation or adsorption.

2.   The Iron Removal Rate (IRR) for the Howe Bridge (HB) oxidation pond treating alkaline mine water is around 21.0 g/day-m^2. This value is typical of other values reported in literature. The C & K Coal (CK) channel system reported significantly higher values. As flow increased in the CK, system the IRR increased. The channel system had rates up to 56.5 g/day-m^2 which corresponded to high flows, and an average of 41.6 g/day-m^2 through the study period. This was not expected and is something to consider when designing a treatment system.

3.   Oxidation rate constants for the heterogeneous and homogeneous reactions for iron were obtained from the field data. Values for these rate constants averaged 2.2 x10^{-8} L/mg-sec and 6.8 x10^{+14} 1/M^3-sec within a temperature range of 11.7 to 19.2 °C. These values were consistent with values reported from laboratory studies.

4.   The heterogeneous oxidation process is dominant in the CK system. This means that the rate of oxidation should be increased by increasing the suspended ferric concentration. Flow was show to increase the rate of ferrous removal and increase the

rate of oxygenation of water. This increased flow may also have created more turbulence that could have stirred up the bottom of the sediments causing increased amounts of ferric to be suspended catalyzing the oxidation of ferrous causing the heterogeneous oxidation process to dominate in the CK system.

5.   Increased flow had a dramatic effect on the oxidation rate of ferrous and oxygenation of the water in the channel system. For the pond system, stirring should increase the rate of oxidation.

6.   The oxygen gas transfer constant ($K_{L(O2)}$) for the HB oxidation pond with relatively constant flow throughout the year was 1.96 cm/hr. The effect of temperature on the $K_{L(O2)}$ was not clear.

7.   The $K_{L(O2)}$ for the CK channel system increased significantly (from 3.9 to 21.5 cm/hr) with an increased flow. The HB race #2 also had higher $K_{L(O2)}$ values compared to the same flow in the pond. Channel systems are more suited for oxygenation of the water. Temperature remained relatively constant during this analysis so the effects of the flow could be considered the cause of the decrease or increase.

6.   Small amounts of sulfate were found in the sludge of the HB system from the core sample analysis, and sulfate was shown to decrease through the system. Since no mineral phases with sulfate were discovered, the decrease is likely due to adsorption of sulfate onto the ferric oxide precipitate. Computer calculations (MINTEQA2) predicted the removal should be between 0.2 % and 4.7 % of the sulfate by adsorption onto ferric oxide.

8. Less alkalinity was removed than predicted by the loss of ferrous through the system. This is partially explained by the substitution of sulfate for the hydroxide in the precipitate. Another possible explanation is the adsorption of ferrous onto ferric oxide. If ferrous is leaving the system as ferrous and not oxidizing to ferric, this would explain why delta ferrous is larger than what is predicted by the alkalinity. It would also explain the color of the sludge as an olive color initially, and while exposed to the air rapidly changes to an orange red color.

9. Bio-oxidation of the samples between the field and lab was one of the hypotheses used to explain the "alkalinity anomaly". However, this was eliminated as a possible reason. This confirmed that alkaline passive treatment systems with pH values greater than 5 can be considered abiotic.

10. Based on XRD analysis, the precipitate that forms under the initial condition for HB pond #2 is goethite. The Bigham model predicted eventual formation of goethite, but with lepidocrocite as an intermediate step. XRD did show lepidocrocite to be a trace signal for the analysis.

11. Quartz was found up to 10% of sludge weight in the lower part of the sediments. The quartz was determined to be detrital and most likely came from the limestone in the anoxic limestone drain or during rain events and being washed into the system. When the limestone dissolves, the impurities are washed out and settle in the lower part of the sediment layer due to Stoke's settling law.

5.2 Design Considerations

The results of this study show that flow has a favorable impact in the IRR, ferrous oxidation and the oxygen gas rate constant for a channel system. The question is how does flow impact these parameters and how are they related. The IRR is a function of the rate of removal of ferrous in the system. Ferrous oxidation is a function of the amount of oxygen and ferric concentrations in the water. Increased flow increases the oxygen gas rate by causing the water to move more rapidly and have more turbulence and mixing. Increased turbulence and mixing causes the rate of oxygenation to increase and suspension of ferric solids to occur. This does not mean that large flows are favorable, but on the contrary, ways must be found to cause the low flows to have this same turbulence and mixing.

For this research, the channel system at CK seemed to be the more efficient of the two systems studied. When building a passive treatment system, enough head should be provided to allow the water to flow over a series of weirs, water falls or rip rap. This will expose greater surface area of the water to the air, while also having a tendency of the waterfall or turbulence to cause the bottom of the sediments to be stirred up. Stirring will cause more ferric to be suspended in the system thereby increasing the heterogeneous oxidation rate.

The current system for CK seems to be working very well. It currently is too large for the flow that it is treating. It is removing the ferrous iron prior to bend #2. When designing a channel system, a settling pond should still be built at the end of the system to receive the solids and allow them to settle out.

For the case of HB, the current system is net acidic and does not have enough alkalinity to treat the amount of iron in the system. The system releases acidic water (pH around 3) with approximately 75 mg/L ferrous into a local stream. Chemical addition into pond #3 is an option, but an expensive one and will require man-hours.

5.3 Future Research

Throughout this paper, many avenues of future study have already been indicated. The following is a short list:

1. Study of the top layer of film that forms in the AMD system and its effect on oxygenation of the water.

2. Study of adsorption of ferrous onto ferric oxides in the AMD system could prove very helpful in understanding another removal mechanism of iron. There has not been a lot of research done in this area.

3. Study of the effect of weirs, rip rap and water falls ability to increase the rate of oxygenation and resuspension of solids on a system, thereby increasing the rate of oxidation of ferrous.

4. Study of the how ferric concentration effect the rate of oxidation of ferrous in the AMD system.

5. The literature indicated other ions that help or inhibit the oxidation of ferrous. Of these ions sulfate seemed to be one of the most prevalent. Since the AMD systems usually have significant amount of sulfate, a study showing sulfate's

effect on the rate of oxidation should be conducted to better understand the mechanics of the overall system.

6. Study the quartz build up in the sediments to predict the life of the limestone drain.

BIBLIOGRAPHY

Alcorn, G. S., 1996. Evaluation and design of passive systems for the treatment of acid mine drainage. Masters thesis. Penn State University.

Allison, J. D., 1991. MINTEQA2/PRODEFA2, A geochemical assessment model for environmental systems. Version 3.0 Users Manual. Environmental Research Laboratory Office of Research and Development. U. S. EPA. Athens, GA.

Alpers, C. N., Blowers, D. W., Nordstrom, D. K., and Jambor, J. L., 1994. Secondary Minerals and Acid Mine Water Chemistry. *In* Short Course Handbook on Environmental Geochemisty of Sulfide Mine-Wastes (J. L. Jambor and D. W. Blowers, eds.) Waterloo, Ontario, May 1994.

Ames, R. P., 1998. Iron oxidation, gas transfer, and solids formation in passive treatment systems for mine drainage. Master thesis. Penn State University.

Appalachian Regional Commision, 1969. Acid Mine Drainage in Appaclachia, Washington D. C.

Bigham, J. M., Schwertmann, U. and Carlson, L., 1992. Mineralogy of precipitates formed by the biogeochemical oxidation of Fe(II) in mine drainage. *In* Biomineralization Processes of Iron and Manganese: Modern and Ancient Environments (H. C. W. Skinner and R. W. Fitzpatrick, eds.). Catena Verlag, Cremlingen-Destedt, Germany, 219-232.

Bigham, J. M., Carlson, L. and Murad, E. 1994. "Schwetmannite, a new iron oxyhydroxysulfate from Pyhasalmi, Finland, and other localities". *Mineral Mag.*

Brady, K. S., Bigham, J. M., Jaynes, W. F. and Logan, T. J., 1986. "Influence of sulfate on Fe-oxide formation: Comparison with a stream receiving acid mine drainage". *Clays Clay Minerals* 34, 266-274.

Brodie, G. A., 1993. Staged, aerobic constructed wetland to treat acid drainage: case history of Fabius Impoundment1 and overview of the Tennessee Valley Authority's Program. *In* Constructed wetlands for water quality improvement, Lewis Publishers, Boca Raton, Florida, pp. 157-165.

Brown, J. B., 1970. "A chemical study of some synthetic potassium-hydronium jarosites". *Can. Mineral.* 10, 696-703.

Brown, J. B., 1971. "Jarosite-goethite stabilities at 25 degrees Celsius, 1 atm". *Mineralium Deposita.* 6, 245-252.

Carlson, L. and Schwertmann, U. 1981. "Natural ferrihydrites in surface depsoits from Finland and their association with silica". *Geochim, Cosmochim. Acta* 45, 421-429.

Chukhrov, F., Zvijagin, B. B., Gorshkov, A. I., Erilova, L. P. and Balashova, V. V., 1973. "Ferrihydrite". *Izv. Akad. Nauk SSSR ser. Geol.* 44, 23-33.

Colmer, A. R. and Hinkle, M. E. 1947. "The role of microorganisms in acid mine drainage: A preliminary report". *Science* 106, 253-256.

Dousma, Jl, Den Otterlander, D. and De Bruyn, P. L., 1979. "The influence of sulfate ion on the formation of Fe(III) oxides". *J. Inorg. Nuclear Chem.* 41, 1565-1568.

Dzombak, D. A., and Morel, F. M. M., 1990. Surface complexation modeling. John Wiley and Sons. New York, NY. 1990.

Eger, P., Melchert, G., Antonson, D., and Wagner, J. 1993. The use of wetland treatment to remove trace metals from mine drainage. In Constructed Wetlands for Water Quality Improvement (G. A. Moshiri, ed.). Lewis Publ., Ann Arbor, Michigan, 177-178.

Faulkner, B., and Skousen, J. G., 1995. "Effects of land reclamation and passive treatment systems on improving water quality". *Greenlands*, 34-40.

Fennessy, M. S. and Mitsch, W. J. 1989. "Treating coal mine drainage with an artificial Wetland". *J. Water Pollution Control Fed.* 61, 1681-1701.

Gazea, B., Adam, K., and Kontopoulos, A., 1996. "A review of passive systems for the treatment of acid mine drainage". *Mineral engineering*, 9 (1): 23-42.

Gould, W. D., Fujikawa, J. I., and Cook, F. D., 1990. Stable isotope composition of sulfate produced during bacterial oxidation of various metal sulfies. In Proceedings Internat. Symp. Biohydrometallurgy (J. D. Alley, R. G. L. McCready and P. L. Wichlacz, eds.) CANMET Report SP 89-10, 81-92. Department of Energy Mines Resources Canada.

Hedin, R. S., and Nairn, R. W., 1992. Designing and sizing passive mine drainage treatment systems. U. S. Bureau of Mines, Pittsburgh Research Center, Pittsburgh, PA.

Hedin, R. S., Watzlaff, G. R., Nairn, R. W., 1994. "Passive Treatment of Acid Mine Drainage with Limestone". *J. Environ. Qual.* 23:1338-1345, 1994.

Hedin, R. S., and Nairn, R. W., 1993. Contaminant removal capabilities of wetlands constructed to treat coal mine drainage. p. 187-195. *In* G. A. Moshiri (ed), <u>Constructed wetlands for water quality improvements</u>. Lewis Publishers, Boca Raton, FL.

Hedin, R. S., 1996. Recovery of iron oxides from polluted coal mine drainage. Technical proposal from Hedin Environmental. Pittsburgh PA, 1996.

Herlihy, A. T., Kaufmann P. R., Mitch, M. E., Brown, D. D., 1990. "Regional estimates of acid mine drainage impact on streams in the mid-Atlantic and southeastern United States". *Water Air Soil Pollution* 50:91-107.

Hustwit, C. C., Ackerman, T. E., and Erickson, P. E., 1992. "The role of oxygen transfer in acid mine drainage (AMD) Treatment. *Water Environment Research*. 64, 817-823.

Jeon, BH., 1998. <u>The characterization of iron oxides produced from passive treatment of mine drainage</u>. Masters Thesis. Penn State University.

Langmuir, D., 1969. <u>The Gibbs free energies of substances in the system $Fe-O_2-H_2O-CO_2$</u>. U.S. Geol. Surv. Prof. Paper 650-B, 180-184.

Leduc, L. G., Trevors, J. T., and Ferroni, G. D., 1993. <u>Thermal characterization of different isolates of Thiobacillus ferrooxidans</u>. FEMS Microbiology Letter 18, 189-194.

Letterman, R. D. and Mitsch, W. J. 1978. "Impact of mine drainage on a mountain stream in Pennsylvania". *Environ. Pollution* 17, 53-73.

Liu, W., 1996. <u>Removal of trace metals by precipitation of ferrites</u>. Master Thesis. Penn State University.

Lowenstam, H. A., and Weiner, S., 1989. <u>On Biomineralization</u>. Oxford University Press, Oxford, UK, 324 pp.

Mills, A. L., 1985. Acid mine waste drainage: Microbial impact on the recovery of soil and water ecosystems. *In* <u>Soil Reclamation Processes</u> (R. L. Tate and D. A. Klein, eds.). Marcel Dekker, Inc., New York, 35-80.

Milnes, A. R., Fitzpatrick, R. W., Self, P. G., Fordham, A. W. and McClure, S. G. 1992. Natural iron precipitates in a mine retention pond near Javiru, Northern Territory, Australia. *In* <u>Biomineralization Processes of Iron and Manganese, Modern and Ancient Environments</u>. Catena Verlag, Cremlingen-Destedt, Germany, 233-261.

Nairn, R. W., Hedin, R. S., and Watzlaf, G. R., 1992. Generation of alkalinity in an anoxic limestone drain. Paper presented at the 1992 National Meeting of the American Society for Surface Mining and Reclamation. Deluth, Minnesota, June 14-18.

Schulze, D. G., 1981. "Identification of soil iron oxide minerals by differential x-ray diffraction." *Soil Sci. Soc. Am. J.* 45, 437-440.

Schwertmann, U. and Fitzpatrick, R. W., 1977. "Occurance of lepidocrocite and its association with goethite in Natal soils". *Soil Sci. Soc. Am. J.* 41, 1013-1018.

Schwertmann, U., Schulze, D. G. and Murad, E. 1982. "Identification of ferrihydrite in soils by dissolution kinetics, differential x-ray diffraction , and Mossbauer spectroscopy". *Soil Sci. Soc. Am. J.* 46, 869-875.

Schwertmann, U., Schulze, D. G. and Murad, E. 1983. "The effect of pH on the formation of goethite and hematite from ferrihydrite. *Clays Clay minerals* 31, 277-284.

Schwertmann, U., 1985. The effect of pedogenic environments on iron oxide minerals. *In* Advances in Soil Science (B. A. Stewart, ed.). Springer-Verlag, New York, 1, 171-200.

Schwertmann, U., and Cornell, R. M., 1991. Iron oxides in the laboratory. Verlag Chemie, Weinheim, Germany.

Schwertmann, U., Bigham, J. M., Traina, S. J., Winland, R. L., and Wolf, M., 1996. "Schwertmannite and the chemical modeling of iron in acid sulfate waters". *Geochimica et Cosmochimica Acta*, Vol. 12, pp. 2111-2121.

Sheetz, Barry, 1999. Conversation held on 26 February 1999 concerning quartz precipitation at the MRL building.

Singer, P. C., and Stumm, W. 1970. "Acid Mine Drainage: the Rate Determining Step." *Science*, Vol. 167, February 20, American Association for the Advancement of Science, pp. 1121-1123.

Skousen, J. G., 1988. "Chemicals for treating acid mine drainage". *Greenlands* 18 (3): 36-40.

Skousen, J. G., Politan, K., Hilton, T., and Meek, A., 1990. "Acid mine drainage treatment systems: chemicals and costs". *Greenlands* 20 (4): 31-37.

Skousen, J. G., 1995. "Acid mine drainage". *Greenlands* 25(2): 52-55.

Skousen, J. G., and Ziemkiewicz, P. F., 1995. Acid mine drainage control and treatment. West Virginia University and the National Mine Land Reclamation Center. Morgantown WV.

Standard Methods for the Examination of Water and Wastewater. Clesceri L. S., Greenberg A. E., and Trussell R. R. (eds.) 1989. American Health Association, Washington.

Stumm W., and Lee G. F., 1961. "Oxygenation of ferrous iron". *Industrial and Engineering Chemistry*. 53, 143-146.

Sung W., and Morgan J. J., 1980. "Kinetics and product of ferrous iron oxygentation in aqueous systems". *Environmental Science and Technology*. 14, 561-568.

Tamura H., and Nagayama, M. 1976. "Effect of anions on the oxygenation of ferrous ion in neutral solutions". *Journal of Inorganic and Nuclear Chemistry*. 38, 113-117/

Torrent, J. and Barron, V., 1993. Laboratory measurement of soil color: Theory and practice. *In* Soil Color (J. M Bigham and E. J. Ciolkosz, eds.). Soil Sci. Soc. Am., Madison, Wisconsin, 21-37.

Watzlaf, G. R., and Hyman, D. M., 1995. Limitations of passive systems for the treatment of mine drainage. Paper presented at the National Association of Abandoned Mine Land Programs, 17th Annual Conference. French Lick, Indiana. October, 1995.

Williams, E. G., Rose, A. W., Parizek, R. R., and Waters, S. A., 1982. Factors controlling the generation of acid mine drainage, final report, Bureau of Mines, U. S. Department of Interior.

Appendix A

Howe Bridge and C & K Sampling Dates and Data

Table A-1: CK raw data from sampling trips.

	31-Jan-98	1-Mar-98	29-Mar-98	13-May-98	6-Jun-98	3-Jul-98	5-Aug-98	26-Aug-98	26-Sep-98	24-Oct-98
FLOW (gal/min)										
#1 (at seep)	129	124	159	191	136	82	50	37.6	21.4	12.9
Air Temp (°C)	-1	8.5	24	21.5	23.9	28	28.3	28.3	23	0.0
PH										
at Pipe	6.47	6.4	6.33	6.15	6.11	6.21	6.23	6.28	6.38	6.1
B1	6.63	6.57	6.54	6.12	6.22	6.51	6.37	6.37	6.36	6.4
B2	6.99	6.85	6.64	6.16	6.47	6.38	6.35	6.4	6.48	6.5
B3	7.14	6.96	6.66	6.24	6.63	6.58	6.48	6.7	6.92	6.7
DO (O_2 ppm)										
at Pipe	0.3	0.4	0.4	0.4	0.1	0.5	0.4	0.3	0.3	0.5
B1	5.8	5.1	5.5	5.9	4.8	5	4.3	5.6	4.6	8.0
B2	8.9	8.5	7	8.5	7	5	3.5	3.8	7.8	11.0
B3	10	8.2	5.1	8.5	6.2	5.4	5.8	6.6	8	10.6
Water Temp (°C)										
at Pipe	10.4	10.5	10.6	10.9	12.5	11.8	12.2	12.4	12.9	12.0
B1	10.1	11.2	13.4	12.2	13		14.5	12.6	19.3	8.8
B2	8	12.8	20.4	21.1	21.1	16.9	24	24.3	25.1	4.0
B3	6.2	12.6	23.4	22.9	23.8	26.8	23.4	23.6	22.5	3.0
Field Alk (mg/L)										
at Pipe					270	270	300			300
B1						270	284	299	290	250
B2							182	160	180	180
B3						180	152	139	170	170
Field Iron (mg/L)										
at Pipe		92.5	100		110	95		92		
B1										
B2										
B3						30				
FE		9.2	0	2						

Table A-2: HB raw data from sampling trips.

	31-Jan-98	1-Mar-98	29-Mar-98	13-May-98	6-Jun-98	3-Jul-98	5-Aug-98	26-Aug-98	26-Sep-98	25-Oct-98	22-Nov-98	14-Dec-98
FLOW (gal/min)												
#1 (at seep)	25.0	27.4	26.2	27.0	25.0	28.0	21.4	20.7	21.0	21.0	22.4	22.1
#2 (pond #1)	7.0	4.6	5.8	5.0	8.0	8.0	14.6	13.0	16.0	15.0	12.0	12.0
Air Temp (°C)	-1.6	4.7	23.0	16.7	13.3	26.0	23.0	29.0	16.0	5.0	1.0	2.0
PH												
at Pipe	6.47	6.41	6.34	6.20	6.13	6.14	6.13	6.18	6.00	6.04	6.09	6.02
IP1	6.60	6.45	6.38	6.17	6.18	6.10	6.26		6.09			
EP1	6.71	6.51	6.39	6.23	6.26	6.25	6.06	6.08	6.13	6	6.14	5.99
IP2	6.72	6.48	6.42	6.28	6.34	6.24	6.16	6.14	6.11	6.05	6.21	6.02
EP2	6.67	6.30	6.25	5.96	6.02	5.86	5.68	5.83	5.80	5.69	5.84	5.75
FE	3.79	3.69	3.37	2.97	2.78	2.55	2.82	2.81	2.73	2.89	3.04	3.09
DO (O$_2$ ppm)												
at Pipe	0.4	0.3	0.3	0.3	0.3	0.8	0.4	0.5	0.5	0.4	0.4	0.6
IP1	4.4	3.7	3.8	3.0	3.0	3.6	2.4		3.7			
EP1	5.8	4.2	4.2	4.0	5.2	4.0	3.0	3.6	3.8	3.4	6.4	7.6
IP2	7.6	6.5	6.4	6.6	6.0	4.4	4.3	4.6	4.2	4.8	7.4	9.2
EP2	9.5	6.0	6.2	5.1	6.8	3.6	3.0	4.1	3.5	8.2	8.0	8.6
FE	7.5	9.8	10.2	6.5	7.5	5.0	4.3	7.7	7.5	9.0	12.1	9.8
Water Temp (°C)												
at Pipe	8.1	8.5	8.6	9.1	9.4	9.7	9.3	9.7	9.7	8.8	8.4	8.3
IP1	7.7	8.1	9.5	9.8	9.7	10.8	10.2		9.8			
EP1	7.1	8.0	10.9	11.9	11.7	13.3	13.0	13.4	11.1	9.4	7.6	7.4
IP2	6.9	8.0	11.3	12.2	11.6	12.5	13.2	14.2	11.5	9.4	7.5	7.2
EP2	4.8	7.1	11.3	12.9	11.1	13.9	16.5	21.2	11.3	7.3	4.8	4.8
FE	1.5	5.6	15.3	16.2	16.4	22.0	22.6	28.2	16.1	8.7	3.3	4.1
Field Iron (mg/L)												
at Pipe		278	274		155	270	251	265	265	250		
IP1						260	249					
EP1												
IP2												
EP2												
FE												
Field Alkalinity (mg/L)												
at Pipe						150	155		148	140		
IP1						140	149		144			
EP1							140	136	126	135		
IP2							137	132	128	118		
EP2						80	42	74	58	40		
FE												

Appendix B

Results of Metal Analysis

Table B-1: Results of CK metals analysis.

	31-Jan-98	1-Mar-98	29-Mar-98	13-May-98	6-Jun-98	3-Jul-98	5-Aug-98	26-Aug-98	26-Sep-98	24-Oct-98
Ferrous Iron (mg/L)										
at Pipe	97.40	97.00	110.80	89.80	104.50	99.99	90.45	88.20	74.70	82.60
B1		94.40	104.50	82.00	96.70		84.02	85.80	71.30	60.90
B2	69.60	73.60	77.20	64.50	64.70	61.90	30.89	8.65	0.00	0.00
B3	0.00	58.50	38.30	37.70	45.20	22.70	7.35	0.00	0.00	0.00
Ferric Iron (mg/L)										
at Pipe	3.18	7.30	0.00	12.30	0.00	1.24				
B1		5.80	0.00	18.40	0.00	45.20				
B2	8.60	8.30	0.00	19.00	13.30	6.60				
B3	0.00	6.70	11.10	23.90	5.60	12.90				
Calcium (mg/L)										
at Pipe			301.10			279.90				337.50
B1			314.30							321.40
B2			301.10			299.00				321.40
B3			301.10			299.00				
Magnesium (mg/L)										
at Pipe			226.20			207.80				173.50
B1			223.60							176.60
B2			225.70			207.80				175.10
B3			223.10			207.80				
Manganese (mg/L)										
at Pipe										48.20
B1										44.90
B2										44.30
B3										

Table B-2: Results of HB metals analysis.

	31-Jan-98	1-Mar-98	29-Mar-98	13-May-98	6-Jun-98	3-Jul-98	5-Aug-98	26-Aug-98	26-Sep-98	25-Oct-98	22-Nov-98	14-Dec-98
Ferrous Iron (mg/L)												
at Pipe	248.40	235.40	253.60	246.30	252.00	256.70	258.13	251.00	246.90	243.5	220.4	225
IP1	243.70	209.70	226.80	213.60	243.70	249.50	252.69		241.90			
EP1	231.40	202.80	220.00	194.20	224.70	230.70	231.92	227.60	225.20	211.8	210.5	196
IP2	178.00	202.80	216.60	194.60	226.50	230.60	227.65	223.40	219.20	210.44	204.9	189
EP2		171.60	184.40	149.80	174.60	182.20	176.40	178.20	177.20	158.4	158.1	159.1
FE	109.30	95.90	94.70	42.10	28.90	6.73	24.00	27.50	27.20	48.6	55.6	74.8
Ferric Iron (mg/L)												
at Pipe	15.90	31.00	3.60	18.10	5.60	0.00						
IP1	13.20	28.70	0.00	26.40	12.00	3.10						
EP1	8.70	26.30	1.10	31.90	10.70	1.70						
IP2	28.70	26.30	0.00	31.50	10.90	9.40						
EP2		35.10	2.90	39.70	16.10	11.70						
FE	8.10	10.20	1.00	39.30	45.80	53.50						
Calcium (mg/L)												
at Pipe			209.60			197.50				225		
IP1												
EP1			168.90			210.10				208.9		
IP2												
EP2			172.20							209.9		
FE			172.20			210.10				192.8		
Magnesium (mg/L)												
at Pipe			152.70			141.10				110.5		
IP1												
EP1										111.9		
IP2			133.60			136.20						
EP2			131.20							108.9		
FE			111.70			120.10				110.5		
Manganese (mg/L)												
at Pipe										37.9		
IP1												
EP1										35.3		
IP2												
EP2										35.9		
FE										35.3		

Appendix C

Quality Control for the AA Machine
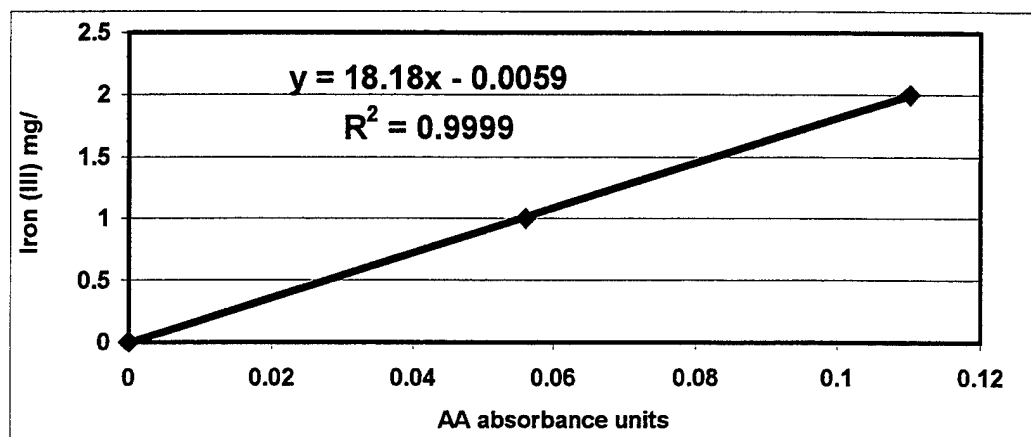
CK STD	AA units
(mg/L)	
0	0
1	0.056
2	0.11

QC number	Iron (mg/L)	AA reading
1	99.4	0.055
2	99.4	0.055
3	99.4	0.055
4	101.2	0.056
Std Dev:	0.909	0.0005
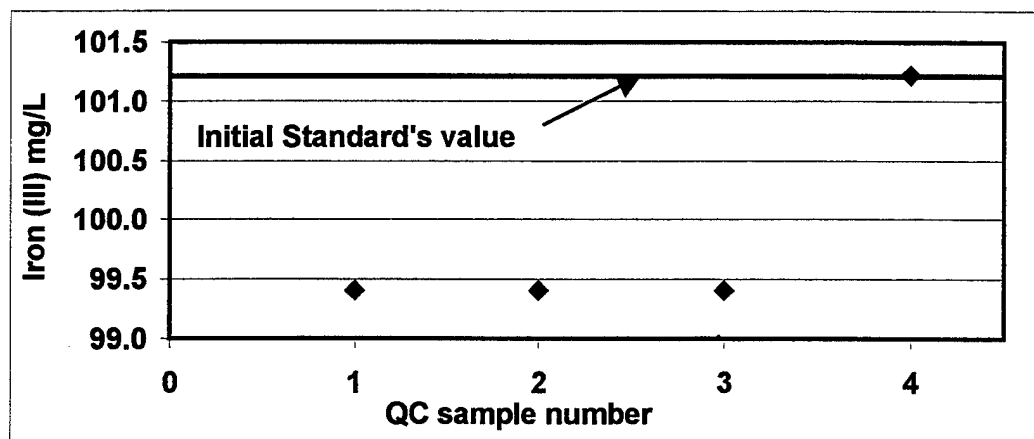
Figure C-1: QC check for 16 July CK total iron experiment.
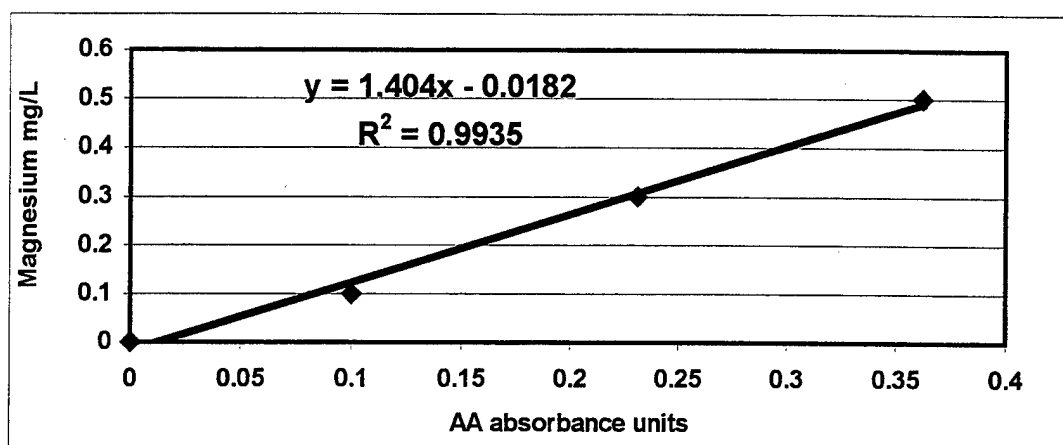
STD	AA units
(mg/L)	
0	0
0.1	0.1
0.3	0.231
0.5	0.362

QC number	Iron (mg/L)	AA reading
1	154.5	0.233
2	155.9	0.235
3	151.0	0.228
4	150.3	0.227
Std Dev:	2.7113	0.0039
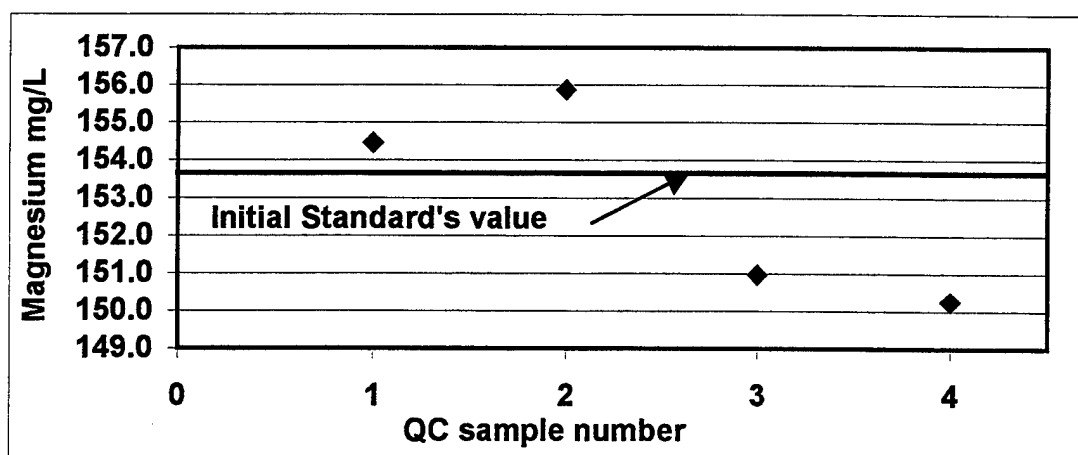
Figure C-2: QC of Magnesium calibration curve on 5 July 1998 for HB and CK samples.
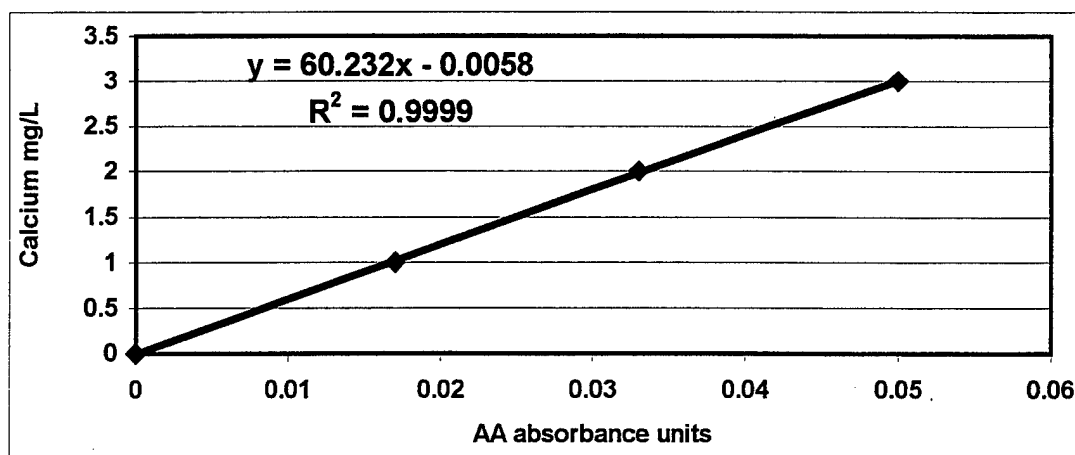
STD	AA units
(mg/L)	
0	0
1	0.017
2	0.033
3	0.05
4	0.062

QC number	Ca (mg/L)	AA reading
1	198.2	0.033
2	204.2	0.034
3	210.2	0.035
4	198.2	0.033
Std Dev:	5.7668	0.0010
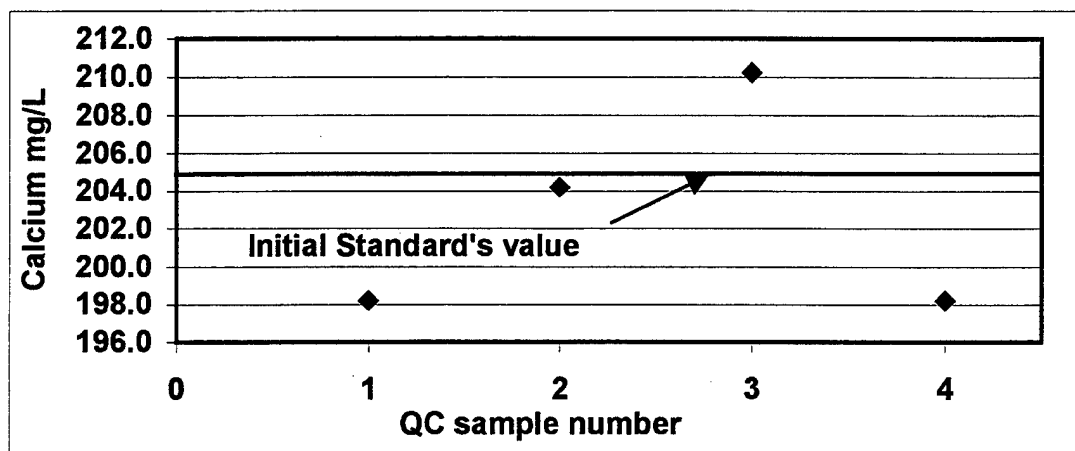
Figure C-3: QC of Calcium calibration curve for 5 July 98 for HB and CK samples.
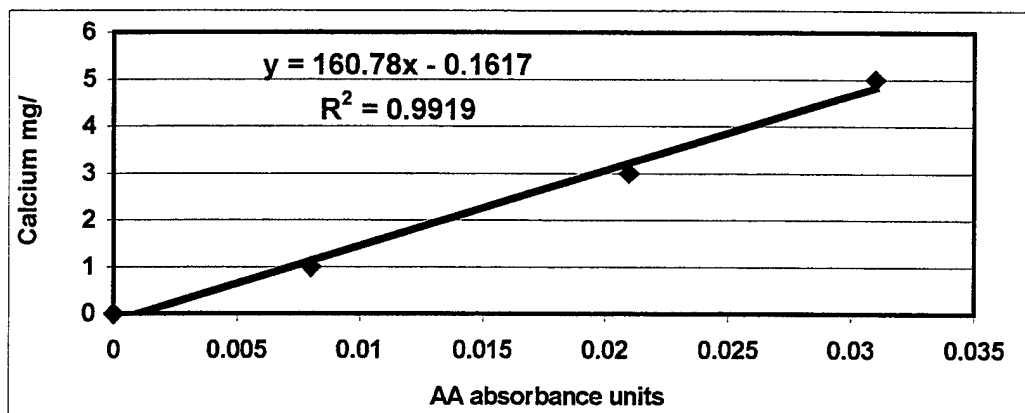
STD (mg/L)	AA units
0	0
1	0.008
3	0.021
5	0.031

QC number	Ca (mg/L)	AA reading
1	337.5	0.022
2	337.5	0.022
3	353.6	0.023
4	321.5	0.021
Std Dev:	13.1276	0.0008
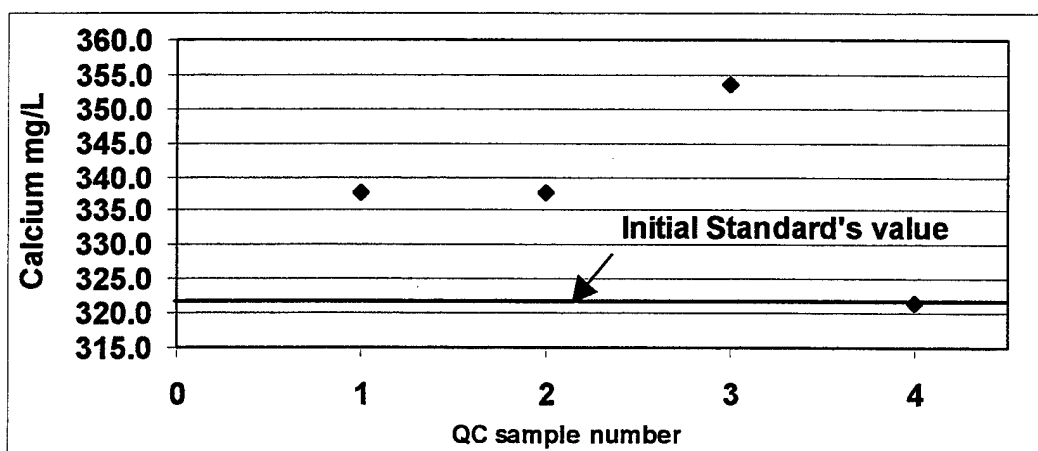
Figure C-4: QC for Calcium calibration curve for 26 Oct 98 for HB and CK samples.
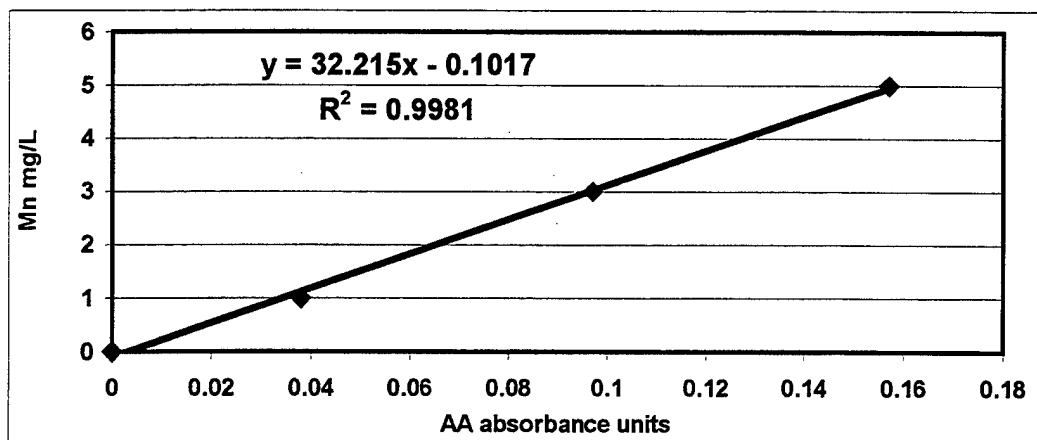
STD (mg/L)	AA units
0	0
1	0.038
3	0.097
5	0.157

QC number	Mn (mg/L)	AA reading
1	23.1	0.039
2	21.2	0.036
3	21.8	0.037
4	22.4	0.038
Std Dev:	0.8318	0.0013
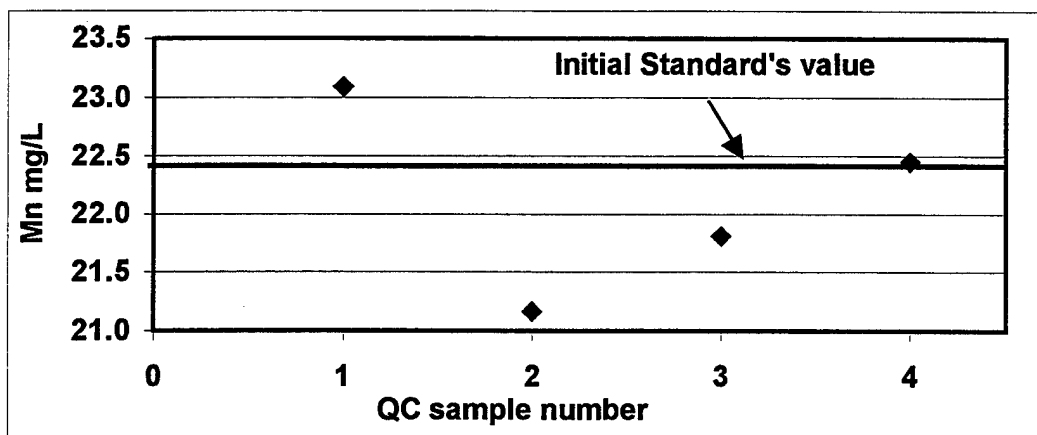
Figure C-5: QC for Mn calibration curve for 26 Oct 98 for HB and CK samples.

$$y = 1.5023x - 0.0067$$
$$R^2 = 0.9989$$
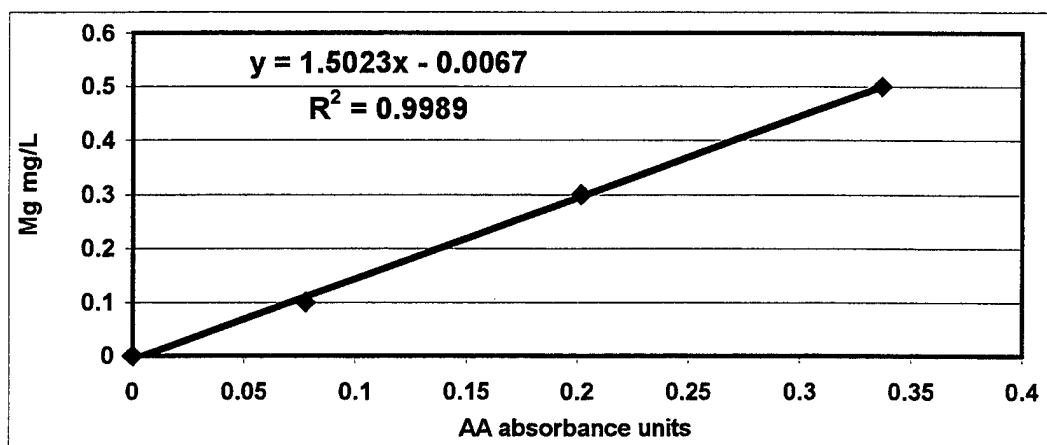
STD (mg/L)	AA units
0	0
0.1	0.078
0.3	0.202
0.5	0.337

QC number	Mg (mg/L)	AA reading
1	107.5	0.076
2	109.0	0.077
3	107.5	0.076
4	110.5	0.078
Std Dev:	1.4383	0.0010
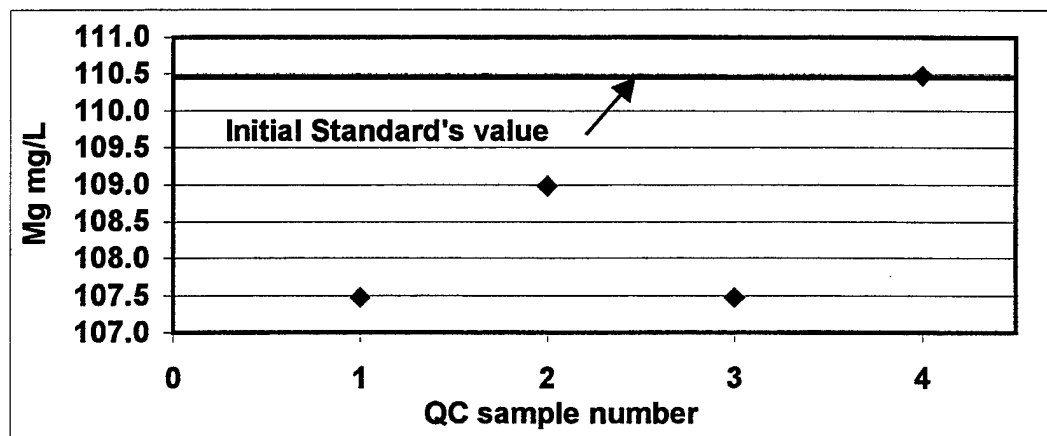
Figure C-6: QC for Magnesium calibration curve for 26 Oct 98 for HB and CK samples.

Appendix D

Quality Control for the UV-Vis Machine

$$y = 4.9711x - 0.5209$$
$$R^2 = 0.9998$$
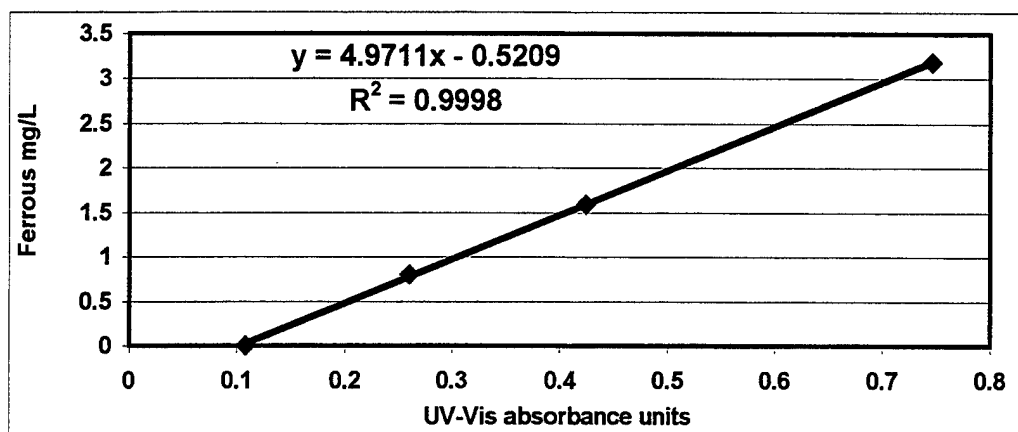
STD	UV-Vis reading
(mg/L)	
0	0.109
0.797	0.26
1.59	0.424
3.18	0.746

QC number	Fe^{2+} (mg/L)	UV-Vis reading
1	1.59	0.424
2	1.58	0.422
3	1.59	0.425
4	1.58	0.423
Std Dev:	0.0064	0.0013
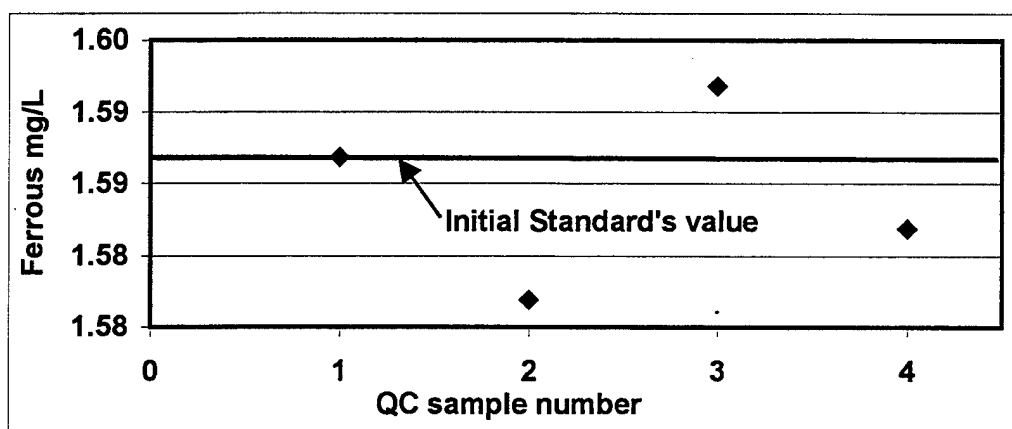
Figure D-1: QC of ferrous calibration curve for UV-Vis on 6 July 98.
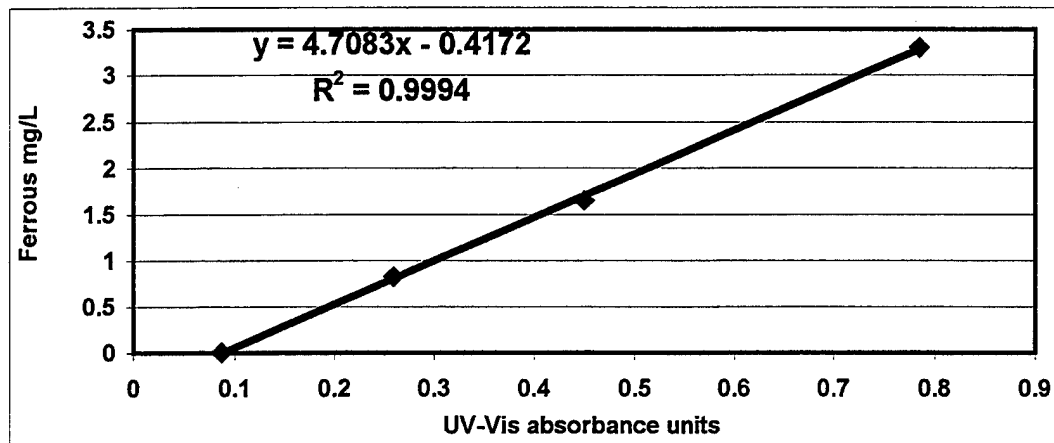
STD	UV-Vis reading
(mg/L)	
0	0.087
0.825	0.259
1.65	0.45
3.3	0.785

QC number	Fe^{2+} (mg/L)	UV-Vis reading
1	1.70	0.45
2	1.71	0.451
3	1.70	0.449
4	1.71	0.452
Std Dev:	0.0061	0.0013
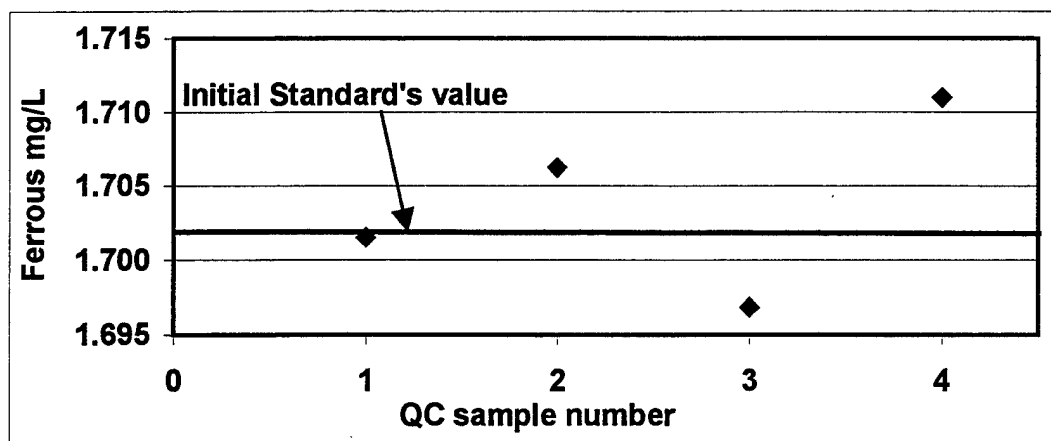
Figure D-2: QC of ferrous calibration curve for UV-Vis on 27 Aug 98.
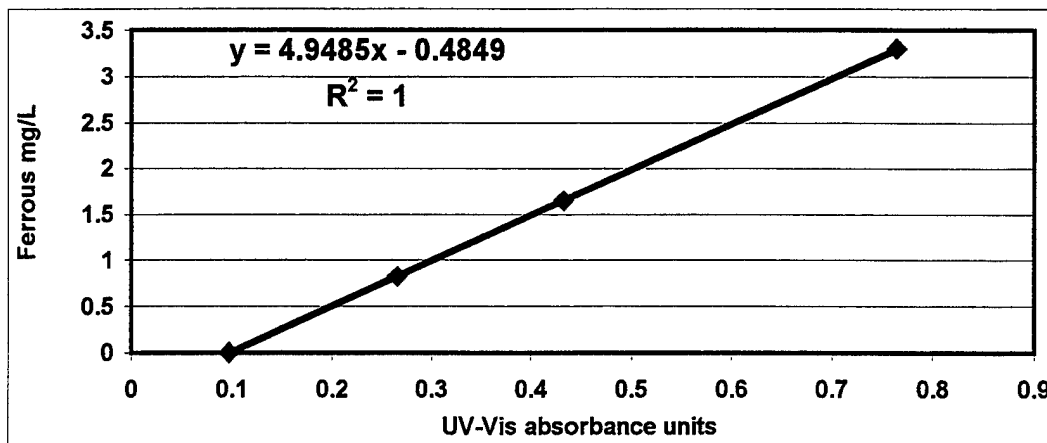
STD	UV-Vis reading
(mg/L)	
0	0.097
0.825	0.265
1.65	0.433
3.3	0.764

QC number	Fe^{2+} (mg/L)	UV-Vis reading
1	1.66	0.434
2	1.66	0.433
3	1.66	0.433
4	1.66	0.433
Std Dev:	0.0025	0.0005
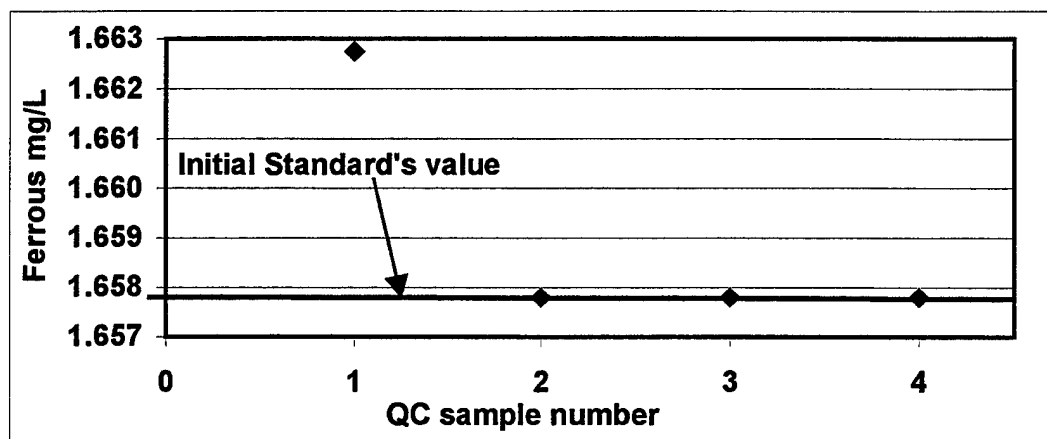
Figure D-3: QC of ferrous calibration curve for UV-Vis on 29 Sept 98.
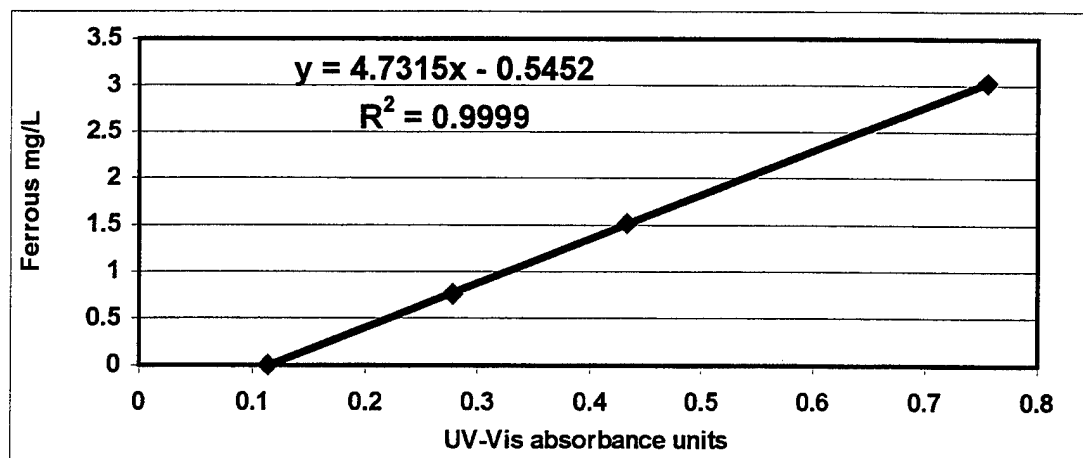
STD	UV-Vis reading
(mg/L)	
0	0.114
0.756	0.278
1.513	0.433
3.026	0.755

QC number	Fe^{2+} (mg/L)	UV-Vis reading
1	1.51	0.434
2	1.49	0.43
3	1.50	0.433
4	1.50	0.432
Std Dev:	0.0081	0.0017
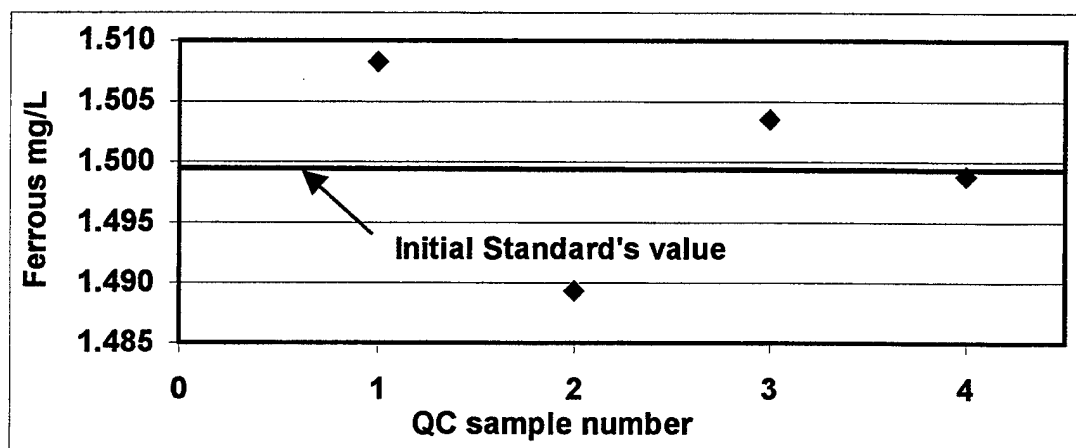
Figure D-4: QC for ferrous calibration curve for UV-Vis on 26 Oct 98.
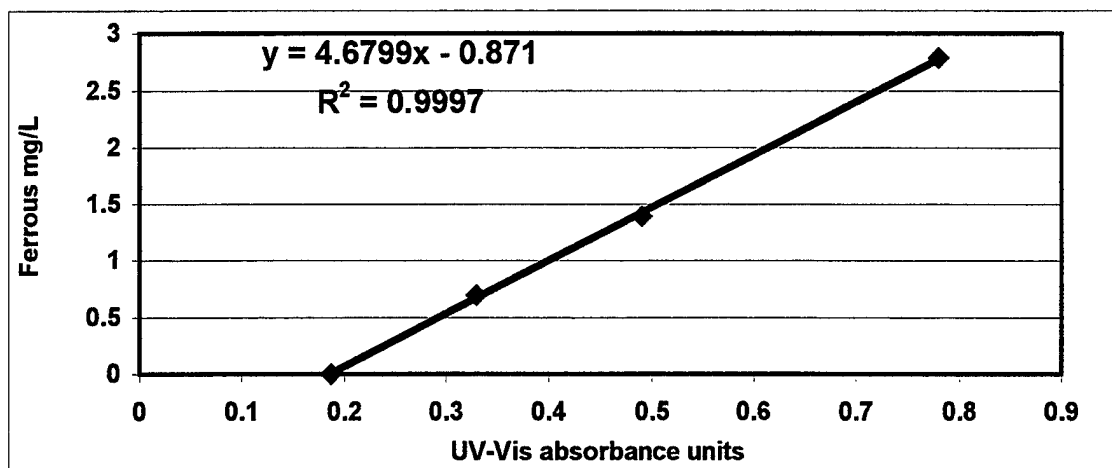
STD	UV-Vis reading
(mg/L)	
0	0.187
0.697	0.33
1.394	0.49
2.788	0.78

QC number	Fe^{2+} (mg/L)	UV-Vis reading
1	0.67	0.329
2	0.68	0.332
3	0.68	0.332
4	0.67	0.33
Std Dev:	0.0070	0.0015
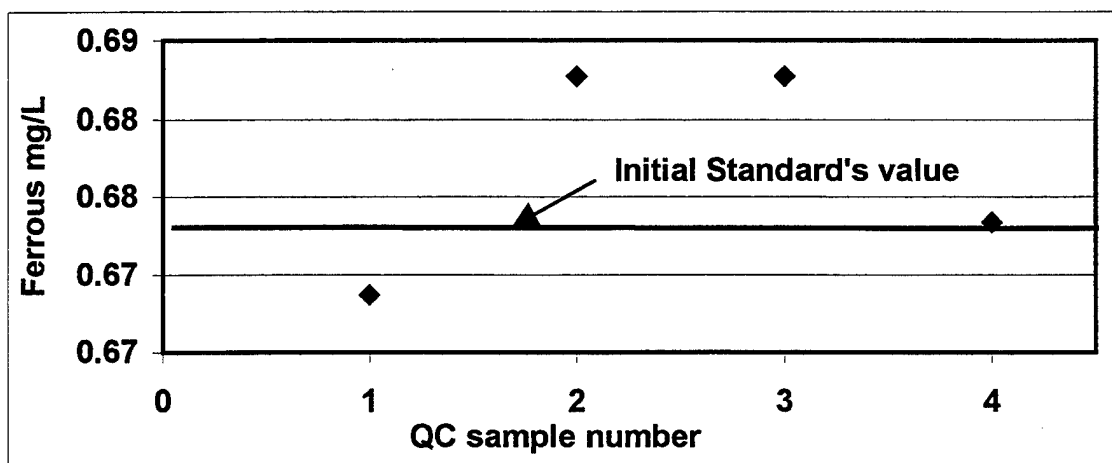
Figure D-5: QC for ferrous calibration curve for UV-Vis on 16 Dec 98.

Appendix E

Quality Control for the TIC Machine

Top chart: Carbon mg vs TIC units

$y = 0.00022x - 0.00032$
$R^2 = 0.99996$
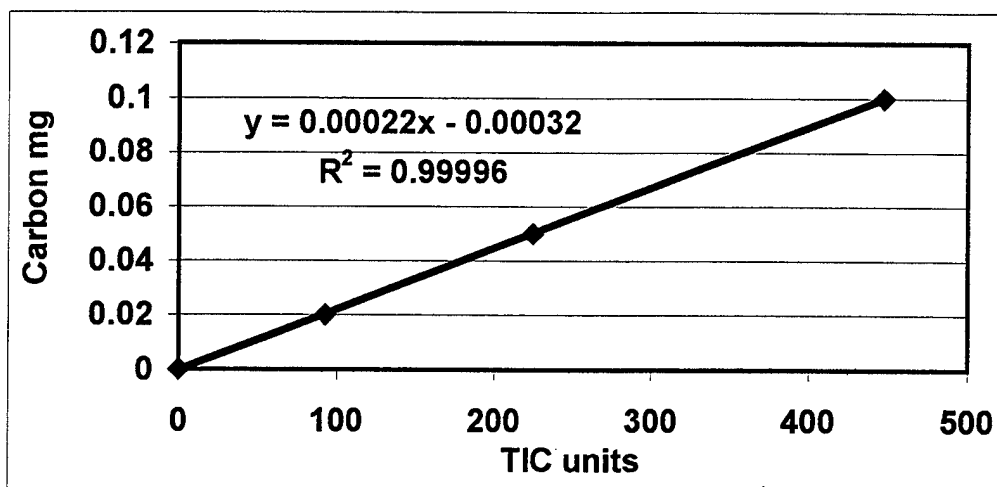
STD (mg)	TIC Units
0	0.0535
0.02	92.26
0.05	225.05
0.1	447.5

QC number	Carbon (mg)	TIC Units
1	0.0489	223.75
2	0.0487	222.95
3	0.0492	225.1
4	0.0490	224.3
5	0.0491	224.85
Std Dev:	0.0002	0.9060

Bottom chart: Carbon mg vs QC sample number

Initial Standard's value
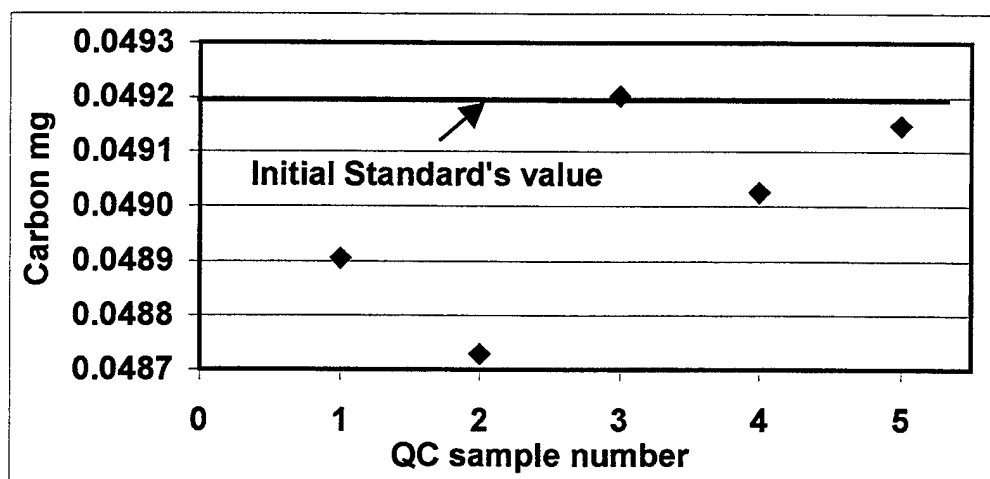
Figure E-1: QC of TIC calibration curve on 5 July 98.
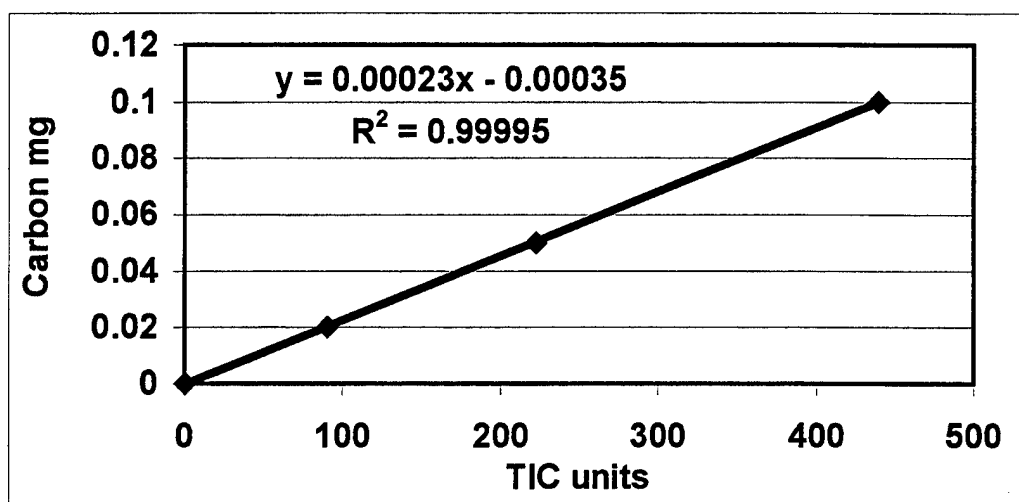
STD	TIC Units
(mg)	
0	0.3515
0.02	89.84
0.05	222.5
0.1	439.45

QC number	Carbon (mg)	TIC Units
1	0.0512	224.1
2	0.0503	220
3	0.0512	224.2
4	0.0516	225.8
5	0.0512	224
Std Dev:	0.0005	2.1545
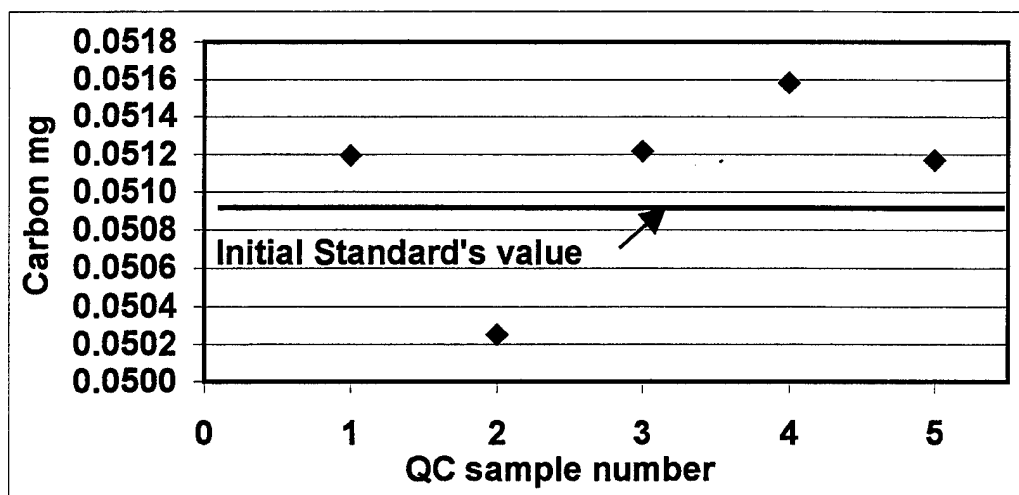
Figure E-2 QC for TIC calibration curve for 6 August 98.

$$y = 0.00022x - 0.00014$$
$$R^2 = 0.99998$$
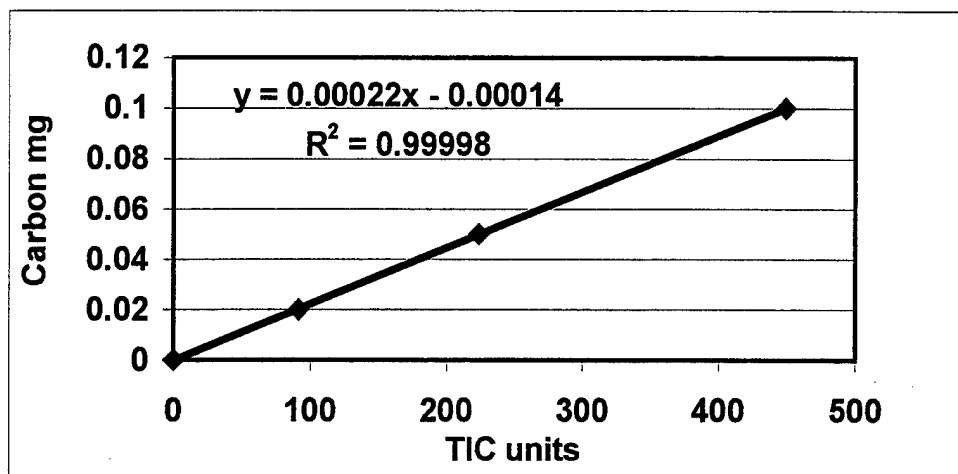
STD	TIC Units
(mg)	
0	0.023
0.02	91.39
0.05	224.1
0.1	448.8

QC number	Carbon (mg)	TIC Units
1	0.0495	225.8
2	0.0492	224.1
3	0.0493	224.9
4	0.0490	223.3
5	0.0491	223.7
Std Dev:	0.0002	0.9990
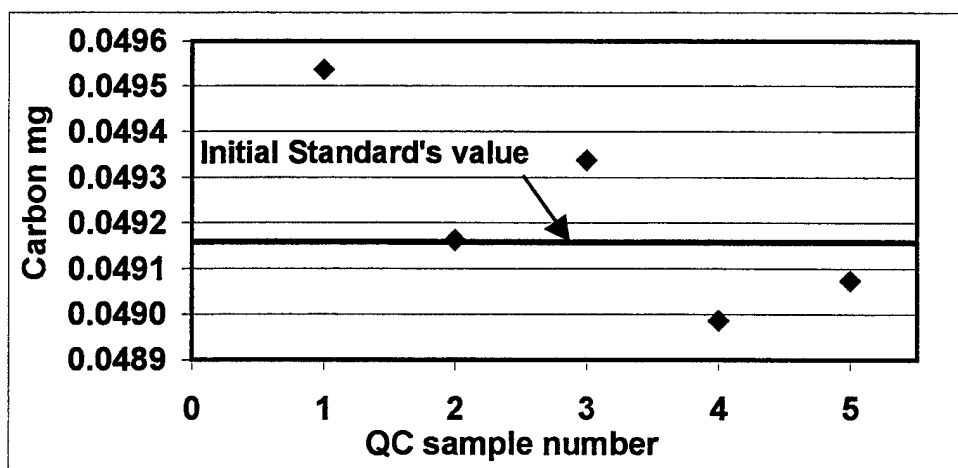
Figure E-3: QC of TIC calibration curve for 27 August 98.
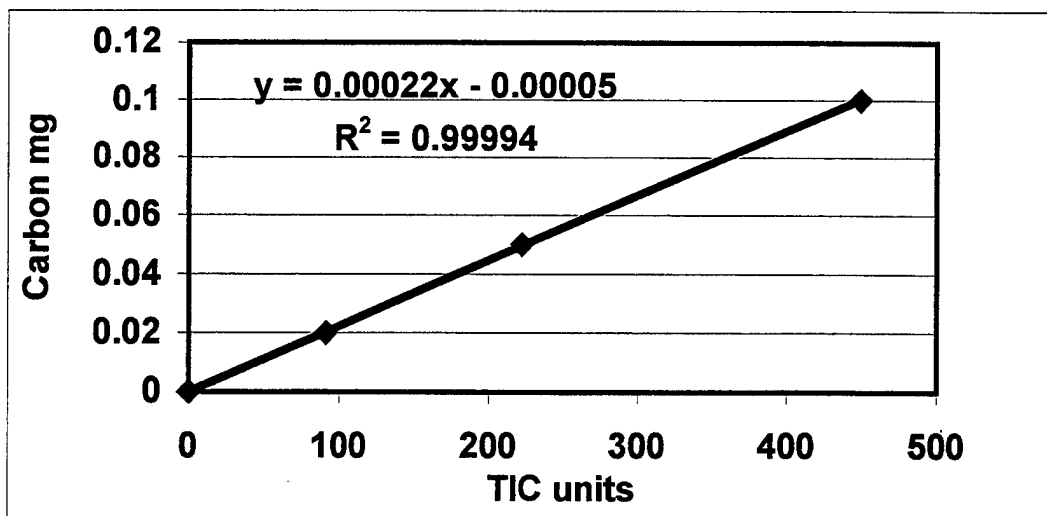
STD (mg)	TIC Units
0	0.0495
0.02	91.465
0.05	222.35
0.1	449.4

QC number	Carbon (mg)	TIC Units
1	0.0486	221
2	0.0489	222.7
3	0.0490	222.9
4	0.0489	222.4
5	0.0490	223.1
Std Dev:	0.0002	0.8349
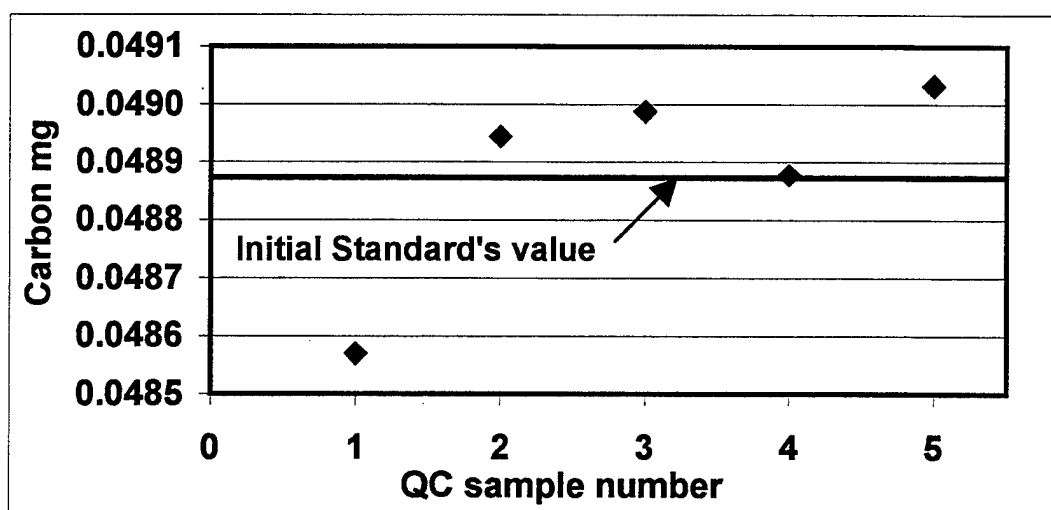
Figure E-4: QC of TIC calibration curve for 28 Sept 98.
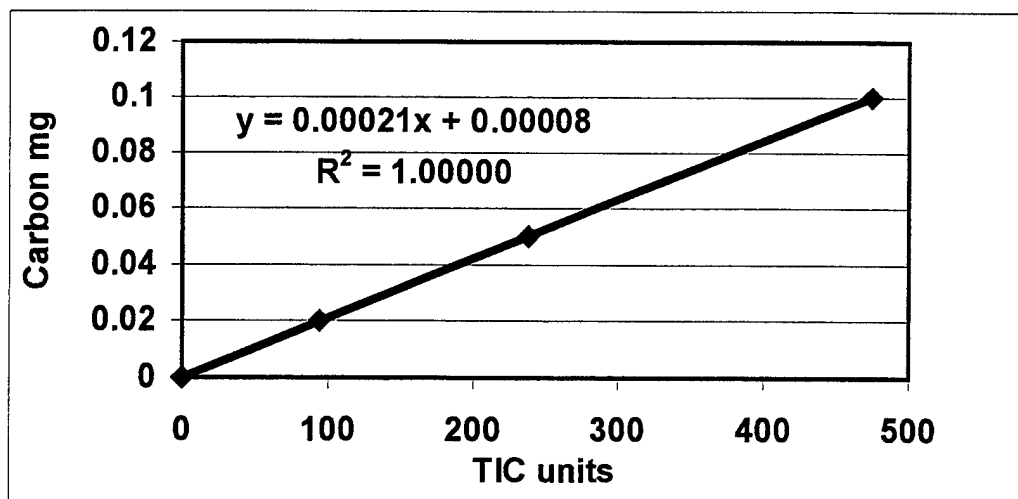
STD	TIC Units
(mg)	
0	0.0085
0.02	94.035
0.05	237.4
0.1	474.85

QC number	Carbon (mg)	TIC Units
1	0.0498	237.7
2	0.0502	239.4
3	0.0499	237.9
4	0.0498	237.4
5	0.0497	237.1
Std Dev:	0.0002	0.8907
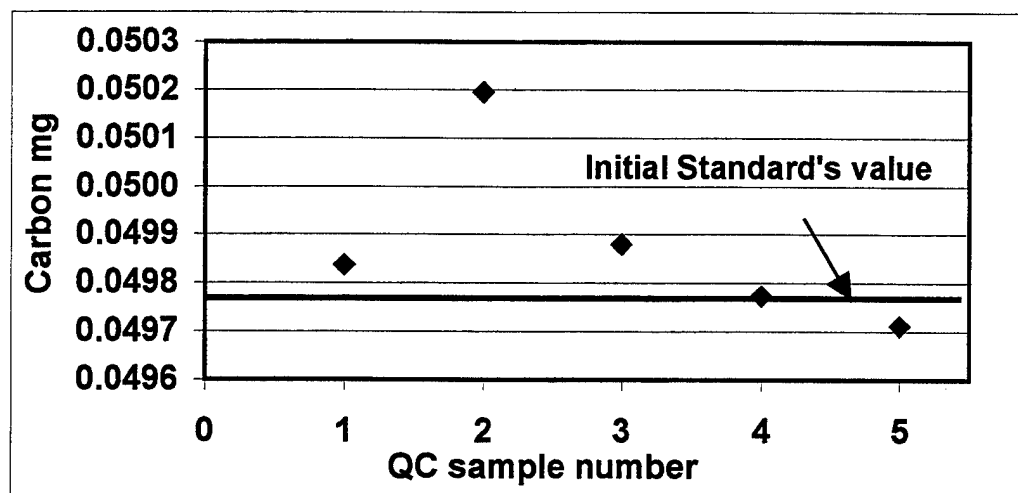
Figure E-5: QC for TIC calibration curve on 16 Dec 98.

Appendix F

MINTEQA2 Output for CK Initial Conditions

C&K Coal Initial Conditions

```
-------------------------------------------------------------------------
Temperature (Celsius):  12.00
Units of concentration: MOLAL
Ionic strength to be computed.
If specified, carbonate concentration represents total inorganic carbon.
Do not automatically terminate if charge imbalance exceeds 30%
Precipitation is allowed only for those solids specified as ALLOWED
  in the input file (if any).
The maximum number of iterations is:  40
The method used to compute activity coefficients is: Davies equation
Intermediate output file
-------------------------------------------------------------------------
       330  0.000E-01   -3.00 y
       280  1.790E-03   -2.75 y
       281  3.500E-05   -4.46 y
       732  1.400E-02   -1.85 y
       470  7.270E-04   -3.14 y
       460  8.230E-03   -2.08 y
       150  7.500E-03   -2.12 y
       140  5.000E-03   -2.30 y

H2O has been inserted as a COMPONENT
  3   1
     330     3.0000      0.0000


  1)  The fixed pH is:    6.00
  2)  The log activity guesses for all components are as computed at
      the point of FIRST convergence in the previous problem.


  PC MINTEQA2 v3.10    DATE OF CALCULATIONS:  2-FEB-99  TIME: 14:23: 2
```

PARAMETERS OF THE COMPONENT MOST OUT OF BALANCE:

ITER	NAME	TOTAL MOL	DIFF FXN	LOG ACTVTY	RESIDUAL
0	Ca+2	7.500E-03	-2.914E-03	-2.59319	2.913E-03
1	Ca+2	7.500E-03	3.015E-04	-2.41562	3.008E-04
2	Ca+2	7.500E-03	3.452E-03	-2.42536	3.452E-03
3	Ca+2	7.500E-03	7.110E-04	-2.56187	7.102E-04
4	Ca+2	7.500E-03	6.297E-05	-2.59318	6.222E-05
5	Ca+2	7.500E-03	5.103E-06	-2.59613	4.353E-06

ID	NAME	ANAL MOL	CALC MOL	LOG ACTVTY	GAMMA	DIFF FXN
140	CO3-2	5.000E-03	1.154E-07	-7.27208	0.463037	4.333E-08
280	Fe+2	1.790E-03	1.400E-03	-3.18815	0.463037	1.574E-07
281	Fe+3	3.500E-05	7.554E-11	-10.87419	0.176862	9.897E-10
732	SO4-2	1.400E-02	9.461E-03	-2.35845	0.463037	1.056E-06
470	Mn+2	7.270E-04	5.504E-04	-3.59370	0.463037	6.198E-08
460	Mg+2	8.230E-03	6.189E-03	-2.54277	0.463037	6.962E-07
150	Ca+2	7.500E-03	5.470E-03	-2.59637	0.463037	6.138E-07
2	H2O	0.000E-01	-7.036E-05	-0.00028	1.000000	0.000E-01
330	H+1	0.000E-01	1.212E-06	-6.00000	0.824905	0.000E-01

Type I - COMPONENTS AS SPECIES IN SOLUTION

ID	NAME	CALC MOL	ACTIVITY	LOG ACTVTY	GAMMA	NEW LOGK
330	H+1	1.212E-06	1.000E-06	-6.00000	0.82490	0.084
280	Fe+2	1.400E-03	6.484E-04	-3.18815	0.46304	0.334
281	Fe+3	7.554E-11	1.336E-11	-10.87419	0.17686	0.752
732	SO4-2	9.461E-03	4.381E-03	-2.35845	0.46304	0.334

470	Mn+2	5.504E-04	2.549E-04	-3.59370	0.46304	0.334
460	Mg+2	6.189E-03	2.866E-03	-2.54277	0.46304	0.334
150	Ca+2	5.470E-03	2.533E-03	-2.59637	0.46304	0.334
140	CO3-2	1.154E-07	5.345E-08	-7.27208	0.46304	0.334

Type II - OTHER SPECIES IN SOLUTION OR ADSORBED

ID	NAME	CALC MOL	ACTIVITY	LOG ACTVTY	GAMMA	NEW LOGK
3301401	H2CO3 AQ	3.015E-03	3.048E-03	-2.51599	1.01092	16.751
3307320	HSO4 -	3.622E-07	2.988E-07	-6.52462	0.82490	1.917
3300020	OH-	4.359E-09	3.596E-09	-8.44421	0.82490	-14.360
4603300	MgOH +	1.753E-09	1.446E-09	-8.83987	0.82490	-12.213
4601400	MgCO3 AQ	1.184E-07	1.197E-07	-6.92183	1.01092	2.888
4601401	MgHCO3 +	5.859E-05	4.833E-05	-4.31576	0.82490	11.583
4607320	MgSO4 AQ	1.983E-03	2.005E-03	-2.69796	1.01092	2.199
1503300	CaOH +	2.531E-10	2.088E-10	-9.68035	0.82490	-13.000
1501400	CaHCO3 +	3.325E-05	2.743E-05	-4.56175	0.82490	11.390
1501401	CaCO3 AQ	1.508E-07	1.524E-07	-6.81702	1.01092	3.047
1507320	CaSO4 AQ	1.997E-03	2.019E-03	-2.69494	1.01092	2.255
2803300	FeOH +	8.997E-08	7.422E-08	-7.12949	0.82490	-9.857
2803301	FeOH3 -1	7.623E-18	6.288E-18	-17.20149	0.82490	-31.929
2807320	FeSO4 AQ	3.897E-04	3.940E-04	-3.40453	1.01092	2.137
2803302	FeOH2 AQ	1.914E-13	1.935E-13	-12.71323	1.01092	-21.529
2813300	FeOH +2	8.364E-08	3.873E-08	-7.41196	0.46304	-2.203
2817320	FeSO4 +	4.368E-10	3.603E-10	-9.44329	0.82490	3.873
2813301	FeOH2 +	3.458E-05	2.853E-05	-4.54475	0.82490	-5.586
2813302	FeOH3 AQ	3.313E-07	3.349E-07	-6.47504	1.01092	-13.605
2813303	FeOH4 -	4.058E-09	3.347E-09	-8.47532	0.82490	-21.516
2817321	Fe(SO4)2 -	5.739E-11	4.734E-11	-10.32479	0.82490	5.350
2813304	Fe2(OH)2+4	1.540E-12	7.079E-14	-13.15005	0.04597	-2.064
2813305	Fe3(OH)4+5	4.879E-14	3.967E-16	-15.40154	0.00813	-4.688
4703300	MnOH +	2.621E-09	2.162E-09	-8.66513	0.82490	-10.988
4703301	Mn(OH)3 -1	4.887E-21	4.031E-21	-20.39454	0.82490	-34.716
4707320	MnSO4 AQ	1.701E-04	1.719E-04	-3.76465	1.01092	2.183
4701400	MnHCO3 +	6.574E-06	5.423E-06	-5.26577	0.82490	11.684
3301400	HCO3 -	1.886E-03	1.556E-03	-2.80801	0.82490	10.548

Type III - SPECIES WITH FIXED ACTIVITY

ID	NAME	CALC MOL	LOG MOL	NEW LOGK	DH
2	H2O	-7.036E-05	-4.153	0.000	0.000
330	H+1	-7.946E-03	-2.100	6.000	0.000

Type VI - EXCLUDED SPECIES (not included in mole balance)

ID	NAME	CALC MOL	LOG MOL	NEW LOGK	DH
3301403	CO2 (g)	8.052E-02	-1.094	18.178	-0.530

PERCENTAGE DISTRIBUTION OF COMPONENTS AMONG
TYPE I and TYPE II (dissolved and adsorbed) species

CO3-2

     60.3   PERCENT BOUND IN SPECIES #3301401   H2CO3 AQ

     1.2   PERCENT BOUND IN SPECIES #4601401   MgHCO3 +

     37.7   PERCENT BOUND IN SPECIES #3301400   HCO3 -

Fe+2

    78.2   PERCENT BOUND IN SPECIES #   280   Fe+2

    21.8   PERCENT BOUND IN SPECIES #2807320   FeSO4 AQ

Fe+3

    98.8   PERCENT BOUND IN SPECIES #2813301   FeOH2 +

SO4-2

    67.6   PERCENT BOUND IN SPECIES #   732   SO4-2

    14.2   PERCENT BOUND IN SPECIES #4607320   MgSO4 AQ

    14.3   PERCENT BOUND IN SPECIES #1507320   CaSO4 AQ

     2.8   PERCENT BOUND IN SPECIES #2807320   FeSO4 AQ

     1.2   PERCENT BOUND IN SPECIES #4707320   MnSO4 AQ

Mn+2

    75.7   PERCENT BOUND IN SPECIES #   470   Mn+2

    23.4   PERCENT BOUND IN SPECIES #4707320   MnSO4 AQ

Mg+2

    75.2   PERCENT BOUND IN SPECIES #   460   Mg+2

    24.1   PERCENT BOUND IN SPECIES #4607320   MgSO4 AQ

Ca+2

    72.9   PERCENT BOUND IN SPECIES #   150   Ca+2

    26.6   PERCENT BOUND IN SPECIES #1507320   CaSO4 AQ

H2O

    98.3   PERCENT BOUND IN SPECIES #2813301   FeOH2 +

     1.4   PERCENT BOUND IN SPECIES #2813302   FeOH3 AQ

H+1

    75.9   PERCENT BOUND IN SPECIES #3301401   H2CO3 AQ

    23.7   PERCENT BOUND IN SPECIES #3301400   HCO3 -


```
      --------------------------------------------------------
      ----------- EQUILIBRATED MASS DISTRIBUTION -----------
```

IDX	NAME	DISSOLVED		SORBED		PRECIPITATED	
		MOL/KG	PERCENT	MOL/KG	PERCENT	MOL/KG	PERCENT
140	CO3-2	5.000E-03	100.0	0.000E-01	0.0	0.000E-01	0.0
280	Fe+2	1.790E-03	100.0	0.000E-01	0.0	0.000E-01	0.0
281	Fe+3	3.500E-05	100.0	0.000E-01	0.0	0.000E-01	0.0
732	SO4-2	1.400E-02	100.0	0.000E-01	0.0	0.000E-01	0.0
470	Mn+2	7.271E-04	100.0	0.000E-01	0.0	0.000E-01	0.0

```
460  Mg+2           8.231E-03   100.0   0.000E-01   0.0   0.000E-01   0.0
150  Ca+2           7.501E-03   100.0   0.000E-01   0.0   0.000E-01   0.0
  2  H2O            7.036E-05   100.0   0.000E-01   0.0   0.000E-01   0.0
330  H+1            7.946E-03   100.0   0.000E-01   0.0   0.000E-01   0.0
```

Charge Balance: SPECIATED

Sum of CATIONS = 2.735E-02 Sum of ANIONS   2.081E-02

PERCENT DIFFERENCE =   1.359E+01   (ANIONS - CATIONS)/(ANIONS + CATIONS)

EQUILIBRIUM IONIC STRENGTH (m) =   4.715E-02

EQUILIBRIUM pH   =   6.000

DATE ID NUMBER: 990202
TIME ID NUMBER: 14230331

Saturation indices and stoichiometry of all minerals

```
    ID #      NAME      Sat. Index        Stoichiometry in [brackets]
  6015000 ANHYDRITE      -0.444    [  1.000] 150  [  1.000] 732
  5015000 ARAGONITE      -1.642    [  1.000] 150  [  1.000] 140
  5046000 ARTINITE      -10.919    [ -2.000] 330  [  2.000] 460  [  1.000] 140
                                   [  5.000]   2
  2046000 BRUCITE        -8.199    [  1.000] 460  [  2.000]   2  [ -2.000] 330
  5015001 CALCITE        -1.456    [  1.000] 150  [  1.000] 140
  5015002 DOLOMITE       -2.960    [  1.000] 150  [  1.000] 460  [  2.000] 140
  6046000 EPSOMITE       -2.669    [  1.000] 460  [  1.000] 732  [  7.000]   2
  2028100 FERRIHYDRITE    2.234    [ -3.000] 330  [  1.000] 281  [  3.000]   2
  2028101 FE3(OH)8        2.839    [ -8.000] 330  [  2.000] 281  [  1.000] 280
                                   [  8.000]   2
  6028100 FE2(SO4)3     -34.379    [  2.000] 281  [  3.000] 732
  2028102 GOETHITE        6.141    [ -3.000] 330  [  1.000] 281  [  2.000]   2
  6015001 GYPSUM         -0.099    [  1.000] 150  [  1.000] 732  [  2.000]   2
  3028100 HEMATITE       17.228    [ -6.000] 330  [  2.000] 281  [  3.000]   2
  5015003 HUNTITE       -10.206    [  3.000] 460  [  1.000] 150  [  4.000] 140
  5046001 HYDRMAGNESIT  -22.782    [  5.000] 460  [  4.000] 140  [ -2.000] 330
                                   [  6.000]   2
  6028101 JAROSITE H      2.916    [ -5.000] 330  [  3.000] 281  [  2.000] 732
                                   [  7.000]   2
  3028101 MAGHEMITE       7.865    [ -6.000] 330  [  2.000] 281  [  3.000]   2
  5046002 MAGNESITE      -1.992    [  1.000] 460  [  1.000] 140
  3028000 MAGNETITE      17.639    [ -8.000] 330  [  2.000] 281  [  1.000] 280
                                   [  4.000]   2
  6028000 MELANTERITE    -2.983    [  1.000] 280  [  1.000] 732  [  7.000]   2
  5046003 NESQUEHONITE   -4.388    [  1.000] 460  [  1.000] 140  [  3.000]   2
  5028000 SIDERITE       -0.088    [  1.000] 280  [  1.000] 140
  2047003 PYROCROITE     -7.437    [ -2.000] 330  [  1.000] 470  [  2.000]   2
  5047000 RHODOCHROSIT   -0.525    [  1.000] 470  [  1.000] 140
  6047000 MNSO4          -9.138    [  1.000] 470  [  1.000] 732
  2015000 LIME          -24.940    [ -2.000] 330  [  1.000] 150  [  1.000]   2
  2015001 PORTLANDITE   -14.297    [ -2.000] 330  [  1.000] 150  [  2.000]   2
  2028000 WUSTITE        -3.537    [ -2.000] 330  [  0.947] 280  [  1.000]   2
  2046001 PERICLASE     -13.261    [ -2.000] 330  [  1.000] 460  [  1.000]   2
  3046001 MAG-FERRITE     4.716    [ -8.000] 330  [  1.000] 460  [  2.000] 281
                                   [  4.000]   2
  3028102 LEPIDOCROCIT    5.754    [ -3.000] 330  [  1.000] 281  [  2.000]   2
```

a

Appendix G

MINTEQA2 Output for HB Pond #2 Initial Conditions

HB IP2 Initial Conditions

```
-------------------------------------------------------------------------------
Temperature (Celsius):  15.00
Units of concentration: MOLAL
Ionic strength to be computed.
If specified, carbonate concentration represents total inorganic carbon.
Do not automatically terminate if charge imbalance exceeds 30%
Precipitation is allowed only for those solids specified as ALLOWED
  in the input file (if any).
The maximum number of iterations is:  40
The method used to compute activity coefficients is: Davies equation
Intermediate output file

-------------------------------------------------------------------------------
      330  0.000E-01   -3.00 y
      280  2.829E-03   -2.54 y
      281  9.320E-04   -3.03 y
      150  5.600E-03   -2.25 y
      460  6.000E-03   -2.22 y
      732  1.400E-02   -1.85 y
      140  4.166E-04   -3.38 y
      470  7.270E-04   -3.14 y

H2O has been inserted as a COMPONENT
  3    1
      330      3.0000     0.0000


INPUT DATA BEFORE TYPE MODIFICATIONS

    ID        NAME     ACTIVITY GUESS   LOG GUESS   ANAL TOTAL
    330  H+1            1.000E-03        -3.000     0.000E-01
    280  Fe+2           2.884E-03        -2.540     2.829E-03
    281  Fe+3           9.333E-04        -3.030     9.320E-04
    150  Ca+2           5.623E-03        -2.250     5.600E-03
    460  Mg+2           6.026E-03        -2.220     6.000E-03
    732  SO4-2          1.413E-02        -1.850     1.400E-02
    140  CO3-2          4.169E-04        -3.380     4.166E-04
    470  Mn+2           7.244E-04        -3.140     7.270E-04
      2  H2O            1.000E+00         0.000     0.000E-01


The input for this sweep is identical to the initial sweep except:
  1)  The fixed pH is:    6.00
  2)  The log activity guesses for all components are as computed at
      the point of FIRST convergence in the previous problem.


PARAMETERS OF THE COMPONENT MOST OUT OF BALANCE:

    ITER      NAME      TOTAL MOL    DIFF FXN   LOG ACTVTY    RESIDUAL
      0   CO3-2        4.166E-04   -4.106E-04   -10.14041    4.106E-04
      1   CO3-2        4.166E-04    2.428E-06    -8.29791    2.386E-06
      2   CO3-2        4.166E-04    2.258E-05    -8.30021    2.254E-05
      3   CO3-2        4.166E-04    3.400E-06    -8.32096    3.358E-06
      4   CO3-2        4.166E-04    2.806E-07    -8.32399    2.389E-07
      5   SO4-2        1.400E-02    7.806E-06    -2.32777    6.406E-06


ID       NAME    ANAL MOL    CALC MOL   LOG ACTVTY    GAMMA     DIFF FXN
470  Mn+2       7.270E-04   5.363E-04   -3.59338    0.475602   5.052E-08
280  Fe+2       2.829E-03   2.134E-03   -2.99358    0.475602   2.012E-07
281  Fe+3       9.320E-04   1.905E-09   -9.44626    0.187845   2.215E-08
150  Ca+2       5.600E-03   3.960E-03   -2.72506    0.475602   3.722E-07
460  Mg+2       6.000E-03   4.401E-03   -2.67921    0.475602   4.144E-07
```

732	SO4-2	1.400E-02	9.881E-03	-2.32795	0.475602	9.286E-07
140	CO3-2	4.166E-04	9.965E-09	-8.32427	0.475602	2.956E-09
2	H2O	0.000E-01	-1.871E-03	-0.00023	1.000000	0.000E-01
330	H+1	0.000E-01	1.204E-06	-6.00000	0.830445	0.000E-01

Type I - COMPONENTS AS SPECIES IN SOLUTION

ID	NAME	CALC MOL	ACTIVITY	LOG ACTVTY	GAMMA	NEW LOGK
330	H+1	1.204E-06	1.000E-06	-6.00000	0.83045	0.081
280	Fe+2	2.134E-03	1.015E-03	-2.99358	0.47560	0.323
281	Fe+3	1.905E-09	3.579E-10	-9.44626	0.18784	0.726
150	Ca+2	3.960E-03	1.883E-03	-2.72506	0.47560	0.323
460	Mg+2	4.401E-03	2.093E-03	-2.67921	0.47560	0.323
732	SO4-2	9.881E-03	4.699E-03	-2.32795	0.47560	0.323
140	CO3-2	9.965E-09	4.739E-09	-8.32427	0.47560	0.323
470	Mn+2	5.363E-04	2.550E-04	-3.59338	0.47560	0.323

Type II - OTHER SPECIES IN SOLUTION OR ADSORBED

ID	NAME	CALC MOL	ACTIVITY	LOG ACTVTY	GAMMA	NEW LOGK
3301401	H2CO3 AQ	2.568E-04	2.594E-04	-3.58611	1.00980	16.734
3307320	HSO4 -	4.181E-07	3.472E-07	-6.45944	0.83045	1.949
3300020	OH-	5.534E-09	4.595E-09	-8.33769	0.83045	-14.257
4603300	MgOH +	1.684E-09	1.398E-09	-8.85438	0.83045	-12.094
4601400	MgCO3 AQ	8.041E-09	8.120E-09	-8.09045	1.00980	2.909
4601401	MgHCO3 +	3.532E-06	2.933E-06	-5.53263	0.83045	11.552
4607320	MgSO4 AQ	1.596E-03	1.612E-03	-2.79275	1.00980	2.210
1503300	CaOH +	2.442E-10	2.028E-10	-9.69302	0.83045	-12.887
1501400	CaHCO3 +	2.205E-06	1.831E-06	-5.73733	0.83045	11.393
1501401	CaCO3 AQ	1.038E-08	1.048E-08	-7.97959	1.00980	3.066
1507320	CaSO4 AQ	1.638E-03	1.654E-03	-2.78141	1.00980	2.267
2803300	FeOH +	1.783E-07	1.481E-07	-6.82956	0.83045	-9.755
2803301	FeOH3 -1	2.069E-17	1.718E-17	-16.76502	0.83045	-31.690
2807320	FeSO4 AQ	6.951E-04	7.019E-04	-3.15370	1.00980	2.164
2803302	FeOH2 AQ	5.071E-13	5.121E-13	-12.29065	1.00980	-21.301
2813300	FeOH +2	2.641E-06	1.256E-06	-5.90101	0.47560	-2.132
2817320	FeSO4 +	1.340E-08	1.113E-08	-7.95368	0.83045	3.901
2813301	FeOH2 +	9.204E-04	7.643E-04	-3.11673	0.83045	-5.589
2813302	FeOH3 AQ	8.888E-06	8.975E-06	-5.04696	1.00980	-13.604
2813303	FeOH4 -	1.080E-07	8.970E-08	-7.04720	0.83045	-21.519
2817321	Fe(SO4)2 -	1.912E-09	1.588E-09	-8.79918	0.83045	5.384
2813304	Fe2(OH)2+4	1.272E-09	6.510E-11	-10.18639	0.05117	-2.002
2813305	Fe3(OH)4+5	1.032E-09	9.920E-12	-11.00347	0.00961	-4.647
4703300	MnOH +	3.395E-09	2.819E-09	-8.54988	0.83045	-10.876
4703301	Mn(OH)3 -1	4.860E-21	4.036E-21	-20.39408	0.83045	-34.719
4707320	MnSO4 AQ	1.902E-04	1.921E-04	-3.71653	1.00980	2.201
4701400	MnHCO3 +	5.795E-07	4.812E-07	-6.31765	0.83045	11.681
3301400	HCO3 -	1.534E-04	1.274E-04	-3.89479	0.83045	10.510

Type III - SPECIES WITH FIXED ACTIVITY

ID	NAME	CALC MOL	LOG MOL	NEW LOGK	DH
2	H2O	-1.871E-03	-2.728	0.000	0.000
330	H+1	1.196E-03	-2.922	6.000	0.000

Type VI - EXCLUDED SPECIES (not included in mole balance)

ID	NAME	CALC MOL	LOG MOL	NEW LOGK	DH
3301403	CO2 (g)	7.070E-03	-2.151	18.173	-0.530

PERCENTAGE DISTRIBUTION OF COMPONENTS AMONG
TYPE I and TYPE II (dissolved and adsorbed) species

Mn+2

    73.8   PERCENT BOUND IN SPECIES #   470   Mn+2

    26.2   PERCENT BOUND IN SPECIES #4707320   MnSO4 AQ

Fe+2

    75.4   PERCENT BOUND IN SPECIES #   280   Fe+2

    24.6   PERCENT BOUND IN SPECIES #2807320   FeSO4 AQ

Fe+3

    98.7   PERCENT BOUND IN SPECIES #2813301   FeOH2 +

Ca+2

    70.7   PERCENT BOUND IN SPECIES #   150   Ca+2

    29.3   PERCENT BOUND IN SPECIES #1507320   CaSO4 AQ

Mg+2

    73.3   PERCENT BOUND IN SPECIES #   460   Mg+2

    26.6   PERCENT BOUND IN SPECIES #4607320   MgSO4 AQ

SO4-2

    70.6   PERCENT BOUND IN SPECIES #   732   SO4-2

    11.4   PERCENT BOUND IN SPECIES #4607320   MgSO4 AQ

    11.7   PERCENT BOUND IN SPECIES #1507320   CaSO4 AQ

    5.0   PERCENT BOUND IN SPECIES #2807320   FeSO4 AQ

    1.4   PERCENT BOUND IN SPECIES #4707320   MnSO4 AQ

CO3-2

    61.6   PERCENT BOUND IN SPECIES #3301401   H2CO3 AQ

    36.8   PERCENT BOUND IN SPECIES #3301400   HCO3 -

H2O

    98.4   PERCENT BOUND IN SPECIES #2813301   FeOH2 +

    1.4   PERCENT BOUND IN SPECIES #2813302   FeOH3 AQ

H+1

    154.0   PERCENT BOUND IN SPECIES #2813301   FeOH2 +

    2.2   PERCENT BOUND IN SPECIES #2813302   FeOH3 AQ

```
                    ---------------------------------------------------------
                    ----------- EQUILIBRATED MASS DISTRIBUTION -----------


    IDX      NAME              DISSOLVED              SORBED              PRECIPITATED
                           MOL/KG    PERCENT     MOL/KG     PERCENT     MOL/KG    PERCENT

    470   Mn+2           7.271E-04    100.0    0.000E-01      0.0     0.000E-01      0.0
    280   Fe+2           2.829E-03    100.0    0.000E-01      0.0     0.000E-01      0.0
    281   Fe+3           9.320E-04    100.0    0.000E-01      0.0     0.000E-01      0.0
    150   Ca+2           5.600E-03    100.0    0.000E-01      0.0     0.000E-01      0.0
    460   Mg+2           6.000E-03    100.0    0.000E-01      0.0     0.000E-01      0.0
    732   SO4-2          1.400E-02    100.0    0.000E-01      0.0     0.000E-01      0.0
    140   CO3-2          4.166E-04    100.0    0.000E-01      0.0     0.000E-01      0.0
      2   H2O            1.871E-03    100.0    0.000E-01      0.0     0.000E-01      0.0
    330   H+1           -1.196E-03    100.0    0.000E-01      0.0     0.000E-01      0.0


         Charge Balance: SPECIATED

            Sum of CATIONS =  2.300E-02 Sum of ANIONS   1.992E-02

            PERCENT DIFFERENCE =    7.176E+00  (ANIONS - CATIONS)/(ANIONS + CATIONS)

         EQUILIBRIUM IONIC STRENGTH (m) =    4.237E-02

         EQUILIBRIUM pH                 =    6.000

         DATE ID NUMBER:           990202
         TIME ID NUMBER:         13550188


Saturation indices and stoichiometry of all minerals

        ID #       NAME       Sat. Index        Stoichiometry in [brackets]
        6015000 ANHYDRITE       -0.512     [   1.000] 150  [   1.000] 732
        5015000 ARAGONITE       -2.799     [   1.000] 150  [   1.000] 140
        5046000 ARTINITE       -12.015     [  -2.000] 330  [   2.000] 460  [   1.000] 140
                                           [   5.000]   2
        2046000 BRUCITE         -8.129     [   1.000] 460  [   2.000]   2  [  -2.000] 330
        5015001 CALCITE         -2.626     [   1.000] 150  [   1.000] 140
        5015002 DOLOMITE        -5.264     [   1.000] 150  [   1.000] 460  [   2.000] 140
        6046000 EPSOMITE        -2.797     [   1.000] 460  [   1.000] 732  [   7.000]   2
        2028100 FERRIHYDRITE     3.662     [  -3.000] 330  [   1.000] 281  [   3.000]   2
        2028101 FE3(OH)8         5.890     [  -8.000] 330  [   2.000] 281  [   1.000] 280
                                           [   8.000]   2
        6028100 FE2(SO4)3      -30.960     [   2.000] 281  [   3.000] 732
        2028102 GOETHITE         7.685     [  -3.000] 330  [   1.000] 281  [   2.000]   2
        6015001 GYPSUM          -0.199     [   1.000] 150  [   1.000] 732  [   2.000]   2
        3028100 HEMATITE        20.330     [  -6.000] 330  [   2.000] 281  [   3.000]   2
        5015003 HUNTITE        -14.747     [   3.000] 460  [   1.000] 150  [   4.000] 140
        5046001 HYDRMAGNESIT   -27.257     [   5.000] 460  [   4.000] 140  [  -2.000] 330
                                           [   6.000]   2
        6028101 JAROSITE H       7.701     [  -5.000] 330  [   3.000] 281  [   2.000] 732
                                           [   7.000]   2
        3028101 MAGHEMITE       10.721     [  -6.000] 330  [   2.000] 281  [   3.000]   2
        5046002 MAGNESITE       -3.131     [   1.000] 460  [   1.000] 140
        3028000 MAGNETITE       21.092     [  -8.000] 330  [   2.000] 281  [   1.000] 280
                                           [   4.000]   2
        6028000 MELANTERITE     -2.780     [   1.000] 280  [   1.000] 732  [   7.000]   2
        5046003 NESQUEHONITE    -5.530     [   1.000] 460  [   1.000] 140  [   3.000]   2
        5028000 SIDERITE        -0.903     [   1.000] 280  [   1.000] 140
        2047003 PYROCROITE      -7.256     [  -2.000] 330  [   1.000] 470  [   2.000]   2
        5047000 RHODOCHROSIT    -1.561     [   1.000] 470  [   1.000] 140
```

```
6047000 MNSO4         -8.984    [  1.000] 470  [  1.000] 732
2015000 LIME         -24.699    [ -2.000] 330  [  1.000] 150  [  1.000]   2
2015001 PORTLANDITE  -14.181    [ -2.000] 330  [  1.000] 150  [  2.000]   2
2028000 WUSTITE       -3.154    [ -2.000] 330  [  0.947] 280  [  1.000]   2
2046001 PERICLASE    -13.109    [ -2.000] 330  [  1.000] 460  [  1.000]   2
3046001 MAG-FERRITE    7.967    [ -8.000] 330  [  1.000] 460  [  2.000] 281
                                [  4.000]   2
3028102 LEPIDOCROCIT   7.182    [ -3.000] 330  [  1.000] 281  [  2.000]   2
```

Appendix H

MINTEQA2 Output for Adsorption onto 1 g/L of ferric oxide

HB IP2 Initial Conditions
Test for cation and anion adsorption to 1 g/L ferric oxide

```
Temperature (Celsius):  10.00
Units of concentration: MOLAL
Ionic strength to be computed.
If specified, carbonate concentration represents total inorganic carbon.
Do not automatically terminate if charge imbalance exceeds 30%
Precipitation is allowed only for those solids specified as ALLOWED
  in the input file (if any).
The maximum number of iterations is:  40
The method used to compute activity coefficients is: Davies equation
Intermediate output file
Adsorption model: Constant Capacitance
Number of adsorbing surfaces: 1
```

```
1.000E+00  600.00 1.400 0.000 81
      330  0.000E-01   -3.00 y
      813  0.000E-01    0.00 y
      812  2.188E-03   -2.66 y
      811  5.495E-05   -4.26 y
      280  3.760E-03   -2.35 y
      140  2.460E-03   -2.70 y
      732  1.460E-02   -1.84 y
      150  5.600E-03   -2.25 y
      460  6.000E-03   -2.22 y

 H2O has been inserted as a COMPONENT
   3   1
     330      3.0000      0.0000
   6   1
     813      0.0000      0.0000
   2  14
8113300 SOH2 +         0.0000    7.2700   0.000   0.000 0.00 0.00 0.00   0.0000
0.00 3  1.000 811   1.000 330   1.000 813   0.000   0   0.000   0   0.000   0
0.000   0   0.000   0   0.000   0   0.000   0   0.000   0   0.000   0

 0.000   0   0.000   0   0.000   0
8113301 SO -          0.0000   -8.9100   0.000   0.000 0.00 0.00 0.00   0.0000
0.00 3  1.000 811  -1.000 330  -1.000 813   0.000   0   0.000   0   0.000   0
0.000   0   0.000   0   0.000   0   0.000   0   0.000   0   0.000   0

 0.000   0   0.000   0   0.000   0
8112800 SOFe +        0.0000   -0.4300   0.000   0.000 0.00 0.00 0.00   0.0000
0.00 4  1.000 811   1.000 280  -1.000 330   1.000 813   0.000   0   0.000   0
0.000   0   0.000   0   0.000   0   0.000   0   0.000   0   0.000   0

 0.000   0   0.000   0   0.000   0
8123300 soh2 +        0.0000    7.2700   0.000   0.000 0.00 0.00 0.00   0.0000
0.00 3  1.000 812   1.000 330   1.000 813   0.000   0   0.000   0   0.000   0
0.000   0   0.000   0   0.000   0   0.000   0   0.000   0   0.000   0

 0.000   0   0.000   0   0.000   0
8123301 so -          0.0000   -8.9100   0.000   0.000 0.00 0.00 0.00   0.0000
0.00 3  1.000 812  -1.000 330  -1.000 813   0.000   0   0.000   0   0.000   0
0.000   0   0.000   0   0.000   0   0.000   0   0.000   0   0.000   0

 0.000   0   0.000   0   0.000   0
8122800 soFe +        0.0000   -3.2500   0.000   0.000 0.00 0.00 0.00   0.0000
0.00 4  1.000 812   1.000 280  -1.000 330   1.000 813   0.000   0   0.000   0
0.000   0   0.000   0   0.000   0   0.000   0   0.000   0   0.000   0

 0.000   0   0.000   0   0.000   0
8117320 SSO4 -        0.0000    7.7800   0.000   0.000 0.00 0.00 0.00   0.0000
0.00 5  1.000 811   1.000 732   1.000 330  -1.000   2  -1.000 813   0.000   0
```

```
 0.000   0   0.000   0   0.000   0   0.000   0   0.000   0   0.000   0

 0.000   0   0.000   0   0.000   0
8117321 SOHSO4 -2        0.0000    0.7900   0.000   0.000 0.00 0.00 0.00   0.0000
0.00 3  1.000 811  1.000 732  -2.000 813   0.000   0   0.000   0   0.000   0
 0.000   0   0.000   0   0.000   0   0.000   0   0.000   0   0.000   0

 0.000   0   0.000   0   0.000   0
8127320 sSO4 -          0.0000    7.7800   0.000   0.000 0.00 0.00 0.00   0.0000
0.00 5  1.000 812  1.000 732  -1.000   2   1.000 330  -1.000 813   0.000   0
 0.000   0   0.000   0   0.000   0   0.000   0   0.000   0   0.000   0

 0.000   0   0.000   0   0.000   0
8127321 sohSO4 -2        0.0000    0.7900   0.000   0.000 0.00 0.00 0.00   0.0000
0.00 3  1.000 812  1.000 732  -2.000 813   0.000   0   0.000   0   0.000   0
 0.000   0   0.000   0   0.000   0   0.000   0   0.000   0   0.000   0

 0.000   0   0.000   0   0.000   0
8111500 SOHCa +2        0.0000    4.7900   0.000   0.000 0.00 0.00 0.00   0.0000
0.00 3  1.000 811  1.000 150  2.000 813   0.000   0   0.000   0   0.000   0
 0.000   0   0.000   0   0.000   0   0.000   0   0.000   0   0.000   0

 0.000   0   0.000   0   0.000   0
8114600 SOHMg +2        0.0000    4.8000   0.000   0.000 0.00 0.00 0.00   0.0000
0.00 3  1.000 811  1.000 460  2.000 813   0.000   0   0.000   0   0.000   0
 0.000   0   0.000   0   0.000   0   0.000   0   0.000   0   0.000   0

 0.000   0   0.000   0   0.000   0
8121500 soCa +          0.0000   -5.8500   0.000   0.000 0.00 0.00 0.00   0.0000
0.00 4  1.000 812  1.000 150  -1.000 330   1.000 813   0.000   0   0.000   0
 0.000   0   0.000   0   0.000   0   0.000   0   0.000   0   0.000   0

 0.000   0   0.000   0   0.000   0
8124600 soMg +          0.0000   -4.6000   0.000   0.000 0.00 0.00 0.00   0.0000
0.00 4  1.000 812  1.000 460  -1.000 330   1.000 813   0.000   0   0.000   0
 0.000   0   0.000   0   0.000   0   0.000   0   0.000   0   0.000   0

 0.000   0   0.000   0   0.000   0
```

INPUT DATA BEFORE TYPE MODIFICATIONS

ID	NAME	ACTIVITY GUESS	LOG GUESS	ANAL TOTAL
330	H+1	1.000E-03	-3.000	0.000E-01
813	ADS1PSIo	1.000E+00	0.000	0.000E-01
812	ADS1TYP2	2.188E-03	-2.660	2.188E-03
811	ADS1TYP1	5.495E-05	-4.260	5.495E-05
280	Fe+2	4.467E-03	-2.350	3.760E-03
140	CO3-2	1.995E-03	-2.700	2.460E-03
732	SO4-2	1.445E-02	-1.840	1.460E-02
150	Ca+2	5.623E-03	-2.250	5.600E-03
460	Mg+2	6.026E-03	-2.220	6.000E-03
2	H2O	1.000E+00	0.000	0.000E-01

The input for this sweep is identical to the initial sweep except:
1) The fixed pH is: 6.00
2) The log activity guesses for all components are as computed at
    the point of FIRST convergence in the previous problem.

PARAMETERS OF THE COMPONENT MOST OUT OF BALANCE:

ITER	NAME	TOTAL MOL	DIFF FXN	LOG ACTVTY	RESIDUAL
0	Ca+2	5.600E-03	-2.078E-03	-2.71665	2.078E-03
1	Ca+2	5.600E-03	2.568E-04	-2.56738	2.562E-04
2	Ca+2	5.600E-03	2.290E-03	-2.58063	2.289E-03

```
        3   Ca+2        5.600E-03   5.278E-04   -2.68815   5.272E-04
        4   Ca+2        5.600E-03   4.117E-05   -2.71782   4.061E-05
        5   Ca+2        5.600E-03   2.839E-06   -2.72030   2.279E-06
```

ID	NAME	ANAL MOL	CALC MOL	LOG ACTVTY	GAMMA	DIFF FXN
460	Mg+2	6.000E-03	4.421E-03	-2.67605	0.476858	3.678E-07
813	ADS1PSIo	3.436E-04	1.983E-01	-0.70259	1.000000	1.481E-11
812	ADS1TYP2	2.188E-03	3.107E-04	-3.50771	1.000000	-7.314E-11
811	ADS1TYP1	5.495E-05	4.737E-07	-6.32446	1.000000	-1.983E-11
280	Fe+2	3.760E-03	2.825E-03	-2.87064	0.476858	2.351E-07
140	CO3-2	2.460E-03	5.350E-08	-7.59326	0.476858	1.617E-08
732	SO4-2	1.460E-02	9.933E-03	-2.32451	0.476858	8.239E-07
150	Ca+2	5.600E-03	3.992E-03	-2.72047	0.476858	3.313E-07
2	H2O	0.000E-01	4.478E-04	-0.00025	1.000000	0.000E-01
330	H+1	0.000E-01	1.203E-06	-6.00000	0.830993	0.000E-01

Type I - COMPONENTS AS SPECIES IN SOLUTION

ID	NAME	CALC MOL	ACTIVITY	LOG ACTVTY	GAMMA	NEW LOGK
330	H+1	1.203E-06	1.000E-06	-6.00000	0.83099	0.080
460	Mg+2	4.421E-03	2.108E-03	-2.67605	0.47686	0.322
812	ADS1TYP2	3.107E-04	3.107E-04	-3.50771	1.00000	0.000
811	ADS1TYP1	4.737E-07	4.737E-07	-6.32446	1.00000	0.000
280	Fe+2	2.825E-03	1.347E-03	-2.87064	0.47686	0.322
140	CO3-2	5.350E-08	2.551E-08	-7.59326	0.47686	0.322
732	SO4-2	9.933E-03	4.737E-03	-2.32451	0.47686	0.322
150	Ca+2	3.992E-03	1.903E-03	-2.72047	0.47686	0.322

Type II - OTHER SPECIES IN SOLUTION OR ADSORBED

ID	NAME	CALC MOL	ACTIVITY	LOG ACTVTY	GAMMA	NEW LOGK
8124600	soMg +	3.263E-06	3.263E-06	-5.48635	1.00000	-4.600
3301401	H2CO3 AQ	1.482E-03	1.496E-03	-2.82501	1.00991	16.764
3307320	HSO4 -	3.688E-07	3.065E-07	-6.51356	0.83099	1.891
3300020	OH-	3.664E-09	3.045E-09	-8.51642	0.83099	-14.436
4603300	MgOH +	1.059E-09	8.798E-10	-9.05564	0.83099	-12.299
4601400	MgCO3 AQ	4.037E-08	4.077E-08	-7.38964	1.00991	2.875
4601401	MgHCO3 +	2.140E-05	1.779E-05	-4.74993	0.83099	11.600
4607320	MgSO4 AQ	1.552E-03	1.567E-03	-2.80489	1.00991	2.191
1503300	CaOH +	1.575E-10	1.309E-10	-9.88310	0.83099	-13.082
1501400	CaHCO3 +	1.178E-05	9.787E-06	-5.00933	0.83099	11.385
1501401	CaCO3 AQ	5.284E-08	5.336E-08	-7.27275	1.00991	3.037
1507320	CaSO4 AQ	1.595E-03	1.610E-03	-2.79306	1.00991	2.248
2803300	FeOH +	1.574E-07	1.308E-07	-6.88339	0.83099	-9.932
2803301	FeOH3 -1	1.078E-17	8.956E-18	-17.04789	0.83099	-32.096
2807320	FeSO4 AQ	8.417E-04	8.500E-04	-3.07057	1.00991	2.120
2803302	FeOH2 AQ	2.789E-13	2.817E-13	-12.55028	1.00991	-21.683
3301400	HCO3 -	9.452E-04	7.854E-04	-3.10489	0.83099	10.569
8113300	SOH2 +	1.750E-06	1.750E-06	-5.75705	1.00000	7.270
8113301	SO -	2.939E-09	2.939E-09	-8.53187	1.00000	-8.910
8112800	SOFe +	4.702E-05	4.702E-05	-4.32769	1.00000	-0.430
8123300	soh2 +	1.147E-03	1.147E-03	-2.94030	1.00000	7.270
8123301	so -	1.927E-06	1.927E-06	-5.71513	1.00000	-8.910
8122800	soFe +	4.667E-05	4.667E-05	-4.33094	1.00000	-3.250
8117320	SSO4 -	6.821E-07	6.821E-07	-6.16614	1.00000	7.780
8117321	SOHSO4 -2	3.517E-07	3.517E-07	-6.45379	1.00000	0.790
8127320	sSO4 -	4.473E-04	4.473E-04	-3.34939	1.00000	7.780
8127321	sohSO4 -2	2.306E-04	2.306E-04	-3.63705	1.00000	0.790
8111500	SOHCa +2	2.187E-06	2.187E-06	-5.66011	1.00000	4.790
8114600	SOHMg +2	2.479E-06	2.479E-06	-5.60569	1.00000	4.800
8121500	soCa +	1.657E-07	1.657E-07	-6.78077	1.00000	-5.850

Type III - SPECIES WITH FIXED ACTIVITY

ID	NAME	CALC MOL	LOG MOL	NEW LOGK	DH
2	H2O	4.478E-04	-3.349	0.000	0.000
330	H+1	-5.441E-03	-2.264	6.000	0.000

Type VI - EXCLUDED SPECIES (not included in mole balance)

ID	NAME	CALC MOL	LOG MOL	NEW LOGK	DH
813	ADS1PSIo	1.983E-01	-0.703	0.000	0.000
3301403	CO2 (g)	3.869E-02	-1.412	18.181	-0.530

PERCENTAGE DISTRIBUTION OF COMPONENTS AMONG
TYPE I and TYPE II (dissolved and adsorbed) species

Mg+2

| 73.7 | PERCENT BOUND IN SPECIES # | 460 | Mg+2 |
| 25.9 | PERCENT BOUND IN SPECIES #4607320 | | MgSO4 AQ |

ADS1PSIo

13.7	PERCENT BOUND IN SPECIES #8112800	SOFe +
333.9	PERCENT BOUND IN SPECIES #8123300	soh2 +
13.6	PERCENT BOUND IN SPECIES #8122800	soFe +
1.3	PERCENT BOUND IN SPECIES #8111500	SOHCa +2
1.4	PERCENT BOUND IN SPECIES #8114600	SOHMg +2

ADS1TYP2

14.2	PERCENT BOUND IN SPECIES # 812	ADS1TYP2
52.4	PERCENT BOUND IN SPECIES #8123300	soh2 +
2.1	PERCENT BOUND IN SPECIES #8122800	soFe +
20.4	PERCENT BOUND IN SPECIES #8127320	sSO4 -
10.5	PERCENT BOUND IN SPECIES #8127321	sohSO4 -2

ADS1TYP1

3.2	PERCENT BOUND IN SPECIES #8113300	SOH2 +
85.6	PERCENT BOUND IN SPECIES #8112800	SOFe +
1.2	PERCENT BOUND IN SPECIES #8117320	SSO4 -
4.0	PERCENT BOUND IN SPECIES #8111500	SOHCa +2
4.5	PERCENT BOUND IN SPECIES #8114600	SOHMg +2

Fe+2

75.1	PERCENT BOUND IN SPECIES # 280	Fe+2
22.4	PERCENT BOUND IN SPECIES #2807320	FeSO4 AQ
1.3	PERCENT BOUND IN SPECIES #8112800	SOFe +

```
          1.2     PERCENT BOUND IN SPECIES #8122800   soFe +


CO3-2
          60.2    PERCENT BOUND IN SPECIES #3301401   H2CO3 AQ

          38.4    PERCENT BOUND IN SPECIES #3301400   HCO3 -


SO4-2
          68.0    PERCENT BOUND IN SPECIES #    732    SO4-2

          10.6    PERCENT BOUND IN SPECIES #4607320   MgSO4 AQ

          10.9    PERCENT BOUND IN SPECIES #1507320   CaSO4 AQ

           5.8    PERCENT BOUND IN SPECIES #2807320   FeSO4 AQ

           3.1    PERCENT BOUND IN SPECIES #8127320   sSO4 -

           1.6    PERCENT BOUND IN SPECIES #8127321   sohSO4 -2


Ca+2
          71.3    PERCENT BOUND IN SPECIES #    150    Ca+2

          28.5    PERCENT BOUND IN SPECIES #1507320   CaSO4 AQ


H2O
          99.9    PERCENT BOUND IN SPECIES #8127320   sSO4 -


H+1
          54.5    PERCENT BOUND IN SPECIES #3301401   H2CO3 AQ

          17.4    PERCENT BOUND IN SPECIES #3301400   HCO3 -

          21.1    PERCENT BOUND IN SPECIES #8123300   soh2 +

           8.2    PERCENT BOUND IN SPECIES #8127320   sSO4 -
```

```
          ----------- EQUILIBRATED MASS DISTRIBUTION -----------


IDX    NAME          DISSOLVED           SORBED            PRECIPITATED
                   MOL/KG   PERCENT    MOL/KG   PERCENT    MOL/KG   PERCENT

460    Mg+2       5.995E-03    99.9   5.742E-06    0.1   0.000E-01    0.0
280    Fe+2       3.667E-03    97.5   9.370E-05    2.5   0.000E-01    0.0
140    CO3-2      2.460E-03   100.0   0.000E-01    0.0   0.000E-01    0.0
732    SO4-2      1.392E-02    95.3   6.790E-04    4.7   0.000E-01    0.0
150    Ca+2       5.598E-03   100.0   2.353E-06    0.0   0.000E-01    0.0
  2    H2O        1.623E-07     0.0  -4.480E-04  100.0   0.000E-01    0.0
330    H+1        3.943E-03    72.5   1.498E-03   27.5   0.000E-01    0.0
```

```
    Charge Balance: SPECIATED

       Sum of CATIONS =  2.251E-02 Sum of ANIONS   2.081E-02

       PERCENT DIFFERENCE =   3.918E+00  (ANIONS - CATIONS)/(ANIONS + CATIONS)
```

EQUILIBRIUM IONIC STRENGTH (m) =   4.283E-02

EQUILIBRIUM pH   =   6.000

**** CONSTANT CAPACITANCE ADSORPTION MODEL ****

**** Parameters For Adsorbent Number 1 ****
 Electrostatic Variables: psi0 = 0.039472   sig0 = 0.055261
                           psib = 0.000000   sigb = 0.000000
                           psid = 0.000000   sigd = 0.000000
 Adsorbent Concentration (g/l):   1.000
 Specific Surface Area (sq. meters/g): 600.00

     DATE ID NUMBER: 990202
     TIME ID NUMBER: 12591472

Saturation indices and stoichiometry of all minerals

ID #	NAME	Sat. Index	Stoichiometry in [brackets]					
6015000	ANHYDRITE	-0.554	[1.000] 150	[1.000] 732				
5015000	ARAGONITE	-2.103	[1.000] 150	[1.000] 140				
5046000	ARTINITE	-11.663	[-2.000] 330	[2.000] 460	[1.000] 140			
			[5.000] 2					
2046000	BRUCITE	-8.472	[1.000] 460	[2.000] 2	[-2.000] 330			
5015001	CALCITE	-1.907	[1.000] 150	[1.000] 140				
5015002	DOLOMITE	-3.905	[1.000] 150	[1.000] 460	[2.000] 140			
6046000	EPSOMITE	-2.753	[1.000] 460	[1.000] 732	[7.000] 2			
6015001	GYPSUM	-0.187	[1.000] 150	[1.000] 732	[2.000] 2			
5015003	HUNTITE	-12.154	[3.000] 460	[1.000] 150	[4.000] 140			
5046001	HYDRMAGNESIT	-25.016	[5.000] 460	[4.000] 140	[-2.000] 330			
			[6.000] 2					
5046002	MAGNESITE	-2.480	[1.000] 460	[1.000] 140				
6028000	MELANTERITE	-2.616	[1.000] 280	[1.000] 732	[7.000] 2			
5046003	NESQUEHONITE	-4.874	[1.000] 460	[1.000] 140	[3.000] 2			
5028000	SIDERITE	-0.121	[1.000] 280	[1.000] 140				
2015000	LIME	-25.314	[-2.000] 330	[1.000] 150	[1.000] 2			
2015001	PORTLANDITE	-14.588	[-2.000] 330	[1.000] 150	[2.000] 2			
2028000	WUSTITE	-3.370	[-2.000] 330	[0.947] 280	[1.000] 2			
2046001	PERICLASE	-13.589	[-2.000] 330	[1.000] 460	[1.000] 2			

Appendix I

MINTEQA2 Output for Adsorption onto 71.5 mg/L of ferric oxide

HB IP2 Initial Conditions
Test for cation and anion adsorption onto 71.5 mg/L ferric oxide

---

Temperature (Celsius): 10.00
Units of concentration: MOLAL
Ionic strength to be computed.
If specified, carbonate concentration represents total inorganic carbon.
Do not automatically terminate if charge imbalance exceeds 30%
Precipitation is allowed only for those solids specified as ALLOWED
  in the input file (if any).
The maximum number of iterations is: 40
The method used to compute activity coefficients is: Davies equation
Intermediate output file
Adsorption model: Constant Capacitance
Number of adsorbing surfaces: 1

```
7.150E-02  600.00 1.400 0.000 81
     330  0.000E-01   -3.00 y
     813  0.000E-01    0.00 y
     812  1.095E-04   -2.66 y
     811  2.750E-06   -4.26 y
     280  3.760E-03   -2.35 y
     140  2.460E-03   -2.70 y
     732  1.460E-02   -1.84 y
     150  5.600E-03   -2.25 y
     460  6.000E-03   -2.22 y

H2O has been inserted as a COMPONENT
   3   1
     330      3.0000      0.0000
   6   1
     813      0.0000      0.0000
   2  14
8113300 SOH2 +          0.0000    7.2700   0.000   0.000 0.00 0.00 0.00   0.0000
0.00 3   1.000 811   1.000 330   1.000 813   0.000   0   0.000   0   0.000   0
0.000   0   0.000   0   0.000   0   0.000   0   0.000   0   0.000   0


  0.000   0   0.000   0   0.000   0
8113301 SO -           0.0000   -8.9100   0.000   0.000 0.00 0.00 0.00   0.0000
0.00 3   1.000 811  -1.000 330  -1.000 813   0.000   0   0.000   0   0.000   0
0.000   0   0.000   0   0.000   0   0.000   0   0.000   0   0.000   0


  0.000   0   0.000   0   0.000   0
8112800 SOFe +         0.0000   -0.4300   0.000   0.000 0.00 0.00 0.00   0.0000
0.00 4   1.000 811   1.000 280  -1.000 330   1.000 813   0.000   0   0.000   0
0.000   0   0.000   0   0.000   0   0.000   0   0.000   0   0.000   0


  0.000   0   0.000   0   0.000   0
8123300 soh2 +         0.0000    7.2700   0.000   0.000 0.00 0.00 0.00   0.0000
0.00 3   1.000 812   1.000 330   1.000 813   0.000   0   0.000   0   0.000   0
0.000   0   0.000   0   0.000   0   0.000   0   0.000   0   0.000   0


  0.000   0   0.000   0   0.000   0
8123301 so -           0.0000   -8.9100   0.000   0.000 0.00 0.00 0.00   0.0000
0.00 3   1.000 812  -1.000 330  -1.000 813   0.000   0   0.000   0   0.000   0
0.000   0   0.000   0   0.000   0   0.000   0   0.000   0   0.000   0


  0.000   0   0.000   0   0.000   0
8122800 soFe +         0.0000   -3.2500   0.000   0.000 0.00 0.00 0.00   0.0000
0.00 4   1.000 812   1.000 280  -1.000 330   1.000 813   0.000   0   0.000   0
0.000   0   0.000   0   0.000   0   0.000   0   0.000   0   0.000   0


  0.000   0   0.000   0   0.000   0
```

```
8117320 SSO4 -           0.0000    7.7800   0.000    0.000 0.00 0.00 0.00   0.0000
0.00 5   1.000 811   1.000 732   1.000 330  -1.000    2  -1.000 813    0.000   0
0.000    0   0.000   0   0.000   0   0.000   0   0.000    0   0.000    0


 0.000    0   0.000   0   0.000   0
8117321 SOHSO4 -2         0.0000    0.7900   0.000    0.000 0.00 0.00 0.00   0.0000
0.00 3   1.000 811   1.000 732  -2.000 813   0.000    0   0.000    0   0.000    0
0.000    0   0.000   0   0.000   0   0.000   0   0.000    0   0.000    0


 0.000    0   0.000   0   0.000   0
8127320 sSO4 -           0.0000    7.7800   0.000    0.000 0.00 0.00 0.00   0.0000
0.00 5   1.000 812   1.000 732  -1.000    2   1.000 330  -1.000 813    0.000   0
0.000    0   0.000   0   0.000   0   0.000   0   0.000    0   0.000    0


 0.000    0   0.000   0   0.000   0
8127321 sohSO4 -2         0.0000    0.7900   0.000    0.000 0.00 0.00 0.00   0.0000
0.00 3   1.000 812   1.000 732  -2.000 813   0.000    0   0.000    0   0.000    0
0.000    0   0.000   0   0.000   0   0.000   0   0.000    0   0.000    0


 0.000    0   0.000   0   0.000   0
8111500 SOHCa +2         0.0000    4.7900   0.000    0.000 0.00 0.00 0.00   0.0000
0.00 3   1.000 811   1.000 150   2.000 813   0.000    0   0.000    0   0.000    0
0.000    0   0.000   0   0.000   0   0.000   0   0.000    0   0.000    0


 0.000    0   0.000   0   0.000   0
8114600 SOHMg +2         0.0000    4.8000   0.000    0.000 0.00 0.00 0.00   0.0000
0.00 3   1.000 811   1.000 460   2.000 813   0.000    0   0.000    0   0.000    0
0.000    0   0.000   0   0.000   0   0.000   0   0.000    0   0.000    0


 0.000    0   0.000   0   0.000   0
8121500 soCa +           0.0000   -5.8500   0.000    0.000 0.00 0.00 0.00   0.0000
0.00 4   1.000 812   1.000 150  -1.000 330   1.000 813   0.000    0   0.000    0
0.000    0   0.000   0   0.000   0   0.000   0   0.000    0   0.000    0


 0.000    0   0.000   0   0.000   0
8124600 soMg +           0.0000   -4.6000   0.000    0.000 0.00 0.00 0.00   0.0000
0.00 4   1.000 812   1.000 460  -1.000 330   1.000 813   0.000    0   0.000    0
0.000    0   0.000   0   0.000   0   0.000   0   0.000    0   0.000    0


 0.000    0   0.000   0   0.000   0
```

INPUT DATA BEFORE TYPE MODIFICATIONS

ID	NAME	ACTIVITY GUESS	LOG GUESS	ANAL TOTAL
330	H+1	1.000E-03	-3.000	0.000E-01
813	ADS1PSIo	1.000E+00	0.000	0.000E-01
812	ADS1TYP2	2.188E-03	-2.660	1.095E-04
811	ADS1TYP1	5.495E-05	-4.260	2.750E-06
280	Fe+2	4.467E-03	-2.350	3.760E-03
140	CO3-2	1.995E-03	-2.700	2.460E-03
732	SO4-2	1.445E-02	-1.840	1.460E-02
150	Ca+2	5.623E-03	-2.250	5.600E-03
460	Mg+2	6.026E-03	-2.220	6.000E-03
2	H2O	1.000E+00	0.000	0.000E-01

The input for this sweep is identical to the initial sweep except:
  1) The fixed pH is: 6.00
  2) The log activity guesses for all components are as computed at
      the point of FIRST convergence in the previous problem.

PARAMETERS OF THE COMPONENT MOST OUT OF BALANCE:

ITER	NAME	TOTAL MOL	DIFF FXN	LOG ACTVTY	RESIDUAL
0	Ca+2	5.600E-03	-2.059E-03	-2.72608	2.059E-03
1	Ca+2	5.600E-03	2.622E-04	-2.58210	2.617E-04
2	Ca+2	5.600E-03	2.238E-03	-2.59435	2.237E-03
3	Ca+2	5.600E-03	5.339E-04	-2.69551	5.334E-04
4	Ca+2	5.600E-03	4.217E-05	-2.72502	4.161E-05
5	Ca+2	5.600E-03	2.879E-06	-2.72752	2.319E-06

ID	NAME	ANAL MOL	CALC MOL	LOG ACTVTY	GAMMA	DIFF FXN
460	Mg+2	6.000E-03	4.382E-03	-2.68262	0.473946	3.753E-07
813	ADS1PSIo	2.353E-05	2.123E-01	-0.67298	1.000000	5.382E-13
812	ADS1TYP2	1.095E-04	1.517E-05	-4.81890	1.000000	-3.897E-12
811	ADS1TYP1	2.750E-06	2.193E-08	-7.65889	1.000000	-1.077E-12
280	Fe+2	3.760E-03	2.868E-03	-2.86672	0.473946	2.458E-07
140	CO3-2	2.460E-03	5.381E-08	-7.59338	0.473946	1.660E-08
732	SO4-2	1.460E-02	1.045E-02	-2.30534	0.473946	8.926E-07
150	Ca+2	5.600E-03	3.950E-03	-2.72769	0.473946	3.375E-07
2	H2O	0.000E-01	2.120E-05	-0.00025	1.000000	0.000E-01
330	H+1	0.000E-01	1.205E-06	-6.00000	0.829721	0.000E-01

Type I - COMPONENTS AS SPECIES IN SOLUTION

ID	NAME	CALC MOL	ACTIVITY	LOG ACTVTY	GAMMA	NEW LOGK
330	H+1	1.205E-06	1.000E-06	-6.00000	0.82972	0.081
460	Mg+2	4.382E-03	2.077E-03	-2.68262	0.47395	0.324
812	ADS1TYP2	1.517E-05	1.517E-05	-4.81890	1.00000	0.000
811	ADS1TYP1	2.193E-08	2.193E-08	-7.65889	1.00000	0.000
280	Fe+2	2.868E-03	1.359E-03	-2.86672	0.47395	0.324
140	CO3-2	5.381E-08	2.550E-08	-7.59338	0.47395	0.324
732	SO4-2	1.045E-02	4.951E-03	-2.30534	0.47395	0.324
150	Ca+2	3.950E-03	1.872E-03	-2.72769	0.47395	0.324

Type II - OTHER SPECIES IN SOLUTION OR ADSORBED

ID	NAME	CALC MOL	ACTIVITY	LOG ACTVTY	GAMMA	NEW LOGK
8124600	soMg +	1.681E-07	1.681E-07	-6.77450	1.00000	-4.600
3301401	H2CO3 AQ	1.481E-03	1.496E-03	-2.82513	1.01013	16.764
3307320	HSO4 -	3.861E-07	3.203E-07	-6.49439	0.82972	1.892
3300020	OH-	3.670E-09	3.045E-09	-8.51642	0.82972	-14.435
4603300	MgOH +	1.044E-09	8.666E-10	-9.06220	0.82972	-12.298
4601400	MgCO3 AQ	3.975E-08	4.015E-08	-7.39632	1.01013	2.875
4601401	MgHCO3 +	2.111E-05	1.751E-05	-4.75662	0.82972	11.600
4607320	MgSO4 AQ	1.597E-03	1.613E-03	-2.79228	1.01013	2.191
1503300	CaOH +	1.551E-10	1.287E-10	-9.89032	0.82972	-13.081
1501400	CaHCO3 +	1.160E-05	9.623E-06	-5.01667	0.82972	11.385
1501401	CaCO3 AQ	5.194E-08	5.247E-08	-7.28009	1.01013	3.037
1507320	CaSO4 AQ	1.639E-03	1.655E-03	-2.78111	1.01013	2.248
2803300	FeOH +	1.591E-07	1.320E-07	-6.87947	0.82972	-9.931
2803301	FeOH3 -1	1.089E-17	9.037E-18	-17.04397	0.82972	-32.095
2807320	FeSO4 AQ	8.875E-04	8.964E-04	-3.04748	1.01013	2.120
2803302	FeOH2 AQ	2.814E-13	2.842E-13	-12.54636	1.01013	-21.684
3301400	HCO3 -	9.464E-04	7.852E-04	-3.10500	0.82972	10.569
8113300	SOH2 +	8.672E-08	8.672E-08	-7.06188	1.00000	7.270
8113301	SO -	1.271E-10	1.271E-10	-9.89591	1.00000	-8.910
8112800	SOFe +	2.352E-06	2.352E-06	-5.62860	1.00000	-0.430
8123300	soh2 +	6.000E-05	6.000E-05	-4.22188	1.00000	7.270
8123301	so -	8.792E-08	8.792E-08	-7.05592	1.00000	-8.910
8122800	soFe +	2.463E-06	2.463E-06	-5.60860	1.00000	-3.250
8117320	SSO4 -	3.083E-08	3.083E-08	-7.51101	1.00000	7.780
8117321	SOHSO4 -2	1.485E-08	1.485E-08	-7.82827	1.00000	0.790
8127320	sSO4 -	2.133E-05	2.133E-05	-4.67101	1.00000	7.780

```
8127321  sohSO4 -2    1.027E-05  1.027E-05   -4.98828   1.00000    0.790
8111500  SOHCa +2     1.141E-07  1.141E-07   -6.94255   1.00000    4.790
8114600  SOHMg +2     1.296E-07  1.296E-07   -6.88748   1.00000    4.800
8121500  soCa +       8.520E-09  8.520E-09   -8.06958   1.00000   -5.850
```

Type III - SPECIES WITH FIXED ACTIVITY

```
  ID      NAME      CALC MOL     LOG MOL   NEW LOGK    DH
    2  H2O          2.120E-05     -4.674     0.000     0.000
  330  H+1         -4.018E-03     -2.396     6.000     0.000
```

Type VI - EXCLUDED SPECIES (not included in mole balance)

```
  ID      NAME      CALC MOL     LOG MOL   NEW LOGK    DH
  813  ADS1PSIo     2.123E-01     -0.673     0.000     0.000
3301403  CO2 (g)    3.868E-02     -1.413    18.181    -0.530
```

PERCENTAGE DISTRIBUTION OF COMPONENTS AMONG
TYPE I and TYPE II (dissolved and adsorbed) species

Mg+2
```
        73.0      PERCENT BOUND IN SPECIES #    460   Mg+2

        26.6      PERCENT BOUND IN SPECIES #4607320   MgSO4 AQ
```

ADS1PSIo
```
        10.0      PERCENT BOUND IN SPECIES #8112800   SOFe +

       254.9      PERCENT BOUND IN SPECIES #8123300   soh2 +

        10.5      PERCENT BOUND IN SPECIES #8122800   soFe +

         1.1      PERCENT BOUND IN SPECIES #8114600   SOHMg +2
```

ADS1TYP2
```
        13.9      PERCENT BOUND IN SPECIES #    812   ADS1TYP2

        54.8      PERCENT BOUND IN SPECIES #8123300   soh2 +

         2.2      PERCENT BOUND IN SPECIES #8122800   soFe +

        19.5      PERCENT BOUND IN SPECIES #8127320   sSO4 -

         9.4      PERCENT BOUND IN SPECIES #8127321   sohSO4 -2
```

ADS1TYP1
```
         3.2      PERCENT BOUND IN SPECIES #8113300   SOH2 +

        85.5      PERCENT BOUND IN SPECIES #8112800   SOFe +

         1.1      PERCENT BOUND IN SPECIES #8117320   SSO4 -

         4.2      PERCENT BOUND IN SPECIES #8111500   SOHCa +2

         4.7      PERCENT BOUND IN SPECIES #8114600   SOHMg +2
```

Fe+2

     76.3   PERCENT BOUND IN SPECIES #   280   Fe+2

     23.6   PERCENT BOUND IN SPECIES #2807320   FeSO4 AQ

CO3-2

     60.2   PERCENT BOUND IN SPECIES #3301401   H2CO3 AQ

     38.5   PERCENT BOUND IN SPECIES #3301400   HCO3 -

SO4-2

     71.5   PERCENT BOUND IN SPECIES #   732   SO4-2

     10.9   PERCENT BOUND IN SPECIES #4607320   MgSO4 AQ

     11.2   PERCENT BOUND IN SPECIES #1507320   CaSO4 AQ

      6.1   PERCENT BOUND IN SPECIES #2807320   FeSO4 AQ

Ca+2

     70.5   PERCENT BOUND IN SPECIES #   150   Ca+2

     29.3   PERCENT BOUND IN SPECIES #1507320   CaSO4 AQ

H2O

   100.6   PERCENT BOUND IN SPECIES #8127320   sSO4 -

H+1

     73.7   PERCENT BOUND IN SPECIES #3301401   H2CO3 AQ

     23.6   PERCENT BOUND IN SPECIES #3301400   HCO3 -

      1.5   PERCENT BOUND IN SPECIES #8123300   soh2 +

----------- EQUILIBRATED MASS DISTRIBUTION -----------

IDX	NAME	DISSOLVED		SORBED		PRECIPITATED	
		MOL/KG	PERCENT	MOL/KG	PERCENT	MOL/KG	PERCENT
460	Mg+2	6.000E-03	100.0	2.976E-07	0.0	0.000E-01	0.0
280	Fe+2	3.755E-03	99.9	4.814E-06	0.1	0.000E-01	0.0
140	CO3-2	2.460E-03	100.0	0.000E-01	0.0	0.000E-01	0.0
732	SO4-2	1.457E-02	99.8	3.165E-05	0.2	0.000E-01	0.0
150	Ca+2	5.600E-03	100.0	1.227E-07	0.0	0.000E-01	0.0
2	H2O	1.639E-07	-0.8	-2.136E-05	100.8	0.000E-01	0.0
330	H+1	3.942E-03	98.1	7.636E-05	1.9	0.000E-01	0.0

    Charge Balance: SPECIATED

      Sum of CATIONS = 2.243E-02 Sum of ANIONS 2.184E-02

      PERCENT DIFFERENCE = 1.344E+00 (ANIONS - CATIONS)/(ANIONS + CATIONS)

    EQUILIBRIUM IONIC STRENGTH (m) = 4.378E-02

```
        EQUILIBRIUM pH              =   6.000


**** CONSTANT CAPACITANCE ADSORPTION MODEL ****


**** Parameters For Adsorbent Number 1 ****
   Electrostatic Variables:  psi0 = 0.037809    sig0 = 0.052932
                             psib = 0.000000    sigb = 0.000000
                             psid = 0.000000    sigd = 0.000000
   Adsorbent Concentration (g/l):   0.071
   Specific Surface Area (sq. meters/g):  600.00

      DATE ID NUMBER:         990202
      TIME ID NUMBER:        13273658
```

Saturation indices and stoichiometry of all minerals

```
    ID #      NAME      Sat. Index       Stoichiometry in [brackets]
  6015000 ANHYDRITE      -0.542    [  1.000] 150  [  1.000] 732
  5015000 ARAGONITE      -2.110    [  1.000] 150  [  1.000] 140
  5046000 ARTINITE      -11.676    [ -2.000] 330  [  2.000] 460  [  1.000] 140
                                   [  5.000]   2
  2046000 BRUCITE        -8.478    [  1.000] 460  [  2.000]   2  [ -2.000] 330
  5015001 CALCITE        -1.915    [  1.000] 150  [  1.000] 140
  5015002 DOLOMITE       -3.919    [  1.000] 150  [  1.000] 460  [  2.000] 140
  6046000 EPSOMITE       -2.740    [  1.000] 460  [  1.000] 732  [  7.000]   2
  6015001 GYPSUM         -0.175    [  1.000] 150  [  1.000] 732  [  2.000]   2
  5015003 HUNTITE       -12.181    [  3.000] 460  [  1.000] 150  [  4.000] 140
  5046001 HYDRMAGNESIT  -25.049    [  5.000] 460  [  4.000] 140  [ -2.000] 330
                                   [  6.000]   2
  5046002 MAGNESITE      -2.487    [  1.000] 460  [  1.000] 140
  6028000 MELANTERITE    -2.593    [  1.000] 280  [  1.000] 732  [  7.000]   2
  5046003 NESQUEHONITE   -4.881    [  1.000] 460  [  1.000] 140  [  3.000]   2
  5028000 SIDERITE       -0.117    [  1.000] 280  [  1.000] 140
  2015000 LIME          -25.321    [ -2.000] 330  [  1.000] 150  [  1.000]   2
  2015001 PORTLANDITE   -14.595    [ -2.000] 330  [  1.000] 150  [  2.000]   2
  2028000 WUSTITE        -3.367    [ -2.000] 330  [  0.947] 280  [  1.000]   2
  2046001 PERICLASE     -13.596    [ -2.000] 330  [  1.000] 460  [  1.000]   2
```

Appendix J

MINTEQA2 Output for Precipitation of Schwertmannite

HB IP2 initial conditions
Test for Schwertmannite precipitation

```
--------------------------------------------------------------------------------
Temperature (Celsius): 15.00
Units of concentration: MOLAL
Ionic strength:  0.020 molal; FIXED
If specified, total carbonate concentration represents total inorganic carbon.
Do not automatically terminate if charge imbalance exceeds 30%
Precipitation is allowed only for those solids specified as ALLOWED
   in the input file (if any).
The maximum number of iterations is:  40
The method used to compute activity coefficients is: Davies equation
Intermediate output file


--------------------------------------------------------------------------------
   330  5.012E-07   -4.50
   280  2.829E-03   -3.00
   140  4.166E-04   -2.00
   150  5.600E-03   -2.52
   732  1.400E-02   -2.00
   460  6.000E-03   -1.70
   281  9.320E-04   -5.00
H2O has been inserted as a COMPONENT
  3   1
   330     4.5000     0.0000
  5   1
2028103   -18.0000     0.0000
```

NPUT DATA BEFORE TYPE MODIFICATIONS

ID	NAME	ACTIVITY GUESS	LOG GUESS	ANAL TOTAL
330	H+1	3.162E-05	-4.500	5.012E-07
280	Fe+2	1.000E-03	-3.000	2.829E-03
140	CO3-2	1.000E-02	-2.000	4.166E-04
150	Ca+2	3.020E-03	-2.520	5.600E-03
732	SO4-2	1.000E-02	-2.000	1.400E-02
460	Mg+2	1.995E-02	-1.700	6.000E-03
281	Fe+3	1.000E-05	-5.000	9.320E-04
2	H2O	1.000E+00	0.000	0.000E+00

The input for this sweep is identical to the initial sweep except:
  1) The fixed pH is: 6.00
  2) The log activity guesses for all components are as computed at
      the point of FIRST convergence in the previous problem.

PARAMETERS OF THE COMPONENT MOST OUT OF BALANCE:

ITER	NAME	TOTAL MOL	DIFF FXN	LOG ACTVTY
0	Fe+3	-1.111E-01	1.111E-01	-12.58960
1	Fe+3	-1.111E-01	1.109E-01	-13.58960
2	Fe+3	-1.111E-01	-1.054E+04	-14.58960
3	Fe+3	-1.111E-01	-4.110E+03	-14.53845
4	Fe+3	-1.111E-01	-1.602E+03	-14.48730
5	Fe+3	-1.111E-01	-6.242E+02	-14.43615
6	Fe+3	-1.111E-01	-2.433E+02	-14.38500
7	Fe+3	-1.111E-01	-9.478E+01	-14.33387
8	Fe+3	-1.111E-01	-3.691E+01	-14.28276
9	Fe+3	-1.111E-01	-1.436E+01	-14.23172
10	Fe+3	-1.111E-01	-5.568E+00	-14.18087
11	Fe+3	-1.111E-01	-2.142E+00	-14.13050
12	Fe+3	-1.111E-01	-8.072E-01	-14.08137
13	Fe+3	-1.111E-01	-2.882E-01	-14.03545
14	Fe+3	-1.111E-01	-8.921E-02	-13.99717
15	Fe+3	-1.111E-01	-1.882E-02	-13.97320
16	Fe+3	-1.111E-01	-1.449E-03	-13.96531

ID	NAME	ANAL MOL	CALC MOL	ACTIVITY	LOG ACTVTY	GAMMA	NEW LOGK	DIFF FXN
281	Fe+3	9.320E-04	3.751E-14	1.085E-14	-13.96461	0.289213	0.5388	-1.045E-05
280	Fe+2	2.829E-03	1.964E-03	1.131E-03	-2.94641	0.576157	0.2395	8.198E-08
140	CO3-2	4.166E-04	8.315E-09	4.791E-09	-8.31958	0.576157	0.2395	-5.013E-15
150	Ca+2	5.600E-03	3.592E-03	2.069E-03	-2.68415	0.576157	0.2395	1.804E-07
460	Mg+2	6.000E-03	4.025E-03	2.319E-03	-2.63464	0.576157	0.2395	1.840E-07

```
      2  H2O        0.000E+00 -2.508E-07 9.995E-01   -0.00022   1.000000   0.0002  0.000E+00
    732  SO4-2      1.400E-02  9.044E-03 5.211E-03   -2.28311   0.576157   0.2395 -1.595E-21
    330  H+1        5.012E-07  1.148E-06 1.000E-06   -6.00000   0.871235   0.0599  5.421E-20
```

Type I - COMPONENTS AS SPECIES IN SOLUTION

```
   ID      NAME      CALC MOL   ACTIVITY   LOG ACTVTY    GAMMA     NEW LOGK      DH
  330  H+1          1.148E-06  0.0000010   -6.00000     0.871235    0.060      0.000
  280  Fe+2         1.964E-03  0.0011313   -2.94641     0.576157    0.239      0.000
  140  CO3-2        8.315E-09  0.0000000   -8.31958     0.576157    0.239      0.000
  150  Ca+2         3.592E-03  0.0020694   -2.68415     0.576157    0.239    . 0.000
  732  SO4-2        9.044E-03  0.0052106   -2.28311     0.576157    0.239      0.000
  460  Mg+2         4.025E-03  0.0023193   -2.63464     0.576157    0.239      0.000
  281  Fe+3         3.751E-14  0.0000000  -13.96461     0.289213    0.539      0.000
```

Type II - OTHER SPECIES IN SOLUTION OR ADSORBED

```
    ID        NAME      CALC MOL   ACTIVITY   LOG ACTVTY    GAMMA     NEW LOGK      DH
3301401  H2CO3 AQ      2.610E-04  0.0002622   -3.58142    1.004616    16.736    -2.247
3307320  HSO4 -        4.418E-07  0.0000004   -6.41460    0.871235     1.928     4.910
3300020  OH-           5.275E-09  0.0000000   -8.33767    0.871235   -14.278    13.345
4603300  MgOH +        1.779E-09  0.0000000   -8.80979    0.871235   -12.115    15.935
4601400  MgCO3 AQ      9.053E-09  0.0000000   -8.04119    1.004616     2.911     2.022
4601401  MgHCO3 +      3.771E-06  0.0000033   -5.48337    0.871235    11.531    -2.430
4607320  MgSO4 AQ      1.971E-03  0.0019800   -2.70333    1.004616     2.212     1.399
1503300  CaOH +        2.557E-10  0.0000000   -9.65210    0.871235   -12.908    14.535
1501400  CaHCO3 +      2.334E-06  0.0000020   -5.69173    0.871235    11.372     1.790
1501401  CaCO3 AQ      1.159E-08  0.0000000   -7.93399    1.004616     3.068     4.030
1507320  CaSO4 AQ      2.006E-03  0.0020153   -2.69565    1.004616     2.270     1.470
2803300  FeOH +        1.895E-07  0.0000002   -6.78237    0.871235    -9.776    13.199
2803301  FeOH3 -1      2.198E-17  0.0000000  -16.71780    0.871235   -31.711    30.300
2807320  FeSO4 AQ      8.636E-04  0.0008676   -3.06168    1.004616     2.166     3.230
2803302  FeOH2 AQ      5.683E-13  0.0000000  -12.24345    1.004616   -21.299    28.565
2813300  FeOH +2       6.609E-11  0.0000000  -10.41935    0.576157    -2.215    10.399
2817320  FeSO4 +       4.292E-13  0.0000000  -12.42718    0.871235     3.880     3.910
2813301  FeOH2 +       2.660E-08  0.0000000   -7.63505    0.871235    -5.610     0.000
2813302  FeOH3 AQ      2.708E-10  0.0000000   -9.56527    1.004616   -13.602     0.000
2813303  FeOH4 -       3.122E-12  0.0000000  -11.56549    0.871235   -21.540     0.000
2817321  Fe(SO4)2 -    6.792E-14  0.0000000  -13.22784    0.871235     5.363     4.600
2813304  Fe2(OH)2+4    5.430E-19  0.0000000  -19.22306    0.110196    -2.336    13.500
2813305  Fe3(OH)4+5    8.673E-24  0.0000000  -24.55846    0.031870    -5.167    14.300
4701401  FeHCO3 +      1.674E-06  0.0000015   -5.83599    0.871235    11.490     0.000
3301400  HCO3 -        1.478E-04  0.0001288   -3.89011    0.871235    10.489    -3.617
```

Type III - SPECIES WITH FIXED ACTIVITY (fixed pH, fixed pe, infinite solids, gases, etc.)
```
   ID      NAME      CALC MOL    LOG MOL    NEW LOGK     DH
    2  H2O         -2.508E-07    -6.601     0.000      0.000
  330  H+1          1.856E-03    -2.731     6.000      0.000
```

Type IV - FINITE SOLIDS (present at equilibrium)
```
   ID        NAME      CALC MOL    LOG MOL    NEW LOGK     DH
2028103  SCHWERTMANIT  1.152E-04    -3.939    -18.000     0.000
```

Type VI - EXCLUDED SPECIES (not included in mole balance)
```
   ID      NAME      CALC MOL    LOG MOL    NEW LOGK     DH
3301403  CO2 (g)      7.147E-03    -2.146    18.173    -0.530
```

PERCENTAGE DISTRIBUTION OF COMPONENTS AMONG TYPE I and TYPE II (dissolved and adsorbed) species

Fe+3
```
           98.7      PERCENT BOUND IN SPECIES #2813301    FeOH2 +
            1.0      PERCENT BOUND IN SPECIES #2813302    FeOH3 AQ
```

Fe+2
```
           69.4      PERCENT BOUND IN SPECIES #    280    Fe+2
```

```
                    30.5    PERCENT BOUND IN SPECIES #2807320   FeSO4 AQ


CO3-2
                    62.6    PERCENT BOUND IN SPECIES #3301401   H2CO3 AQ
                    35.5    PERCENT BOUND IN SPECIES #3301400   HCO3 -


Ca+2
                    64.1    PERCENT BOUND IN SPECIES #    150   Ca+2
                    35.8    PERCENT BOUND IN SPECIES #1507320   CaSO4 AQ


Mg+2
                    67.1    PERCENT BOUND IN SPECIES #    460   Mg+2
                    32.8    PERCENT BOUND IN SPECIES #4607320   MgSO4 AQ


H2O
                     2.1    PERCENT BOUND IN SPECIES #3300020   OH-
                    75.5    PERCENT BOUND IN SPECIES #2803300   FeOH +
                    21.2    PERCENT BOUND IN SPECIES #2813301   FeOH2 +


SO4-2
                    65.1    PERCENT BOUND IN SPECIES #    732   SO4-2
                    14.2    PERCENT BOUND IN SPECIES #4607320   MgSO4 AQ
                    14.4    PERCENT BOUND IN SPECIES #1507320   CaSO4 AQ
                     6.2    PERCENT BOUND IN SPECIES #2807320   FeSO4 AQ


H+1
                    76.9    PERCENT BOUND IN SPECIES #3301401   H2CO3 AQ
                    21.8    PERCENT BOUND IN SPECIES #3301400   HCO3 -



            --------------------------------------------------------
            ----------- EQUILIBRATED MASS DISTRIBUTION -----------

IDX     NAME            DISSOLVED           SORBED           PRECIPITATED
                     MOL/KG   PERCENT    MOL/KG   PERCENT    MOL/KG   PERCENT

281  Fe+3            2.694E-08    0.0    0.000E+00    0.0    9.215E-04   100.0
280  Fe+2            2.829E-03  100.0    0.000E+00    0.0    0.000E+00     0.0
140  CO3-2           4.166E-04  100.0    0.000E+00    0.0    0.000E+00     0.0
150  Ca+2            5.600E-03  100.0    0.000E+00    0.0    0.000E+00     0.0
460  Mg+2            6.000E-03  100.0    0.000E+00    0.0    0.000E+00     0.0
  2  H2O             2.508E-07  100.0    0.000E+00    0.0    0.000E+00     0.0
732  SO4-2           1.388E-02   99.2    0.000E+00    0.0    1.152E-04     0.8
330  H+1             6.789E-04  100.0    0.000E+00    0.0    0.000E+00     0.0

     CHARGE BALANCE: SPECIATED
            SUM OF CATIONS =  1.917E-02 SUM OF ANIONS   1.824E-02
            PERCENT DIFFERENCE =   2.500E+00   (ANIONS - CATIONS)/(ANIONS + CATIONS)
     EQUILIBRIUM IONIC STRENGTH (m) =   2.000E-02
     EQUILIBRIUM pH                 =   6.000
```

Saturation indices and stoichiometry of all minerals

```
    ID #      NAME      Sat. Index      Stoichiometry (in parentheses) of each component
  2028103 SCHWERTMANIT    0.000    (  8.000)281  (  1.000)732  (-22.000)330
  6015000 ANHYDRITE      -0.426    (  1.000)150  (  1.000)732
  5015000 ARAGONITE      -2.754    (  1.000)150  (  1.000)140
  5046000 ARTINITE      -11.921    ( -2.000)330  (  2.000)460  (  1.000)140  (  5.000)  2
  2046000 BRUCITE        -8.084    (  1.000)460  (  2.000)  2  ( -2.000)330
  5015001 CALCITE        -2.581    (  1.000)150  (  1.000)140
  5015002 DOLOMITE       -5.169    (  1.000)150  (  1.000)460  (  2.000)140
  6046000 EPSOMITE       -2.708    (  1.000)460  (  1.000)732  (  7.000)  2
  2028100 FERRIHYDRITE   -0.856    ( -3.000)330  (  1.000)281  (  3.000)  2
  2028101 FE3(OH)8       -3.099    ( -8.000)330  (  2.000)281  (  1.000)280  (  8.000)  2
  6028100 FE2(SO4)3     -39.862    (  2.000)281  (  3.000)732
  2028102 GOETHITE        3.167    ( -3.000)330  (  1.000)281  (  2.000)  2
  6015001 GYPSUM         -0.113    (  1.000)150  (  1.000)732  (  2.000)  2
  3028100 HEMATITE       11.294    ( -6.000)330  (  2.000)281  (  3.000)  2
  5015003 HUNTITE       -14.554    (  3.000)460  (  1.000)150  (  4.000)140
  5046001 HYDRMAGNESIT  -27.015    (  5.000)460  (  4.000)140  ( -2.000)330  (  6.000)  2
  6028101 JAROSITE H     -5.764    ( -5.000)330  (  3.000)281  (  2.000)732  (  7.000)  2
  3028101 MAGHEMITE       1.684    ( -6.000)330  (  2.000)281  (  3.000)  2
```

```
5046002 MAGNESITE      -3.082    (  1.000)460   (  1.000)140
3028000 MAGNETITE      12.103    ( -8.000)330   (  2.000)281   (  1.000)280   (  4.000)  2
6028000 MELANTERITE    -2.688    (  1.000)280   (  1.000)732   (  7.000)  2
5046003 NESQUEHONITE   -5.481    (  1.000)460   (  1.000)140   (  3.000)  2
5028000 SIDERITE       -0.852    (  1.000)280   (  1.000)140
2015000 LIME          -24.658    ( -2.000)330   (  1.000)150   (  1.000)  2
2015001 PORTLANDITE   -14.140    ( -2.000)330   (  1.000)150   (  2.000)  2
2028000 WUSTITE        -3.109    ( -2.000)330   (  0.947)280   (  1.000)  2
2046001 PERICLASE     -13.064    ( -2.000)330   (  1.000)460   (  1.000)  2
3046001 MAG-FERRITE    -1.025    ( -8.000)330   (  1.000)460   (  2.000)281   (  4.000)  2
3028102 LEPIDOCROCIT    2.664    ( -3.000)330   (  1.000)281   (  2.000)  2
```

Appendix K

Determination Ferrous Oxidation Rate Constants

Location	Flow Time (Hours)	Ferrous (mg/L)	DO (mg/L)	Ferric (mg/L)	pH	d(fe)/dt mg/L-hr	d[Fe+2]/dt*[H]^2 [DO]*[Fe+2] M/sec
At Pipe	0	104.5	0	0	6.11	0	
Bend #2	3	64.7	7	13.4	6.47	13.26666667	5.2377E-14
Bend #3	74	45.2	6.2	5.6	6.63	0.274647887	5.69199E-16

Location	Converson to [OH] units 1/M^3 sec	AVE [H] mol	AVE[Fe+2] mg/L	AVE[Fe+3] mg/L	[H]*[Fe+3] M mg/L
At Pipe					
Bend #2	5.2377E+14	5.13E-07	84.6	6.7	3.436E-06
Bend #3	5.69199E+12	2.82E-07	54.95	9.5	2.677E-06
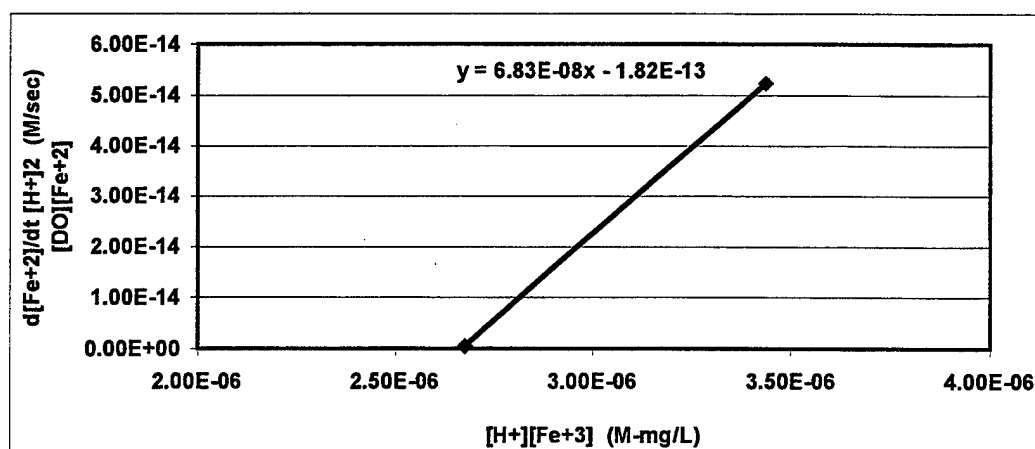
Figure K-1: Determination of rate constants for CK sampling trip, 6 June 1998.

Location	Flow Time (Hours)	Ferrous (mg/L)	DO (mg/L)	Ferric (mg/L)	pH	d(fe)/dt mg/L-hr	d[Fe+2]/dt*[H]^2 [DO]*[Fe+2] M/sec
At Pipe	0	97	0	7.3	6.4	0	
Bend #2	3.83	73.6	8.5	8.3	6.85	6.109660574	4.21208E-15
Bend #3	7.2	58.5	8.2	6.5	6.9	4.480712166	1.3077E-15

Location	Converson to [OH] units 1/M^3 sec	AVE [H] mol	AVE[Fe+2] mg/L	AVE[Fe+3] mg/L	[H]*[Fe+3] M mg/L
At Pipe					
Bend #2	4.21208E+13	2.37E-07	85.3	7.8	1.85E-06
Bend #3	1.3077E+13	1.33E-07	66.05	7.4	9.868E-07
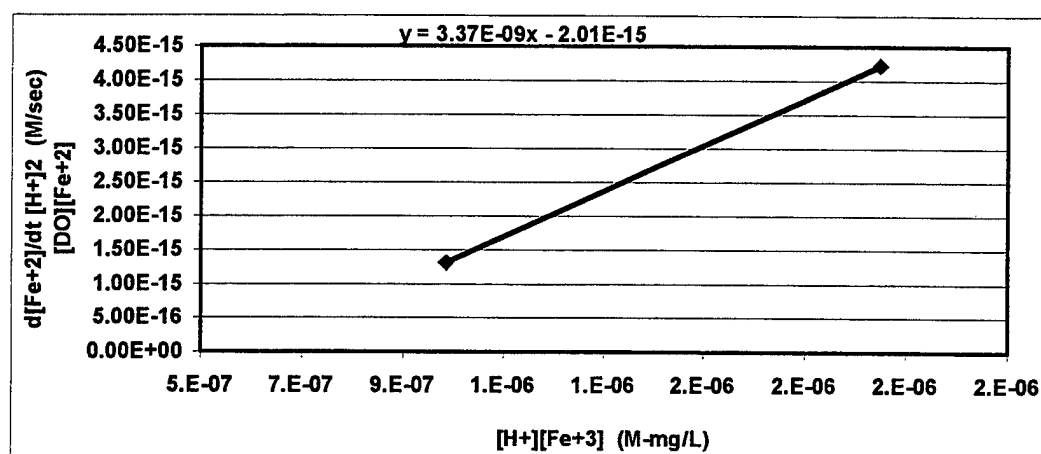
Figure K-2: Determination of rate constants for CK sampling trip, 1 March 1998.

Location	Flow Time (Hours)	Ferrous (mg/L)	DO (mg/L)	Ferric (mg/L)	pH	d(fe)/dt mg/L-hr	d[Fe+2]/dt*[H]^2 [DO]*[Fe+2] M/sec
At Pipe	0	110	0	0	6.33	0	
Bend #2	3.83	77.2	7	2	6.64	8.563968668	1.24494E-14
Bend #3	7.2	38.2	5.1	11.1	6.66	11.5727003	1.75201E-14

Location	Converson to [OH] units 1/M^3 sec	AVE [H] mol	AVE[Fe+2] mg/L	AVE[Fe+3] mg/L	[H]*[Fe+3] M mg/L
At Pipe					
Bend #2	1.24494E+14	3.27E-07	93.6	1	3.273E-07
Bend #3	1.75201E+14	2.24E-07	57.7	6.55	1.466E-06
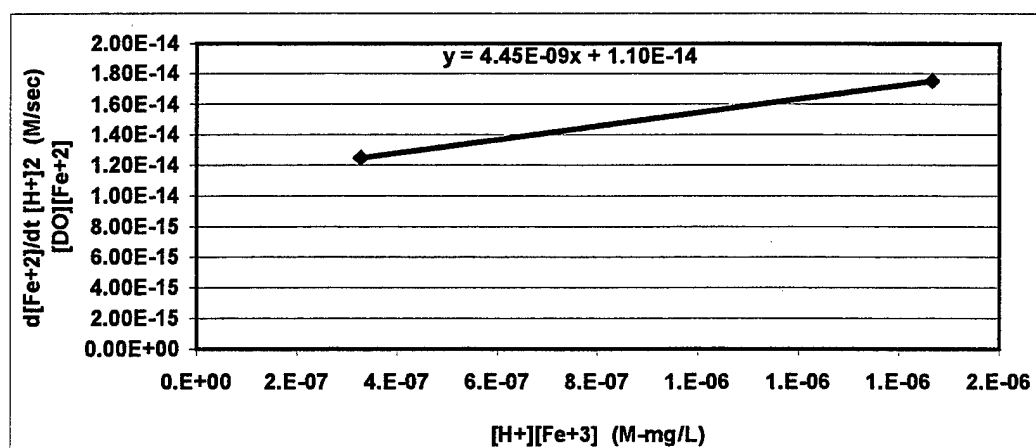
Figure K-3: Determination of rate constants for CK sampling trip, 29 March 1998.

Location	Flow Time (Hours)	Ferrous (mg/L)	DO (mg/L)	Ferric (mg/L)	pH	d(fe)/dt mg/L-hr	d[Fe+2]/dt*[H]^2 [DO]*[Fe+2] M/sec
At Pipe	0	100	0	1.24	6.21	0	
Bend #2	5.8	61.9	5	6.6	6.38	6.568965517	3.70815E-14
Bend #3	10.86	22.7	5.4	12.9	6.58	7.747035573	3.30559E-14

Location	Converson to [OH] units 1/M^3 sec	AVE [H] mol	AVE[Fe+2] mg/L	AVE[Fe+3] mg/L	[H]*[Fe+3] M mg/L
At Pipe					
Bend #2	3.70815E+14	5.07E-07	80.95	3.92	1.987E-06
Bend #3	3.30559E+14	3.31E-07	42.3	9.75	3.229E-06
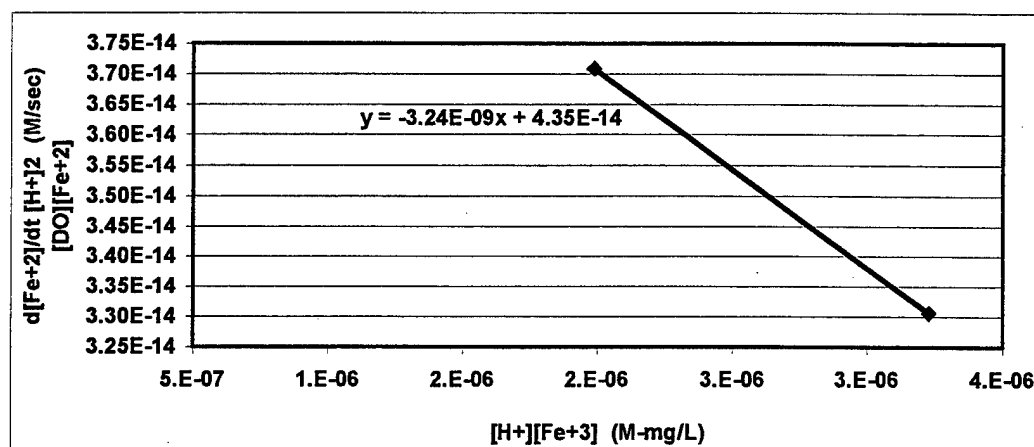
Figure K-4: Determination of rate constants for CK sampling trip, 3 July 1998.

Appendix L

Bulk Analysis of HB IP2 Water and Sludge Samples

Table L-1: Bulk analysis on the core sample taken from HB pond #2 on 24 Jan 1998.

Wt. %	HB IP2 Top layer	HB IP2 Middle layer	HB IP2 Bottom layer
Al_2O_3	0.053	0.158	1.550
B_2O_3	0.004	0.005	0.008
BaO	<0.002	<0.002	0.007
CaO	0.034	0.036	0.054
CoO	<0.002	<0.002	<0.002
Cr_2O_3	<0.002	<0.002	<0.002
Fe_2O_3	13.7	16.4	15.4
K_2O	0.005	0.021	0.260
MgO	0.020	0.024	0.079
MnO	0.034	0.049	0.051
MoO_3	<0.002	0.003	0.004
Na_2O	0.004	0.008	0.060
NiO	<0.002	<0.002	<0.002
SiO_2	0.35	1.27	10.5
SrO	<0.002	<0.002	<0.002
TiO_2	<0.002	0.007	0.118
V_2O_5	<0.002	<0.002	<0.002
ZnO	0.01	0.016	0.015
F	<0.001	<0.001	<0.001
Cl	0.008	0.006	<0.001
Nitrate	<0.001	<0.001	<0.001
Phosphate	<0.002	<0.002	<0.002
SO_3	0.127	0.084	0.108
Moisture	81.7	76.6	66.9
$LOI-1000^0C$	84.6	80.0	70.4

Table L-2: Bulk analysis on filtered sample taken from HB IP2 on 24 January 1998. The cation sample was acidified, the anion sample was not.

HB IP2 water sample	mg/L
Al	0.25
B	0.03
Ba	0.03
Ca	110
Co	0.33
Cr	0.03
Fe	100
K	4.3
Mg	53
Mn	20.3
Mo	0.10
Na	9.5
Ni	0.27
Si	4.2
Sr	0.7
Ti	0.02
V	0.03
Zn	0.28
F	<0.02
Cl	4.3
Nitrate	<0.05
Phosphate	<0.2
SO$_4$	610

Appendix M

Results from TIC Experiments

Table M-1: CK results for TIC analysis.

	31-Jan-98	1-Mar-98	29-Mar-98	13-May-98	6-Jun-98	3-Jul-98	5-Aug-98	26-Aug-98	26-Sep-98	24-Oct-98
Alkalinity (mg/L)										
at Pipe					253.6	266.4	309.4	333.2	379.5	311.0
B1		338.2			247.8	275.9	290.9	288.4	283.3	221.2
B2		246.1			219.8	197.0	181.9	141.4	164.9	160.0
B3		206.5			177.7	140.0	140.2	136.6	175.5	170.7
TIC (mg/L)										
at Pipe					134.1	124.7	142.0	144.8	150.0	167.0
B1		114.5			102.1	98.8	116.0	115.0	114.0	91.0
B2		71.7			65.0	77.0	74.0	55.2	60.0	57.2
B3		58.3			46.3	47.8	50.0	43.0	50.0	55.0

Table M-2: HB results for TIC analysis.

	31-Jan-98	1-Mar-98	29-Mar-98	13-May-98	6-Jun-98	3-Jul-98	5-Aug-98	26-Aug-98	26-Sep-98	25-Oct-98	22-Nov-98	14-Dec-98
Alkalinity (mg/L)												
at Pipe	207.1	181.9			144.5	144.4	147.8	157.2	121.4	138.4	104.2	116.6
IP1	180.8	153.5			132.5		148.2		126.2			
EP1	169.3	141.7			114.2	133.4	100.5	111.3	121.5	105.3	71.6	71.8
IP2	152.0	133.8			119.9	118.9	107.4	111.5	109.2	95.6	72.6	67.0
EP2	62.1	87.3			38.4	47.1	33.2	53.4	47.8	23.1	26.2	37.4
FE	-8.0	-10.0			-82.9	-140.0	-75.0	-77.0	-93.0	-64.0	-55.0	-45.0
TIC (mg/L)												
at Pipe	76.8	71.1			76.0	74.9	77.0	77.8	76.0	82.0	58.5	70.9
IP1	61.3	58.7			65.6	55.9	66.0		68.6			
EP1	53.6	51.7			51.7	61.1	57.0	62.0	64.0	66.0	37.5	46.5
IP2	47.8	49.3			25.0	54.8	54.0	58.0	59.0	56.0	34.7	41.2
EP2	25.5	37.9			23.4	36.6	35.0	43.5	41.0	25.0	21.3	29.3
FE	21.3	2.9			2.1	2.6	1.6	2.0	4.0	4.0	0.6	7.8

Appendix N

Results of TOC Experiment

Table N-1: Results of the TOC machine for 3 July samples.

Location	TOC (mg/L)
CK @ pipe	1.316
CK B2	1.355
HB IP2	1.110
HB @ pipe	0.99

Appendix O

XRD Signature Cards used for Analysis of the Sludge

Table O-1: XRD card for Silicon Oxide.

46-1045																		Quality:S

Si O2
Silicon Oxide
Quartz, syn
Rad:CuKa1   Lambda:1.540598   Filter:Monochromator crystal used   d sp:Diffractometer
Cutoff: Int:Diffractometer   I/Icor:3.41
Ref:Kern, A., Eysel, W., Mineralogisch-Petrograph.Inst., Univ. Heidelberg, Germany.Swanson, Fuyat., (1993)
Sys:Hexagonal   S.G.:P3221
a:4.91344±4E-5   b: c:5.40524±8E-5
α: β: γ: Z:3   mp
Ref2
Dx:2.65   Dm:2.649   SS/FOM: F30=538.7(0.0018,31)   Volume[CD]:113.01
εα: ηωβ:1.544   εγ:1.553   Sign:+   2V:
Ref3
Color:White
Pattern taken at 23(1) C. Low temperature quartz. 2SGU determination based on profile fit method. To replace 33-1161.

58 reflections in pattern.

d A	Int.	h	k	l	d A	Int.	h	k	l	d A	Int.	h	k	l	d A	Int.	h	k	l
4.2550	16	1	0	0	1.3821	6	2	1	2	1.0477	1	1	0	5	0.8972	1	2	1	5
3.3435	100	1	0	1	1.3750	7	2	0	3	1.0438	1	4	0	1	0.8889	1	3	1	4
2.4569	9	1	1	0	1.3719	5	3	0	1	1.0346	1	2	1	4	0.8814	1	1	0	6
2.2815	8	1	0	2	1.2879	2	1	0	4	1.0149	1	2	2	3	0.8782	1	4	1	2
2.2361	4	1	1	1	1.2559	3	3	0	2	0.9896	1	1	1	5	0.8598	1	3	0	5
2.1277	6	2	0	0	1.2283	1	2	2	0	0.9872	1	3	1	3	0.8458	1	1	1	6
1.9799	4	2	0	1	1.1998	2	2	1	3	0.9783	1	3	0	4	0.8407	1	5	0	1
1.8180	13	1	1	2	1.1978	1	2	2	1	0.9762	1	3	2	0	0.8359	1	4	0	4
1.8017	1	0	0	3	1.1840	2	1	1	4	0.9608	1	3	2	1	0.8296	1	2	0	6
1.6717	4	2	0	2	1.1802	2	3	1	0	0.9285	1	4	1	0	0.8254	2	4	1	3
1.6592	2	1	0	3	1.1530	1	3	1	1	0.9182	1	3	2	2	0.8189	1	3	3	0
1.6083	1	2	1	0	1.1407	1	2	0	4	0.9161	2	4	0	3	0.8117	3	5	0	2
1.5415	9	2	1	1	1.1145	1	3	0	3	0.9152	2	4	1	1	0.8097	1	3	3	1
1.4529	2	1	1	3	1.0816	2	3	1	2	0.9089	1	2	2	4					
1.4184	1	3	0	0	1.0638	1	4	0	0	0.9009	1	0	0	6					

Table O-2: XRD card for Fibroferrite.

38-0481										Quality:S	

| Fe (SO4) (O H) !5 H2 O |
| Iron Sulfate Hydroxide Hydrate |
| Fibroferrite |

Rad:CoKa1	Lambda:1.7889	Filter:Beta filter used		d sp:Diffractometer
Cutoff:	Int:Diffractometer	I/Icor:		

Ref:Sabelli, C., Santucci, A., 1987 171, (1987)

Sys:Rhombohedral		S.G.:R-3		
a:24.152±0.003	b:	c:7.645±0.002		
α:	β:	γ:	Z:18	mp
Ref2				
Dx:	Dm:2.004	SS/FOM: F30=10.3(0.03,98)	Volume[CD]:3862.02	
εα:	ηωβ:	εγ:	Sign:	2V:
Ref3				

| Color:Yellow, green |
| Specimen from Cetine mine, Tuscany, Italy. To replace 16-935. |

33 reflections in pattern.

d A	Int.	h	k	l	d A	Int.	h	k	l	d A	Int.	h	k	l	d A	Int.	h	k	l
12.1000	100	1	1	0	3.5880	5	2	0	2	2.6800	8	1	5	2	1.7040	3	5	1	4
6.9800	42	3	0	0	3.5050	5	2	4	1	2.5290	7	5	4	1	1.6780	5	6	8	1
6.1800	13	0	2	1	3.4850	7	6	0	0	2.4230	8	2	7	1	1.5750	3	13	0	1
6.0300	8	2	2	0	3.4430	22	1	2	2	2.3290	10	8	1	1					
5.5000	10	2	1	1	3.3460	33	5	1	1	2.2820	5	2	8	0					
4.6200	5	1	3	1	3.3460	33	2	5	0	2.1570	8	8	0	2					
4.5700	53	1	4	0	3.1340	17	4	3	1	2.1080	5	6	5	1					
4.3100	13	4	0	1	2.9890	25	2	3	2	2.0450	5	3	8	1					
4.0700	35	3	2	1	2.7840	30	7	0	1	1.9890	8	9	2	1					
3.7540	5	0	1	2	2.7130	8	6	2	1	1.9390	3	5	7	1					

Table O-3: XRD card for Amarantite.

17-0158

Fe S O4 (O H) !3 H2 O
Iron Sulfate Hydroxide Hydrate
Amarantite

Rad:CuKa	Lambda:1.5418	Filter:Monochromator crystal used		d sp:
Cutoff:	Int:	I/Icor:		
Ref:Cesbron.. 87 125. (1964)				

Sys:Anorthic (triclinic)		S.G.:P-1		
a:8.9	b:11.56	c:6.64		
α:95.55	β:90.52	γ:97.42	Z:4	mp
Ref2				
Dx:2.197	Dm:2.197	SS/FOM: F30=1.8(0.11,149)	Volume[CD]:674.09	
ea:1.516	ηωβ:1.598	εγ:1.621	Sign:-	2V:30SDE
Ref3				

Color:Red, brownish red
Specimen from Sierra Gorda. Chile. Analysis (%): \Fe2 O3\ 36.10, \S O3\ 35.10, \H2 O\ 28.80.

36 reflections in pattern.

d A	Int.	h	k	l	d A	Int.	h	k	l	d A	Int.	h	k	l	d A	Int.	h	k	l
11.3000	100	0	1	0	4.1300	10	0	2	1	2.7420	5	0	2	2	2.0620	10	0	4	2
8.6900	100	1	0	0	3.7400	10	-2	2	0	2.6750	20	-2	0	2	2.0400	10	-4	2	1
7.3400	10	-1	1	0	3.6500	20	2	-1	1	2.6220	40	0	-3	2	1.9810	5	1	5	1
6.5000	30	1	1	0	3.5700	80	-2	1	1	2.5490	20	-2	4	0	1.9500	5	-2	4	2
5.8800	5	0	-1	1	3.4100	40	0	-3	1	2.4760	20	2	1	2	1.8630	10	4	2	1
5.6100	10	0	2	0	3.1100	60	-1	0	2	2.4240	10	-2	-2	2	1.8010	10	-1	5	2
5.3900	10	-1	0	1	3.0500	80	-1	-1	2	2.2840	5	-1	5	0					
5.1600	40	-1	2	0	2.9900	30	0	-2	2	2.2390	10	1	3	2					
4.9800	40	1	-1	1	2.9350	10	3	0	0	2.1600	5	-1	-4	2					
4.4600	20	1	1	1	2.8180	20	-1	4	0	2.1130	10	4	1	0					

Table O-4: XRD card for Siderite.

Quality:S

29-0696

Fe C O3

Iron Carbonate

Siderite

| Rad:CuKa1 | Lambda:1.540598 | Filter:Monochromator crystal used | d sp: |

Cutoff: Int: I/Icor:

Ref:. 15 32. (1978)

Sys:Rhombohedral   S.G.:R-3c

a:4.6935±0.0002   b: c:15.386±0.008

α: β: γ: Z:6   mp

Ref2

Dx:3.932   Dm:3.932   SS/FOM: F30=75.3(0.0102,39)   Volume[CD]:293.53

εα: ηωβ:1.8728(1)   εγ:1.6331   Sign:-   2V:

Ref3

Color:Light yellowish brown

Optical data on specimen from Camborne. Specimen from Ivigtut, Greenland (NMNH 132849). Spectrographic analysis indicates 1-2% Mn. Pattern taken at 25 C. To replace 8-133.

33 reflections in pattern.

d A	Int.	h	k	l	d A	Int.	h	k	l	d A	Int.	h	k	l	d A	Int.	h	k	l
3.5930	25	0	1	2	1.5063	14	1	2	2	1.1977	4	3	0	6	0.9358	2	1	0	16
2.7950	100	1	0	4	1.4390	3	1	0	10	1.1737	2	2	2	0	0.9309	6	3	2	1
2.5640	1	0	0	6	1.4266	11	2	1	4	1.1254	4	1	1	12	0.9256	3	2	3	2
2.3460	20	1	1	0	1.3969	6	2	0	8	1.1154	1	3	1	2					
2.1340	20	1	1	3	1.3818	3	1	1	9	1.0872	3	2	1	10					
1.9650	20	2	0	2	1.3548	11	3	0	0	1.0820	5	1	3	4					
1.7968	12	0	2	4	1.2823	5	0	0	12	1.0671	4	2	2	6					
1.7382	30	0	1	8	1.2593	1	2	1	7	0.9825	5	4	0	4					
1.7315	35	1	1	6	1.2269	3	0	2	10	0.9724	5	3	1	8					
1.5291	3	2	1	1	1.2002	5	1	2	8	0.9666	2	2	0	14					

Table O-5: XRD card for Magnesioferrite.

Mg Fe2 O4

Magnesium Iron Oxide

Magnesioferrite, ordered svn

| Rad:CuKa | Lambda:1.542 | Filter:Beta filter used | d sp: |
| Cutoff: | Int: | I/Icor: | |

Ref:Allen, W., School of Ceramics, RutgersUniv., New Brunswick, NJ, USA., (1965)

Sys:Cubic		S.G.:Fd3m		
a:8.375	b:	c:		
α:	β:	γ:	Z:8	mp
Ref2				
Dx:4.522	Dm:4.523	SS/FOM: F22=21.7(0.032,32)	Volume[CD]:587.43	

| εα: | ηωβ:2.35 | εγ: | Sign: | 2V: |
| Ref3 | | | | |

Color:Red brown

Synthetic, by solid state reaction of MgO, \Fe2 O3\ in air at 1600 C equilibrated at temperatures below 350 C and quenched. Magnesioferrites, equilibrated at temperatures between 350 and 950 and quenched, have cell sizes which range linearly between this form and the high temperature form.

22 reflections in pattern.

d A	Int.	h	k	l	d A	Int.	h	k	l	d A	Int.	h	k	l	d A	Int.	h	k	l
4.8400	4	1	1	1	1.2080	2	4	4	4	0.8210	4	10	2	0					
2.9600	40	2	2	0	1.1190	4	6	4	2	0.8100	8	9	5	1					
2.5250	100	3	1	1	1.0900	12	7	3	1										
2.4180	2	2	2	2	1.0470	6	8	0	0										
2.0940	25	4	0	0	0.9870	4	6	6	0										
1.7090	14	4	2	2	0.9670	8	7	5	1										
1.6120	30	5	1	1	0.9360	2	8	4	0										
1.4810	35	4	4	0	0.8930	1	6	6	4										
1.3240	6	6	2	0	0.8780	6	9	3	1										
1.2770	8	5	3	3	0.8550	10	8	4	4										

Table O-6: XRD card for Magnetite.

19-0629   Quality:S

Fe Fe2 O4

Iron Oxide

Magnetite, svn

| Rad:CuKa1 | Lambda:1.54056 | Filter:Beta filter used | d sp: |
| Cutoff: | Int: | I/Icor:4.9 | |

Ref:. 5 31. (1967)

Sys:Cubic		S.G.:Fd3m		
a:8.396	b:	c:		
α:	β:	γ:	Z:8	mp

Ref2

| Dx:5.197 | Dm:5.197 | SS/FOM: F26=58(0.0132,34) | Volume[CD]:591.86 |

| εα: | ηωβ:2.42 | εγ: | Sign: | 2V: |

Ref3

Color:Black

a=8.3967 refined in 1975. Other data 25-1376. Sample obtained from the Columbian Carbon Co., New York, NY, USA.
Spectrographic analysis showed the following major impurities: 0.01 to 0.1% Co, 0.001 to 0.01% Ag, Al, Mg, Mn, Mo, Ni, Si, Ti
and Zn. Pattern taken at 25 C. Opaque mineral optical data on specimen from Braastad, Norway: RR#2R#e=20.1, Disp.=16.
VHN#1#0#0=592, Color values=.311, .314, 20.1, Ref.: IMA Commission on Ore Microscopy QDF. To replace 11-614. See also
26-1136.

26 reflections in pattern.

d A	Int.	h	k	l	d A	Int.	h	k	l	d A	Int.	h	k	l	d A	Int.	h	k	l
4.8520	8	1	1	1	1.2807	10	5	3	3	0.8952	2	6	6	4					
2.9670	30	2	2	0	1.2659	4	6	2	2	0.8802	6	9	3	1					
2.5320	100	3	1	1	1.2119	2	4	4	4	0.8569	8	8	4	4					
2.4243	8	2	2	2	1.1221	4	6	4	2	0.8233	4	10	2	0					
2.0993	20	4	0	0	1.0930	12	7	3	1	0.8117	6	9	5	1					
1.7146	10	4	2	2	1.0496	6	8	0	0	0.8080	4	10	2	2					
1.6158	30	5	1	1	0.9896	2	6	6	0										
1.4845	40	4	4	0	0.9695	6	7	5	1										
1.4192	2	5	3	1	0.9632	4	6	6	2										
1.3277	4	6	2	0	0.9388	4	8	4	0										

Table O-7: XRD card for Hematite.

33-0664   Quality:S

| Fe2 O3 |
| Iron Oxide |
| Hematite, syn |

Rad:CuKa1	Lambda:1.540598	Filter:Monochromator crystal used	d sp:Diffractometer
Cutoff:	Int:Diffractometer	I/Icor:2.4	
Ref:, 18 37. (1981)			

Sys:Rhombohedral		S.G.:R-3c		
a:5.0356±0.0001	b:	c:13.7489±0.0007		
α:	β:	γ:	Z:6	mp
Ref2				
Dx:5.27	Dm:5.27	SS/FOM: F30=69.3(0.0111,39)	Volume[CD]:301.93	

| εα:2.94 | ηωβ:3.22 | εγ: | Sign:- | 2V: |
| Ref3 | | | | |

| Color:Dark reddish brown |

1350-1360$DE Sample from Pfizer, Inc., NY, USA, heated at 800 C for 3 days. Pattern taken at 25 C. To replace 13-534 and validated by calculated pattern 24-72. Opaque mineral optical data on specimen from Elba, R#1R#0=30.2, RR#2R#e=26.1, Disp.=16, VHN=1038 (mean at 100, 200, 300), Color values=1 .299, .309, 29.8, 2 .299, .309, 25.7, Ref.: IMA Commission on Ore Microscopy QDF. Pattern reviewed by Syvinski, W., McCarthy, G., North Dakota State Univ., Fargo, ND, USA. \ITICDD Grant-in-Aid\RG (1990). Agress well with experimental and calculated patterns. Additional weak reflection [indicated by brackets] was observed. Also called: crocus mantis. Also called: venetian red. Also called: ferrite. Also called: indian red. Also called: crocus.

45 reflections in pattern.

d A	Int.	h	k	l	d A	Int.	h	k	l	d A	Int.	h	k	l	d A	Int.	h	k	l
3.6840	30	0	1	2	1.4538	30	3	0	0	1.0768	2	0	4	2	0.8998	1	3	0	12
2.7000	100	1	0	4	1.4138	1	1	2	5	1.0557	7	2	1	10	0.8954	3	2	0	14
2.5190	70	1	1	0	1.3497	3	2	0	8	1.0428	1	1	1	12	0.8789	6	4	1	6
2.2920	3	0	0	6	1.3115	10	1	0	10	1.0393	3	4	0	4	0.8648	1	2	3	8
2.2070	20	1	1	3	1.3064	6	1	1	9	0.9892	4	3	1	8	0.8543	3	4	0	10
2.0779	3	2	0	2	1.2592	8	2	2	0	0.9715	1	2	2	9	0.8436	5	1	2	14
1.8406	40	0	2	4	1.2276	4	3	0	6	0.9606	5	3	2	4	0.8392	3	3	3	0
1.6941	45	1	1	6	1.2141	2	2	2	3	0.9581	4	0	1	14	0.8089	4	3	2	10
1.6367	1	2	1	1	1.1896	5	1	2	8	0.9516	5	4	1	0	0.8014	4	2	4	4
1.6033	5	1	2	2	1.1632	5	0	2	10	0.9318	2	4	1	3					
1.5992	10	0	1	8	1.1411	7	1	3	4	0.9206	2	0	4	8					
1.4859	30	2	1	4	1.1035	7	2	2	6	0.9081	5	1	3	10					

Table O-8: XRD card for Jarosite.

| 22-0827 | | | | | | | | | | | | | | | | | | | Quality:S |

| K Fe3 (S O4)2 (O H)6 |
| Potassium Iron Sulfate Hydroxide |
| Jarosite, syn |

Rad:CoKa	Lambda:1.7902	Filter:		d sp:Guinier
Cutoff:	Int:Guinier	I/Icor:		
Ref:Smith, Plessev Company, Limited, Caswell,Towcaster, Northants, UK.				

Sys:Rhombohedral		S.G.:R-3m		
a:7.29	b:	c:17.16		
α:	β:	γ:	Z:3	mp
Ref2				
Dx:3.158	Dm:3.159	SS/FOM: F30=20(0.038,40)	Volume[CD]:789.77	

| εα:1.715 | ηωβ:1.820 | εγ: | Sign: | 2V: |
| Ref3 | | | | |

| Color:Yellow, brown |

\Fe2 (S O4)3\ + \K2 S O4\ + \H2 S O4\. Heated 170 C for 24 hours in sealed tube. Occurs as mineral at Meadow Valley 1, Pioche, Nevada, USA, with a=7.304, c=17.268, S.G.=`R-3m` (166), Dx=3.158, Kato, T., Miura, \IT Mineral. J. Japan\RG, \BF8\RG 419 (1977). To replace 10-443.

42 reflections in pattern.

d A	Int.	h	k	l	d A	Int.	h	k	l	d A	Int.	h	k	l	d A	Int.	h	k	l	d A	Int.	h	k	l
5.9300	45	1	0	1	2.3680	4	2	1	1	1.6560	2	1	0	10	1.4280	4	2	3	2					
5.7200	25	0	0	3	2.3020	12	1	2	2	1.6210	6	1	3	4	1.4230	4	1	3	7					
5.0900	70	0	1	2	2.2870	40	1	0	7	1.5950	6	1	2	8	1.4120	4	3	0	9					
3.6500	40	1	1	0	1.9770	45	3	0	3	1.5720	4	4	0	1	1.3990	4	2	0	11					
3.5500	4	1	0	4	1.9370	10	0	2	7	1.5600	6	3	1	5	1.3790	4	4	1	0					
3.1100	75	0	2	1	1.9090	8	0	0	9	1.5520	6	0	4	2	1.3380	12	4	1	3					
3.0800	100	1	1	3	1.8250	45	2	2	0	1.5360	20	2	2	6	1.3260	2	4	0	7					
3.0200	6	0	1	5	1.7760	6	2	0	8	1.5070	20	0	2	10	1.3140	2	2	2	9					
2.9650	15	2	0	2	1.7380	6	2	2	3	1.4800	8	4	0	4	1.2870	2	1	0	13					
2.8610	30	0	0	6	1.7170	6	3	1	2	1.4420	4	3	2	1										
2.5420	30	0	2	4	1.6900	2	1	1	9	1.4320	4	0	4	5										

Table O-9: XRD card for Schwertmannite.

47-1775

Fe16 O16 (S O4)3 (O H)10 !10 H2 O

Iron Oxide Sulfate Hydroxide Hydrate

Schwertmannite

Rad:CoKa	Lambda:1.7902	Filter:Monochromator crystal used	d sp:Diffractometer
Cutoff:	Int:Diffractometer	I/Icor:	

Ref:Bigham. J., Carlson. L.. Murad. E.. 58 641. (1994)

Sys:Tetragonal		S.G.:P4/m		
a:10.66±0.04	b:	c:6.04±0.01		
α:	β:	γ:	Z:1	mp
Ref2				
Dx:	Dm:4.326	SS/FOM: F8=0.4(0.219,89)	Volume[CD]:686.36	
αx:	ηωβ:	εγ:	Sign:	2V:
Ref3				

Color:Yellowish brown

Specimen from Pyhasalmi sulfide mine. Oulu Province. Finland (Finnish Museum of Natural History B8659). Chemical analysis (wt.%): \Fe2 O3\ 62.6. \S O3\ 12.7. \C O2\ 1.5. \H2 O\@- 10.2. \H2 O\@+ 12.9. Structurally related to akaganeite-\IT M\RG.

9 reflections in pattern.

d A	Int.	h	k	l	d A	Int.	h	k	l	d A	Int.	h	k	l	d A	Int.	h	k	l
4.8600	37	2	1	0															
3.3900	46	3	1	0															
2.5500	100	2	1	2															
2.2800	23	3	0	2															
1.9500	12	1	1	3															
1.6600	21	5	2	2															
1.5100	24	0	0	4															
1.4600	18	2	0	4															
1.4600	18	5	4	2															

Table O-10: XRD card for Ferrihydrite.

				Quality:B

29-0712

FeS O7 (O H) !4 H2 O

Iron Oxide Hydroxide Hydrate

Ferrihydrite. svn

Rad:MoKa	Lambda:0.7107	Filter:Beta filter used	d sp:
Cutoff:	Int:	I/Icor:	

Ref:Chukhrov. F. et al. Van der Giessen., 23. (1973)

Sys:Hexagonal		S.G.:P		
a:5.08	b:	c:9.4		
α:	β:	γ:	Z:1	mp
Ref2				
Dx:3.796	Dm:3.796	SS/FOM: F6=2(0.109,27)	Volume[CD]:210.08	
ea:	ηωβ:	εγ:	Sign:	2V:
Ref3				

Color:Yellow. dark brown

Prepared by slow hydrolysis of ferric salts at pH>3. and below 9.5. To replace 22-1117. Measured density and color from \IT Am. MineraL\RG. 'BF60\RG 485 (1975).

6 reflections m pattern.

d A	Int.	h	k	l	d A	Int.	h	k	l	d A	Int.	h	k	l	d A	Int.	h	k	l
2.5000	100	1	1	0															
2.2100	80	2	0	0															
1.9600	80	1	1	3															
1.7200	50	1	1	4															
1.5100	70	1	1	5															
1.4800	80	1	0	6															

Table O-11: XRD card for Lepidocrocite.

44-1415

Fe O (O H)
Iron Oxide Hydroxide
Lepidocrocite. svn

Rad:CuKa1	Lambda:1.54056	Filter:Monochromator crystal used	d sp:Diffractometer
Cutoff:	Int:Diffractometer	I/Icor:1.2	

Ref:Martin. K., McCarthv. G., North DakotaState University. Fargo, North Dakota, USA.Posniak, E., Merwin. H.Christensen. H.

Sys:Orthorhombic		S.G.:Amam		
a:12.52±0.006	b:3.873±0.002	c:3.071±0.006		
α:	β:	γ:	Z:4	mp
Ref2				
Dx:3.964	Dm:3.963	SS/FOM: F30=52.6(0.0146.39)	Volume[CD]:148.91	
ea:1.94	ηωβ:2.20	ey:2.51	Sign:-	2V:83SDE
Ref3				

Color:Red-brown
Sample from Johnson Matthey Electronics. The I/I#c value for integrated reflection is 6.8. The discrepency results from broad reflections (FWHM = 0.92SDE at d=3.294). 250

34 reflections in pattern.

d A	Int.	h	k	l	d A	Int.	h	k	l	d A	Int.	h	k	l	d A	Int.	h	k	l	d A	Int.	h	k	l
6.2700	61	2	0	0	1.8502	12	2	2	0	1.4192	3	6	2	0	1.1845	7	1	3	1					
3.2940	100	2	1	0	1.8375	8	6	1	0	1.3916	12	2	1	2	1.1814	7	2	2	2					
2.9810	8	1	0	1	1.7350	21	5	1	1	1.3711	12	5	2	1	1.1781	4	6	1	2					
2.4730	76	3	0	1	1.6238	5	1	2	1	1.2984	4	4	1	2	1.0960	1	8	0	2					
2.4340	34	4	1	0	1.5650	3	8	0	0	1.2672	3	9	0	1										
2.3620	36	1	1	1	1.5344	33	0	0	2	1.2637	5	2	3	0										
2.0860	9	6	0	0	1.5248	30	3	2	1	1.2175	2	8	2	0										
2.0860	9	3	1	1	1.4915	5	2	0	2	1.2045	9	9	1	1										
1.9404	53	5	0	1	1.4510	5	8	1	0	1.2030	11	0	2	2										
1.9351	72	0	2	0	1.4357	8	7	1	1	1.1914	7	10	1	0										

Table O-12: XRD card for Goethite.

Quality:S

29-0713

| FeO(OH) |
| Iron Oxide Hydroxide |
| Goethite |

			d sp:
Rad:CoKa	Lambda:1.7902	Filter:	
Cutoff:	Int:	I/Icor:	
Ref:Harrison. R. et al., 52 51, (1975)			

Sys:Orthorhombic		S.G.:Pbnm		
a:4.608	b:9.956	c:3.0215		
α:	β:	γ:	Z:4	mp
Ref2				
Dx:	Dm:4.258	SS/FOM: F30=47.1(0.0155,41)	Volume[CD]:138.62	
εα:2.260	ηωβ:2.393	εγ:2.398	Sign:-	2V:15(15)SDE
Ref3				

Color:Dark brown

Specimen from Hindlow quarry, Derbyshire. England, UK (E35891). Lead nitrate used as internal standard (a=7.8568). Dx for \Fe3.88 Six (O H)4.31 O3.69\ (x </= 0.012), formula from chemical analysis with impurities deducted. Chemical analysis (wt.%): \Si O2\ 1.84, \Fe2 O3\ 86.30, \H2 O\ (<105C) 10.79, \H2 O\ (<105C) 0.86, and minor MgO, CaO, \C O2\ and organic C. To replace 17-536. Opaque mineral optical data on specimen from Restornel, Cornwall, England. UK: R#1R#o=17.5, RR#2R#e=15.6, Disp.=16. VHN=667 (mean at 100, 200, 300). Color values=1 .291, .296, 17.5, 2 .294, .299, 15.5, Ref.: IMA Commission on Ore Microscopy QDF.

38 reflections in pattern.

d A	Int.	h	k	l	d A	Int.	h	k	l	d A	Int.	h	k	l	d A	Int.	h	k	l
4.9800	12	0	2	0	2.1900	18	1	4	0	1.5637	10	1	5	1	1.3173	3	1	3	2
4.1830	100	1	1	0	2.0890	1	2	2	0	1.5614	8	1	6	0	1.2921	1	0	4	2
3.3830	10	1	2	0	2.0110	2	1	3	1	1.5091	8	0	0	2	1.2654	1	3	3	1
2.6930	35	1	3	0	1.9200	5	0	4	1	1.4675	2	3	2	0	1.2437	1	1	4	2
2.5830	12	0	2	1	1.8020	6	2	1	1	1.4541	5	0	6	1	1.1994	1	3	4	1
2.5270	4	1	0	1	1.7728	1	1	4	1	1.4207	2	1	1	2	1.1506	1	0	8	1
2.4890	10	0	4	0	1.7192	20	2	2	1	1.3936	3	3	3	0	1.1445	1	4	1	0
2.4500	50	1	1	1	1.6906	6	2	4	0	1.3694	2	3	0	1	1.1263	1	2	4	2
2.3030	1	2	0	0	1.6593	3	0	6	0	1.3590	3	1	7	0					
2.2530	14	1	2	1	1.6037	4	2	3	1	1.3459	1	2	6	0					

Appendix P

XRD Raw Data Checked Against Mineral Signatures
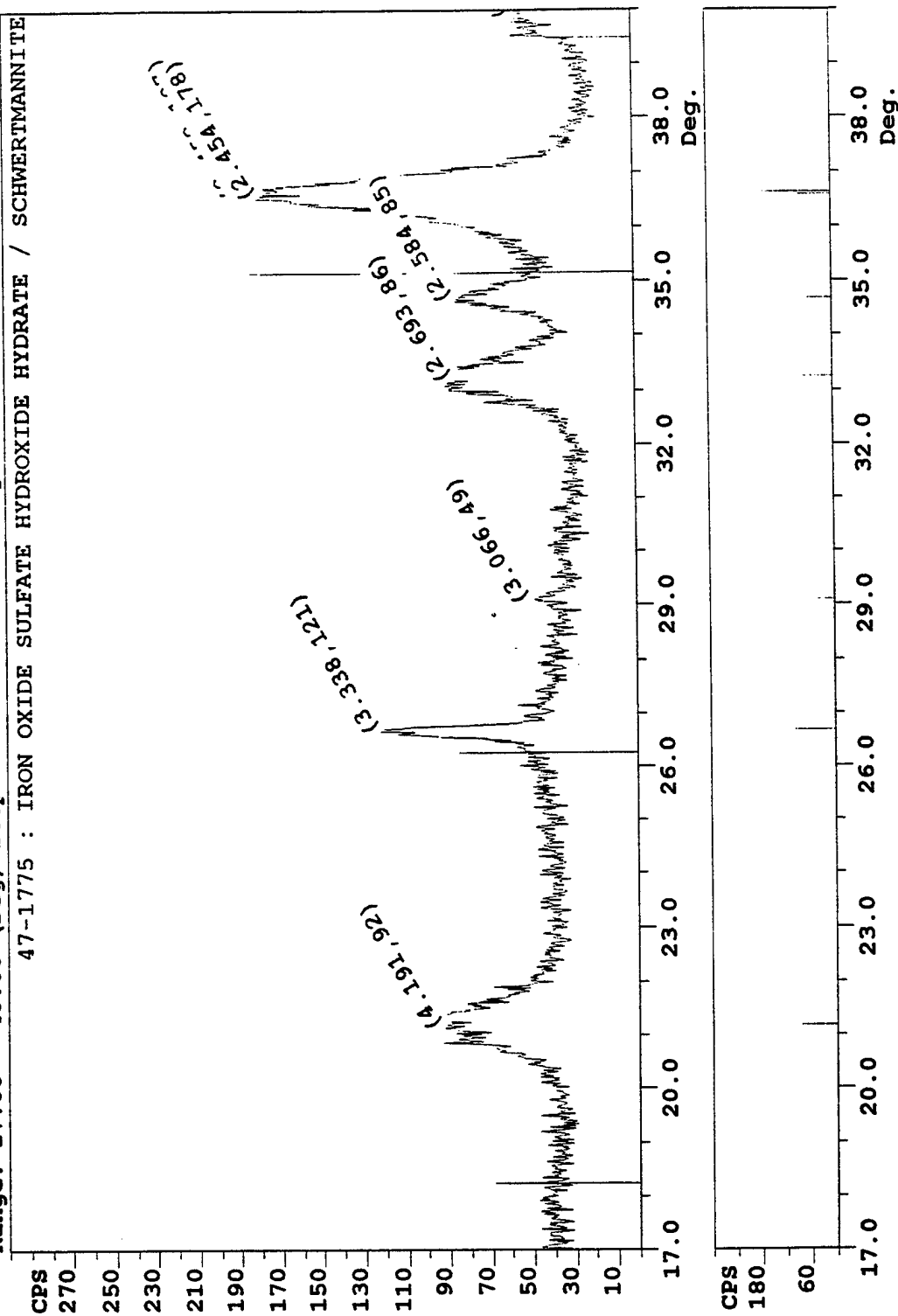
Figure P-1: Schwertmannite signature on the raw data.
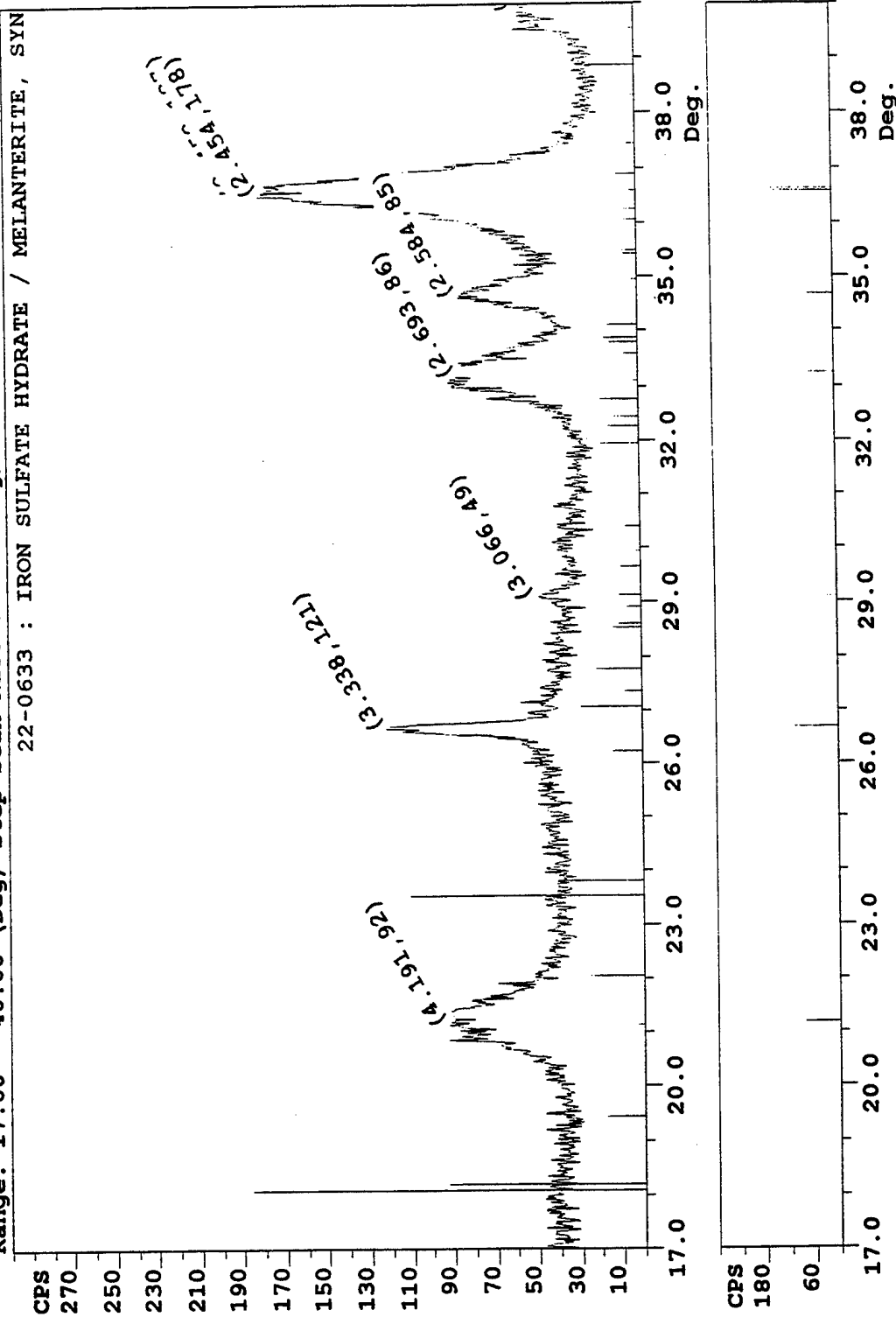
Figure P-2: Melanterite signature on the raw data.

206
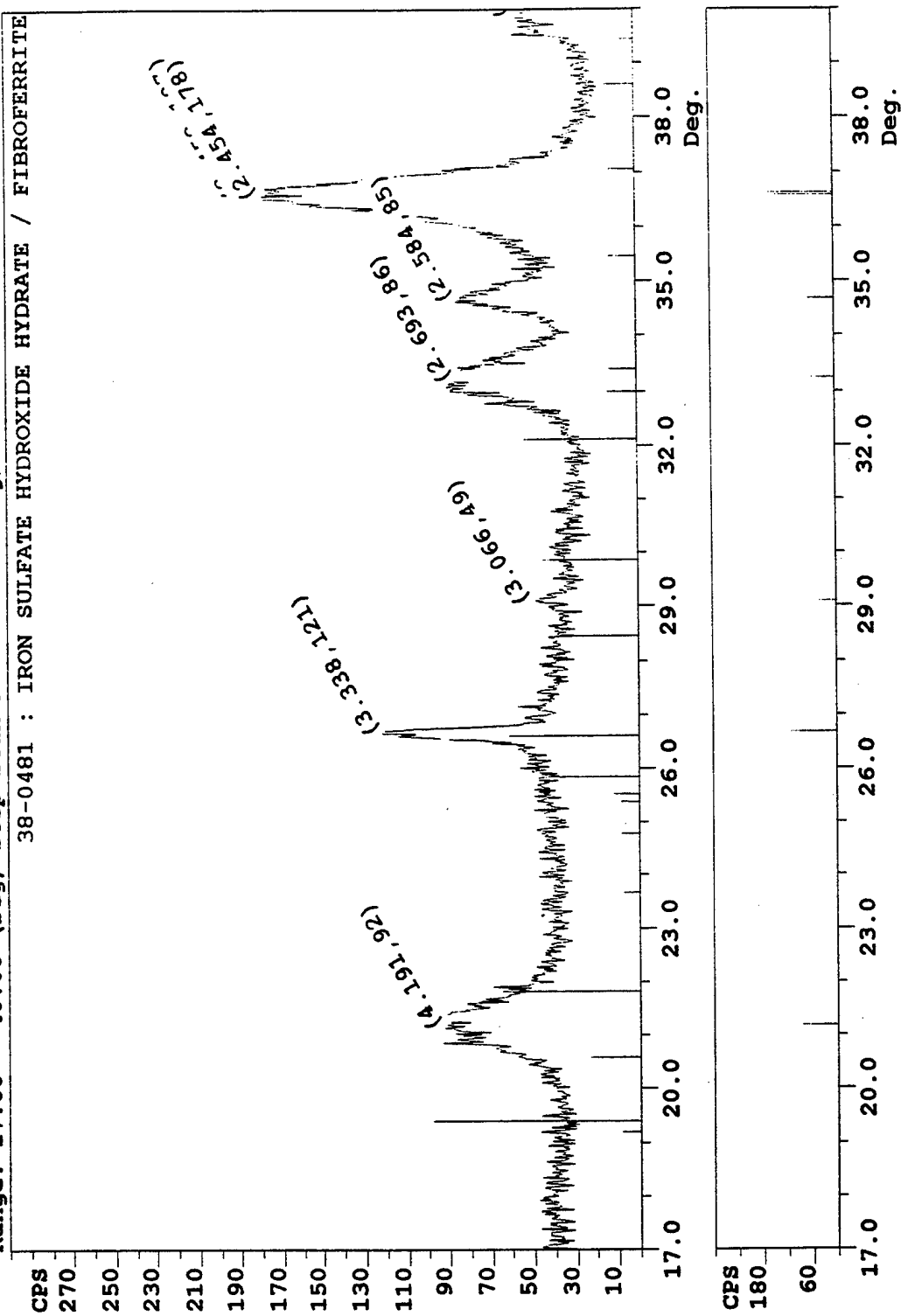
Figure P-3: Fibroferrite signature on the raw data.

Figure P-4: Amarantite signature on the raw data.
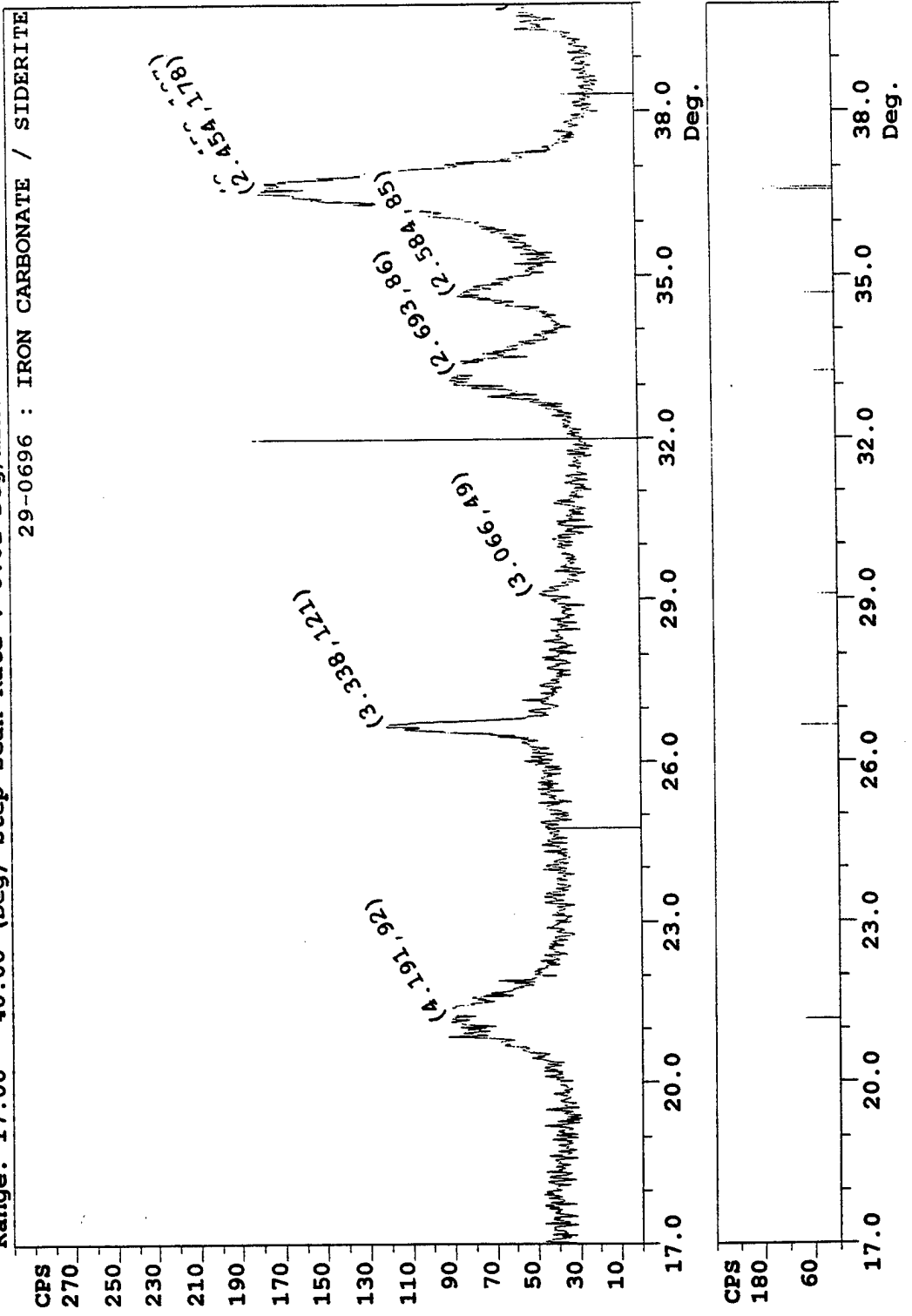
Figure P-5: Siderite signature on the raw data.
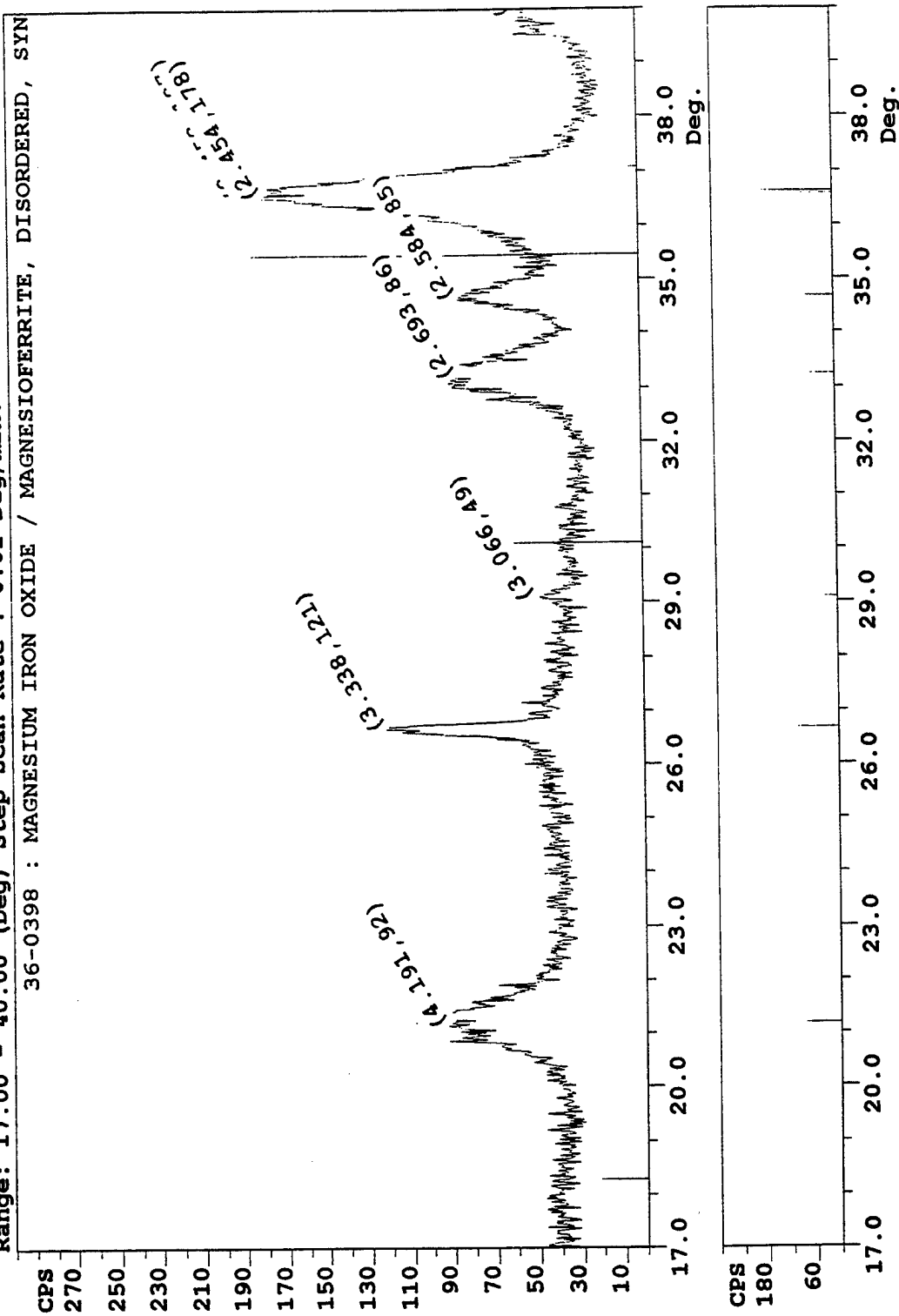
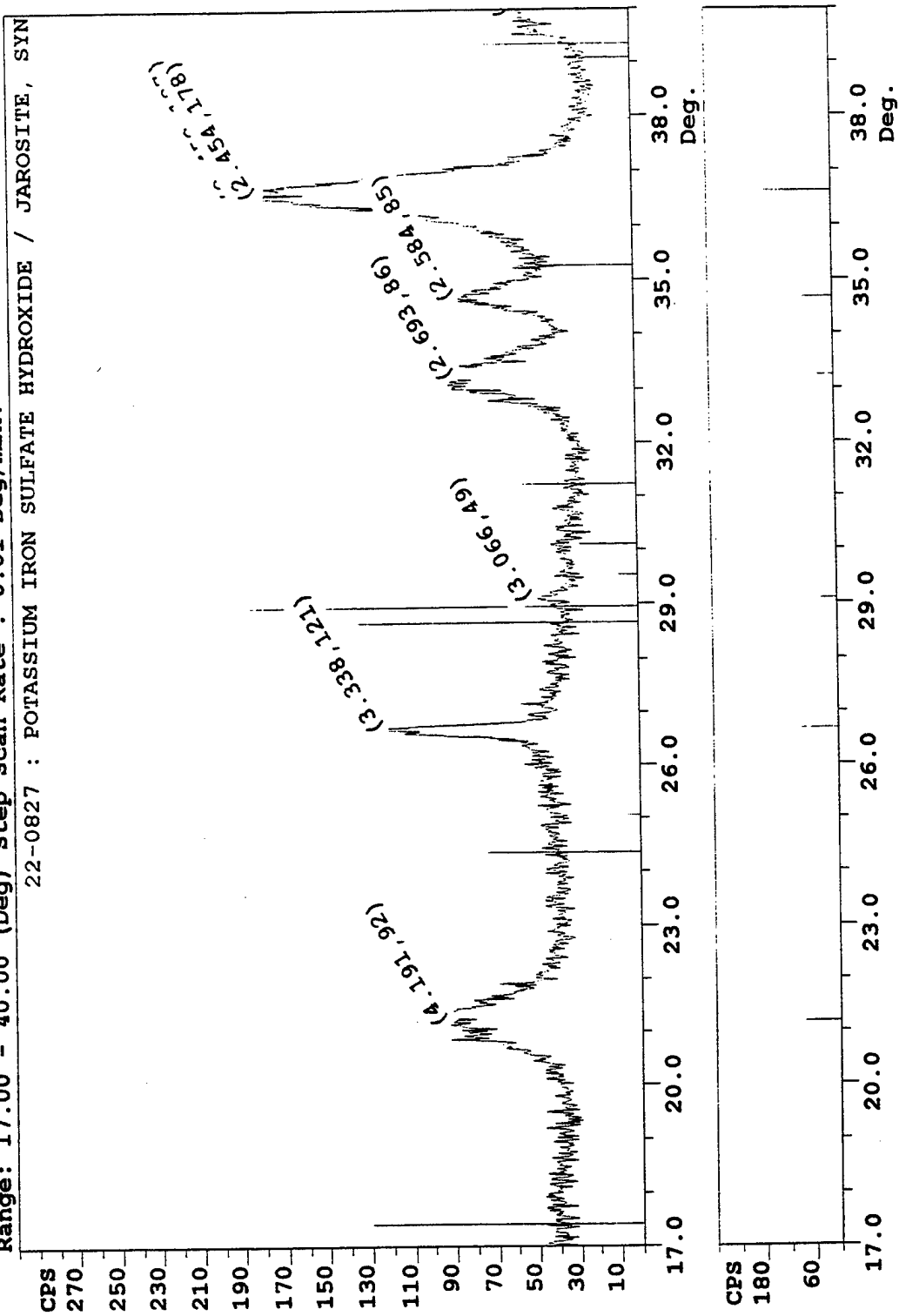Figure P-6: Magnesioferrite signature on the raw data.
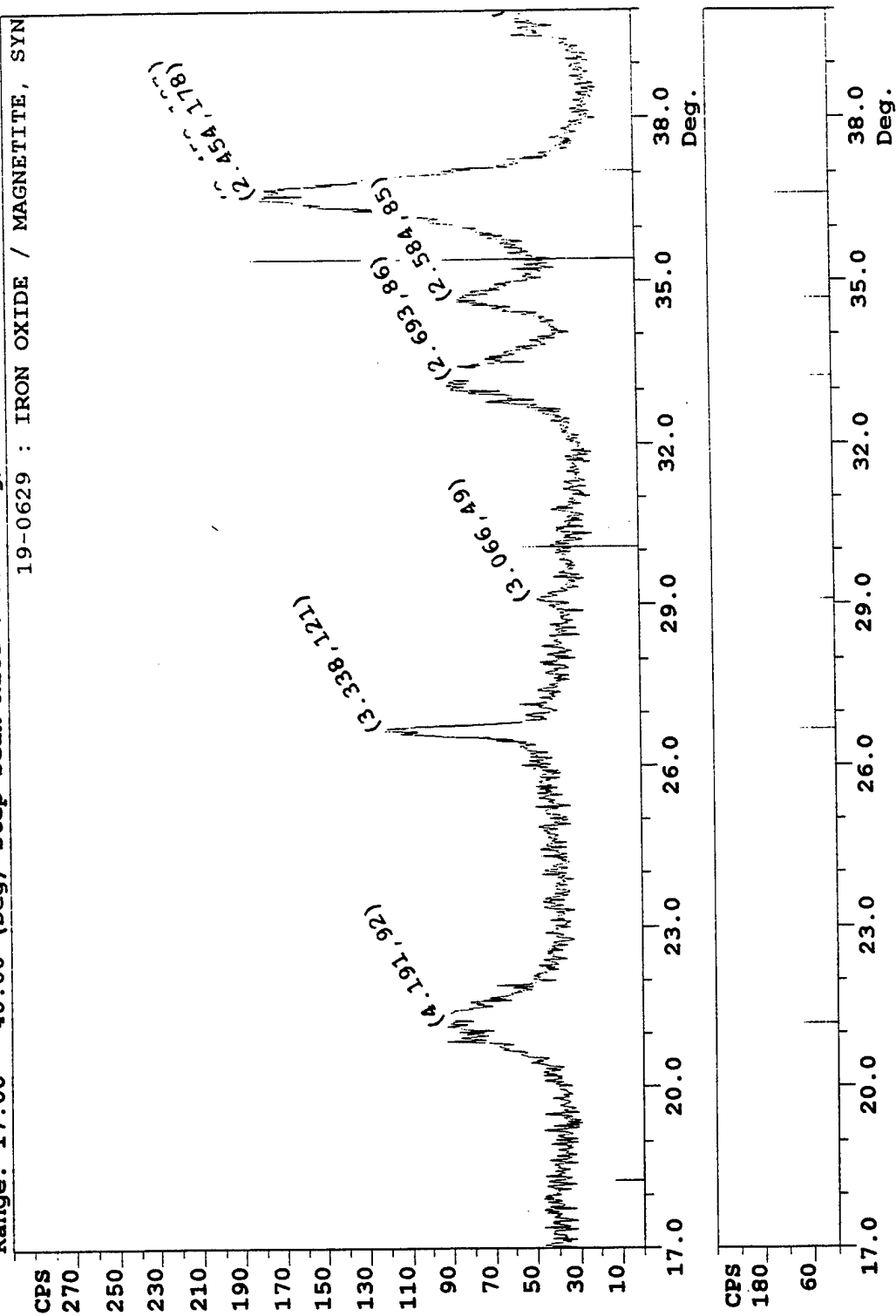
Figure P-7: Magnetite signature on the raw data.

File: HB IP2 middle slowscan, ID: HB IP2 middle, slow scan (4 Jan 99)
Date: 01/04/99 23:11 Step : 0.020° Cnt Time: 2.400 Sec.
Range: 17.00 - 40.00 (Deg) Step Scan Rate : 0.01 Deg/min.

33-0664 : IRON OXIDE / HEMATITE, SYN
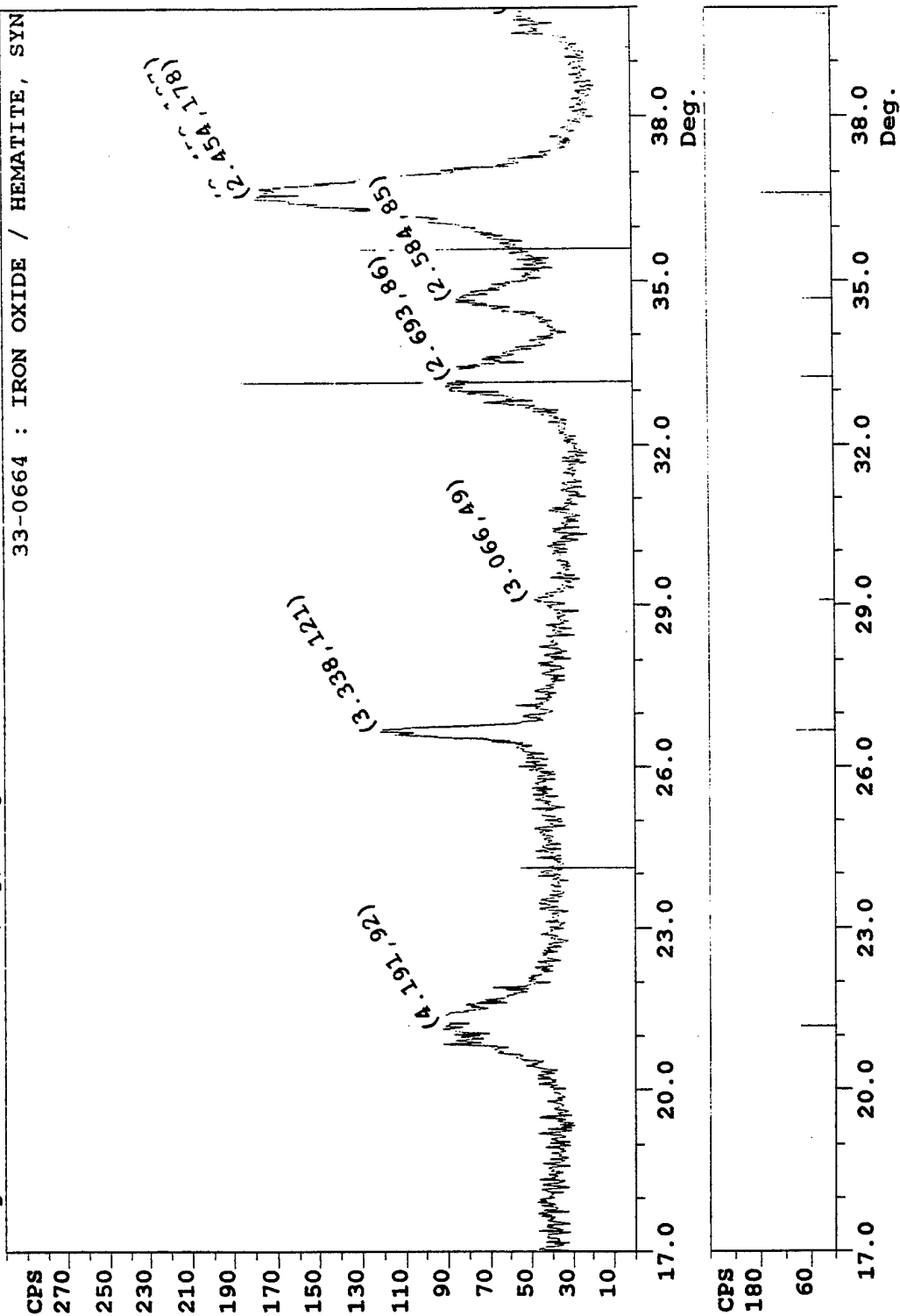
Figure P-8: Hematite signature on the raw data.

212

Figure P-9: Jarosite signature on the raw data.

File: HB IP2 middle slowscan, ID: HB IP2 middle, slow scan (4 Jan 99)
Date: 01/04/99 23:11 Step : 0.020° Cnt Time: 2.400 Sec.
Range: 17.00 - 40.00 (Deg) Step Scan Rate : 0.01 Deg/min.

29-0712 : IRON OXIDE HYDROXIDE HYDRATE / FERRIHYDRITE, SYN
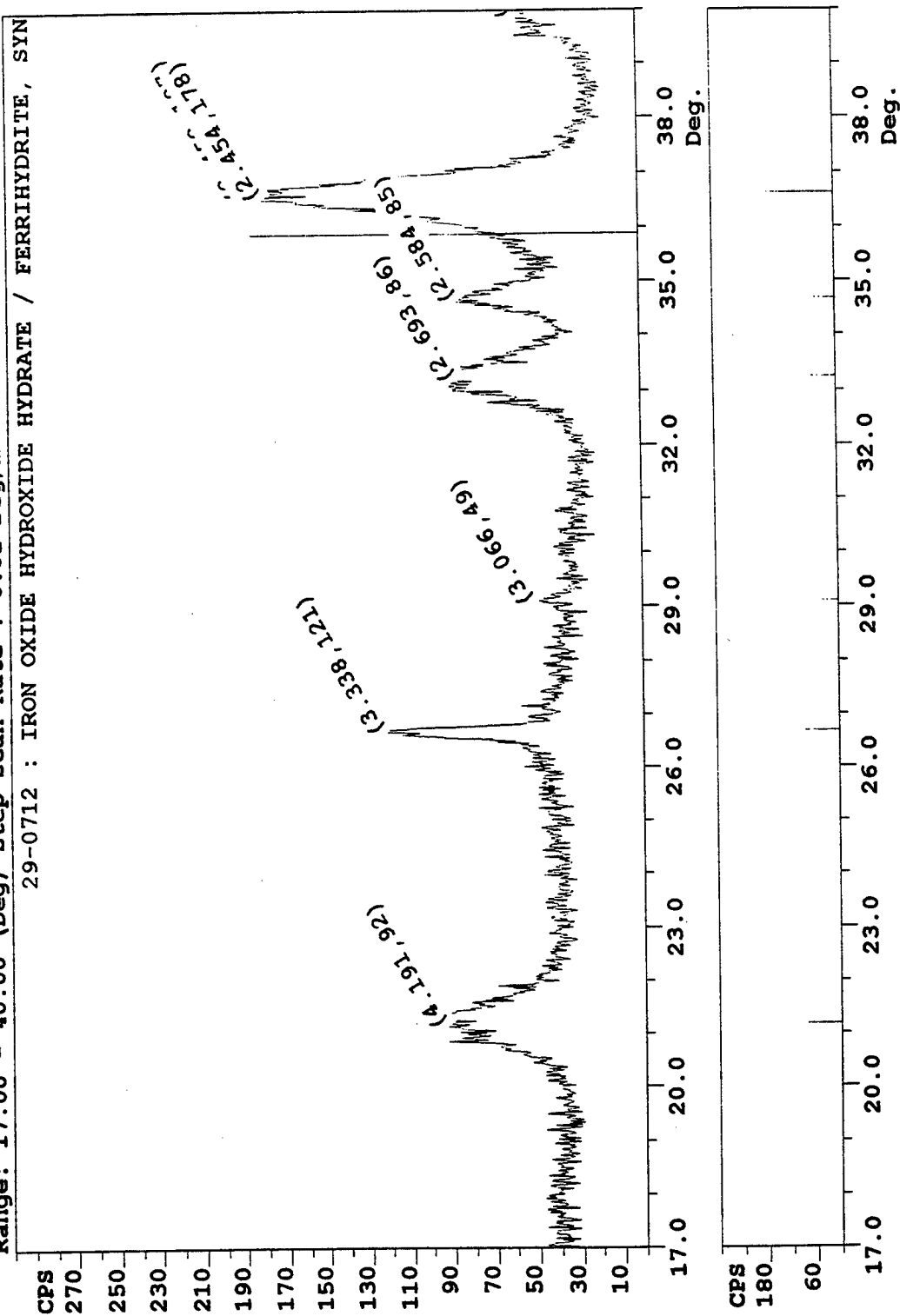
Figure P-10: Ferrihydrite signature on the raw data.

PLEASE CHECK THE APPROPRIATE BLOCK BELOW:

AQ #_____

☐ _____/_____ copies are being forwarded. Indicate whether Statement A. B. C. D. E, F. or X applies.

☒ DISTRIBUTION STATEMENT A:
   APPROVED FOR PUBLIC RELEASE: DISTRIBUTION IS UNLIMITED

☐ DISTRIBUTION STATEMENT B:
   DISTRIBUTION AUTHORIZED TO U.S. GOVERNMENT AGENCIES
   ONLY; (Indicate **Reason** and Date). OTHER REQUESTS FOR **THIS**
   DOCUMENT SHALL BE REFERRED TO (Indicate Controlling DoD Office).

☐ DISTRIBUTION STATEMENT C:
   DISTRIBUTION AUTHORIZED TO U.S. GOVERNMENT AGENCIES AND
   THEIR CONTRACTORS; (Indicate Reason and Date). OTHER REQUESTS
   FOR THIS DOCUMENT SHALL BE REFERRED TO (Indicate Controlling DoD **Office**).

☐ DISTRIBUTION STATEMENT D:
   DISTRIBUTION AUTHORIZED TO DoD AND U.S. DoD CONTRACTORS
   ONLY; (Indicate Reason and Date). OTHER REQUESTS SHALL BE REFERRED TO
   (Indicate Controlling DoD Office).

☐ DISTRIBUTION STATEMENT E:
   DISTRIBUTION AUTHORIZED TO DoD COMPONENTS ONLY; (Indicate
   Reason and Date). OTHER REQUESTS SHALL BE REFERRED TO (Indicate Controlling DoD Office).

☐ DISTRIBUTION STATEMENT F:
   FURTHER DISSEMINATION ONLY AS DIRECTED BY (Indicate Controlling DoD Office and Date) or HIGHER
   DoD AUTHORITY.

☐ DISTRIBUTION STATEMENT X:
   DISTRIBUTION AUTHORIZED TO U S GOVERNMENT AGENCIES
   AND PRIVATE INDIVIDUALS OR ENTERPRISES ELIGIBLE TO OBTAIN EXPORT-CONTROLLED
   TECHNICAL DATA IN ACCORDANCE WITH LoD DIRECTIVE 5230.25 WITHHOLDING OF
   UNCLASSIFIED TECHNICAL DAT A FROM PUBLIC DISCLOSURE. 6 Nov 1984 (indicate date of determination).
   CONTROLLING DoD OFFICE IS (Indicate Controlling DoD Office).

☐ This document was previously forwarded to DTIC on _____ (date) and the
   AD number is _____

☐ [n accordance with provisions of DoD instructions. the document requested is not supplied because:
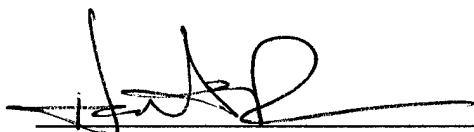
☐ It will be published at a later date. (Enter approximate date. if known).

☐ Other. (Give Reason)

DoD Directive 5230.24, "Distribution Statements on Technical Documents," 18 Mar 87, contains seven distribution statements, as described briefly above. Technical Documents must be assigned distribution statements.

9 April 99

Authorized Signature/Date

HEATH C. ROSCOE
Print or Type Name

814-861-3344
Telephone Number